UNIVERSIDADE DE SÃO PAULO
FACULDADE DE ZOOTECNIA E ENGENHARIA DE ALIMENTOS

SIMARA LARISSA FANALLI

Effect of the addition of different sources of fatty acids in the pig diet on the transcriptomic profile of different tissues

Pirassununga
2022

SIMARA LARISSA FANALLI

Effect of the addition of different sources of fatty acids in the pig diet on the transcriptomic profile of different tissues

Versão corrigida

Dissertação apresentada à Faculdade de Zootecnia e Engenharia de Alimentos da Universidade de São Paulo, como parte dos requisitos para a obtenção do titulo de Mestre em Ciências do programa de Mestrado em Biociência Animal.

Área de Concentração: Biociência Animal

Orientadora: Profa. Dra. Aline Silva Mello Cesar

Pirassununga

2022

Ficha catalográfica elaborada pelo
Serviço de Biblioteca e Informação, FZEA/USP,
com os dados fornecidos pelo(a) autor(a)

Fanalli, Simara Larissa

F199e Effect of the addition of different sources of fatty acids in the pig diet on the transcriptomic profile of different tissues / Simara Larissa Fanalli ; orientadora Aline Silva Mello Cesar. -- Pirassununga, 2022.

262 f.

Dissertação (Mestrado - Programa de Pós-Graduação em Biociência Animal) -- Faculdade de Zootecnia e Engenharia de Alimentos, Universidade de São Paulo.

1. RNA-Seq. 2. liver. 3. immune response. 4. metabolic disease. 5. skeletal muscle. I. Cesar, Aline Silva Mello, orient. II. Título.

UNIVERSIDADE DE SÃO PAULO
ESCOLA SUPERIOR DE AGRICULTURA "LUIZ DE QUEIROZ"

Comissão de Ética no Uso de Animais – CEUA
www4.esalq.usp.br – fone (19)34294400

CERTIFICADO

Certificamos que a proposta intitulada "Efeito da adição de ácido oleico na dieta de suínos sobre o perfil da resposta imunológica e de ácidos graxos de diferentes tecidos", registrada com o número de protocolo 2018.5.1787.11.6, n° CEUA: 2018-28, sob a responsabilidade de Aline Silva Mello Cesar, que envolve a produção, manutenção e/ou utilização de animais pertencentes ao filo Chordata, subfilo Vertebrata (exceto o homem), para fins de pesquisa científica (ou ensino), encontra-se de acordo com os preceitos da Lei nº 11.794, de 08 de outubro de 2008, do Decreto nº 6.899, de 15 de julho de 2009, e com as normas editadas pelo Conselho Nacional de Controle da Experimentação Animal-CONCEA, e foi aprovada pela Comissão de Ética no Uso de Animais (CEUA) da Escola de Agricultura Luiz de Queiroz-ESALQ/USP, em reunião ordinária no dia 18 de setembro de 2018.

Finalidade	**( ) Ensino (X) Pesquisa Científica**
Vigência da autorização	22/11/2018 a 31/07/2022
Espécie/Linhagem/raça	Suíno/Comercial
Nº de animais	72
Peso/Idade	125 dias / 70Kg
Sexo	M
Origem	Estação Experimental Fazenda São Gabriel – DB Genética Suína – Presidente Olegário - MG

CERTIFICATE

This is to certify that study "Effect off dietary oleic acid on fatty acid composition and inflammatory response profile in different tissues of pigs", protocol number 2018.5.1787.11.6, under the responsibility of Aline Silva Mello Cesar, has been approved by the Institutional Animal Care and Use Committee, College of Agriculture "Luiz de Queiroz", Piracicaba, SP, Brazil, University of São Paulo.

Piracicaba, 25 de setembro de 2018.

Prof. Dr. Urbano dos Santos Ruiz
Coordenador da CEUA/ESALQ/USP

Folha de Aprovação

Simara Larissa Fanalli

Effect of the addition of different sources of fatty acids in the pig diet on the transcriptomic profile of different tissues

Dissertação apresentada à Faculdade de Zootecnia e Engenharia de Alimentos da Universidade de São Paulo, como parte dos requisitos para a obtenção do título de Mestre em Ciências do programa de Mestrado em Biociência Animal.

Data de aprovação: 04/03/2022

Banca Examinadora:

_____

Aline Silva Mello Cesar – Presidente da Banca Examinadora
Profª. Drª. Faculdade de Zootecnia e Engenharia de alimentos – Orientadora

_____

Profª. Drª. Vivian Vezzoni de Almeida
Universidade Federal de Goiás - GO

_____

Dr. Gabriel Costa Monteiro Moreira
University of Liège - GIGA/ULg

À Maria do Carmo, Fausto, Mirian e família

pelo amor e incentivo, dedico!

AGRADECIMENTOS

Agradeço a Deus que me deu forças e me guiou até aqui.

À Profa. Dra. Aline Silva Mello Cesar por essa oportunidade incrível, pela orientação, paciência, compreensão, ensinamentos, confiança, imensa e incansável ajuda em todos os momentos, pelo amor a docência, dedicação e profissionalismo. Por ser inspiração!

Ao Prof. Dr. Robson Carlos Antunes por acreditar em mim, pelo incentivo, apoio e por tornar essa caminhada possível.

À Profa. Dra. Janine França, pela amizade e apoio constante.

A Universidade de São Paulo – Faculdade de Zootecnia e Engenharia de Alimentos, ao programa de Biociência Animal e a Escola Superior de Agricultura "Luiz de Queiroz" pela oportunidade e por toda equipe de técnicos, funcionários e professores.

À Coordenação de Aperfeiçoamento de Pessoal de Nível Superior (CAPES) pela bolsa concedida - Código de Financiamento 001.

À DB Genética Suína, a Fundação de Amparo à Pesquisa do Estado de São Paulo (FAPESP) e o Conselho Nacional de Desenvolvimento Científico e Tecnológico (CNPq) foram imprescindíveis na realização desta pesquisa.

À Bruna, Julia Dezen e Julia Martins pela intensa parceria. Aos integrantes do Laboratório de Biologia Molecular e Micotoxinas (LABMIC), Janaína, Débora, Laura, Natalia, Milena, Tota e Ivani, pelo acolhimento, ajuda e pela parceria. À Fernanda e ao Felipe pelo auxílio nessa reta final. À Profa. Dra. Daniele Maffei, a Denise, ao Laboratório de Qualidade e Processamento de Carnes e ao Laboratório de Biotecnologia Animal (LBA) por todo apoio e auxílio.

Aos professores e pesquisadores, em especial ao Dr. Luiz Lehmann Coutinho, Dr. Heidge Fukumasu, Dra. Luciana Correia de Almeida Regitano, Dra Vivian Vezzoni de Almeida, Dr. Gabriel Costa, Dr. Albino Luchiari Filho, Dra.Bárbara Silva-Vignato, Dra. Juliana Afonso, Dra. Bruna Petry, Dra. Priscila Trevisoli, Dra Ariana Meira, Dra Karine Assis, pelo ensinamento, ajuda e sugestões.

Aos membros da banca examinadora pelo aceite, tempo e pelas valiosas colaborações.

À Ingrid e Natália pela amizade e recepção em Piracicaba, à Silvia pelo acolhimento e ao Atio *(in memoriam)* por toda ajuda. À Helen, pela compreensão, ajuda e por me deixar fazer parte da sua vida. Às amigas de uma vida, Alana e Lorena por sempre me apoiarem.

Aos meus pais, pela força, confiança e amor, aos meus irmãos, em especial a Mirian que com sua família foram essenciais na minha vida acadêmica e meus sobrinhos por serem minha força. Amo vocês.

À todos, muito obrigada!

INSTITUIÇÃO E FONTE FINANCIADORA

Este trabalho foi desenvolvido nos laboratórios: Laboratório de Biologia Molecular e Micotoxinas (Departamento de Agroindústria Alimentos e Nutrição - LAN - ESALQ/USP); Laboratório de Qualidade e Processamento de Carnes (Departamento de Agroindústria Alimentos e Nutrição - LAN - ESALQ/USP); Laboratório do Centro de Genômica Animal (Departamento de Zootecnia - LZT - ESALQ/USP), Piracicaba, São Paulo, Brasil.

Recebeu apoio financeiro da Coordenação de Aperfeiçoamento de Pessoal de Nível Superior (CAPES). Programa Demanda Social - Processo: 88887.509276/2020-00, da Fundação de Amparo à Pesquisa do Estado de São Paulo (FAPESP) - Jovem Pesquisador (JP) Processo número: 2017/25180-2 e do Conselho Nacional de Desenvolvimento Científico e Tecnológico (CNPq) Processo número: 301083/2018-5.

RESUMO

FANALLI, S.L., Efeito da adição de diferentes fontes de ácidos graxos na dieta de suínos sobre o perfil do transcriptoma de diferentes tecidos, 2022, p.276 Dissertação (Mestrado) – Faculdade de Zootecnia e Engenharia de Alimentos, Universidade de São Paulo, Pirrassununga (FZEA/USP), 2022.

A espécie *Sus Scrofa* é uma das mais importantes para a produção de carne e outros produtos de origem animal em todo o mundo e são modelo animal para doenças metabólicas em humanos. Além disso, a carne suína é uma das principais fontes de ácidos graxos (AG) na dieta humana. O consumo de AG está associado à deposição de gordura e aumento da ocorrência de doenças metabólicas. Por outro lado, existem estudos que divergem sobre o papel dos AG envolvidos nas respostas inflamatórias celulares em doenças metabólicas. O objetivo deste estudo foi identificar os genes diferencialmente expressos (GDE) e os fatores de transcrição de amostras de músculo e fígado de suínos machos imunocastrados alimentados com dieta adicionada de diferentes fontes e níveis de AG. Os tratamentos dietéticos consistiram em dieta basal de milho e farelo de soja suplementadas com 1,5% de óleo de soja (SOY1,5, nível comum usado na produção comercial de suínos) ou 3% de óleo de soja (SOY3,0), ou 3% de óleo de canola (CO) ou 3% de óleo de peixe (FO) por um período experimental de 98 dias durante as fases de crescimento e terminação (18 animais/tratamento). Foi realizada a análise dos parâmetros bioquímicos do sangue, assim como o perfil de AG depositados nos tecidos. Os GDE (FDR 10%) foram identificados em 72 amostras de músculo esquelético e fígado através do pacote DESeq2 R, seguido da análise de qualidade dos dados. A partir da análise do transcriptoma de amostras do músculo esquelético e fígado, a análise de enriquecimento funcional (FDR<0,10) pelo MetaCore resultou em mapas de vias de sinalização associadas a processos metabólicos, estresse oxidativo doenças metabólicas e neurodegenerativas, assim como redes gênicas relacionadas à resposta imune e processos biológicos. O enriquecimento da dieta basal com fontes de óleo contendo diferentes perfis de AG influenciou a composição do perfil depositado na gordura intramuscular (*Longissimus lomborum*) e fígado, os parâmetros sanguíneos e a expressão gênica em vias metabólicas e processos de redes no tecido muscular esquelético e fígado dos animais durante as fases de crescimento e terminação. Quando a comparação foi relacionada à adição de óleo de soja e óleo de peixe a maior quantidade de GDE total foi identificada. Além disso, fatores de transcrição foram relacionados ao metabolismo lipídico e resposta imune quando utilizado óleo de soja 1.5% ou 3%. Em suma, esses resultados contribuem para o campo de pesquisa da nutrigenômica que visa elucidar a influência da dieta na saúde animal e humana e impulsionar a tecnologia e a ciência dos alimentos.

Palavras–chave: RNA-Seq, fígado, resposta imune, doença metabólica, músculo esquelético.

ABSTRACT

FANALLI, S.L. Effect of the addition of different sources of fatty acids in the pig diet on the transcriptomic profile of different tissues, 2022, p.276 M.Sc. Dissertation - Faculdade de Zootecnia e Engenharia de Alimentos, Universidade de São Paulo, Pirassununga, 2022.

The *Sus Scrofa* species is one of the most important for the production of meat and other animal products worldwide and is an animal model for metabolic diseases in humans. Furthermore, pork is one of the main sources of fatty acids (FA) in the human diet. The FA consumption is associated with fat deposition and increased occurrence of metabolic diseases. On the other hand, some studies diverge on the role of FAs involved in cellular inflammatory responses in metabolic diseases. The aim of this study was to identify differentially expressed genes (GDE) and transcription factors from muscle and liver samples from immunocastrated male pigs fed a diet added from different sources and levels of FA. Dietary treatments consisted of corn-soybean meal growing-finishing diets supplemented with 1.5% soybean oil (SOY1.5, common level used in commercial pig production) or 3% soybean oil (SOY3.0) or 3% canola oil (CO) or 3% fish oil (FO) for an experimental period of 98 days during the growing and finishing phases (18 pigs/treatment). The analysis of the parameters of the blood was performed, as well as the profile of AG deposited in the tissues. The DEG (FDR 10%) was identified in 72 samples of skeletal muscle and liver using the DESeq2 R., followed by data quality analysis. From the transcriptome analysis of skeletal muscle and liver samples, the functional enrichment analysis (FDR <0.10) by MetaCore revealed maps of signaling pathways associated with metabolic processes, oxidative stress, metabolic and neurodegenerative diseases, as well as gene networks related to immune response and biological processes. The enrichment of the basal diet with oil sources containing different FA profiles influenced the composition of the deposited profile, the blood parameters, and the gene expression in metabolic pathways and network processes in the skeletal muscle tissue and liver of animals during the growth and termination. When the comparison was related to the addition of soybean oil and fish oil, the highest amount of total DEG was identified. In addition, transcription factors related to lipid metabolism and immune response were identified when using 1.5% or 3% soybean oil. It could contribute to the nutrigenomics research field that aims to elucidate dietary interventions in animal and human health, as well as to drive food technology and science.

Keywords: RNA-Seq, liver, immune response, metabolic disease, skeletal muscle.

CONTENTS

CHAPTER 1. GENERAL INTRODUCTION

1.1 BACKGROUND AND JUSTIFICATION

The domestic pig (*Sus scrofa*) is one of the most important species for the production of meat and other animal products worldwide (SUMMERS et al., 2020; OECD-FAO, 2021) and, consequently, meat quality and fatty acids (FA) composition is economically relevant and can affect human health (MARTINS et al., 2018). Among its many benefits are its supply of unsaturated fatty acids, such as oleic acid (OA, C18:1 cis 9) and linoleic acid (AL, C18: 2 cis9, 12), which have positive effects on human health (LAAKSONEN et al., 2005; FARAG; GAD, 2022). Pigs have been increasingly used to nutrigenomics research and for investigation of metabolic diseases in humans due to role as a biomedical model for humans (LUNNEY, 2007; BROWN et al., 2010; MALGWI et al., 2022). They have a system to emulate a series of aspects related to human health, such as obesity, diabetes, cancer, neurological, cardiovascular and infectious diseases (KRAGH et al., 2009; REDDY et al., 2009), as they have similarities in terms of anatomy, biochemistry, pathology, pharmacology and physiology with humans what makes them to be used as a biomedical model (KRAGH et al., 2009; REDDY et al., 2009; PAN et al., 2021).

Many studies of fat sources in pig have been carried out in nutrigenomics, as the reflected FA profiles of dietary components can alter gene expression (PARK et al., 2012; KIM et al., 2014; LI et al., 2015; SZOSTAK et al., 2016; KELLNER; GABLER; PATIENCE, 2017; NONG et al., 2020). The fat content in the tissues directly impacts important pork qualities as juiciness, flavor, as well as tenderness and firmness. Low levels of saturated fatty acids (SFA) are highly desirable, due to their frequent association with high levels of blood cholesterol, such as low-density lipoprotein cholesterol (LDL-c). However, high levels of MUFA (Monounsaturated) and PUFA (Polyunsaturated fatty acids) are useful in decreasing LDL-c levels and increasing high-density lipoprotein cholesterol, which reduces the risk of heart disease (ALBUQUERQUE et al., 2021).

In muscle, FA are substrates for oxidation (FRAYN; ARNER; YKI-JÄRVINEN, 2006), skeletal muscle is an insulin-sensitive peripheral tissue, essential for blood lipid profile and lipid homeostasis, such as FA oxidation and in the cholesterol efflux (SHIMIZU et al., 2015; LI et al., 2016). Fundamental to maintaining glycemic control,

muscle plays an important role in energy metabolism and is important for insulin-mediated glucose metabolism (SHIMIZU et al., 2015; LI et al., 2016). In addition, its nutritional value and benefits impact human health (PUIG-OLIVERAS et al., 2014). In the liver, triglyceride hydrolysis is substrates for the assembly of very low-density lipoprotein (FRAYN; ARNER; YKI-JÄRVINEN, 2006). The liver is a metabolic organ that plays a central role in lipid metabolism, energy, immunomodulation, detoxification and endocrine activity in a healthy organism, in addition to degrading products such as circulating Aβ peptides important for the liver-brain axis (WIĘCKOWSKA-GACEK et al. 2021).

Nutritionally important FA such as MUFA oleic acid (OA, C18:1), PUFA as omega-6 (n-6) linoleic acid (LA, C18:2 n-6), and omega-3 (n-3) fatty acids such as docosahexaenoic acid (DHA, C22:6 n-3) and eicosapentaenoic acid (EPA, C22:5 n-3) and alpha-linolenic acid (ALA, C18:3 n-3), can regulate gene transcription in different tissues (CESAR et al., 2016; KELLNER; GABLER; PATIENCE, 2017; MOGHADASIAN; SHAHIDI, 2017). Major sources of MUFA OA include olive oil and canola oil, LA can be found in soybean oil, ALA in soybean oil, flaxseed oil and canola oil, EPA and DHA in fish oil (MOGHADASIAN; SHAHIDI, 2017). Pig diets added with vegetable oils rich in unsaturated fatty acids can be a source of healthier products for consumers (PARK et al., 2012).

Important components of pro-inflammatory lipid mediators are n-6 PUFA (BORDONI et al., 2021). Linoleic acid can be converted to arachidonic acid (AA, 20:4n-6) (a precursor of inflammatory mediators), an important component of membrane phospholipids and a substrate for cytochrome P450 (CYP), cyclooxygenase-2 (COX-2), 5-lipoxygenase (5-LOX) and in the production of eicosanoid mediators, such as hydroperoxyeicosatetraenoic acid (HPETE), leukotrienes (LTs), thromboxanes (TXs), prostaglandins (PGs), and lipoxins (MARION-LETELLIER; SAVOYE; GHOSH, 2015; BORDONI et al., 2021).

In contrast, PUFA such as n-3 are fundamental in modulating immune system functions, decreasing the severity of inflammatory disorders (YATES et al., 2014). The increase in n-3 from oily fish and fish oil can decrease the amount of AA's in the membrane phospholipids of cells involved in inflammation (CALDER, 2015). The n-3 can inhibit AA's metabolism by competing for enzymes that catalyze the biosynthesis of thromboxanes, prostaglandins and leukotrienes. In addition, n-3 PUFA such as ALA can be metabolized into EPA and DHA which give rise to eicosanoids with anti-

inflammatory functions, originating mediators accelerating the resolution of inflammation by inhibiting the migration of immune cells, among them, the release of inflammatory cytokines such as inflammatory disease-associated interleukins IL-1α, IL-1β, IL-6, and IL-8, interferon γ (IFNγ), and tumor necrosis factor α (TNF-alpha) (CALDER, 2015; MARION- LETELLIER; SAVOYE; GHOSH, 2015; BORDONI et al., 2021). Blockade performed by n-3 PUFA may be through suppression of inflammatory nuclear factor kappa B (NF-κB) signaling (BORDONI et al., 2021), in addition, many cellular systems and functions can be impacted and regulated by FA long-chain n-3 such as EPA or DHA via transcription factors including 4-sterol regulatory element binding protein-1c (SREBP-1c), peroxisome proliferator-activated receptors *(PPARα, β, γ1 and γ2),* and *NF-κB* that is related to important regulatory systems of protein encoding of inflammatory processes, lipid and carbohydrate metabolism, directly or indirectly modulating various cellular activities related to inflammation (RODRÍGUEZ-CRUZ; SERNA, 2017).

Thus, the balance between the ratio of n-6 and n-3 is fundamental especially for the health of the consumer. Conversion of LA and ALA to long-chain PUFA *in vivo* is a limiting step due to a competition between these n-6 and n-3 FA as they share a common enzymatic pathway (LI et al., 2015). When there is an imbalance with excessive concentration of n-6 PUFA, it is related with the development of cardiovascular, neuropsychiatric and metabolic pathogenesis and a high concentration of n-3, that is, a low ratio between n-6 and n-3 exert suppressive effects (SIMOPOULOS, 2002, 2008; LI et al., 2015) A lower proportion of this ratio was related to increased lipolysis in pigs fed different proportions of PUFA in the study by Nong et al. (2020).

The understanding at the molecular level of FA is still quite limited and there is a gap in the knowledge between the effect and importance of fatty acids on the level of gene expression and consequently on the biological pathways involved with metabolic diseases and the pig immune system. Thus, our hypothesis is that the addition of oils with different fatty acid profiles in the diet of pigs during the growing and finishing phases alters the transcriptome expression profile of different tissues. And our objectives were (1) to evaluate changes in gene expression in skeletal and liver muscle tissue and to identify the metabolic pathways and gene networks impacted by the fatty acid composition of pigs fed a diet with different levels of soybean oil (1.5 % or 3.0%); (2) to identify the main transcription factors related to lipid metabolism and the immune

response linked to differentially expressed genes (DEG) from liver tissue of immunocastrated male pigs fed diets with two levels of soybean oil (1.5% or 3.0%) and (3) to evaluate the effect of the addition of different sources of fatty acids on the transcriptome profile of skeletal muscle and liver and to identify the metabolic pathways and impacted gene networks.

REFERENCES

ALBUQUERQUE, A. et al. Transcriptomic profiling of skeletal muscle reveals candidate genes influencing muscle growth and associated lipid composition in portuguese local pig breeds. **Animals**, v. 11, n. 5, 2021.

BORDONI, L. et al. Nutrigenomics of dietary lipids. **Antioxidants**, v. 10, n. 7, 2021.

BROWN, M. S.; RADHAKRISHNAN, A.; GOLDSTEIN, J. L. Retrospective on Cholesterol Homeostasis: The Central Role of ScapAnnual **Review of Biochemistry**, 2018.

CALDER, P. C. **Marine omega-3 fatty acids and inflammatory processes: Effects, mechanisms and clinical relevanceBiochimica et Biophysica Acta - Molecular and Cell Biology of Lipids**, 2015. .

CESAR, A. S. M. et al. Differences in the skeletal muscle transcriptome profile associated with extreme values of fatty acids content. **BMC Genomics**, p. 1–16, 2016. Disponível em: <http://dx.doi.org/10.1186/s12864-016-3306-x>.

FRAYN, K. N.; ARNER, P.; YKI-JÄRVINEN, H. Fatty acid metabolism in adipose tissue, muscle and liver in health and disease. **Essays in Biochemistry**, v. 42, 2006.

KELLNER, T. A.; GABLER, N. K.; PATIENCE, J. F. The composition of dietary fat alters the transcriptional profile of pathways associated with lipid metabolism in the liver and adipose tissue in the pig. **Journal of Animal Science**, v. 95, n. 8, 2017.

KIM, S.-C. et al. Changes in expression of insulin signaling pathway genes by dietary fat source in growing-finishing pigs. **Journal of Animal Science and Technology**, v. 56, n. 1, 2014.

KRAGH, P. M. et al. Hemizygous minipigs produced by random gene insertion and handmade cloning express the Alzheimer's disease-causing dominant mutation APPsw. **Transgenic Research**, v. 18, n. 4, 2009.

LI, F. et al. Effects of dietary n-6:n-3 PUFA ratio on fatty acid composition, free amino acid profile and gene expression of transporters in finishing pigs. **British Journal of Nutrition**, v. 113, n. 5, 2015.

LUNNEY, J. K. Advances in swine biomedical model genomicsInternational **Journal of Biological Sciences**, 2007.

MALGWI, I. H. et al. Genes Related to Fat Metabolism in Pigs and Intramuscular Fat Content of Pork: A Focus on Nutrigenetics and Nutrigenomics. 2022

MARION-LETELLIER, R.; SAVOYE, G.; GHOSH, S. **Polyunsaturated fatty acids and inflammationIUBMB Life**, 2015. .

MARTINS, T. da S. et al. Fat Deposition, Fatty Acid Composition, and Its Relationship with Meat Quality and Human Health. In: **Meat Science and Nutrition**. [s.l: s.n.]

MOGHADASIAN, M. H.; SHAHIDI, F. Fatty Acids. **International Encyclopedia of Public Health**, p. 114–122, 1 jan. 2017. Disponível em: <https://www.sciencedirect.com/science/article/pii/B9780128036785001570?via%3Dihub>. Acesso em: 2 nov. 2021.

NONG, Q. et al. Low dietary N-6/N-3 Pufa ratio regulates meat quality, reduces triglyceride content, and improves fatty acid composition of meat in Heigai pigs. **Animals**, v. 10, n. 9, 2020.

OECD-FAO. OECD-FAO Agricultural Outlook 2021–2030. **OECD-FAO Agricultural Outlook 2021–2030**, p. 163–177, 2021.

PAN, Z. et al. Pig genome functional annotation enhances the biological interpretation of complex traits and human disease. **Nat Commun**, v. 12, 2021.

PARK, J. C. et al. Effects of dietary fat types on growth performance, pork quality, and gene expression in growing-finishing pigs. **Asian-Australasian Journal of Animal Sciences**, v. 25, n. 12, 2012.

PUIG-OLIVERAS, A. et al. Differences in muscle transcriptome among pigs phenotypically extreme for fatty acid composition. **PLoS ONE**, v. 9, n. 6, 2014.

REDDY, A. M. et al. Cloning, characterization and expression analysis of porcine microRNAs. **BMC Genomics**, v. 10, 2009.

SIMOPOULOS, A. P. The importance of the ratio of omega-6/omega-3 essential fatty acids. **Biomedicine & Pharmacotherapy**, v. 56, n. 8, p. 365–379, 1 out. 2002.

SIMOPOULOS, A. P. **The importance of the omega-6/omega-3 fatty acid ratio in cardiovascular disease and other chronic diseasesExperimental Biology and Medicine**, 2008. .

SUMMERS, K. M. et al. Functional Annotation of the Transcriptome of the Pig, *Sus scrofa*, Based Upon Network Analysis of an RNAseq Transcriptional Atlas. **Frontiers in Genetics**, v. 10, 2020.

SZOSTAK, A. et al. Effect of a diet enriched with omega-6 and omega-3 fatty acids on the pig liver transcriptome. **Genes and Nutrition**, v. 11, n. 1, p. 1–17, 2016.

WIĘCKOWSKA-GACEK, A. et al. Western Diet Induces Impairment of Liver-Brain Axis Accelerating Neuroinflammation and Amyloid Pathology in Alzheimer's Disease. **Frontiers in Aging Neuroscience**, v. 13, 2021.

CHAPTER 2: Differential gene expression associated with soybean oil level in the diet of pigs

Simara Larissa Fanalli[1], Bruna Pereira Martins da Silva[1], Julia Dezen Gomes[2], Vivian Vezzoni de Almeida[3], Felipe André Oliveira Freitas[2], Gabriel Costa Monteiro Moreira[4], Bárbara Silva-Vignato[2], Juliana Afonso[5], James Reecy[6], James Koltes[6], Dawn Koltes[6], Luciana Correa Almeida Regitano[5], Dorian Garrick[7], Júlio Cesar de Carvalho Baileiro[8], Ariana Nascimento Meira[2], Luciana Freitas[8], Luiz Lehmann Coutinho[2], Heidge Fukumasu[1]; Gerson Barreto Mourão[2], Severino Matias de Alencar[2], Albino Luchiari Filho[2], and Aline Silva Mello Cesar[1,2]*

[1] Faculty of Animal Science and Food Engineering, University of São Paulo, Pirassununga, São Paulo, Brazil.
[2] Luiz de Queiroz College of Agriculture, University of São Paulo, Piracicaba, São Paulo, Brazil.
[3] Federal University of Goiás, College of Veterinary Medicine and Animal Science, Goiânia, Goiás, Brazil.
[4] University of Liège, GIGA Medical Genomics, Unit of Animal Genomics, Liège,
[5] Embrapa Pecuária Sudeste, São Carlos, São Paulo, Brazil.
[6] Iowa State University, College of Agriculture and Life Sciences, Ames, Iowa, USA;
[7] AL Rae Centre for Genetics and Breeding, Massey University, Hamilton, New Zealand.
[8] College of Veterinary Medicine and Animal Science, University of São Paulo, Pirassununga, São Paulo, Brazil.
[8] DB Genética de Suínos, Patos de Minas, MG, Brazil.
*****_Correspondence: E-mail address_: alinecesar@usp.br (A.S.M. Cesar)

ABSTRACT

Fatty acids (FA) are involved in several essential roles in cell structure, from modulating functions to influencing metabolic processes. The aim of this study was to identify the differentially expressed genes (DEG) from the skeletal muscle and liver samples of pig model for metabolic diseases. To perform the study, we did a comparative analysis between the FA profile and RNA sequencing (RNA-Seq) data of 35 samples of liver tissue (SOY1.5, n=17 and SOY3.0, n=18) and 36 samples from skeletal muscle (SOY1.5, n=18 and SOY3.0, n=18) of *Large White* pigs were analyzed. The DESEq2 R package was used to perform the differential gene expression analysis, after quality control of the RNA-Seq data. The FA profile in the tissues was modified by the diet mainly related to MUFA and PUFA. The skeletal muscle transcriptome analysis revealed 45 DEG (FDR 10%), and the functional enrichment analysis identified network maps related to inflammation, immune process, and pathways associated with the oxidative stress in adipocyte syndrome in type 2 diabetes and metabolic dysfunction X. For the liver tissue, the transcriptome analysis revealed 281 DEG, which participate in network maps related to neurodegenerative diseases. With this nutrigenomics study, we verified that different levels of soybean oil in the swine diet, an animal model for metabolic diseases in humans, affected the transcriptome profile of skeletal muscle and liver tissue. These findings may help to better understand the biological mechanisms that can be modulated by the diet.

Keywords: fatty acid, RNAseq, transcriptome, immune response, Huntington's disease, metabolism, hepatic tissue, *Longissimus lomborum,* biomedical model.

1.INTRODUCTION

The World Health Organization, (2021) estimated that 41 million people died in 2018 due to chronic non-communicable diseases (NCDs) including cardiovascular diseases (CVDs), cancers, and metabolic diseases such as type 2 diabetes, obesity, and neurodegenerative diseases. These diseases have in common the influence of genetic factors, oxidative stress, and inflammation as result of sedentary lifestyle, diet, and consumption of drugs and alcohol. Pigs have been used as a biomedical model for diseases and in nutrigenetics and nutrigenomics (BROWN et al., 2010; HAO et al., 2021; PAN et al., 2021; MALGWI et al., 2022).

Metabolic diseases are any of the diseases or disorders that disrupt the normal process of converting food to energy into the cell, which involves the activity of thousands of enzymes. Among the metabolic processes that occurs into the cell are the process and transport of the proteins, carbohydrates, lipids, and their small organic molecules such as amino acids, sugars and starches, and fatty acids (FA), respectively (LI; TRUSH, 2016; LOBO et al., 2010).

The main efficient process that generates a lot of energy is the cellular respiration that uses organic molecules (sugar and lipids) and oxygen. Part of the oxygen used in this process is transformed into superoxide or reactive oxygen species (ROS) that can cause harm to cells, tissues and organ (LOBO et al., 2010). Free radical such as ROS is a highly toxic and reactive molecule capable to transform other molecules such as proteins, lipids, and nucleic acids (DNA and RNA). This transformation changes the chemical structure and biological function of these molecules, disrupting the normal cellular metabolic processes and, as a consequence, leads to an inflammatory state and a pro-inflammatory immune response (LI; TRUSH, 2016).

Meat has high nutritional importance and FA profile has impact on human health. Among its many benefits are its supply of unsaturated fatty acids, such as oleic acid (OA, C18:1 cis 9) and linoleic acid (AL, C18: 2 cis9, 12), which have positive effects on human health (LAAKSONEN et al., 2005). Pigs have been increasingly used to nutrigenomics research and for investigation of metabolic diseases in humans due to role as a biomedical model for humans (LUNNEY, 2007; BROWN et al., 2010; MALGWI et al., 2022). Pigs are similarities in terms of anatomy, biochemistry, pathology, pharmacology and physiology with humans what makes them to be used as a biomedical model (LUNNEY, 2007; KRAGH et al., 2009; REDDY et al., 2009; PAN et al., 2021).

In pigs, the liver is the main site for the de novo synthesis of oxidation of FA and cholesterol. It is a highly specialized organ, related to the regulation of several metabolic processes, along with the skeletal muscle, is essential for the regulation of lipid metabolism in mammals (RAMAYO-CALDAS et al., 2012). Muscle tissue metabolism can be regulated by several molecules, some of which are contained in adipose tissue, which can be considered an endocrine organ and is responsible for maintaining organism homeostasis (SON; PATON, 2020). Free fatty acids are released from adipose tissue and enter skeletal muscle via intermembrane proteins. In addition, free fatty acids can regulate several genes and skeletal muscle lipogenesis, including Sterol regulatory-element binding proteins (SREPBs), Nuclear factor kappa B (NFkB), liver X receptors, retinoid X receptors, receptors activated by peroxisome proliferators (PPARs) (SON; PATON, 2020).

The characterization of gene networks involved in immune cell function and metabolic in health and disease is important to understand immunodeficiency or

autoimmunity disorders caused by an unbalanced immune response (DI CARA et al., 2019). Dysfunctional peroxisomes result in overall lipid alterations, such as accumulation of very long-chain fatty acids (VLCFA) and VLCFA-cholesteryl esters (DI CARA et al., 2019). Lipid metabolic dysregulation can cause inflammation, participating in the modulation of the immune system responses (BERNARDI et al., 2018; DI CARA et al., 2019; HOTAMISLIGIL, 2017). Furthermore, among the proteins that drive inflammation are cytokines that are previously secreted by immune cells and vascular endothelial cells (BERNARDI et al., 2018; DI CARA et al., 2019).

Lipids are a major class of biological molecules, ubiquitously distributed in all types of cells. They regulate transcription, store energy, and contribute to many biological processes, such as cellular structure and energy storage (NAKAMURA and NARA, 2003). Consumption of FA has been linked to metabolic effects, including altered blood parameters; such as lipid and lipoprotein composition (WOOD et al., 2008). Nevertheless, past studies and meta-analyses have noted contrasting opinions regarding the role of FA in animal and human health (SCHWINGSHACKL and HOFFMANN, 2014).

The FA are among the most important dietary components found in meat, which is rich in polyunsaturated (PUFA), saturated (SFA), and monounsaturated (MUFA) fatty acids (WOOD et al., 2008). Since consumers are more concerned about food safety and the quality of the food they consume, the production of meat with has abundant nutritional value has grown significantly (MOREL et al., 2013; DOKMANOVIC et al., 2015).

Our previous studies in different species revealed a significant number of genes differentially expressed between animals with divergent values of FA content in skeletal muscle, associated with biological processes such as insulin receptor signaling, activated T cell nuclear factors (NFAT) in cardiac hypertrophy, mitochondrial disorder, and neurodegenerative disorders such as Huntington's and Alzheimer's disease. The study shows that fatty acids have a significant impact on gene expression associated with important biological processes, such as oxidative phosphorylation, cell growth, survival, and migration (CESAR et al., 2016).

Human consumption of MUFA and PUFA has been related with low levels of low-density lipoprotein (LDL) and with potentially increased levels of high-density lipoprotein (HDL) in the blood. Pig meat has a high unsaturation fatty acid profile, mainly due to oleic acid (OA), and plays a significant role in human nutrition and health

(SCHMID, 2011; KRITCHEVSKY, 2000; TERES et al., 2008; PAUWELS, 2008; PAUWELS, 2011). Another important aspect of unsaturated FA content is the relationship with meat quality characteristics, such as juiciness, flavor, and shelf life (TSIMIKAS AND REAVEN, 1998). In the context of improving our knowledge about the biological processes associated with FA content in different tissues, scientific studies of this kind are extremely important. This knowledge can be applied both in animal production (genetic improvement, nutrition, and environment) as in animal and human health.

Pig diets added with vegetable oils rich in unsaturated fatty acids can be a source of healthier products for consumers (PARK et al., 2012). Thus, vegetable oils such as canola, sunflower and soybean oil are interesting options due to the amount of PUFA (ALENCAR et al., 2021). On the other hand, there is a need to fill in the knowledge gaps regarding the impact of the amount of soybean oil added on gene expression and the functional and nutritional knowledge of lipids. Thus, our hypothesis is that different levels of soybean oil (1.5%*vs*3%) added in the diet of *Large White* pigs can affect the variation in the fatty acid profile deposition could be associated with gene expression profile of the skeletal muscle and liver tissue of these animals, modulating biological processes involved with lipid metabolism and metabolic diseases.

The present study aimed to (1) evaluate changes in fatty acid profile and gene expression of the skeletal muscle and liver tissue of pigs fed a diet with different levels of soybean oil; (2) identify metabolic pathways and gene networks impacted by the dietary fatty acid composition of the pigs' tissues that were fed with different proportions of degummed soybean oil.

2.METHODS

2.1 Ethics statement

All animal procedures were approved by the Animal Care and Use Committee of Luiz de Queiroz College of Agriculture (University of São Paulo, Piracicaba, Brazil, protocol: 2018.5.1787.11.6 and number CEUA 2018-28) and followed ethical principles in animal research, according to the Guide for the Care and Use of Agricultural Animals in Agricultural Research and Teaching (FASS, 2010).

2.2 Animals

In our 98-day feeding study, thirty-six genetically lean immunocastrated male pigs (offspring of *Large White* sires x *Large White* dams) with an average initial body weight (BW) of 28.44 ± 2.95 kg and an average age of 71 ± 1.8 days were used. All the animals were genotyped for the halothane mutation (RYR1 gene) according to Fujii et al. (1991); thus, pigs selected for this trial were all halothane homozygous-negative (NN). The animals were randomly allotted to one of two dietary treatments with six replicate pens per treatment and three pigs per pen, which were housed in an all-in/all-out double-curtain-sided building. Each pen was equipped with a three-hole dry self-feeder and a nipple drinker, allowing pigs ad libitum access to feed and water throughout the experimental period. Immunocastration of the intact males was performed by the administration of two 2-mL dose of Vivax® (Pfizer Animal Health, Parkville, Australia) on day 56 (127 days of age) and day 70 (141 days of age) (ALMEIDA et al., 2021), in accordance with the manufacturer's recommendations.

As discussed in our previous works, the experimental diet consisted in a six-phase diet that was as follows: two in the grower and four for finisher. Dietary treatments consisted of corn-soybean meal growing-finishing diets supplemented with 1.5% soybean oil (SOY1.5, common level used in commercial pig production) or 3% soybean oil (SOY3.0). The diets were formulated to reach or exceed Rostagno et al. (2011) recommendations for growing-finishing pigs. No antibiotic growth promoters were used, and all diets were provided in a mash meal form (ALMEIDA et al., 2021; FANALLI et al., 2022, in review).

2.3 Fatty acid profile of samples

Sample collection and fatty acid profile

Sample collection, fatty acid profile was previously described in Almeida et al., (2021), and Fanalli et al., (2022, in review). In summary, liver and skeletal muscle (*Longissimus lumborum)* samples were collected, and then stored at -80 °C until fatty acid profile and RNA sequencing analyses. The FA profile was performed by Bligh and Dyer (1959) and methylated according to the procedure outlined by AOCS (2004; Method AM 5-04).

Statistical analyzes to verify differences in the FA profile of skeletal muscle and liver tissue between the diets were performed using the "proc mixed" procedure of the

SAS statistical software (v. 9.4), where the mixed model was adopted using the restricted maximum likelihood (REML) methodology. In the model, the block effects were declared as a random effect and the treatments as a fixed effect. A normal distribution of the data was assumed and exploratory analyzes were performed previously to verify the consistency of the data. The SAS “proc univariate” procedure (v. 9.4) was used to verify the fit of the normal distribution and homogeneity of residuals for each of the variables. Diagnostics of the density distribution of the Studentized Residual of the model were made with the Shapiro-Wilk test and also, graphs were plotted as a histogram with normal density, Scatterplot and "QQ plot" for visual analysis of the dispersion of residues with the option "residual” of the “mixed proc” (SAS v.9.4).

2.4 Tissue RNA extraction and RNA-sequencing

Total RNA was extracted from skeletal muscle and liver tissue samples using commercial RNA extraction kits (RNeasy® Mini Kit, Qiagen), according to the manufacturer instructions. With the spectrophotometer Nanodrop 1000 and Bioanalyzer, RNA quantification, purity and integrity were evaluated, respectively. All samples presented an RNA Integrity Number (RIN) higher or equal to seven. From the total RNA from each sample, 2µg were used for library preparation according to the protocol described in the TruSeq RNA Sample Preparation kit v2 guide (Illumina, San Diego, CA). The estimation of libraries average size was made with the Agilent Bioanalyzer 2100 (Agilent, Santa Clara, CA, USA) and the libraries were quantified using quantitative PCR with the KAPA Library Quantification kit (KAPA Biosystems, Foster City, CA, USA). Quantified samples were diluted and pooled (five pools of all 36 samples each), using TruSeq DNA CD Index Plate (96 indexes, 96 samples, Illumina, San Diego, CA, USA). All samples are pooled and sequenced in five lanes of a sequencing flowcell, using the TruSeq PE Cluster kit v4-cBot-HS kit (Illumina, San Diego, CA, USA), were clustered and sequenced using HiSeq2500 equipment (Illumina, San Diego, CA, USA) with a TruSeq SBS Kit v4-HS (200 cycles), according to manufacturer instructions. All the sequencing analyses were per-formed at the Genomics Centre at ESALQ, localized in the Animal Biotechnology Laboratory at ESALQ – USP, Piracicaba, São Paulo, Brazil.

Sequencing adaptors and low complexity reads were removed in an initial data filtering step by Trim Galore 0.6.5 software. Phred score lower than 33; only the reads

with a length higher than 70 nucleotides were kept after trimming. Quality control and reads statistics were estimated with FASTQC version 0.11.8 software [http://www.bioinformatics.bbsrc.ac.uk/projects/fastqc/]. Sus Scrofa 11.1 reference assembly available at Ensembl [http://www.ensembl.org/Sus_scrofa/Info/Index]. The abundance (read counts) of mRNAs for all annotated genes was calculated using STAR-2.7.6a [http://bioinformatics.oxfordjournals.org/content/29/1/15].

2.5 Data analysis, differentially expressed genes, and functional enrichment analysis

Differentially expressed genes (DEG) between the two diets (SOY1.5vsSOY3.0) from skeletal muscle and liver tissue were identified using the DESeq2 available at Bioconductor open-source software for bioinformatics, using a multi-factor design (LOVE; HUBER; ANDERS, 2014) statistical package in R. Prior to statistical anal-ysis the read count data was filtered as follows: i) genes with zero counts for all samples, that is, unexpressed genes, ii) genes with less than one read per sample on average were removed (very lowly expressed); iii) genes that were not present in at least 50% of the samples were removed (rarely expressed). Sire was fit as factor in the multi-factor model. The cut-off approach performed to identify the DEG was control the false discovery rate (FDR) at 10% (CESAR et al., 2016), by using the Benjamini- Hochberg (1995) methodology.

For skeletal muscle between SOY1.5*vs*SOY3.0 the functional enrichment analysis by MetaCore was applied to identify the pathway maps from 45 DEG, and in the liver 281 DEG using. The functional enrichment analysis of DEG (FDR <0.10) was performed to obtain comparative networks by ‘analyze single experiment’ using a standard parameter of MetaCore software v.21.4 build 70700 using *Homo sapiens* genome annotation as background reference and a default parameter. The filters used were metabolic maps: energy metabolism, lipid metabolism, steroid metabolism; cardiovascular diseases: atherosclerosis; regulation of metabolism; nutritional and metabolic diseases, and nervous system diseases. To understand the behavior of genes and their interactions, gene net-works were created using the Process Networks tool in MetaCore.

3.RESULTS AND DISCUSSION

3.1 Fatty acid profile for skeletal muscle and liver tissue

To analyze the changes in FA profiles, we identified the FA composition in the tissues, resulting in lipidic profile changes in skeletal muscle and liver of growing and finishing pigs receiving a diet enriched with different proportions of soybean oil (SOY1.5*vs*SOY3.0).

The *Longissimus lumborum* intramuscular fat composition (Table 1) was not modified with the increase in the proportion of oil to saturated fat acids: C14:0 (P =0.20); C16:0 (P =0.21) and C18:0 (P =0.42), to the MUFA C20:1 n-9 (P =0.11), C20:5 n-3, EPA (P =0.12), and Atherogenic index (P =0.43). In other hand, C18:1 n-9) (P <0.01) presented the biggest percentage in the diet enriched with 3% of soy oil (SOY3.0). In addition, in our results SFA not presented changes with the modification between oil proportions (P =0.26), like the MUFA C20:1.

Table 1: Effects of dietary treatments on fatty acid profile of *Longissimus lumborum* intramuscular fat of immunocastrated male pigs

	Dietary treatment			
Fatty Acid (%)	**SOY1.5**	**SOY3.0**	**Pooled SEM[2]**	***P*-value**
Saturated fatty acid (SFA)				
Myristic acid (C14:0)	1.14	1.19	0.04	0.20
Palmitic acid (C16:0)	25.50	25.01	0.21	0.21
Stearic acid (C18:0)	12.18	11.89	0.15	0.42
Monounsaturated fatty acid (MUFA)				
Palmitoleic acid (C16:1)	2.86 [a]	3.17 [b]	0.13	0.02
Eicosenoic acid (C20:1)	0.51	0.55	0.03	0.11
Oleic acid (C18:1 n-9)	38.93 [a]	44.15 [b]	1.40	<0.01
Polyunsaturated fatty acid (PUFA)				
Linoleic acid (C18:2 n-6)	17.90[a]	13.28[b]	1.12	<0.01
Alpha-linolenic acid (C18:3 n-3)	0.77[a]	0.56[b]	0.06	<0.01
Eicosapentaenoic acid (C20:5 n-3)	0.30	0.15	0.09	0.12
Docosahexaenoic acid (C22:6 n-3)	0.36 [a]	0.16 [b]	0.08	0.03
Total SFA	38.83	38.09	0.65	0.26
Total MUFA	42.29 [a]	47.70 [b]	1.48	<0.01
Total PUFA	19.28[a]	14.80[b]	1.72	<0.05
Total n-3 PUFA[3]	1.35[a]	0.87[b]	0.15	<0.01
Total n-6 PUFA[4]	17.90[a]	13.28[b]	1.12	<0.01
PUFA:SFA ratio[5]	0.50[a]	0.39[b]	0.05	0.03
n-6:n-3 PUFA ratio[6]	14.20	17.29	1.70	0.10
Atherogenic index	0.49	0.48	0.09	0.43

[1]Pigs (*n* = 36) were fed either a corn-soybean meal diet containing 1.5% soybean oil (SOY1.5) or diet containing with 3% soybean oil (SOY3.0). Values represent the least square means from a subset of pigs (*n*= 36; 18 pigs/treatment).
[2]SEM = standard error of the least square means.
[3]Total n-3 PUFA = {[C18:3 n-3] + [C20:5 n-3] + [C22:6 n-3]}.
[4]Total n-6 PUFA = C18:2 n-6.

[5]PUFA:SFA ratio = total PUFA/total SFA.
[6]Σ n-6/Σ n-3 PUFA ratio.
[a–b]Within a row, values without a common superscript differ ($P \leq 0.05$) or tended to differ ($0.05 < P \leq 0.10$) using Student's t test. (Adapted from ALMEIDA et al., 2021).

In addition, the composition of the FA profile was also performed in the liver. The FA profile in the liver (Table 2) presented a different pattern as of the observed in the skeletal muscle in relation to the SFA as the C14:0 and C16:0 that presented differences (P <0.01) with high percentage in the samples from animals that received a diet enriched with 3% of oil, what can be due to the increase in Palmitic and Myristic acid. The C18:0 (P <0.01) presented a higher contented in samples from animals with the diet enriched in SOY1.5 (P <0.01). As it occurred in muscle, high values of OA were identified in liver, C18:2 n-6 (P <0.01) was higher in SOY1, and C18:3 n-3 do not presented difference between diets (P =0.07). The C22:6 n-3 presented difference in intramuscular fat (P =0.03) and not in liver (P =0.11). The Atherogenic index was lower in SOY1.5 compared to SOY3.0 (P<0.01).

Table 2: Effects of dietary treatments on fatty acid profile of liver tissue of immunocastrated male pigs

Fatty acid (%)	Dietary treatment		Pooled SEM[2]	*P*-value
	SOY1.5	SOY3.0		
Saturated fatty acid (SFA)				
Myristic acid (C14:0)	0.73[a]	0.98[b]	0.05	<0.01
Palmitic acid (C16:0)	20.92[a]	22.98[b]	0.40	<0.01
Stearic acid (C18:0)	25.48[a]	21.28[b]	1.06	<0.01
Monounsaturated fatty acid (MUFA)				
Palmitoleic acid (C16:1)	0.66[a]	0.93[b]	0.05	<0.01
Oleic acid (C18:1 n-9)	21.36[a]	27.84[b]	1.06	<0.01
Polyunsaturated fatty acid (PUFA)				
Linoleic acid (C18:2 n-6)	27.02[a]	23.64[b]	0.67	<0.01
Alpha-linolenic acid (C18:3 n-3)	1.42	1.17	0.10	0.07
Eicosapentaenoic acid (C20:5 n-3, EPA)	0.58[a]	0.27[b]	0.11	0.04
Docosahexaenoic acid (C22:6 n-3, DHA)	1.18	0.99	0.11	0.17
Total SFA	46.69	45.24	1.03	0.31
Total MUFA	22.01[a]	28.78[b]	1.04	<0.01
Total PUFA	30.79[a]	26.06[b]	0.55	<0.01
Total n-3 PUFA[3]	3.75[a]	2.42[b]	0.37	<0.01
Total n-6 PUFA[4]	27.02[a]	23.64[b]	0.67	<0.01
PUFA:SFA ratio[5]	0.67[a]	0.58[b]	0.02	<0.01
n-6:n-3 PUFA ratio[6]	8.51[a]	9.90[b]	0.50	0.05
Atherogenic index	0.42[a]	0.51[b]	0.01	<0.01

[1]Pigs (*n* = 35) were fed either a corn-soybean meal diet containing 1.5% soybean oil (SOY1.5) or diet containing with 3% soybean oil (SOY3.0). Values represent the least square means from a subset of pigs (*n*= 35; 17pigs/SOY1.5; 18 pigs/SOY3.0).
[2]SEM = standard error of the least square means.
[3]Total n-3 PUFA = {[C18:3 n-3] + [C20:5 n-3] + [C22:6 n-3]}.
[4]Total n-6 PUFA = C18:2 n-6.
[5]PUFA:SFA ratio = total PUFA/total SFA.
[6]Σ n-6/Σ n-3 PUFA ratio.
[a–b]Within a row, values without a common superscript differ ($P \leq 0.05$) or tended to differ ($0.05 < P \leq 0.10$) using Student's t test.

3.2 Sequencing data and differential expression analysis

Thus, 36 samples (SOY1.5*vs*SOY3.0) of skeletal muscle and 35 samples (17 of SOY1.5 and 18 of SOY3.0) of liver tissue were used in subsequent RNA sequencing (RNA-Seq) data analysis. The total average number of sequenced reads before and after filtering for samples from the skeletal muscle of SOY1.5 group was 33,459,142 and 32,965,842, and of SOY3.0 group were 31,955,613 e 31,491,236. The total average number of reads before and after filtering for samples from liver tissue of the SOY1.5 group was 33,561,721 and 33,072,908, and of the SOY3.0 group were 34,078,903 e 33,610,858. On average, 78.59% of the total read pairs were mapped against the *Sscrofa11.1* reference genome assembly (APPENDIX A - Table S1) for both tissues and for each treatment.

Differential gene expression analysis was performed for each tissue by comparing gene expression levels between the two groups of animals that were fed with diets enriched with different levels of soybean oil (SOY1.5*vs*SOY3.0) (APPENDIX A - Table S2a). A total of 45 DEG (log2fold-change ≥1 or ≤−1; FDR-corrected p-value< 0.1) were identified in the skeletal muscle between the two groups, where 35 were down-regulated (log2FC ranging from -5.8 to -0.41) and 10 up-regulated (log2FC ranging from 2.3 to 0.53) in the SOY1.5 group compared with the SOY3.0 (APPENDIX A - Table S2b). For liver tissue, a total of 281 DEG (log2fold-change ≥1 or ≤−1; FDR-corrected p-value < 0.1) were identified, where 129 were down-regulated (log2FC ranging from -3.0 to -0.20) and 152 up-regulated (log2FC ranging from 4.8 to 0.24) in the SOY1.5 group (Table S3b). The Figure 1 shows the Volcano plot of log2 fold change (x-axis) *vs* -log10FDR-corrected p-value (y-axis) for skeletal muscle and liver tissue from the differential gene expression analysis between SOY1.5*vs*SOY3.0 groups comparison.

(A)

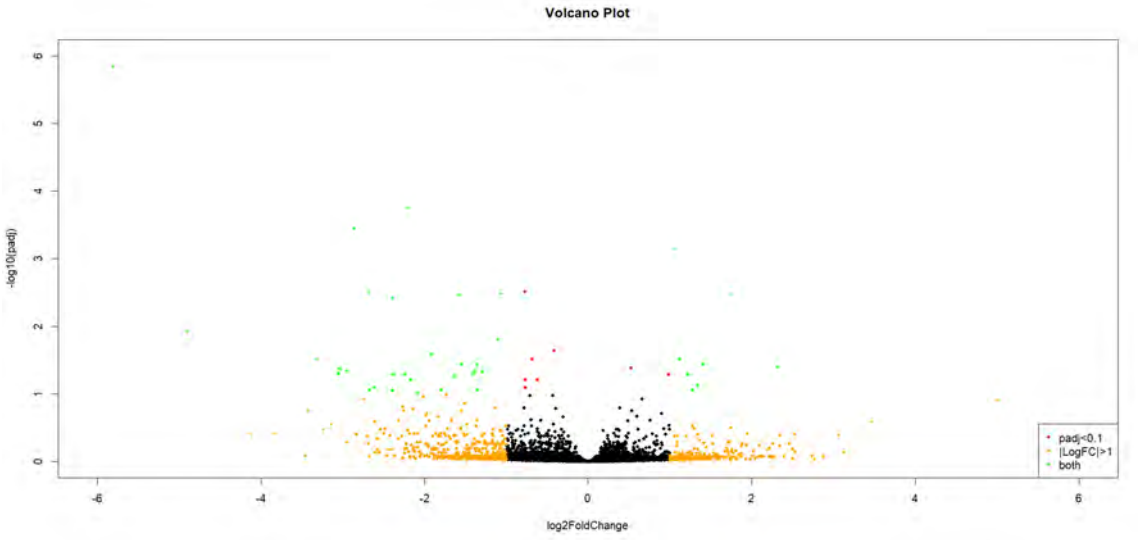

(B)

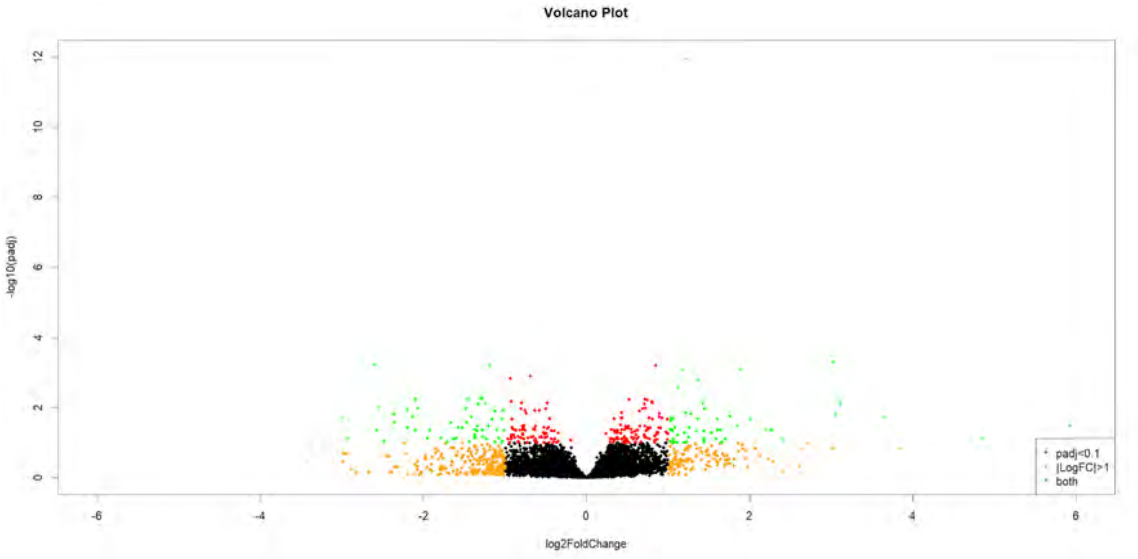

Figure 1. Volcano plot of log2 fold change (x-axis) versus -log10FDR-corrected p-value in RNA-Seq data from (A) skeletal muscle and (B) liver tissue of immunocastrated male pigs fed with two level of soybean oil in the diet (1.5 % and 3.0 % of soybean oil).

3.3 Common differentially expressed genes between skeletal muscle and liver tissue

From the total of DEG, six genes were common between the two comparisons, in the skeletal muscle and liver tissue (Table 3). The *CDK20* gene, identified as DEG both in the skeletal muscle and liver of pigs fed with different levels of soybean oil, showed a higher expression in the SOY1.5 group for both tissues (log2 fold change +1.04 in the skeletal muscle, and log2 fold change +0.98 in the liver). In the same way,

the *CCDC90B* was less expressed in the SOY1.5 group for both tissues (log2 fold change -0.41, skeletal muscle, and log2 fold change -0.45, liver). The ENSSSCG00000022842 or *LOC100525692* also was less expressed in the SOY1.5 group in both skeletal muscle (log2 fold change -1.8) and liver (log2 fold change -2.1), and the same occurred for *ALG6* (log2 fold change -0.68, skeletal muscle, and log2 fold change -0.74, liver). Finally, the ENSSSCG00000051557 showed higher expression in the SOY1.5 group for both the skeletal muscle (log2 fold change +1.28) and liver (log2 fold change +1.36).

Table 3. Common differentially expressed genes between the two tissues comparisons, in the skeletal muscle and liver tissue of immunocastrated male pigs fed two levels of soybean oil in the diet (1.5 % and 3.0 % of soybean oil).

Gene common	**Description**	**Reference**
ENSSSCG00000009578 Cyclin dependent kinase 20 (*CDK20)*	Cell cycle related kinase. Its expression is related to the activation of β-catenin-TCF signaling and cell cycle progression. Can activate cyclin-dependent kinase 2 which is related to cell growth.	MALUMBRES, (2014) STELZER, G. *et al*, (2016)
ENSSSCG00000014903 Coiled-coil domain containing 90B *(CCDC90B)*	Paralog of the MCUR1 gene (Mitochondrial Calcium Uniporter Regulator 1) which is related to the Ca, cAMP and lipid signaling pathways.	STELZER, G. *et al*, 2016
ENSSSCG00000022842 LOC100525692	Protein encoding gene.	STELZER, G. *et al*, 2016
ENSSSCG00000022842 Alpha-1,3-Glucosyltransferase *(ALG6)*	Related to N-Linked Glycosylation.	STELZER, G. *et al*, 2016
ENSSSCG00000017914 Glycolipid Transfer Protein Domain-Containing Protein 2 *GLTPD2*	Participates in the transfer of glycolipids.	STELZER, G. *et al*, 2016
ENSSSCG00000051557	-	-

3.4 Functional enrichment analysis for skeletal muscle differential expression

Seven different pathway maps were detected (p-value <0.1), which are linked to the Fatty Aldehyde Dehydrogenase or Aldehyde Dehydrogenase Family 3 Member A2 *(AL3A2)*, Alpha-2-Glycoprotein 1, Zinc-Binding *(AZGP1)*, and T-Cell Surface Glycoprotein *(CD4)* genes (Table 4).

Table 4. Pathway maps by MetaCore software (p-value <0.1) from the list of differentially expressed genes (FDR 10%) in the skeletal muscle of immunocastrated male pigs fed with two different levels of soybean oil in the diet

Pathway maps	p-value	DEG[1]
Fatty Acid Omega Oxidation	3,33E-02	*AL3A2*
Leukotriene 4 biosynthesis and metabolism	4,42E-02	*AL3A2*
TNF-alpha, IL-1 beta induces dyslipidemia and inflammation in obesity and type 2 diabetes in adipocytes	4,64E-02	*AZGP1*
Breakdown of CD4+ T cell peripheral tolerance in type 1 diabetes mellitus	5,39E-02	*CD4*
Triacylglycerol metabolism p.1	6,56E-02	*AL3A2*
Oxidative stress in adipocyte dysfunction in type 2 diabetes and metabolic syndrome X	6,99E-02	*AL3A2*
Peroxisomal branched chain fatty acid oxidation	9,08E-02	*AL3A2*

[1]Differentially Expressed Genes

The DEG *AL3A2* was present in five (Figure 2, 3, 4, 5 and 6) of the seven pathway maps identified, which encodes the AL3A2 enzyme In this study the *AL3A2* was identified as a DEG in skeletal muscle of pigs that was fed with different levels of soybean oil (1.5 % *vs* 3%), which was less expressed in SOY1.5 group (log2 fold change -0.77).

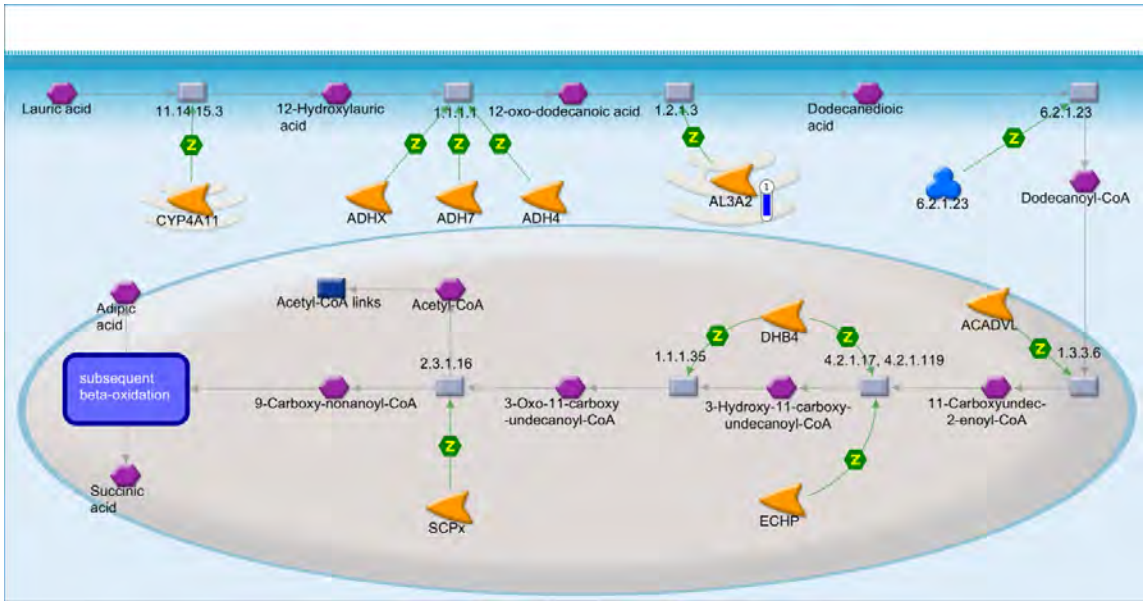

Figure 2. Fatty Acid Omega Oxidation pathway map created by using MetaCore software (p-value <0.10) and the list of differentially expressed genes (FDR 10%) in the skeletal muscle of immunocastrated male pigs fed with two different levels of soybean oil in the diet (1.5 % and 3.0 % of soybean oil). The blue thermometer indicates that the DEG is down-regulated (log2 fold change -0.77) in the diet with 1.5 % of soybean oil (SOY1.5). Green arrows indicate positive interaction and gray arrows indicates unspecified interaction. For a detailed definition, see https://portal.genego.com/legends/MetaCoreQuickReferenceGuide.pdf.

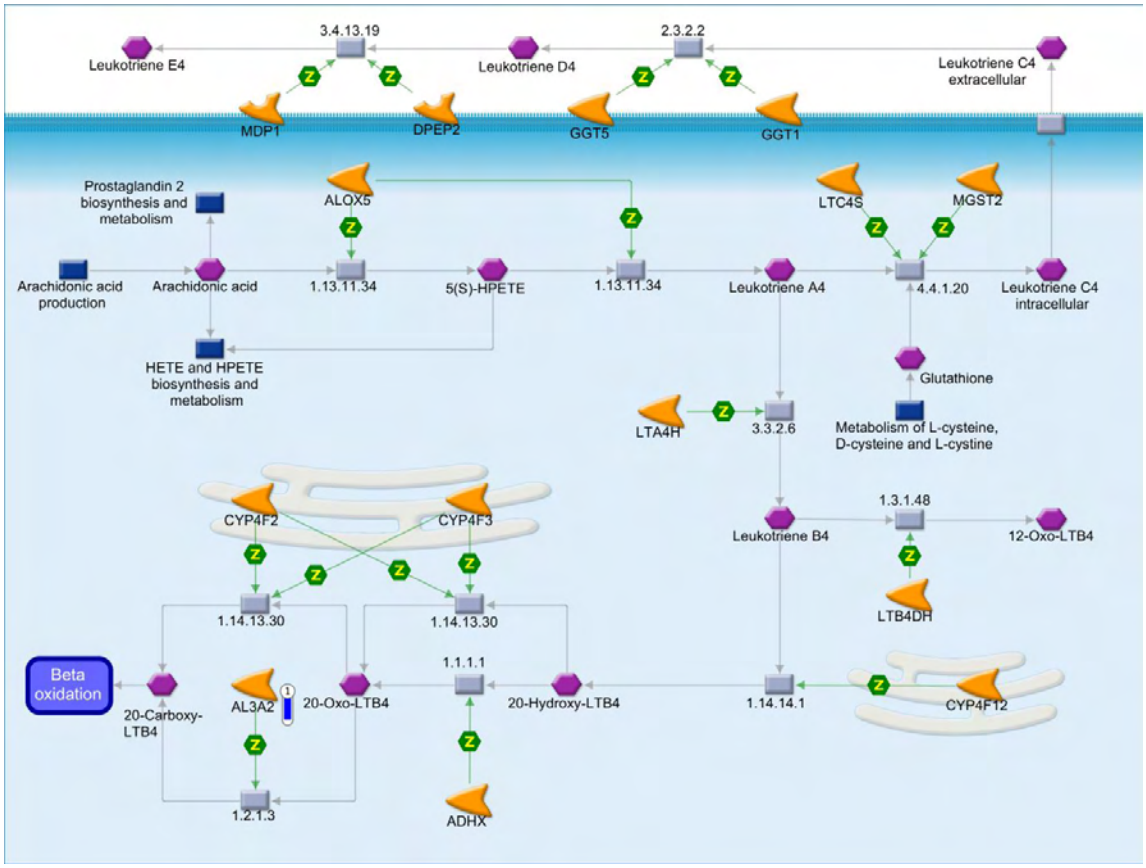

Figure 3. Leukotriene 4 biosynthesis and metabolism pathway map created by using MetaCore software (p-value <0.10) and the list of differentially expressed genes (FDR 10%) in the skeletal muscle of immunocastrated male pigs fed with two different levels of soybean oil in the diet (1.5 % and 3.0 % of soybean oil). The blue thermometer indicates that the DEG is downregulated (log2 fold change -0.77) in

the diet with 1.5 % of soybean oil (SOY1.5). Green arrows indicate positive interaction and gray arrows indicate unspecified interaction. For a detailed definition, see https://portal.genego.com/legends/MetaCoreQuickReferenceGuide.pdf.

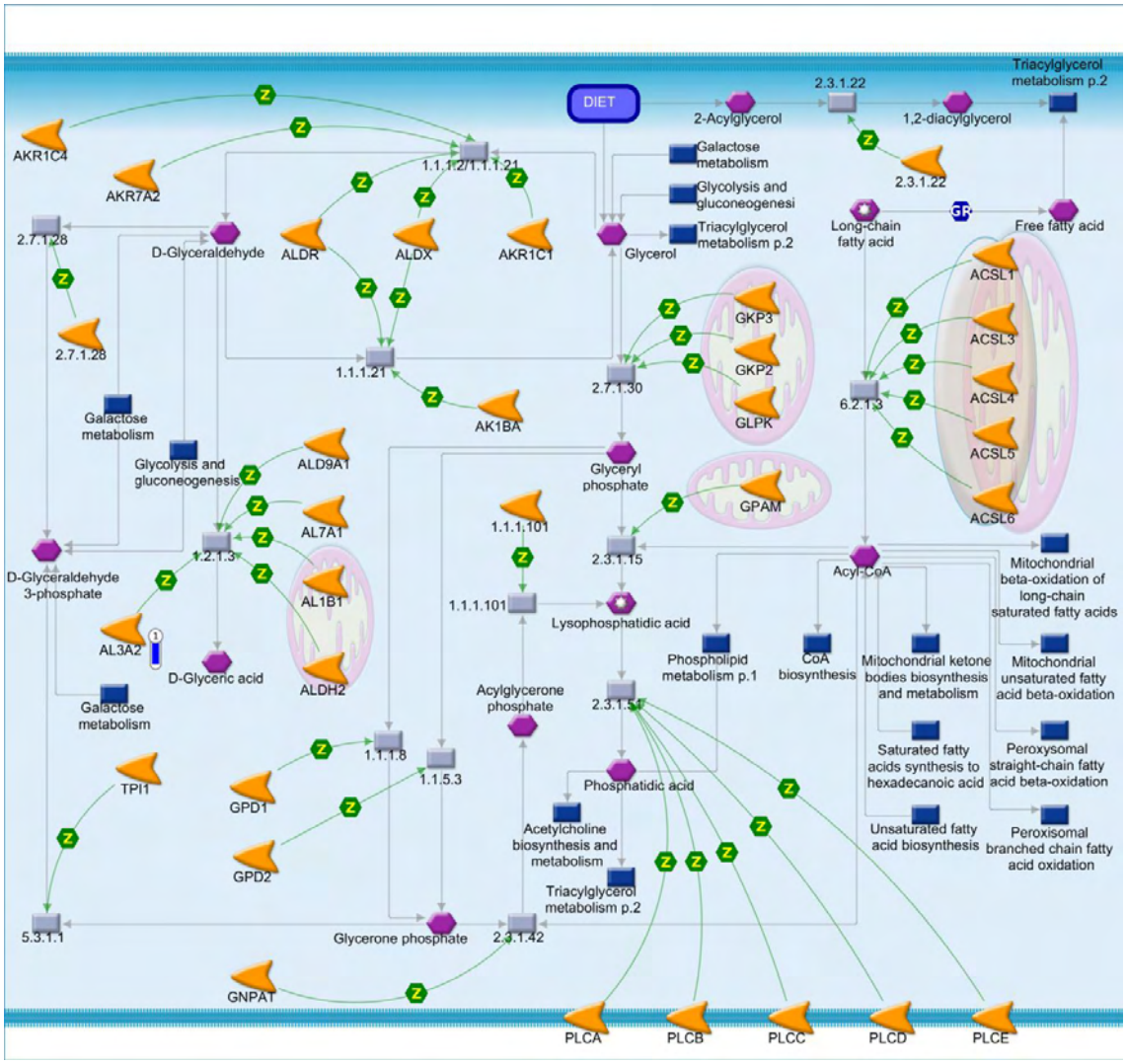

Figure 4. Triacylglycerol metabolism p.1 pathway map created by using MetaCore software (p-value <0.10) and the list of differentially expressed genes (FDR 10%) in the skeletal muscle of immunocastrated male pigs fed with two different levels of soybean oil in the diet (1.5 % and 3.0 % of soybean oil). The blue thermometer indicates that the DEG is downregulated (log2 fold change -0.77) in the diet with 1.5 % of soybean oil (SOY1.5). Green arrows indicate positive interaction and gray arrows indicate unspecified interaction. For a detailed definition, see https://portal.genego.com/legends/MetaCoreQuickReferenceGuide.pdf.

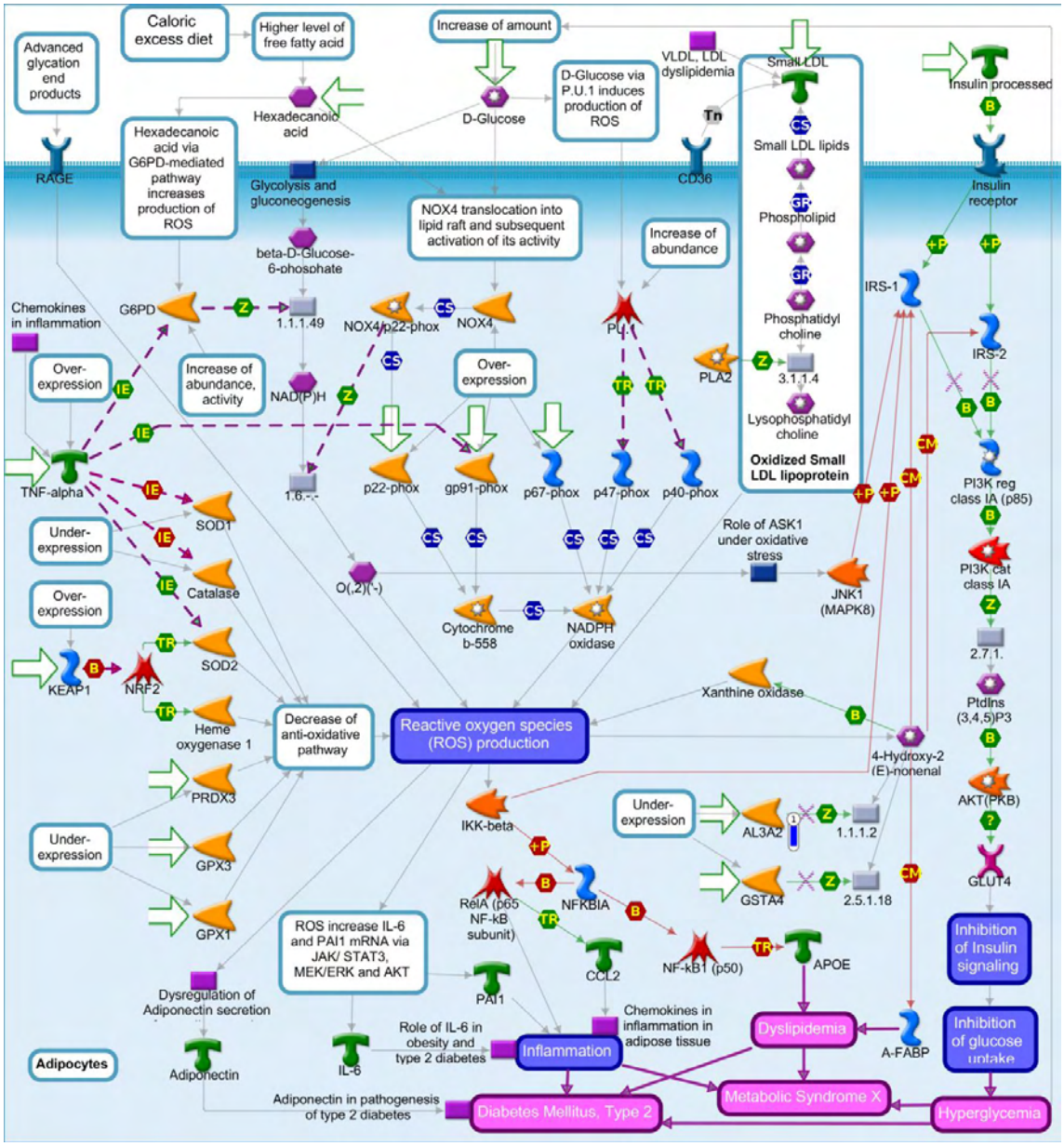

Figure 5. Oxidative stress in adipocyte dysfunction in type 2 diabetes and metabolic syndrome X pathway map created by using MetaCore software (p-value <0.10) and the list of differentially expressed genes (FDR 10%) in the skeletal muscle of immunocastrated male pigs fed with two different levels of soybean oil in the diet (1.5 % and 3.0 % of soybean oil). The blue thermometer indicates that the DEG is downregulated (log2 fold change -0.77) in the diet with 1.5 % of soybean oil (SOY1.5). Green arrows indicate positive interactions, red arrows indicate negative interaction and gray arrows indicate unspecified interaction. For a detailed definition, see https://portal.genego.com/legends/MetaCoreQuickReferenceGuide.pdf.

.

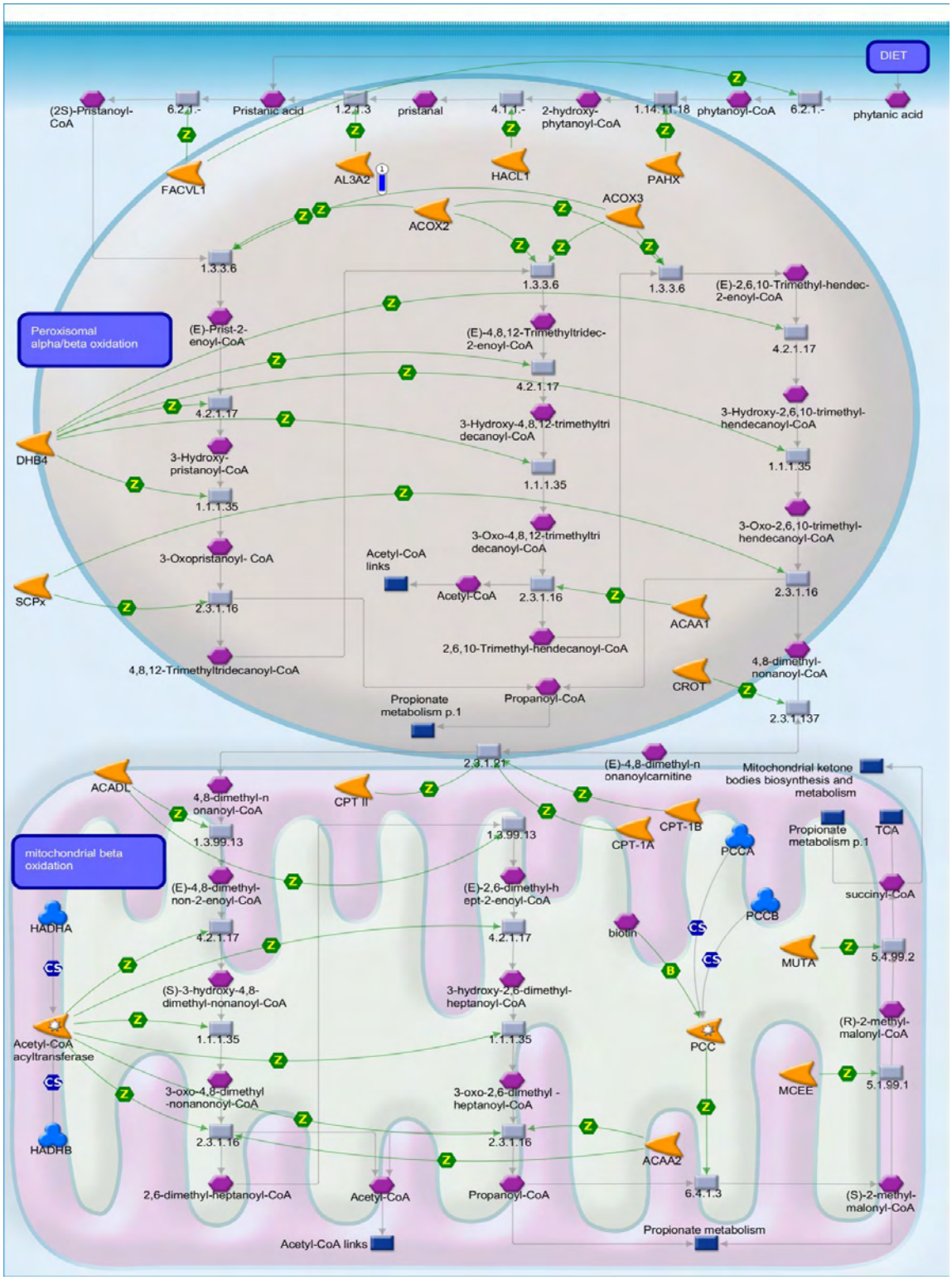

Figure 6. Peroxisomal branched chain fatty acid oxidation pathway map created by using MetaCore software (p-value <0.10) and the list of differentially expressed genes (FDR 10%) in the skeletal muscle of immunocastrated male pigs fed with two different levels of soybean oil in the diet (1.5 % and 3.0 % of soybean oil). The blue thermometer indicates that the DEG is downregulated (log2 fold change -0.77) in the diet with 1.5 % of soybean oil (SOY1.5). Green arrows indicate positive interaction and gray arrows indicate unspecified interaction. For a detailed definition, see https://portal.genego.com/legends/MetaCoreQuickReferenceGuide.pdf.

The *AZGP1* gene is involved in the *TNF-alpha* and *IL-1 beta (IL-1b)* pathways, which are involved with the occurrence of dyslipidemia and inflammation in adipocytes, leading to development of obesity and type 2 diabetes diseases (Figure 7). Herein, we identified the *AZGP1* gene as a DEG in skeletal muscle of pigs that was fed with different levels of soybean oil (1.5% *vs* 3%), which was less expressed in the SOY1.5 group (log2 fold change -2.67). Another DEG identified in this study was *CD4* enriched in the "Breakdown of CD4+ T cell peripheral tolerance in type 1 diabetes mellitus" pathway in muscle (Figure 8), which was less expressed in SOY1.5 group (log2 fold change -1.57).

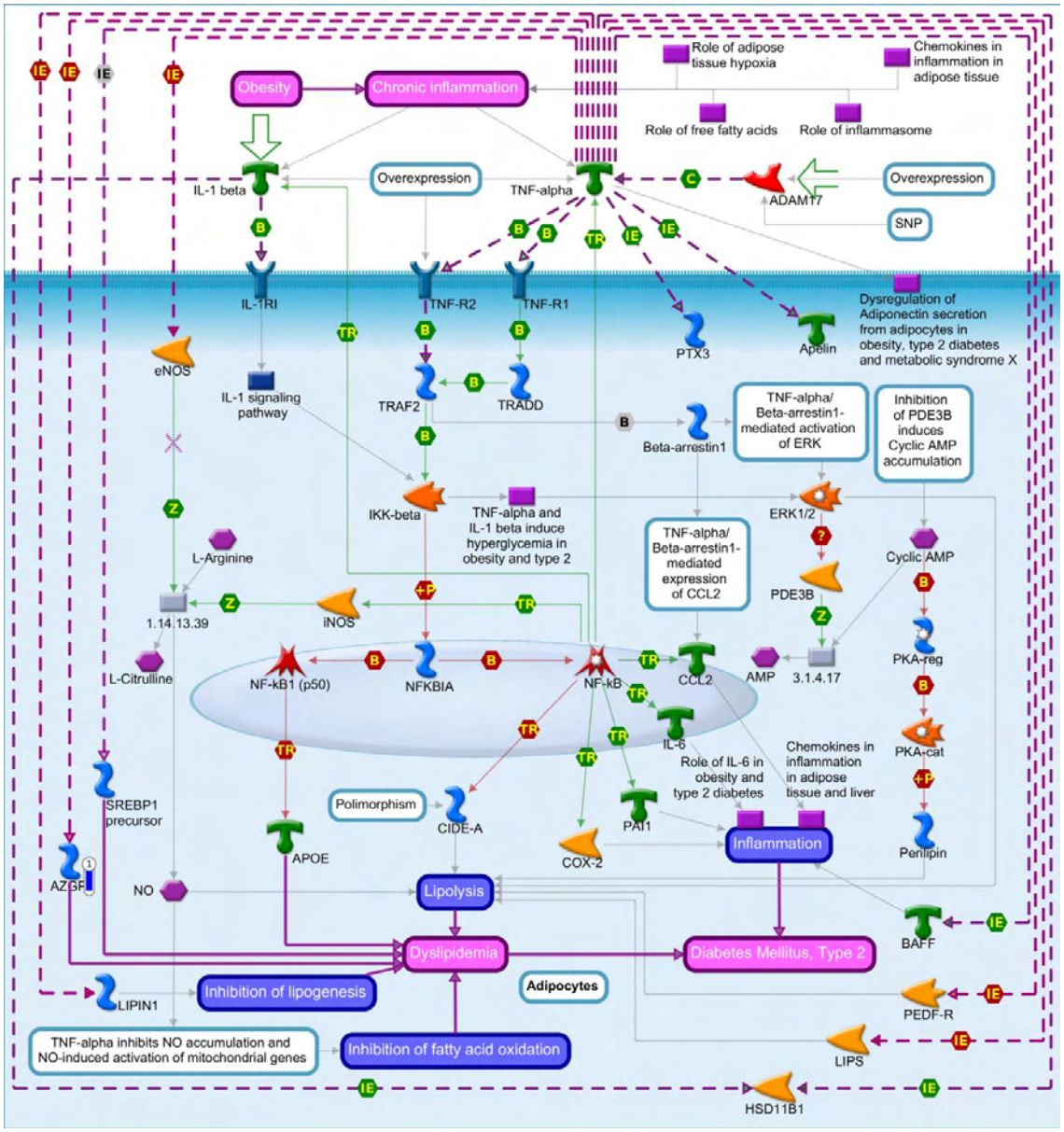

Figure 7. *TNF-alpha, IL-1 beta* induces dyslipidemia and inflammation in obesity and type 2 diabetes in adipocytes pathway map created by using MetaCore software (p-value <0.10) from the list of differentially expressed genes (FDR 10%) in the skeletal muscle of immunocastrated male pigs fed with two different levels of soybean oil in the diet (1.5 % and 3.0 % of soybean oil). The blue thermometer indicates that the DEG is downregulated (log2 fold change -2.67) in the diet with 1.5 % of soybean oil (SOY1.5). Purple lines indicates enhancement in diseases and purple dotted line emerges in diseases. Green arrows indicates positive interactions, red arrows indicates negative interaction and gray arrows indicates unspecified interaction. For a detailed definition, see https://portal.genego.com/legends/MetaCoreQuickReferenceGuide.pdf.

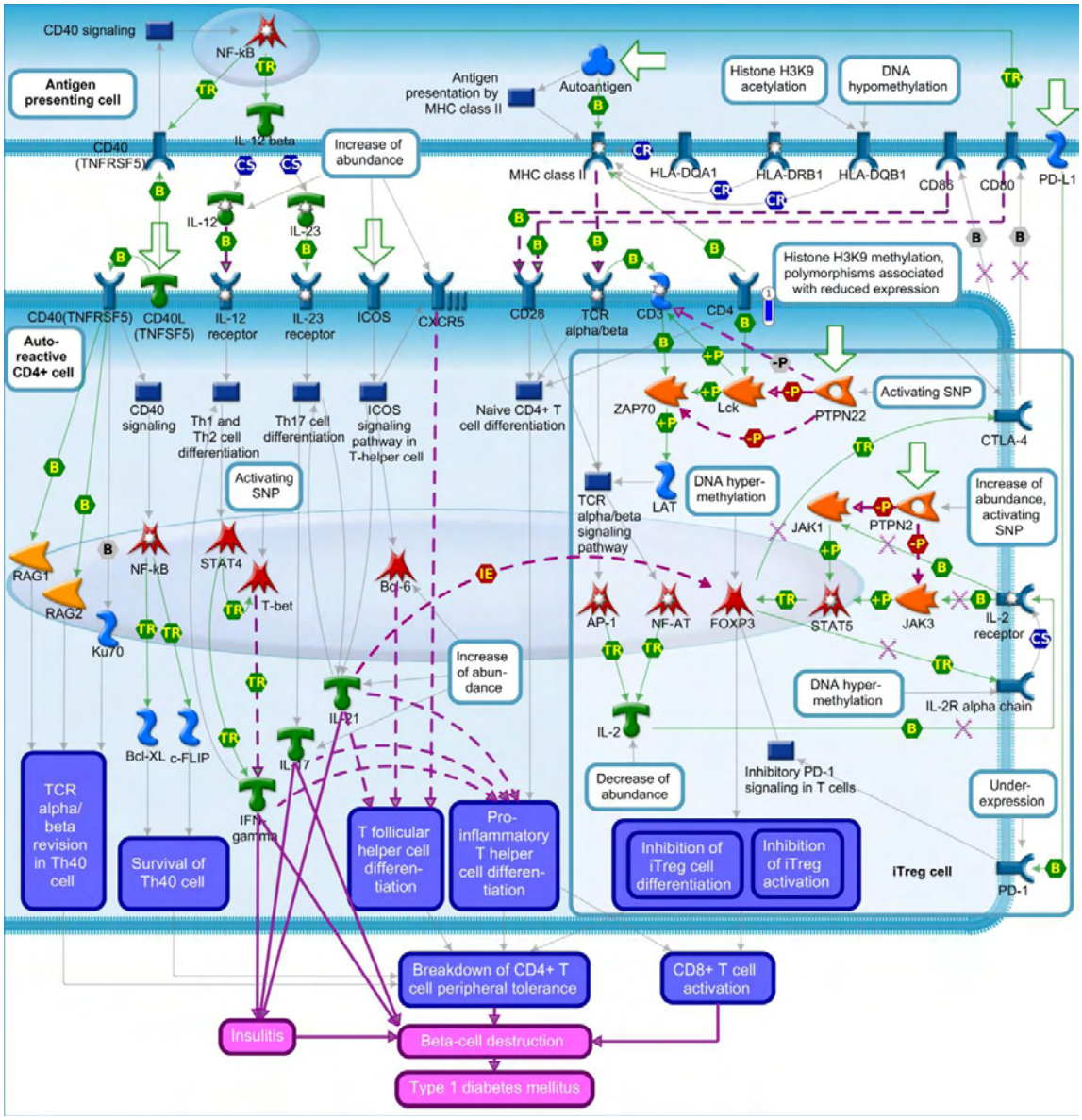

Figure 8: Breakdown of CD4+ T cell peripheral tolerance in type 1 diabetes mellitus pathway map created by MetaCore software (p-value <0.10) from the list of differentially expressed genes (FDR 10%) in the skeletal muscle of immunocastrated male pigs fed with two different levels of soybean oil in the diet (1.5 % and 3.0 % of soybean oil). The blue thermometer indicates that the DEG is downregulated (log2 fold change -1.57) in the diet with 1.5 % of soybean oil (SOY1.5). Purple lines indicates enhancement in diseases and purple dotted line emerge in diseases. Green arrows indicates positive interactions, red arrows indicates negative interaction and gray arrows indicates unspecified interaction. For a detailed definition, see https://portal.genego.com/legends/MetaCoreQuickReferenceGuide.pdf.

The enriched pathways show our DEG identified by DESeq2 with an important role in metabolism and diseases (Table 5). The majority of the top 10 enriched (p-value <0.05) processs networks identified are associated with immune response, the same observed in the pathway maps. The identified networks; such as, “immune response antigen presentation” with the DEG *AZGP1* and *CD4* (log2 fold change -2,67; log2 fold

change -1.57), and "Kallikrein- kinin system" with the DEG *A2M* (alpha-2-macroglobulin; log2 fold change -1,79), are shown in Figures 9 and 10.

Table 5. Process Networks by MetaCore software (p-value <0.1) from the list of differentially expressed genes (FDR 10%) in the skeletal muscle of immunocastrated male pigs fed with two different levels of soybean oil in the diet

Process Networks	p-value	DEG[1]
Chemostaxis	1,80E-03	*CCR10, GPCRs, CD4*
Cell adhesion_Leucocyte chemostaxis	3,78E-03	*CCR10, GPCRs, CD4*
Immune response_Antigen presentation	4,60E-03	*CD4, AZGP1*
Signal transduction_Leptin signling	1,56E-02	*A2M, T-A2MG*
Inflammation_Kallikrein-kinin system	4,43E-02	*A2M, T-A2MG*
Reproduction_Male sex differentiation	6,99E-02	*Tektin 1, AKAP3*

[1]Differentially Expressed Genes

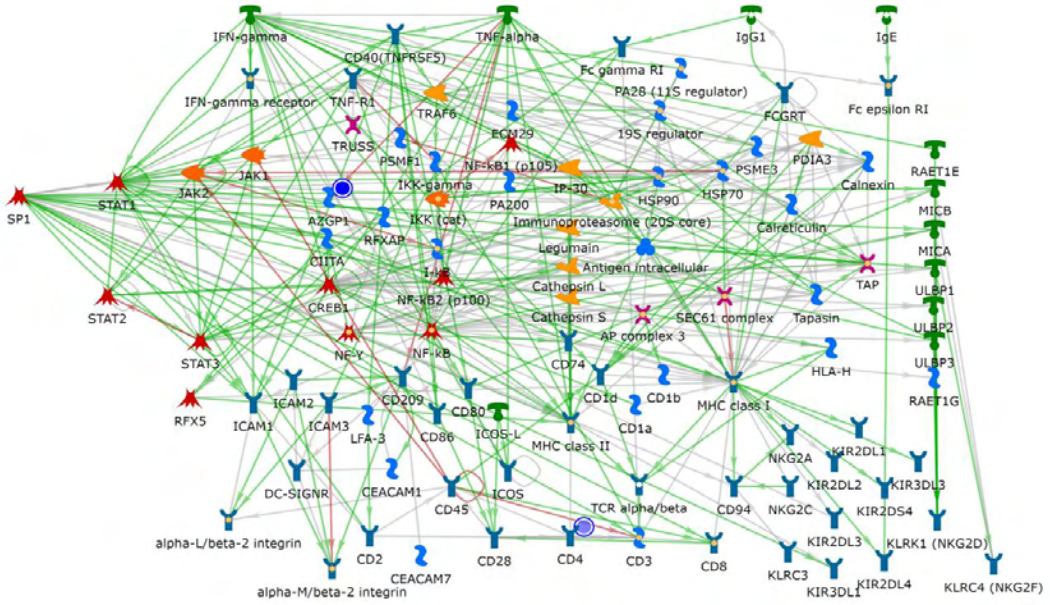

Figure 9. Process network Immune response antigen presentation identified by MetaCore software using the list of differentially expressed genes (FDR 10%) in the skeletal muscle of immunocastrated male pigs fed with two different levels of soybean oil in the diet (1.5 % and 3.0 % of soybean oil). Green arrows indicates positive interactions, red arrows indicates negative interactions, and gray arrows indicates unspecified interactions. For a detailed definition, see https://portal.genego.com/legends/MetaCoreQuickReferenceGuide.pdf.

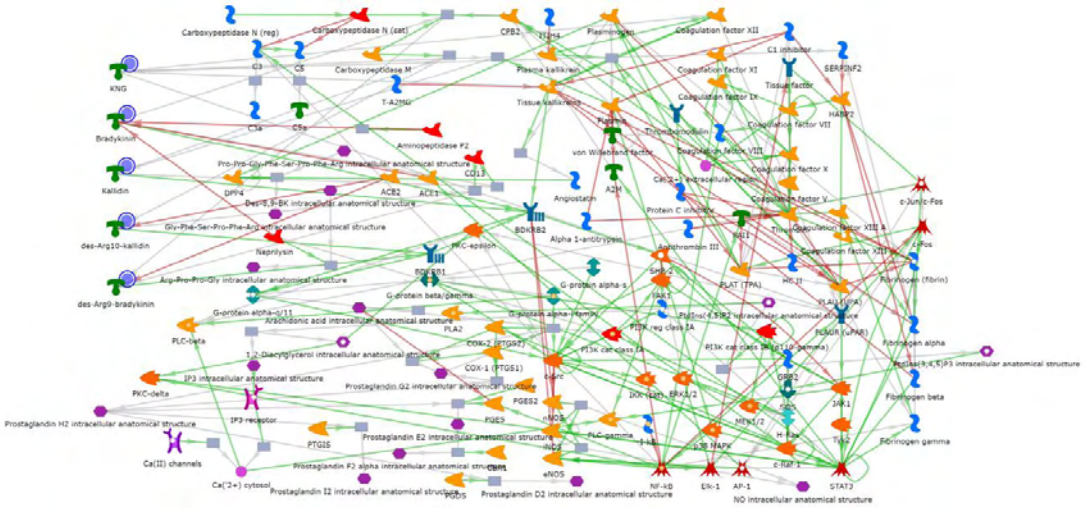

Figure 10. Process network Inflammation_Kallikrein-kinin system identified by MetaCore software using the list of differentially expressed genes (FDR 10%) in the skeletal muscle of immunocastrated male pigs fed with two different levels of soybean oil in the diet (1.5 % and 3.0 % of soybean oil). Green arrows indicates positive interactions, red arrows indicates negative interactions and gray arrows indicates unspecified interactions. For a detailed definition, see https://portal.genego.com/legends/MetaCoreQuickReferenceGuide.pdf.

3.5 Functional enrichment analysis for liver differential expression

Six different pathway maps were detected (p-value <0.10), which are linked to BAG chaperone 1 *(BAG-1)*, *ST13* Hsp70 Interacting Protein (Hip), Microtubule Associated Protein Tau *(MAPT)*, group of non-phosphorylatable alkali light chains of Myosin II *(MELC)*, Protein Phosphatase 2 Catalytic *(PP2C)*, Adenine nucleotide translocases Protein group *(ANT)*, Peptidylprolyl Isomerase F *(PPIF)*, and cyclin dependent kinase inhibitor 1A *(CDKN1A ou p21)* genes (Table 6).

Table 6: Pathway maps with DEG between SOY1.5 vs SOY3.0 in liver tissue enriched in significant pathways (p <0.1)

Pathway maps	p-value	DEG[1]
HSP70 and HSP40-dependent folding in Huntington's disease	1.034E-2	*BAG-1*, *ST13 (Hip)*
Inhibition of remyelination in multiple sclerosis: regulation of cytoskeleton proteins	3.022E-2	*MAPT*, *MELC*
Tau pathology in Alzheimer disease	4.543E-2	*MAPT*, *PP2C*
Mitochondrial dysfunction in neurodegenerative diseases	5.153E-2	*ANT*
Dual role of *p53* in transcription deregulation in Huntington's Disease	7.179E-2	*p21*
LRRK2 in neuronal apoptosis in Parkinson's disease	9.869E-.0.2	*ANT*

[1] Differentially expressed genes (DEG).

Herein, we identified the DEG *BAG-1* as an up-regulated gene (log2 fold change +0.35) in liver samples from pigs fed 1.5% of soybean oil. This gene participates in the pathway map named “HSP70 and HSP40-dependent folding in Huntington's disease *BAG-1”* (Figure 11). We identified the *ST13* gene as a DEG in the liver of pigs that were fed with different levels of soybean oil (1.5% *vs* 3%), being less expressed in the SOY1.5 group (log2 fold change -0.35). In the "HSP70 and HSP40-dependent folding in Huntington's disease" pathway (Figure 11) ST13 is related to the folding process of mutant Huntington via stimulation of HSP70.

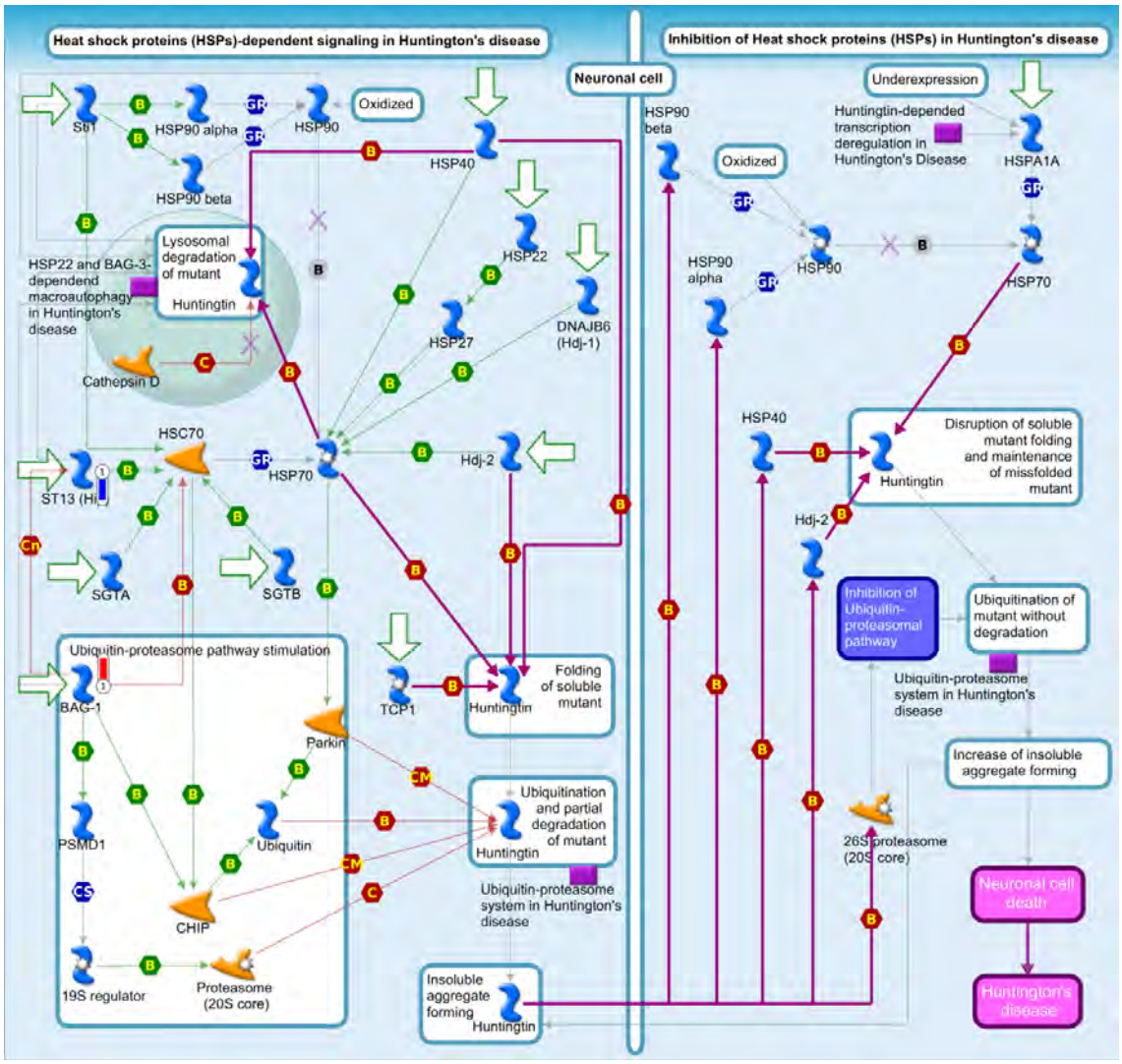

Figure 11. HSP70 and HSP40-dependent folding in Huntington's disease pathway map created by MetaCore software (p-value <0.10) and the list of differentially expressed genes (FDR 10%) in the liver of immunocastrated male pigs fed with two different levels of soybean oil in the diet (1.5 % and 3.0 % of soybean oil). The blue thermometer indicates that the DEG is downregulated (log2 fold change -0.35) and the red thermometer indicates that the DEG is up-regulated (log2 fold change +0.35) in the diet with 1.5 % of soybean oil (SOY1.5). Purple lines indicates enhancement in diseases and purple dotted line emerges in diseases. A green arrow indicates positive interactions, red arrows indicate negative

interactions, and grey arrows indicate unspecified interactions. For a detailed definition, see https://portal.genego.com/legends/MetaCoreQuickReferenceGuide.pdf.

The microtubule associated protein *Tau (MAPT)* gene was identified as DEG in the liver of our pig population, showing lower expression (log2 fold change -1.18) in the SOY1.5 group and enriched in "Inhibition of remyelination in multiple sclerosis: regulation of cytoskeleton proteins" (Figure 12) and "Tau pathology in Alzheimer disease" (Figure 13). Another interesting DEG identified herein, also enriched in the "Iinhibition of remyelination in multiple sclerosis: regulation of cytoskeleton proteins" pathway, was the Myosin light chain 3 (*MYL3*). The *MYL3* participates in the pathway as a MELC group with lower expression (log2 fold change -1.37) in SOY1.5 group.

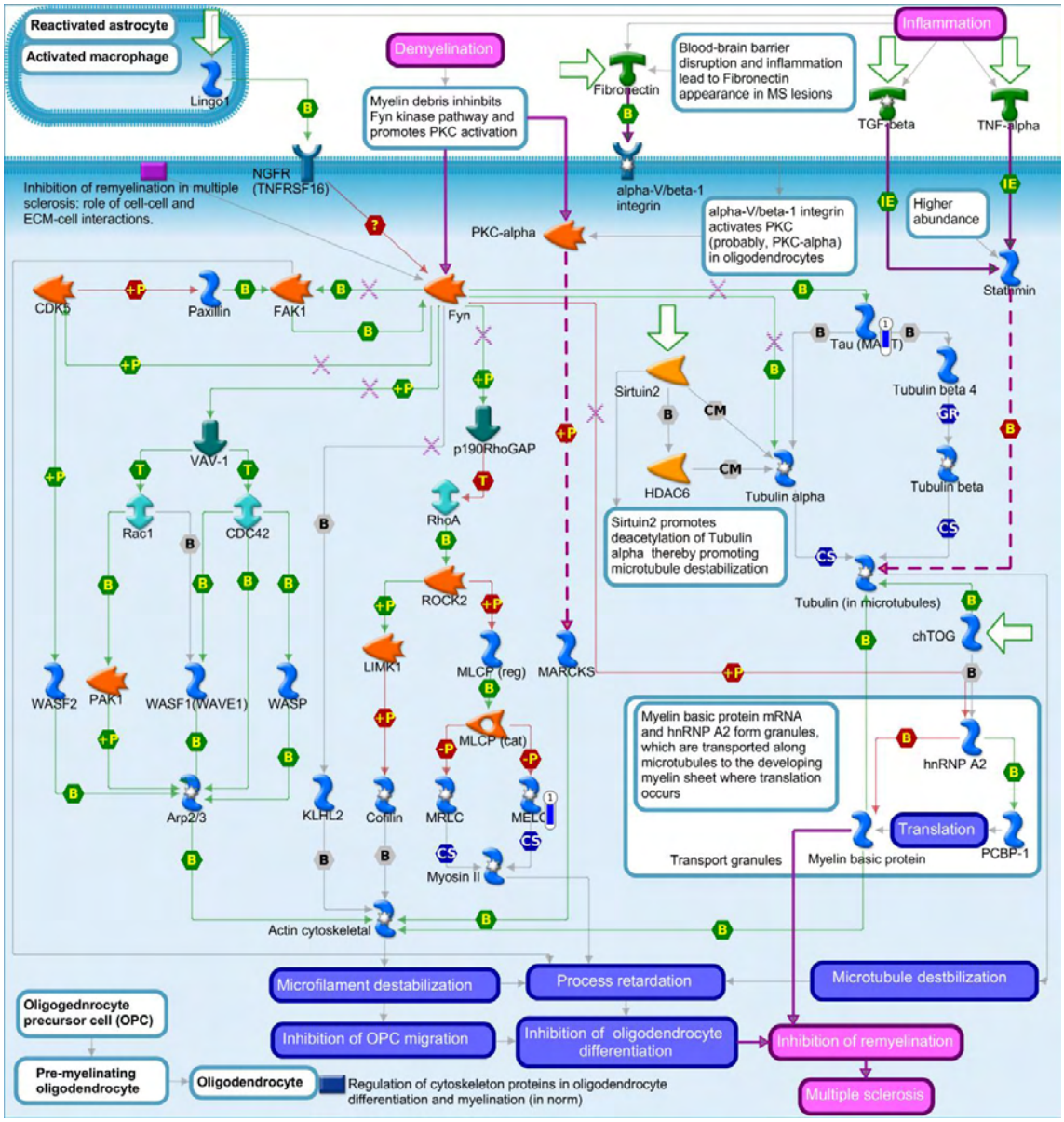

Figure 12. Inhibition of remyelination in multiple sclerosis: regulation of cytoskeleton proteins pathway map created by using MetaCore software (p-value <0.10) and the list of differentially expressed genes (FDR 10%) in the liver of immunocastrated male pigs fed with two different levels of soybean oil in the diet (1.5 % and 3.0 % of soybean oil). The blue thermometer indicates that the DEG is downregulated (log2 fold change -1.18 and -1.37) in the diet with 1.5 % of soybean oil (SOY1.5). Purple lines indicates enhancement in diseases and purple dotted line emerges in diseases. Green arrows indicates positive interactions, red arrows indicates negative interactions and grey arrows indicates unspecified interactions. For a detailed definition, see https://portal.genego.com/legends/MetaCoreQuickReferenceGuide.pdf.

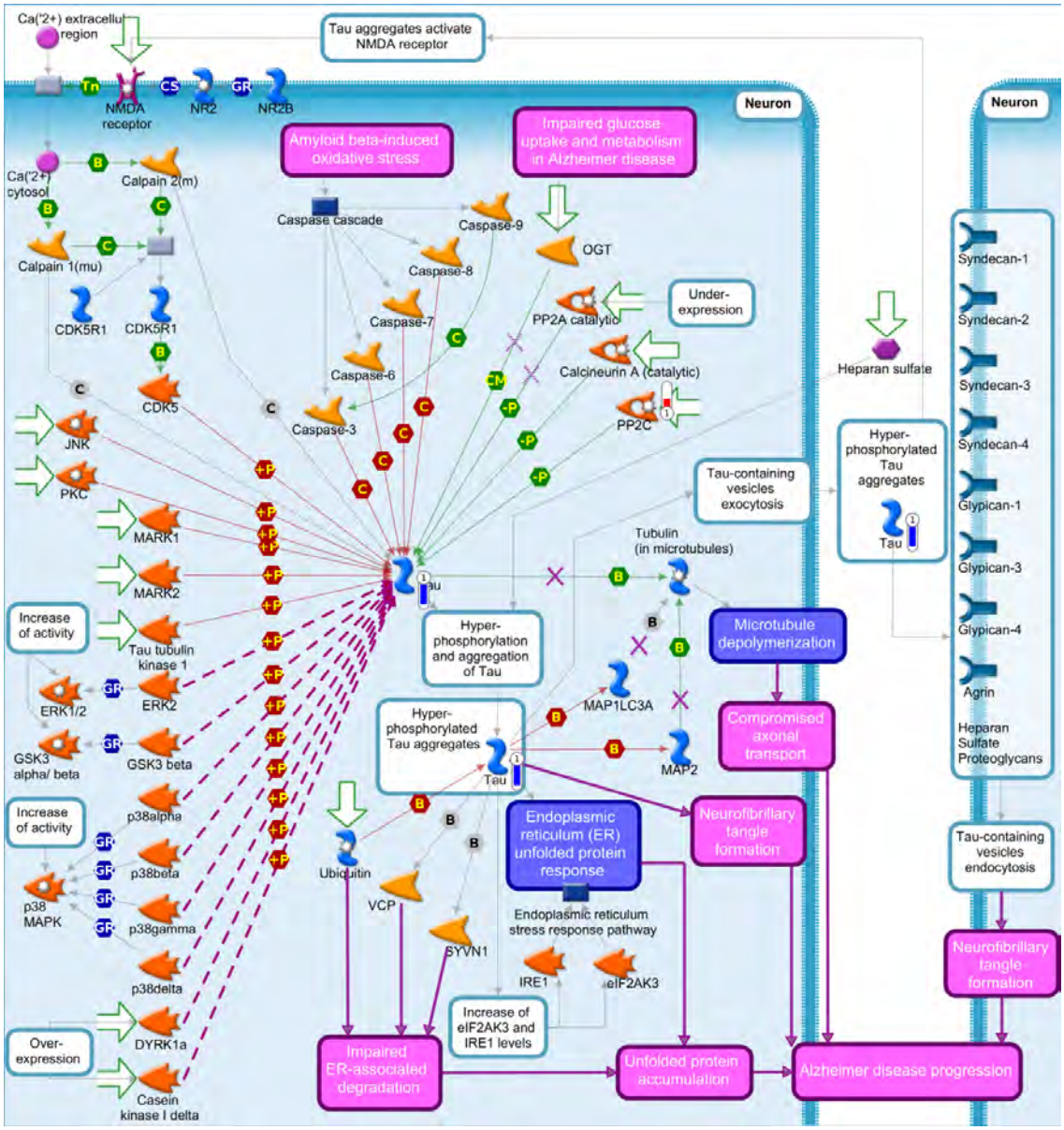

Figure 13. Tau pathology in Alzheimer disease pathway map created by using MetaCore software (p-value <0.10) and the list of differentially expressed genes (FDR 10%) in the liver of immunocastrated male pigs fed with two different levels of soybean oil in the diet (1.5 % and 3.0 % of soybean oil). The blue thermometer indicates that the DEG is downregulated (log2 fold change -1.18) and red thermometer indicates that the DEG is up-regulated (log2 fold change +0.42) in the diet with 1.5 % of soybean oil (SOY1.5). Purple lines indicates enhancement in diseases and purple dotted line emerges in diseases. Green arrows indicates positive interactions, red arrows indicates negative interactions and grey arrows indicates unspecified interactions. For a detailed definition, see https://portal.genego.com/legends/MetaCoreQuickReferenceGuide.pdf.

The solute carrier family 25 member 4 *(SLC25A4)* gene was identified as DEG in liver of pigs that were fed with different levels of soybean oil (1.5 *vs* 3%), more expressed (log2 fold change +0.57) in the SOY1.5 group. The DEG *SLC25A5* was involved in the "mitochondrial dysfunction in neurodegenerative diseases" enriched pathway (Figure 14), as the adenine nucleotide translocases protein group (*ANT*).

Another gene identified as a DEG in liver is the peptidylprolyl isomerase F (*PPIF*), member of the peptidil-prolil cis-trans isomerase family *(PPIas*e), that was more expressed (log2 fold change +0.81) in the SOY1.5 group. In the "mitochondrial dysfunction in neurodegenerative disease" pathway (Figure 14), the DEG *PPIF* is linked to the *ANT* gene.

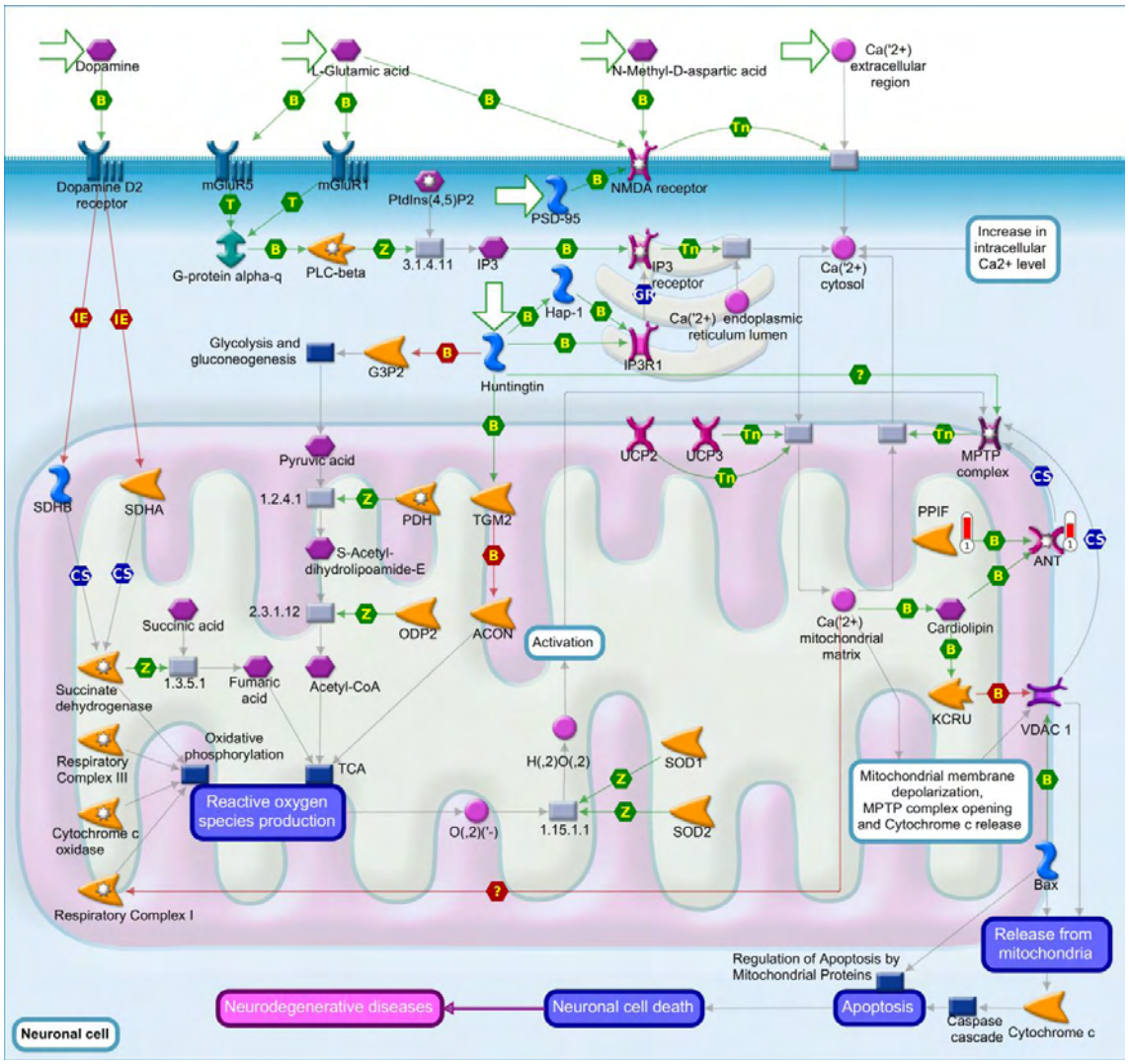

Figure 14. Mitochondrial dysfunction in neurodegenerative diseases pathway map created by using MetaCore software (p-value <0.10) and the list of differentially expressed genes (FDR 10%) in the liver of immunocastrated male pigs fed with two different levels of soybean oil in the diet (1.5 % and 3.0 % of soybean oil). The red thermometer indicates that the DEG is up-regulated (log2 fold change +0.81 and +0.57) in the diet with 1.5 % of soybean oil (SOY1.5). Purple lines indicate enhancement in diseases and purple dotted line emerges in diseases. Green arrows indicate positive interactions, red arrows indicate negative interactions and grey arrows indicate unspecified interactions. For a detailed definition, see https://portal.genego.com/legends/MetaCoreQuickReferenceGuide.pdf.

In this study, *p21* gene showed higher expression (log2 fold change +0.81) in the SOY1.5 group and was enriched in the "dual role pathway of *p53* in transcription deregulation in Huntington's Disease" (Figure 15).

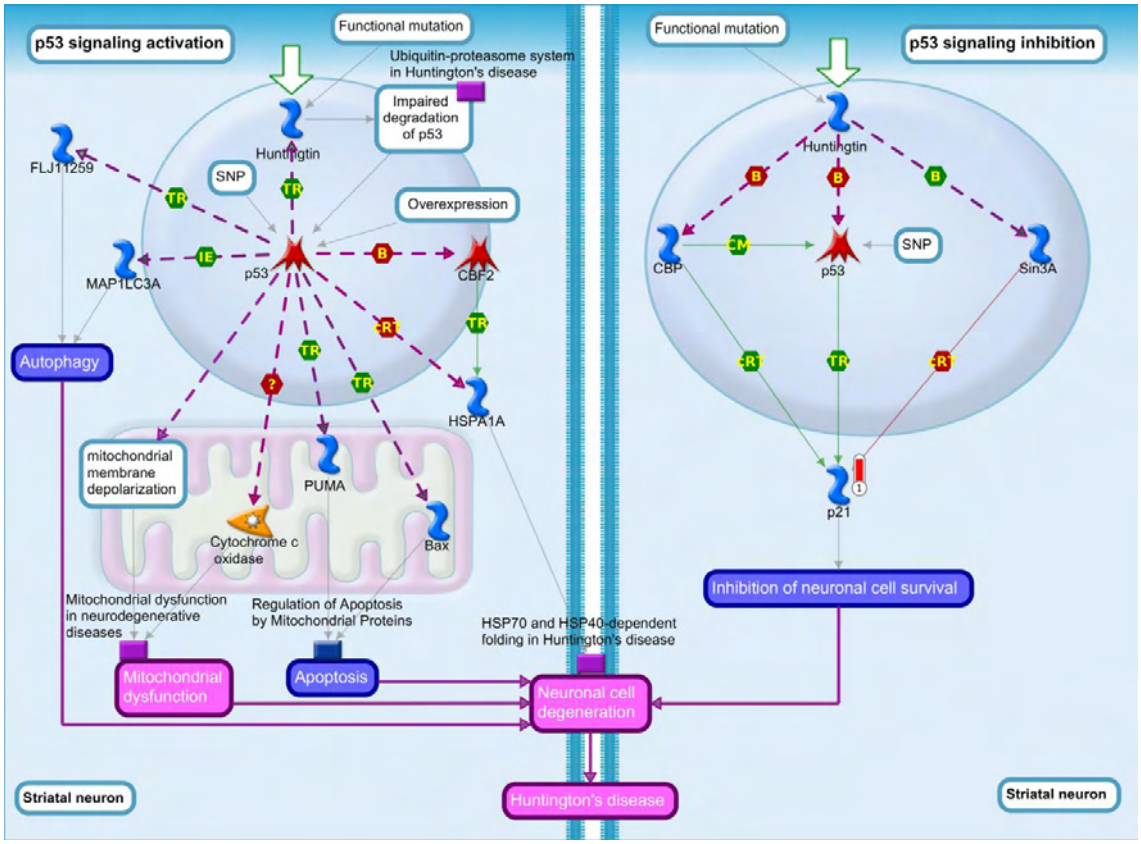

Figure 15. Dual role of p53 in transcription deregulation in Huntington's Disease pathway map created by using MetaCore software (p-value <0.10) and the list of differentially expressed genes (FDR 10%) in the liver of immunocastrated male pigs fed with two different levels of soybean oil in the diet (1.5 % and 3.0 % of soybean oil). The red thermometer indicates that the DEG is downregulated (log2 fold change +0.81) in the diet with 1.5 % of soybean oil (SOY1.5). Purple lines indicate enhancement in diseases and purple dotted line emerges in diseases. Green arrows indicate positive interactions, red arrows indicate negative interactions and grey arrows indicate unspecified interactions. For a detailed definition, see https://portal.genego.com/legends/MetaCoreQuickReferenceGuide.pdf.

The Top10 GO network pathways ($p<0.1$) were identified using the program's default in analyze single experiment (Figure 16).

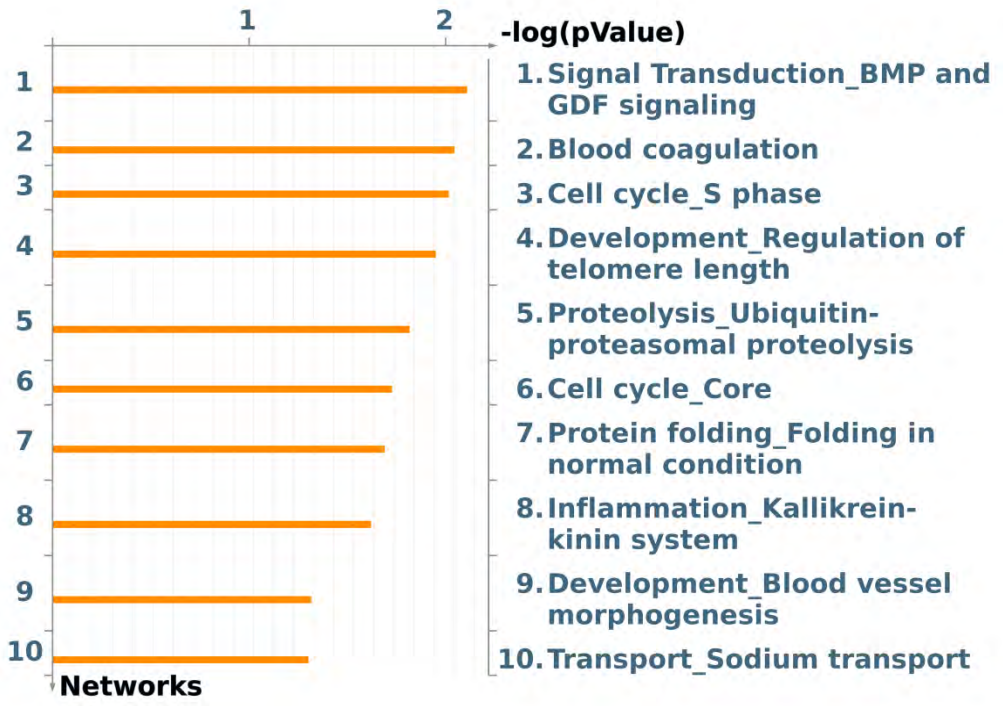

Figure 16. Top 10 enriched networks identified by MetaCore software from the list of differentially expressed genes (FDR 10%) in the liver of immunocastrated male pigs fed with two different levels of soybean oil in the diet (1.5 % and 3.0 % of soybean oil).

The "Protein folding in normal condition" network presents the DEG *PPID* (+0.48log2 fold change), HSP105 (+0.83log2 fold change), *BAG-1* (+0.35log2 fold change), and *ST13* (Hip) (-0.35log2 fold change) (Figure 17). The "inflammation_Kallikrein-kinin system", contains the DEG *KNG1* (-0.67log2 fold change), which in the gene network appears enriched as a receptor ligand, and has bioactive metabolites of bradykinin as can be seen in Figure 18 (within a blue circle).

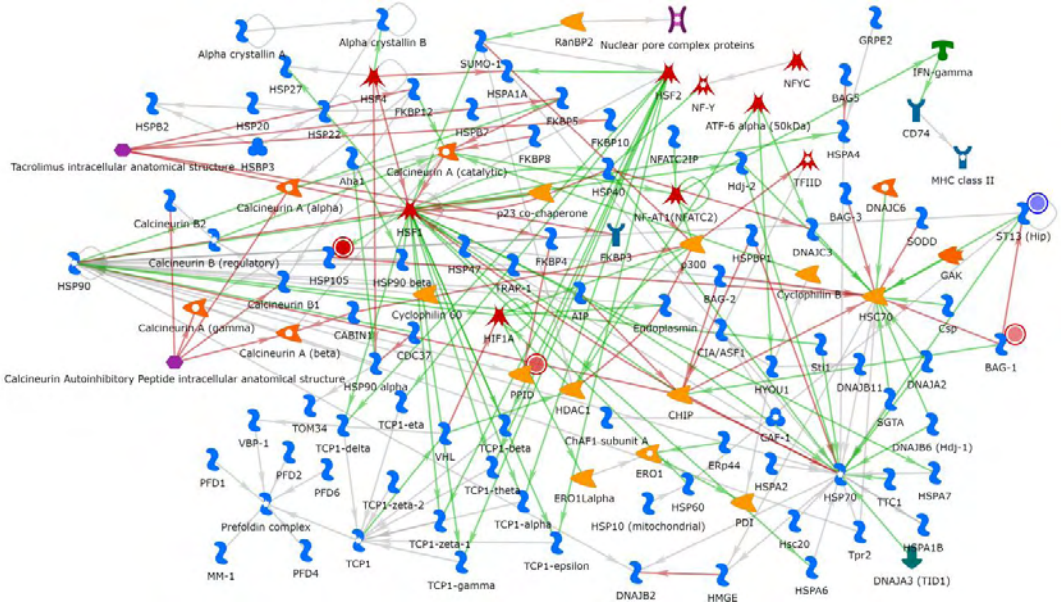

Figure 17. Process network Protein folding in normal condition identified by MetaCore software from the list of differentially expressed genes (FDR 10%) in the liver of immunocastrated male pigs fed with two different levels of soybean oil in the diet (1.5 % and 3.0 % of soybean oil). Green arrows indicates positive interactions, red arrows indicates negative interaction and gray arrows indicates unspecified interaction. For a detailed definition, see https://portal.genego.com/legends/MetaCoreQuickReferenceGuide.pdf.

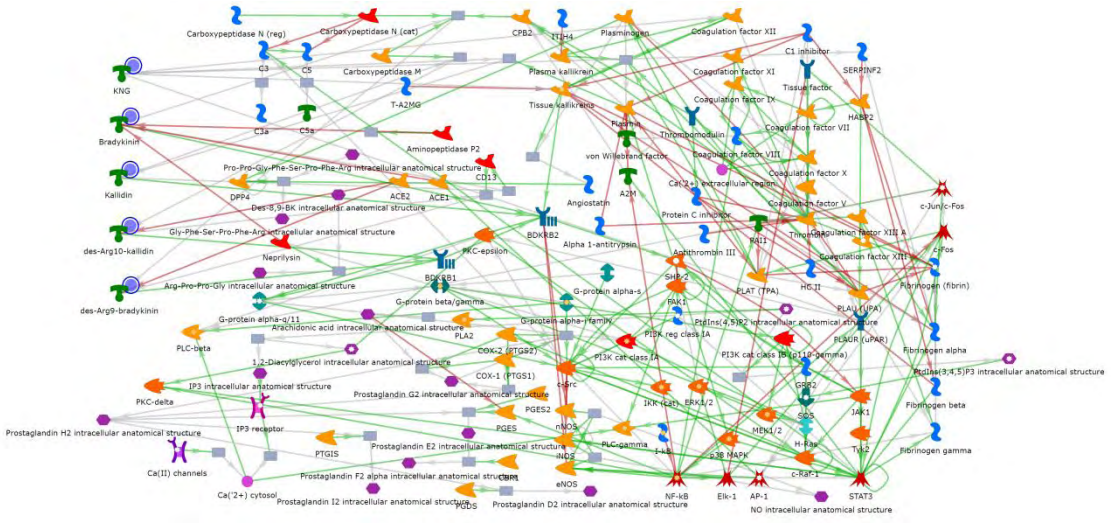

Figure 18. Process network Inflammation_Kallikrein-kinin system identified by MetaCore software from the list of differentially expressed genes (FDR 10%) in the liver of immunocastrated male pigs fed with two different levels of soybean oil in the diet (1.5 % and 3.0 % of soybean oil). Green arrows indicates positive interactions, red arrows indicates negative interaction and gray arrows indicates unspecified interaction. For a detailed definition, see https://portal.genego.com/legends/MetaCoreQuickReferenceGuide.pdf.

4. DISCUSSION

Different levels of dietary soybean oil modulates fat deposition: We identified differences between diets with different addition of soybean oil. In addition to the group's previous study (Almeida et al., 2021), Alencar et al., (2021) and other studies revealed that soybean oil modulates FA composition in gilts in pork.

Both n-6 and n-3 PUFAs decreased as the amount of diet varied. The PUFA n-3 presented a fundamental role in the development and manteinance in the health animal and its ingestion is related to action effects of insulin, neurologic development, reproduction, innate and acquired immunity and with transcription factors expression (WEI et al., 2016). In a study with L*ongissimus dorsi* muscle samples from pigs receiving a diet enriched with linseed (reach in AL), in the growing and finishing, WEI et al., (2016) identified genes anotated as involved in apoptose, muscle organs development and transcriptional regulation. Beyond genes involved in the metabolic process of glicose, aminoacid metabolismo, the quinase IκB cascade *NF-κB*, FA metabolic process, IGF-1/insulin and of genes that code for Wnt pathway elements. As in Alencar et al. (2021) regardless of the amount of soybean oil adopted, the values were above the recommended (ratio <4:1). The n-6:n-3 ratio above the recommended are related to pro-inflammatory immune responses, and metabolic diseases.

The SFA and MUFA in the pigs have in vivo sinthesis with low influency by diet that PUFA, as AL and ALA that are sintetize and reflect changes in diet (ENSER et al., 2000), that can be observed in our results in which SFA not presented changes with the modification between oil, like the MUFA C20:1. We identified a difference in both muscle and liver related to the amount of MUFA, the diet is responsible for a considerable amount of OA in the adipose tissue; the *de novo* synthesis is the main one in the supply of MUFA to the body, so the tissue content is not so influenced by the diet. In our study, the LL intramuscular fat EPA and DHA showed higher deposition in the SOY1.5 group and, consequently, of the total n-3, the same can be observed with n-6, which showed higher LA deposition. However, in the liver, only EPA showed higher deposition in the SOY1.5 group, as well as n-3 and AL, which helped SOY1.5 to present a lower n-6:n-3 ratio than in SOY3.0, but keeping it above 8.

Most serum parameters showed no difference with the addition of soybean oil to the diet as shown in our previous study (FANALLI et al., 2021). With the increase in oil, we observed lower values of albumin, triglycerides and VLDL. In the DEG identified in (APPENDIX B - Table S1), we observed *APOO* with higher expression

(log2 fold change +0.60) in SOY1.5 encoded protein associated with HDL, LDL and VLDL lipoproteins (STELZER, G. et al, 2016), alterations in members of the apolipoprotein family may result in changes in the regulation of particle metabolism (GLUSZKA et al., 2017); as VLDL which may be related to the higher VLDL content found in SOY1.5.

Different levels of dietary soybean oil modulates gene expression in skeletal muscle: The *AL3A2* gene showed the highest amounts of enriched pathway maps, the AL3A2 enzyme helps to detoxify aldehydes produced by alcohol metabolism and lipid peroxidation, the development of the central and peripheral nervous systems, and the oxidation of long-chain aliphatic aldehydes to fatty acid (STELZER, G. et al, 2016). Previous study demonstrated that the *AL3A2* gene participates in the oxidation of 12-oxo-dodecanoic acid to dodecanedioic acid through the activation effect by the catalysis mechanism (KELSON et al., 1997). This gene also participates in the "leukotriene 4 biosynthesis and metabolism" pathway, where the Leukotriene E4 is formed by a family of inflammatory lipid mediators and synthesized from arachidonic acid (AA) through a diversity of cells, such as basophils, mast cells, eosinophils, and macrophages, being the final step of inactivation in Leukotriene B4 metabolism (PETERS-GOLDEN et al., 2006). Furthermore, *AL3A2* gene is involved in "triacylglycerol metabolism and in the oxidative stress in adipocyte dysfunction in type 2 diabetes" and "metabolic syndrome X" pathway, in which the accumulation of oxidative products occurs due to an imbalance in the net levels of reactive oxygen species (ROS) in relation to the antioxidant capacity of the body (MASLOV et al., 2019). The different levels of soybean oil in the diet could be affecting the *AL3A2* expression level. Thus, the consumption of higher levels of soybean oil could improve the rate of lipid oxidation, accumulation of free radicals into the cells causing cell damage and, consequently, the inflammatory condition that would lead to metabolic diseases such as type 2 diabetes and atherosclerosis (PAN et al., 2016). These results confirm previous studies that identified the fatty aldehyde dehydrogenase isozymes, such as *AL3A2* have cell-specific functions associated to inflammation, differentiation, or oxidative stress responses (BAZEWICZ et al., 2019; CHU et al., 2019).

The DEG *AZGP1* is related to stimulation of the breakdown of lipids within adipocytes, which causes fat to be lost in some advanced cancers, and it is also capable of binding to polyunsaturated fatty acids (KRAHMER; FARESE; WALTHER, 2013). Studies shown that the *AZGP1* gene can be inhibited by *TNF-alpha* and other genes

related to the development of metabolic disorders. Also, this gene encodes a soluble protein classified as an adipokine (GOHDA et al., 2003; TZANAVARI; BING; TRAYHURN, 2007). In an obese adipose tissue, the overexpression of *TNF-alpha* together with IL-1b activates the ERK1/2 pathways leading to impaired gene expression that are involved in inflammation, FA oxidation, lipolysis, lipogenesis in addition to oxidative stress (JAGER et al., 2010). Our studies corroborating with previous nutrigenomics studies which showed that the *AZGP1* expression level can be affected by the diet (FAULCONNIER et al., 2018; OLLIER et al., 2007). *AZGP1* gene plays a fundamental role in lipid metabolism and others metabolic diseases such as cancer, being considered as a lipid-metabolizing factor (HIRAI et al., 1998) that impacts the fatty acid metabolism, increasing lipolysis process and decreasing the inflammation signs (CHOI et al., 2012; LIU et al., 2019). According to our findings, diets with higher level of soybean oil change the expression level of *AZGP1* gene in the skeletal muscle leading to a dyslipidemia, inflammatory response mediated by *TNF-alpha* and *IL-1b*, and metabolic diseases.

The *CD4* membrane glycoprotein of T lymphocytes, which is expressed in T lymphocytes, B cells, macrophages, and granulocytes (STELZER et al., 2016). As well as facilitating T-cell activation, *CD4* is an important mediator of indirect neuronal damage in infections and immune-mediated conditions affecting the nervous system. Studies have been shown that diet-induced obesity increases the expression of T-cell and MHC II molecules in adipose tissue and fat spots in this tissue (MORRIS et al., 2013). Skeletal muscle is an important organ for insulin response, thus, presents a significant contribution in systemic insulin sensitivity (FERACO et al., 2021). Hong et al. (2009) suggested that the obesity condition affects the inflammatory state of skeletal muscle. Corroborating, Varma et al. (2009), showed that diets with high level of fat can induce obesity inflammation by the macrophage infiltration into skeletal muscle. However, dietary intake of specific PUFA can modulate the inflammatory responses that can be explained by the influence of the dietary fatty acid profile into n-6:n-3 PUFA ratio of the membrane phospholipids. The n-6 PUFA metabolism generates lipid mediators that have pro-inflammatory functions while n-3 has an anti-inflammatory effect (CALDER, 2011; DJURICIC AND CALDER, 2021; INNES AND CALDER, 2018). Therefore, the overexpression of lipid mediators generated by n-6 are associated with inflammatory diseases (CALDER, 2011; DJURICIC AND CALDER, 2021; INNES AND CALDER, 2018). These previous findings corroborate with our results

that pointed out CD4 gene as downregulated DEG (log2 fold change -1,57) in skeletal muscle of pigs fed with lower level of soybean oil (SOY1.5).

Soybean oil added to pig's diet modulates gene expression in liver tissue: The liver plays a fundamental role in the energy balance of the entire body, removes toxins such as ammonia and is responsible for the detoxification of most endogenous and exogenous toxic compounds. When some hepatic mechanism fails, it causes problems that can reach the brain, affecting brain function and causing several neurodegenerative diseases including Huntington's and Alzheimer (CARROLL et al., 2015; FELIPO, 2013). In Huntington's disease (HD) the majority of symptoms are related to neuronal damage although additional peripheral tissue abnormalities such as energy metabolism deficiency, skeletal muscle atrophy and adipose tissue dysfunction have been reported in both humans and mice with HD (CHIANG et al., 2011). In mice, the aggregates of the resultant mutant Htt protein (mHtt) were found from the transgenic mouse model, mHtt is related with the suppression of the transcription factor *C/EBPα* (TF critical for energy homeostasis) and the *PPARγ* protein function, there is an evidence that defects in liver function may contribute to peripheral abnormalities in HD mice (CHIANG et al., 2011).

The DEG BAG co-chaperone 1 *(BAG-1)* is a protein-coding gene, which is involved in binding to the membrane protein *BCL2,* which participates in the regulation of apoptosis, oncogenesis, neuronal differentiation and the reactions of cellular regulatory proteins, including glucocorticoid receptor (SHEN et al., 2016). *BAG-1* when associated with *BCL2,* it acts activating the degradation of the Huntingtin mutation, probably via activation of U-box containing protein 1 (CHIP) and proteasome (SROKA et al., 2009). Members of the *BAG* and *CHIP* family may also play an important role in modulating neurodegeneration by targeting misfolded mutant proteins to the ubiquitin-proteasome system (KALIA; KALIA; MCLEAN, 2010). *BAG-1* is a co-chaperone for HSP70 and HSC70 chaperone proteins, that participates as a nucleotide exchange factor (NEF) promoting ADP release from HSP70 and HSC70 proteins (STELZER et al., 2016). The HPS70 plays a protective role in several different models of nervous system injury, although it has an association with a deleterious role in some diseases (GERACI; TURTURICI; SCONZO, 2011). Pathologies related to misfolded proteins affect different classes of neurons and are related to numerous diseases such as Parkinson disease (PD), Alzheimer disease (AD), amyotrophic lateral sclerosis (ALS), and

inheritable polyglutamine (PolyQ) diseases (GERACI; TURICI; SCONZO, 2011). In the study by Nollen et al., (2000), with mammalian tissue culture cell lines, *BAG-1* participates as an inhibitor of Hsp70-dependent refolding the authors showed that a two-fold increase in cellular levels of *BAG-1* can inhibit Hsp70 refolding. Adrie et al. (2010) showed that *BAG-1, BAG-3,* cellular inhibitor of apoptosis 1 (cIAP1) and myeloid cell leukemia sequence 1 (MCL-1) were more expressed in brain-dead patients than in hip surgery patients, demonstrating an inhibition of the apoptosis process. In addition, Kalia, Kalia and McLean (2010) demonstrated evidence that HSP70 and the co-chaperones *BAG-1,* HSP40, Hip and CHIP exert a protective role in relation to neurodegenerative diseases. These results confirm the study by Sroka et al. (2009), who demonstrated that BAG-1 plays a key role in neuronal survival and differentiation, and is essential for the proper development and maintenance of the central nervous system. In disease-related pathways, BAG-1 has its function compromised and this causes BAG-1 accumulation as in the enriched pathway "HSP70 and HSP40-dependent folding in Huntington's disease", which in the SOY1.5 group with higher expression would lead to even more in ubiquitin-proteasome activation, but that with HD disease, proteasome functionality is impaired and with impairment of proteasome function, it leads to changes in neurotransmitter systems (JANA et al., 2001).

ST13 or *Hip* co-chaperone is a gene encoding the HSP70 interaction protein, which can also collaborate with other positive cofactors, such as the organizer protein HSP70-HSP90 (Hop), or compete with negative cofactors such as *BAG-1* (SHI; ZHANG; ZHENG, 2007). *ST13* can also act as a facilitator of the Hsc/HSP70 chaperone, aiding in protein folding and repair, and controlling the activity of proteins responsible for regulation, such as steroid receptors and regulators of proliferation or apoptosis (SHI; ZHANG; ZHENG, 2007). According to Hou et al. (2012), in case of functional alteration of the ST13 gene, the HSP70 protein can lose control over the apoptosis process, and thus generate an incorrect proliferation. Freitas et al. (2016), studying miRNA and mRNA expression in peripheral blood cells, found miR-107 downregulated and its target the *ST13* mRNA, showing high expression in patients with high platelet reactivity. miR-107 is associated with expression inhibition of genes involved in metabolism, cell division, angiogenesis and stress response (FINNERTY et al., 2010), and has been associated with neurodegenerative diseases and cancer (NELSON et al., 2010). In the SOY1.5 group, the expression was lower, decreasing its ability to prevent the newly formed Hsc/Hsp70-substrate complex from prematurely

dissociating in the "HSP70 and HSP40-dependent folding in Huntington's disease" pathway.

Alzheimer's disease (AD) is characterized by the extracellular accumulation of amyloid beta peptides or plaques (Aβ) and the intracellular accumulation of phosphorylated tau protein species (tau tangles) in the brain. The Hsp-70/Hsc-70 chaperone, mentioned above, can bind to the *Tau/MAPT* protein, reducing its phosphorylation and inducing its proteasomal degradation. In addition, Hsp-70 is involved in mediating the degradation of Tau/MAPT by recruiting the CHIP E3 ubiquitin ligase, whereas *BAG-1* can associate with *Tau/MAPT* in a Hsc-70-dependent manner and inhibit its proteasomal degradation (CAECILIE SIGNORE et al., 2021; ELLIOTT; LAUFER; GINZBURG, 2009). In the study by Elliott; Laufer; Ginzburg, (2009) in AD hippocampi, the authors reported that *BAG-1* co-localizes with both tau tangles and intracellular amyloid which may indicate that BAG-1 plays a significant role in AD pathology. DEG *Tau/MAPT* was also enriched in the "*Tau* pathology in Alzheimer disease" (Figure 15) pathway together with protein phosphatase, Mg2+/Mn2+ dependent 1F (*PPM1F*) identified in the pathway as the PP2C group with the highest expression (0.42log2 fold change) in the SOY1.5 group. *PPM1F* phosphatase dephosphorylates and negatively regulates the activities of MAP kinases, in addition to being able to interact with guanine Rho nucleotide exchange factors (LIU et al., 2005).

Neurodegenerative disease such as AD is characterized by the microtubule-associated neuronal protein *MAPT* that undergoes hyperphosphorylation by multiple kinases resulting in microtubule disintegration, and this phosphorylation can be regulated by several phosphatases including *PP2C* (LIU et al., 2005). In the study by Liu et al. (2002) with several pools of Tau proteins isolated from AD brain, observed that Tau is abnormally hyperphosphorylated and glycosylated when there is an imbalance between phosphorylation and dephosphorylation, favoring the formation of intraneuronal neurofibrillary tangles (NFTs) which is one of the histopathology's characteristics of AD. Thus, the authors suggested that tau glycosylation is an early abnormality that facilitates hyperphosphorylation in the AD brain (LIU et al. 2002). *I*n the "Inhibition of remyelination in multiple sclerosis: regulation of cytoskeleton proteins", *MAPT* in which Fyn suppression inactivates the guanine nucleotide exchange factor Vav 2 via *CDC42*, destabilizing the actin microfilaments. Fyn suppresses glucocorticoid receptor DNA binding factor 1 leading to RhoA activation. This

suppression of Fyn also impairs the interaction with *Tau (MAPT)* and alpha tubulin (BUSTELO, 2000). In the "Iinhibition of remyelination in multiple sclerosis: regulation of cytoskeleton proteins" RhoA binds to protein kinase 2 (ROCK2), which contains association with Rho and promotes phosphorylation and activation of protein phosphatase 1 (MLCP (reg))/protein phosphatase 1, isoenzyme beta (MLCP) (cat)), with dephosphorylation of Myosin II regulatory light chains (MRLC and MELC) (BAER et al., 2009; MAEKAWA et al., 1999). This activation of RhoA can lead to a growth-related inhibition of the oligodendrocyte process and impair remyelination in multiple sclerosis (STELZER, G. et al, 2016). As Tau (MAPT) are the proteins that stabilize microtubules, the SOY1.5 group was less expressed, thus potentiating the non-stabilization of microtubules, which is harmful. Duan et al. (2012) suggested that the abnormal hyperphosphorylation of *Tau/MAPT* is caused by the conformational change of this protein in the diseased brain, making this a favorable environment for phosphorylation or an unfavorable one for dephosphorylation.

The neurodegenerative diseases can be involved in the intracelular Ca2+ both by its lose by homeostase and excitotoxicity (REGO and OLIVEIRA, 2003). An overload of intracellular Ca2+ high concentration reflect in na overlod of the UCP2 and UCP3 pathway in the mitochondrial Ca2+, which can induce the depolarization of the mitochondrial membrane and, as one of the consequences, activate the production of reactive oxigene species (ROS) and stimulate the MPTP complex by the Cardiolipin/ANT pathways in PPIF (BEAL, 1998; BRUSTOVETSKY et al., 2003).

The expression of *p21* is controlled by the *p53* tumor suppressor protein that in response to stress stimuli mediates the *p53*-dependent cell cycle G1 phase (STELZER et al., 2016). Huntingtin mutation can either activate or decrease *p53* activity and an inhibition of p53 in the "mitochondrial dysfunction in neurodegenerative diseases" pathway can lead to *p21* under expression, leading to inhibition of neuronal cell survival (STEFFAN et al., 2000). The gene expression analysis performed in transgenic mice with fatty livers in the study by Yahagi et al. (2004), resulted in increased expression of *p21* mRNA, considered an indicator of *p53* activity. Thus, the cellular toxicity of excess free fatty acid (FFA), lipid peroxidation and oxidative stress may be associated with the mechanisms of activation of the *p53* protein (YAHAGI et al., 2004).

Bradykinin plays an important role in mediating inflammation resulting in vasodilation in addition to stimulating prostaglandin synthesis (Bennett, 2007). Process networks were related to both the chaperone group (HSP90) and pro-inflammatory

activity, respectively. These results from the gene networks corroborate with the pathway maps shown above, highlighting that the change in the amount of oil in the diet of male pigs causes a change in the gene expression.

Genes common to dietary treatments and overview of the effect of soybean oil addition in different tissues: By identifying the common genes between the tissues, we observed the influence on modulation and important relationship to Cell cycle related kinase, in addition to the relationship to the Ca, cAMP and lipid signaling pathways and glycosylation.

As observed and discussed regarding the genes that showed differential expression, we observed a better relationship when using SOY3.0 associated with the enriched pathways presented and the association with gene function. In liver tissue SOY1.5vsSOY3.0 showed less DEG (45) and relation to neurodegenerative diseases, which highlights the importance of the liver in disease regulation. In contrast, in skeletal muscle 281 DEG were identified with greater relation to FA metabolism, metabolic diseases and inflammatory processes. Our findings show similar function signaling pathways and networks and DEG with respect to the changes that were obtained by modulating the FA profile, making an important contribution to nutrigenomics studies.

The main processes involved are related to the immune response and inflammation, again we observe the DEG that have relation to important genes and that can modulate several processes, both in muscle and in the liver.

5.CONCLUSIONS

In this nutrigenomics study, we verified that increasing the level of soybean oil in the diet of swine, an animal model for metabolic diseases in humans, affected the transcriptome profile of skeletal muscle and liver tissue. The differentially expressed genes identified here participate in network maps associated with metabolic and neurodegenerative diseases in pathways such as "TNF-alpha, IL-1 beta induces dyslipidemia and inflammation in obesity and type 2 diabetes in adipocytes" and "HSP70 and HSP40-dependent folding in Huntington's disease" in addition to DEG that are related to relevant biological processes. The FA profile showed changes according to the increase in oil in the diet. These findings may help us to better understand the biological mechanisms that can be modulated through the diet, in this study specifically by increasing the level of soybean oil (an important source of unsaturated fatty acids) in the diet of immunocastrated male pigs.

REFERENCES

ABBAS, A. K.; LICHTMAN, A. H.; POBER, J. S. **Cellular and Molecular Immunology**. 4th. ed. [s.l.] W.B. Saunders., 2000, 2000.

ALMEIDA, V. V. et al. Effects of increasing dietary oil inclusion from different sources on growth performance, carcass and meat quality traits, and fatty acid profile in genetically lean immunocastrated male pigs. **Livestock Science**, v. 248, p. 104515, 1 jun. 2021.

AOAC. Official Method 963.15. Fat in Cacao Products Soxhlet Extrac tion Method. **AOAC**, 2006.

AOCS. Official approved procedure Am 5-04, Rapid determination of oil/fat utilizing high temperature solvent extraction. **American Oil Chemist's Society**, 2005.

BENJAMINI, Y.; HOCHBERG, Y. Controlling the False Discovery Rate: A Practical and Powerful Approach to Multiple Testing. **Journal of the Royal Statistical Society: Series B (Methodological)**, v. 57, n. 1, 1995.

BLIGH, E. G.; DYER, W. J. A rapid method of total lipid extraction and purification. **Canadian journal of biochemistry and physiology**, v. 37, n. 8, 1959.

BROWN, M. S.; RADHAKRISHNAN, A.; GOLDSTEIN, J. L. **Retrospective on Cholesterol Homeostasis: The Central Role of ScapAnnual Review of Biochemistry**, 2018. .

CALDER, P. C. **ImmunonutritionBritish Medical Journal**, 2003. .

CESAR, A. S. M. et al. Differences in the skeletal muscle transcriptome profile associated with extreme values of fatty acids content. **BMC Genomics**, p. 1–16, 2016. Disponível em: <http://dx.doi.org/10.1186/s12864-016-3306-x>.

FESSLER, M. B. **The Intracellular Cholesterol Landscape: Dynamic Integrator of the Immune ResponseTrends in Immunology**Elsevier Current Trends, , 1 dez. 2016. .

FUJII, J. et al. Identification of a mutation in porcine ryanodine receptor associated with malignant hyperthermia. **Science**, v. 253, n. 5018, 1991.

GORNALL, A. G.; BARDAWILL, C. J.; DAVID, M. M. Determination of serum proteins by means of the biuret reaction. **The Journal of biological chemistry**, v. 177, n. 2, 1949.

HEGAZI, R. A.; WISCHMEYER, P. E. **Clinical review: Optimizing enteral nutrition for critically ill patients - a simple data-driven formulaCritical Care**, 2011. .

JUMP, D. B. et al. Polyunsaturated fatty acids inhibit S14 gene transcription in rat liver and cultured hepatocytes. **Proceedings of the National Academy of Sciences of the United States of America**, v. 90, n. 18, 1993.

JUMP, D. B. **The biochemistry of n-3 polyunsaturated fatty acidsJournal of Biological Chemistry**, 2002. .

KUSNADI, A. et al. The Cytokine TNF Promotes Transcription Factor SREBP Activity and Binding to Inflammatory Genes to Activate Macrophages and Limit Tissue Repair. **Immunity**, v. 51, n. 2, p. 241- 257.e9, 20 ago. 2019.

LANDS, B. Highly unsaturated fatty acids (HUFA) mediate and monitor food's impact on health. **Prostaglandins & Other Lipid Mediators**, v. 133, p. 4–10, 1 nov. 2017.

LEE, S. H.; LEE, J. H.; IM, S. S. **The cellular function of SCAP in metabolic signalingExperimental and Molecular Medicine**, 2020. .

LOVE, M. I.; HUBER, W.; ANDERS, S. Moderated estimation of fold change and dispersion for RNA-seq data with DESeq2. **Genome Biology**, v. 15, n. 12, 2014.

LUNNEY, J. K. **Advances in swine biomedical model genomicsInternational Journal of Biological Sciences**, 2007. .

MALGWI, I. H. et al. Genes Related to Fat Metabolism in Pigs and Intramuscular Fat Content of Pork: A Focus on Nutrigenetics and Nutrigenomics. 2022

MARTIN, C. A. et al. Ácidos graxos poliinsaturados ômega-3 e ômega-6: Importância e ocorrência em alimentos. **Revista de Nutricao**, v. 19, n. 6, 2006.

MATER, M. K. et al. Arachidonic acid inhibits lipogenic gene expression in 3T3-L1 adipocytes through a prostanoid pathway. **Journal of Lipid Research**, v. 39, n. 7, 1998.

MEDZHITOV, R.; JANEWAY, C. A. **Innate immunity: The virtues of a nonclonal system of recognitionCell**, 1997. .

MetaCore (Clarivate Analytics). , 2021. . Disponível em: <portal.genego.com>.

MI, H. et al. The PANTHER database of protein families, subfamilies, functions and pathways. **Nucleic Acids Research**, v. 33, n. DATABASE ISS., 2005.

MOGHADASIAN, M. H.; SHAHIDI, F. Fatty Acids. **International Encyclopedia of Public Health**, p. 114–122, 1 jan. 2017. Disponível em: <https://www.sciencedirect.com/science/article/pii/B9780128036785001570?via%3Dihub>. Acesso em: 2 nov. 2021.

OECD-FAO. OECD-FAO Agricultural Outlook 2021–2030. **OECD-FAO Agricultural Outlook 2021–2030**, p. 163–177, 2021.

PAN, Z. et al. Pig genome functional annotation enhances the biological interpretation of complex traits and human disease. **Nat Commun**, v. 12, 2021.

RADHAKRISHNAN, A. et al. Switch-like Control of SREBP-2 Transport Triggered by Small Changes in ER Cholesterol: A Delicate Balance. **Cell Metabolism**, v. 8, n. 6, p. 512–521, 6 dez. 2008.

ROSTAGNO, H. S. Tabelas brasileiras para aves e suínos: composição de alimentos e

exigências nutricionais. **Tabelas brasileiras para aves e suínos: composição de alimentos e exigências nutricionais**, 2011.

SILVA, J. P. M. da et al. Fatty acid profile in brain and hepatic tissues from pigs supplemented with canola oil. **Revista Brasileira de Agrotecnologia**, v. 11, n. 2, 2021.

SIMOPOULOS, A. P. Importance of the omega-6/omega-3 balance in health and disease: Evolutionary aspects of diet. **World Review of Nutrition and Dietetics**, v. 102, 2011.

SUMMERS, K. M. et al. Functional Annotation of the Transcriptome of the Pig, Sus scrofa, Based Upon Network Analysis of an RNAseq Transcriptional Atlas. **Frontiers in Genetics**, v. 10, 2020.

TRINDER, P. Determination of Glucose in Blood Using Glucose Oxidase with an Alternative Oxygen Acceptor. **Annals of Clinical Biochemistry: International Journal of Laboratory Medicine**, v. 6, n. 1, 1969.

WILLIAMS, N. H.; STAHLY, T. S.; ZIMMERMAN, D. R. Effect of Chronic Immune System Activation on the Rate, Efficiency, and Composition of Growth and Lysine Needs of Pigs Fed from 6 to 27 kg. **Journal of Animal Science**, v. 75, n. 9, 1997.

YATES, C. M.; CALDER, P. C.; ED RAINGER, G. **Pharmacology and therapeutics of omega-3 polyunsaturated fatty acids in chronic inflammatory diseasePharmacology and Therapeutics**, 2014. .

YEHUDA, S.; RABINOVITZ, S.; MOSTOFSKY, D. I. **Essential fatty acids are mediators of brain biochemistry and cognitive functionsJournal of Neuroscience Research**, 1999. .

CHAPTER 3: EFFECT OF DIETARY SOYBEAN OIL INCLUSION ON LIVER-RELATED TRANSCRIPTION FACTORS IN A PIG MODEL FOR METABOLIC DISEASES

Doi:10.20944/preprints202202.0149.v1

Simara Larissa Fanalli[1], Bruna Pereira Martins da Silva[1], Julia Dezen Gomes[2], Fernanda Nery Ciconello[2], Vivian Vezzoni de Almeida[3], Felipe André Oliveira Freitas[2], Gabriel Costa Monteiro Moreira[4], Bárbara Silva-Vignato[2], Juliana Afonso[5], James Reecy[6], James Koltes[6], Dawn Koltes[6], Luciana Correa Almeida Regitano[5], Júlio Cesar de Carvalho Baileiro7, Luciana Freitas[8], Luiz Lehmann Coutinho[2], Heidge Fukumasu[1]; Severino Matias de Alencar[2], Albino Luchiari Filho[2], and Aline Silva Mello Cesar[1,2]*

[1]Faculty of Animal Science and Food Engineering, University of São Paulo, Pirassununga, São Paulo, Brazil.
[2]Luiz de Queiroz College of Agriculture, University of São Paulo, Piracicaba, São Paulo, Brazil.
[3]Federal University of Goiás, College of Veterinary Medicine and Animal Science, Goiânia, Goiás, Brazil;
[4]University of Liège, GIGA Medical Genomics, Unit of Animal Genomics, Liège,
[5]Embrapa Pecuária Sudeste, São Carlos, São Paulo, Brazil.
[6]Iowa State University, College of Agriculture and Life Sciences, Ames, Iowa, USA;
[7]College of Veterinary Medicine and Animal Science, University of São Paulo, Pirassununga, São Paulo, Brazil.
[8]DB Genética de Suínos, Patos de Minas, MG, Brazil.

ABSTRACT

Fatty acids (FA) have several essential roles in cell structure, transcriptional regulation and physiological processes, modulating cell functions and influencing metabolic processes. The consumption of FA is associated with fat deposition and increased occurrence of metabolic diseases. On the other hand, there are studies that diverge on the role of FA involved in cell inflammatory responses in metabolic diseases. For the first time, we performed a study to identify key transcription factors (TF) involved in lipid metabolism and inflammatory response by transcriptome analysis from liver samples. The key TF were identified by functional enrichment analysis from the list of differentially expressed genes identified in liver samples between 35 pigs fed with 1.5% or 3.0% soybean oil (SOY1.5; SOY3.0). The functional enrichment analysis detected TF linked to lipid homeostasis and inflammatory response, such as *RXRA*, *EGFR*, and *SREBP2* precursor. These findings demonstrated that key TF related to lipid metabolism could be modulated by the dietary inclusion of soybean oil. It could contribute to the nutrigenomics research field that aims to elucidate dietary interventions in animal and human health, as well as to drive food technology and science.

Keywords: immune response; fatty acid; lipid metabolism; RNA-Seq; transcriptome.

1.INTRODUCTION

Fatty acids are the main compound of lipids, which are a class of molecules present in animals and vegetal cell types. The main vegetal sources of dietary fatty acids in animal and human nutrition are soybean, canola, sunflower, corn, and flaxseed oil (MOGHADASIAN; SHAHIDI, 2017). Its oils are rich sources of unsaturated fatty acids, such as monounsaturated (MUFA) and polyunsaturated (PUFA) fatty acids, which are previously associated with the prevention of health disorders because of their anti-inflammatory effects and cell membrane properties and structure (LANDS, 2017). Essential FA, mainly polyunsaturated fatty acids (PUFA), may modulate gene expression in diverse biological processes thought regulating transcription factors (TF), including peroxisome proliferator receptors *(PPAR)*, liver X receptors *(LXR)*, and sterol regulatory element-binding proteins *(SREBP)* (JUMP, 2002).

Soybean oil is considered an excellent source of unsaturated FA, such as linoleic acid (LA, C18:2 n-6), alpha-linoleic acid (ALA, C18:3 n-3), oleic acid (OA, C18:1 n-9), and palmitoleic acid (C16:1), which participate in lipid metabolism, inflammatory response, and cholesterol synthesis. Special attention has been focused on PUFA, specifically LA and ALA, given their functions of maintaining cell membranes under normal conditions, as well as their brain functions and the transmission of nerve impulses (MARTIN et al., 2006; LANDS, 2017). An increased proportion of omega (n)-6:n-3 PUFA, which is observed typically in Western diets, leads to a wide range of

pathologies, such as cardiovascular, inflammatory, autoimmune, and diabetic diseases. On the other hand, a low ratio of n-6: n-3 PUFA in the diet may be linked to cholesterol reduction and prevention of cardiovascular diseases (YEHUDA; RABINOVITZ; MOSTOFSKY, 1999; SIMOPOULOS, 2011).

The immune system is defined as the set of cells, tissues, and molecules that act as intermediates in defense of the organism against infections, conferring immunity, which comprises two functional systems: innate and adaptive (ABBAS; LICHTMAN; POBER, 2000). In general, the main difference between these two immune systems lies in the mechanisms and receptors used for immunological recognition (MEDZHITOV; JANEWAY, 1997). Immunonutrition refers to circumstances where feeding specific nutrients present a potential to modulate the activity of the immune system. This concept can be applied to any situation where a source of nutrients is used to modify the immune system or immune responses (CALDER, 2003).

It is already known that macro and micronutrients have immunomodulatory action (immune nutrients), which have been studied in intensive production systems, such as poultry and swine where animals are in contact with a wide range of potentially pathogenic microorganisms. The manifestation of infectious or pathological diseases has a nutritional cost to the animals since there are studies showing that animals raised in low sanitary environments grow slower and consume less food than animals raised in cleaner environments. This occurs because some nutrients that would be directed to the growth of the animal can be redirected to aid the response to the animal health, and is a critical point in a production system (WILLIAMS; STAHLY; ZIMMERMAN, 1997).

Among the most studied immune nutrients are: conditionally-essential amino acids such as arginine and glutamine, which may become essential in stress situations; vitamins E and C, important antioxidants that prevent the aggressive effects of oxidative stress and help to preserve the proper functioning of the immunity; fatty acids that participate in the synthesis of inflammatory mediators, such as leukotrienes, prostaglandins, and thromboxanes, interceding in the immune system response(HEGAZI; WISCHMEYER, 2011).

The use of immune nutrients such as fatty acids to modify inflammatory and immunologic responses has become of increasing interest both in animal and human health. It is because PUFA such as n-3 modulate immune system functions and thereby decrease the severity of inflammatory disorders (YATES; CALDER; ED RAINGER, 2014).

It is well documented that sterol regulatory element-binding protein 2 *(SREBP2)* preferentially activates genes involved in cholesterol biosynthesis and homeostasis (RADHAKRISHNAN et al., 2008; BROWN; RADHAKRISHNAN; GOLDSTEIN, 2018; LEE; LEE; IM, 2020). The SREBPs modulate the transcription of genes encoding enzymes for FA synthesis and uptake, including fatty acid synthase *(FAS),* acetyl CoA carboxylase *(ACC),* and stearoyl CoA desaturase-1 *(SCD1),* and lipoprotein lipase *(LPL)*. Furthermore, *SREBP* has been associated with immune responses (KUSNADI et al., 2019), primarily because the sterols mediate the *SREBP* effects on immune function by altering membrane lipid composition, thus affecting signaling, stress responses, or binding to specific cellular receptors (FESSLER, 2016).

The liver is a target tissue for FA-regulated gene expression and there is evidence that the PUFA are the principal FA regulating liver lipogenic gene expression (JUMP et al., 1993; MATER et al., 1998). The pig is an ideal animal model for investigating the effects of feeding different levels of soybean oil on liver transcriptome profiling and metabolic diseases that occurs also in humans. Pigs and humans show similarities in their anatomy, morphology, metabolism, and physiology, which indicates that the pigs are an important animal model in studies of metabolic diseases in humans such as obesity, atherosclerosis, diabetes, cancer, neurological, cardiopulmonary, and infectious diseases (LUNNEY, 2007; PAN et al., 2021). It was hypothesized that increasing the inclusion of soybean oil at different levels in the diets of growing-finishing pigs would modulate the liver gene expression profile and point out the main TF involved in fatty acid biological processes. Therefore, we have used the pig model to investigate key TF involved in lipid metabolism and immune response linked to differentially expressed genes (DEG), which were identified from liver tissue of immunocastrated male pigs fed either 1.5 or 3.0% added dietary soybean oil.

.

2.MATERIALS AND METHODS

All animal procedures were approved by the Animal Care and Use Committee of Luiz de Queiroz College of Agriculture (University of São Paulo, Piracicaba, Brazil, protocol number: 2018.5.1787.11.6 and number CEUA 2018-28) and followed ethical principles in animal research, according to the Guide for the Care and Use of Agricultural Animals in Agricultural Research and Teaching. This study was carried out in compliance with the ARRIVE guidelines.

2.1. Animals and experimental diets

The current study used data from ALMEIDA *et al.* (2021) and SILVA et al. (2021). Briefly, a total of 36 immunocastrated and halothane homozygous-negative (NN) male pigs *(Large White)* were used in a 98-day feeding trial. Pigs were housed in an all-in/all-out double-curtain-sided building with partially slatted concrete floor pens. Immunocastration of intact males was performed by administering two 2-mL doses of Vivax® (Pfizer Animal Health, Parkville, Australia) at 127 and 141 days of age. The animals used herein were from a population genotyped for the halothane mutation (RYR1 gene) (FUJII et al., 1991).

Pigs were blocked by initial body weight (28.44 ± 2.95 kg) and assigned to one of two dietary treatments: 1.5% soybean oil (SOY1.5) or 3.0% of soybean oil (SOY3.0). The levels of soybean oil to be tested in this study were decided based on the usual nutritional program in pig production, which is 1,5% of soybean oil. Each treatment had six pens containing three pigs. Diets were formulated to meet or exceed the nutritional requirements of growing-finishing pigs, as defined by Rostagno (ROSTAGNO, 2011). Feed treatments consisted of corn-soybean meal in the growing period, while diets in the finishing period were added with SOY1.5 or SOY3.0. Pigs were fed in a phase feeding program that lasted from day 0 to 21 for grower I; days 21 to 42 for grower II; days 42 to 56 for finisher I; days 56 to 63 for finisher II; days 63 to 70 for finisher III; and days 70 to 98 for finisher IV (ALMEIDA et al., 2021). All pigs had ad libitum access to feed and water throughout the experimental period. Individual pig Body weight was measured on days 0, 21, 42, 56, 63, 70, and 98.

At the end of the 98-day study, pigs with an average final body weight of 133.9 ± 9.4 kg (169 days old) were slaughtered by electrical stunning followed by exsanguination, according to the industry standards and Brazilian legislation, after a 16-hour rest period. After slaughter, liver tissue samples were collected, snap-frozen in liquid nitrogen, and stored at -80ºC until analysis.

2.2. Blood biochemical parameters and fatty acid profile of liver

Blood was sampled from the jugular vein four days before the slaughter and immediately transferred into non-anticoagulant vacuum tubes (Becton Dickinson Vacutainer Systems, Franklin Lakes, NJ, USA). Then, the samples were stored at room temperature for 2 hours, subsequently centrifuged at 3,000 × g for 10 min to obtain serum, and stored in duplicated 1.5-mL tubes at −80°C. Serum lipid and biochemistries

were analyzed by the Mindray, BS120 (Guangdong, China) in the Pathology Laboratory at the University of São Paulo, Pirassununga, SP, Brazil. Blood serum glucose content was quantified by the colorimetric enzymatic method according to Trinder (TRINDER, 1969) using commercial kits, following the use recommendations proposed by the manufacturer. The quantification of total cholesterol and fractions was also performed by the enzymatic-colorimetric method, but by selective precipitation. This procedure was performed using commercial kits, according to the manufacturer's instructions. The analysis for the determination of total proteins was performed using commercial kits, following the used protocol proposed by the manufacturer, using the Biureto method with some modifications (GORNALL; BARDAWILL; DAVID, 1949). The composition of FA was previously investigated by our group and described in ALMEIDA et al. (2021) and SILVA et al. (2021). Fatty acid composition analyses: Ether extract was obtained from 5 g of skeletal muscle (*Longissimus lomborum*) and liver using the Soxhlet method according to AOAC (Method 963.15) (AOAC, 2006). For fatty acid profile determination, total lipid was isolated from 100 g of skeletal muscle and 25 g of the liver; following the cold extraction method proposed by Bligh and Dyer (BLIGH; DYER, 1959) and methylated according to the procedure outlined by AOCS (Method AM 5-04) (AOCS, 2005).

2.3. RNA extraction, libraries, and sequencing

Total RNA was extracted from 30 mg of frozen liver samples using RNeasy® Mini Kit (QIAGEN, Hilden, Germany) following the manufacturer's guidelines. The RNA integrity was verified by Bioanalyzer 2100 (Agilent, Santa Clara, CA, USA) and only samples with RIN score > 7.8 were used. A total of 2 μg of total RNA from each sample was used for library preparation according to the protocol described in the TruSeq RNA Sample Preparation kit v2 guide (Illumina, San Diego, CA) (CESAR et al., 2016). The average insert size of the libraries was estimated using the Agilent Bioanalyzer 2100 (Agilent, Santa Clara, CA, USA) and quantified using quantitative PCR with the KAPA Library Quantification kit (KAPA Biosystems, Foster City, CA, USA). Then, samples were diluted and pooled (three pools of six samples each). Five lanes with 36 pooled samples were performed in two sequencing flowcell, using the TruSeq PE Cluster kit v4-cBot-HS kit (Illumina, San Diego, CA, USA), clustered, and sequenced using HiSeq2500 ultra-high-throughput sequencing system (Illumina, San Diego, CA, USA) with the TruSeq SBS Kit v4-HS (200 cycles), according to

manufacturer instructions(CESAR et al., 2016). The sequencing analyses were performed at the Genomics Center at ESALQ, Piracicaba, São Paulo, Brazil.

2.4 Data analysis, differentially expressed genes, and functional enrichment analysis

The RNA-Sequencing (RNA-Seq) data quality was checked using the FastQC, v. 0.11.8 software [http://www.bioinformatics.bbsrc.ac.uk/projects/fastqc/]. Adapters and bases with low PHRED scores were removed using the Trim Galore v. 0.6.5. Reads with a minimum length of 70 bases were aligned and mapped to the reference pig genome (*Sus Scrofa* 11.1) using the assembly available at Ensembl Release 102 [http://www.ensembl.org/Sus_scrofa/Info/Index]. Alignment and mapping were performed using the STAR v. 2.7.6a.

All DEG were compared between treatments (SOY1.5 *vs* SOY3.0) from liver tissue, which were identified using the DESeq2 package available at Bioconductor open-source software for bioinformatics (LOVE; HUBER; ANDERS, 2014), using a multi-factor design. Before statistical analysis, the read count data was filtered as follows: i) genes with zero counts for all samples, that is, unexpressed genes, ii) genes with less than 1 read per sample on average were removed (very lowly expressed); iii) genes that were not present in at least 50% of the samples were removed. For statistical analysis of transcript abundance, sire was fit as a factor in the multi-factor model. To control false discovery, a false discovery rate (FDR) was set at 10% (CESAR et al., 2016) with FDR determined using the Benjamini-Hochberg (BENJAMINI; HOCHBERG, 1995) methodology. Significance differences were set at log2fold-change ≥ 1 or ≤ -1; FDR-corrected p-value < 0.1.

The functional enrichment analysis of DEG was performed to obtain comparative networks by analyzing the single network (TF) using a standard parameter of MetaCore software (Clarivate Analytics) v. 21.3 build 70600, which were filtered for liver tissue and *Homo sapiens* species dataset to show activating and inhibiting effects. The overexpression test from the list of up and down-regulated DEG was performed by Panther v.17 [http://www.pantherdb.org/] (MI et al., 2005) to identify the GO terms related to Biological Processes. The *Sus scrofa* genome reference was used as background.

For the functional analysis to identify important TF related to lipid homeostasis and immune response, the construction of the gene network by the TF mechanism was

performed. For each TF of the master list, the algorithm generated a subnetwork with all the shortest paths to which the TF from the nearest recipient with direct ligands on the list. The construction favors networks, in which the terminal nodes (recipient targets) of transcription-regulated pathways on the original gene list provide a TF-specific network on the gene list.

3.RESULTS

The blood biochemical parameters, body weight, muscle and liver fat content (ether extract), and the fatty acid composition of the liver of the animals fed with diets containing different levels of soybean oil (1.5% SOY1.5 vs 3.0% SOY3.0) were shown in the APPENDIX B (Table S1). Among the blood biochemical parameters evaluated the albumin (g/dL), triglycerides (mg/dL), and very low-density lipoprotein (VLDL mg/dL) were statistically different ($p < 0.05$) between the two groups of diet, where the animals from SOY1.5 presented higher values of these parameters. The saturated (SFA), monounsaturated (MUFA), PUFA, and their ratio were statistically different ($p < 0.05$) between the groups, where we can observe a higher proportion of the sum of MUFA and PUFA and omega 3 (n-3) in the SOY3.0 group of diet. The same group presents lower triglycerides and VLDL in the blood. However, the animals did not present differences in the body weight, and subcutaneous, intramuscular, and liver fat deposition between the diets (APPENDIX B - Table S1).

The RNA-Seq data from liver tissue of 35 pigs fed diets containing different levels of soybean oil (SOY1.5 n = 17 and SOY3.0 n = 18) was used for further analysis, once one of the samples presented a RIN value below the threshold. The mapping analysis statistic showed that 78% on average of total paired reads generated in this study were aligned against the reference genome. After quality filtering, 19,250 genes were considered for differential gene expression analysis between the SOY1.5 and SOY3.0 groups. A total of 281 DEG (log2fold-change ≥ 1 or ≤ -1; FDR-corrected p-value < 0.1) were identified, in which 129 were down-regulated (log2FC ranging from -3.0 to -0.20) and 152 were up-regulated (log2FC ranging from 4.8 to 0.24) in SOY1.5 group (APPENDIX B - Table S2). The functional analysis from the list of down and up-regulated DEG in SOY1.5 by PANTHER applying the overrepresentation test showed no enrichment for GO terms from up-regulated DEG. However, we observed GO terms associated (p-value < 0,05) with Biological Processes from the list of down-regulated DEG, such as glucose metabolic process (GO:0006006), negative regulation of

endopeptidase activity (GO:0010951), hexose metabolic process (GO:0019318), and others (APPENDIX B - Table S3). The functional analysis detected important TF associated with lipid metabolisms, such as lipogenesis and adipogenesis, lipid homeostasis, and immune response (APPENDIX B - Table S4).

The genes and TF, including CK1, AKT2, Beta-catenin, CDK6, Cyclin D1, EGFR, p21, and Rb protein, are displayed in APPENDIX B (Table S5). Both mechanisms of activation and inactivation of other genes and TF are shown in Figure 1. The genes and TF, such as Beta-catenina, EGFR, and ESR1, lead to the primary activation of transcription (APPENDIX B - Table S6). The genes ACK1, AKT, CDK1, and CDK4, cause phosphorylation effects with activation and inhibition mechanisms. From these, the TF, such as TSHZ1 and SOX9, were also DEG with -0.45 log2FC and -1.02 log2FC, respectively.

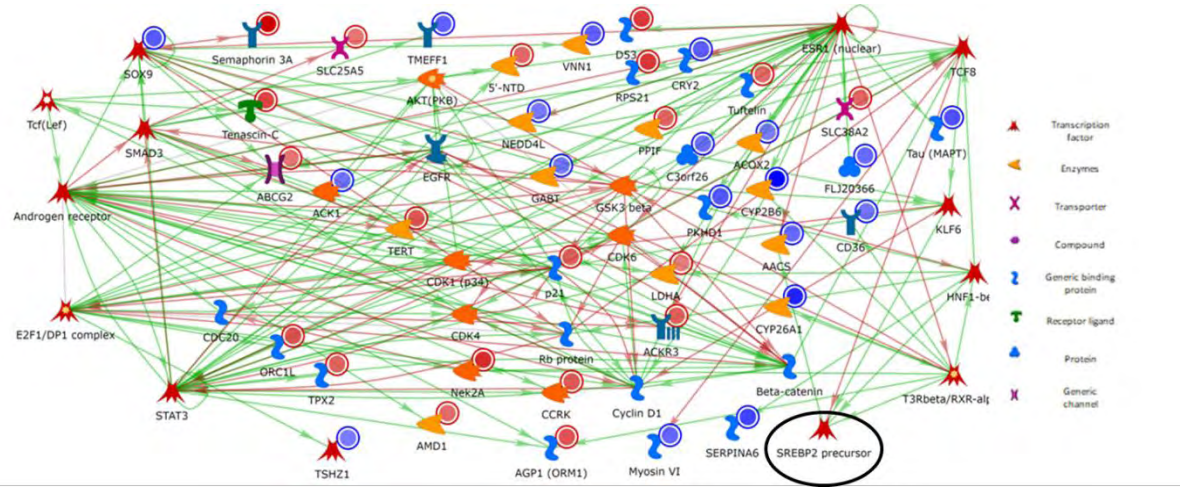

Figure 1. The network was created with MetaCore basic analysis networks (transcription factor) algorithm using DEG list (FDR <0.10) from liver tissue of immunocastrated male pigs fed diets containing different levels of soybean oil (SOY1.5: 1.5% and SOY3.0: 3.0% soybean oil). The green lines represent the activation of other genes, whereas the red lines represent an inactivation. In the blue circles, genes down-regulated and up-regulated are highlighted with red circles. The SREBP2 precursor is highlighted with a black circle. Image created by MetaCore (Clarivate Analytics) [https://portal.genego.com/].

The RXRA exhibited transcriptional regulatory response on some DEG, including *CYP25A1*, which codes for a cytochrome P450 enzyme superfamily and is related to the synthesis of steroids, cholesterol, and other lipids involved in activation mechanism (STELZER et al., 2016). Our results highlighted that RXRA could be involved in the regulation of other DEG, such as *HNF1-beta*, *ORM1*, *Nek2A*, *CD36*, and *CYP2B6*. Other TF are related to DEG, including ESR1, with binding, phosphorylate,

and transcriptional regulate effects combined, as well as a co-regulatory effect with the *SOX9* and *TCF8* TF.

Based on the interactions observed in the network (Figure 1), SREBP2 precursor is one of the key genes involved in the control of cholesterol and FA biosynthesis. This TF takes part in "SCAP/SREBP transcriptional control of cholesterol and FA biosynthesis". The activation of SREBP2 precursor in sterol regulatory element-binding protein cleavage-activating protein (SCAP) is vital for targeting genes for FA and cholesterol biosynthesis (Figure 2). The *SREBP2 precursor* was enriched in MetaCore analysis and undergoes transcriptional regulation via inhibition mechanisms by *TCF8*. The SREBP2 precursor is activated by *KLF6*, *T3Rbeta/RXR-alpha*, and *HNF1-beta*. Furthermore, SREBP2 directly activates acetoacetyl-CoA synthetase (*AACS*) and was down-regulated in the SOY1.5 group compared to SOY3.0 group (-0.75log2FC).

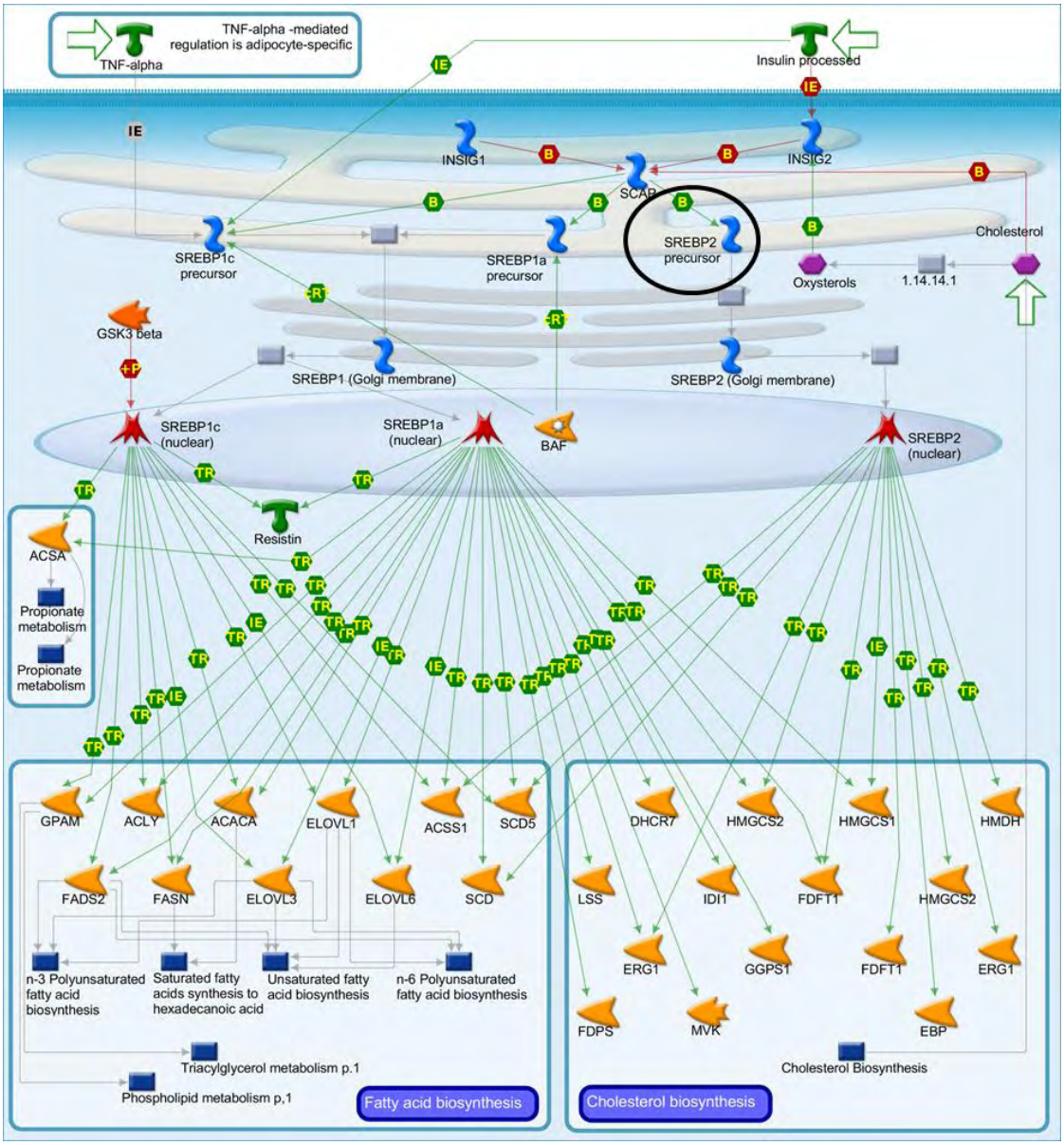

Figure 2. SCAP/SREBP transcriptional control of cholesterol and fatty acid biosynthesis pathway map. Image created by MetaCore (Clarivate Analytics) [https://portal.genego.com/]. Activation is indicated by green arrows, inhibition is indicated by red arrows, and unspecific relationship is indicated by gray arrows. The SREBP2 precursor is highlighted with a black circle. Nodes represent GeneGo Network objects (genes or gene complexes). For more information, see https://portal.genego.com/legends/MetaCoreQuickReferenceGuide.pdf

Additionally, SREBP2 precursor may be involved in the angiogenesis via interleukin-8 (IL-8), considering IL-8 acts as a key mediator for inflammatory responses linked to angiogenesis (Figure 3).

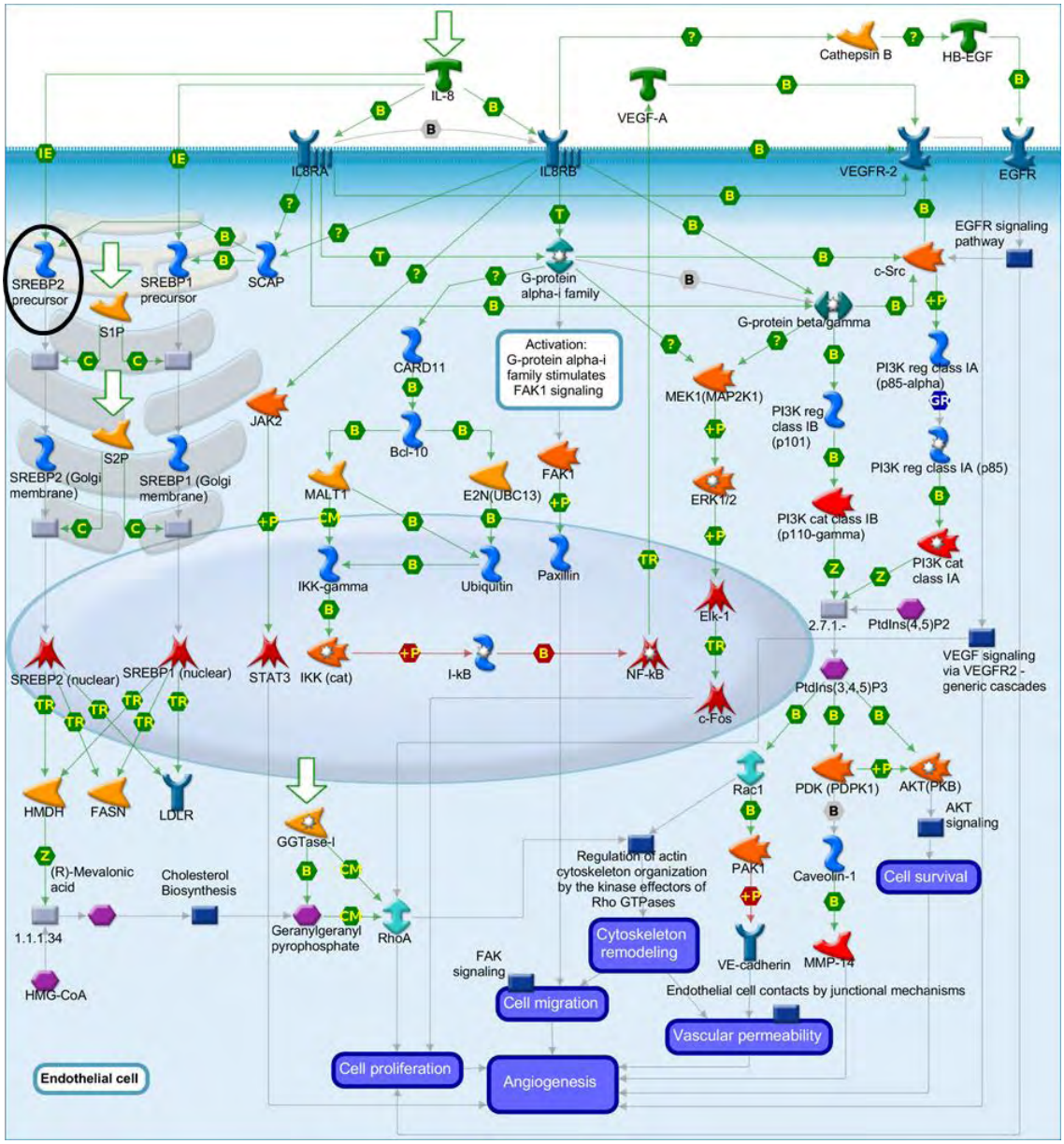

Figure 3. Development role of interleukin-8 (IL-8) in angiogenesis pathway map. Image created by MetaCore (Clarivate Analytics) [https://portal.genego.com/]. Activation is indicated by green arrows, inhibition is indicated by red arrows, and unspecific relationship is indicated by gray arrows. The SREBP2 precursor is highlighted with a black circle. Nodes represent GeneGo Network objects (genes or gene complexes). For more information, see https://portal.genego.com/legends/MetaCoreQuickReferenceGuide.pdf

4.DISCUSSION

In this study, we observed that the increased level of soybean oil, an important source of MUFA, PUFA, and n-3 fatty acids, in the diet of animal models for metabolic diseases in humans such as type 2 diabetes, obesity, and coronary diseases, increased the proportion of these FA in the liver tissue. It also demonstrated a lower level of

triglycerides and VLDL in the blood of the animals (SOY3.0), which did not affect the body weight and fat deposition (ALMEIDA et al., 2021).

The transcriptome profile analysis identifies network connections, TF, and the behavior of interrelated genes in liver tissue in response to the increased levels of soybean oil in the diet of growing-finishing pigs. The enriched network showed that the DEG are involved in key regulatory mechanisms and soybean oil may alter the behavior of TF, such as inhibition of canonical Wnt signaling, adipogenic/lipogenic regulation, cholesterol metabolism, and others.

The RXRA was one of the TF detected herein, being fundamental for metabolism, development, differentiation, proliferation, and cell death. Moreover, RXRA acts on gene expression regulation and shows receptor behavior for FA and oxysterols (STELZER et al., 2016). According to Inoue et al. (2005) RXRA is related to hepatic triglyceride metabolism, in addition to being a transcriptional target of PPAR. The RXRA may display a transcriptional regulatory effect by the activation of DEG found in our study between SOY1.5 and SOY3.0 groups, such as the *CD36*, which was down-regulated in the SOY1.5 group.

It has been reported that the levels of the *CD36* protein are increased in nonalcoholic fatty liver disease (NAFLD) patients, which is associated with dyslipidemia, obesity, and type 2 diabetes (SHEEDFAR et al., 2014). Moreover, *CD36* gene is involved in liver steatoses (ZHOU et al., 2008), with previous studies indicating an increase in liver steatoses in mice induced by a fat-rich diet (INOUE et al., 2005). In addition to the FFA transporter, *CD36* has an essential role in adipogenesis, mostly due to its high FA affinity (ZHOU et al., 2008). The *CD36* deletion in mice resulted in the elimination of the LXR agonistic effect on the triglycerides and FFA in the liver and surrounding tissues (ZHOU et al., 2008). Zhou et al. (2008) suggested that the *CD36* induction is related to an increase in PPARγ activation by the steatoses rather than an increase in FFA capitation. Our findings demonstrated a decrease in hepatic *CD36* expression in pigs fed SOY1.5 diet, suggesting that dietary inclusion of soybean oil altered *CD36* expression levels.

Another DEG with an activation interaction through RXRA transcriptional regulation was *CYP26A1*, a gene involved in lipid metabolism, which was negatively regulated in the SOY1.5 group. The *CYP26A1* alters fat deposition (XING et al., 2014) and takes part in the CYP450 family, thus exhibiting a fundamental role in catalytic metabolic reactions and unsaturated FA oxidation (STELZER et al., 2016).

The ESR1 TF shows a vital role in hepatic lipid and carbohydrate metabolism and is involved in the liver response to estrogen mediation (KHRISTI et al., 2019). Evaluating the changes in mice liver gene expression after the loss of the ESR1 transcription regulation, Khristi et al. (2019) demonstrated a pattern of sex-related corporal body weight gain in females. While females became obese, the males do not even reach the normal corporal body weight, thus emphasizing the ESR1 importance on lipid and carbohydrate metabolisms. Nuthikattu et al. (2019) identified the ESR1 TF as a DEG modulated by the Western diet when comparing the gene expression between female mice groups with a deficiency of low-density lipoprotein receptors in the hippocampus microvessels fed either a control or occidental diet. According to Więckowska-Gacek et al. (2021) occidental diet may cause metabolic syndromes and diseases due to several factors, including the low consumption of unsaturated FA. The ESR1 TF (nuclear) participates in several DEG-related mechanisms and effects in our study, inhibiting the RXRA TF and the NED4L DEG and activating other genes such as *MAPT, ABT,* and *ACOX2*.

Another important connection factor is the EGFR. Considering the phosphorylation effect, EGFR acts as an activation mechanism in ESR1. The EGFR gene signaling may stimulate lipid metabolism; however, when overexpressed, this gene is linked to several types of cancer, including lung cancer (STELZER et al., 2016). In liver hepatocytes of adult mice, EGFR is more pronounced and has a critical function related to the liver repair and regeneration (NATARAJAN; WAGNER; SIBILIA, 2007). Furthermore, a novel FA synthesis is involved in EGFR activation, and in cells that store and secrete lipids, lipid metabolism may be stimulated by EGFR signaling (PENROSE et al., 2016). In our study, EGFR appears to be involved in the mechanisms of phosphorylation to *AKT1* with an activation effect. In contrast, *beta-catenin* effect is of inhibition by the phosphorylation mechanism. Furthermore, the network interaction demonstrated that ESR1 inhibits the SRY-box transcription factor 9 (*SOX9*).

The *SOX9* was a DEG up-regulated in the liver of pigs fed SOY1.5 diet compared to those fed SOY3.0 diet, and relevant to NAFLD development (FENG et al., 2021). The authors suggested that SOX9 may be considered a biomarker for NAFLD because it is involved in liver metabolic diseases since NAFLD pathology involves both molecular pathways and cellular alterations (FENG et al., 2021). According to Stelzer et al. (2016) *FOXO* (*FOXO1* and *FOXO3*) promotes *SOX9* expression when the lipid levels are low, which is in agreement with our findings, given that *SOX9* expression was

down-regulated in the SOY1.5 group. Moreover, *SOX9* shows transcriptional regulation effects on the inhibition mechanism of *HNF1-beta*, *Semaphorin 3A,* and *CDK1* (p34), whereas activation effects were observed for *ABCG2, VNN1, RXRA, and KLF6* genes.

In the current study, we also highlighted the TCF8/ZEB1 TF, which represses the expression of several genes, such as the interleukin-2 (IL-2), since TCF8/ZEB1, is involved in the up-regulation of neuronal differentiation (STELZER et al., 2016). The *TCF8/ZEB1* has an inhibitory effect on myosin VI, which was down-regulated (-0.802 log2 fold change) in SOY1.5 group. Evaluating obesity/anti-obesity genes in parametrial fat cells from mutation or polymorphism in knockout *TCF8/ZEB1* mice, Saykally et al. (2009) demonstrated an association of *TCF8/ZEB1* with glucose uptake and adipose tissue accumulation.

The SREBP and TF regulate cholesterol, and along with the liver X receptor (LXR) family integrate cholesterol homeostasis with FA metabolism (SPANN; GLASS, 2013). Furthermore, SREBP and LXR may be involved in the regulation of genes involved in immune system cells (SPANN; GLASS, 2013). Herein, we found SREBP2 precursor related to some DEG, indicating the involvement of our DEG in important regulations, such as cholesterol metabolism and other essential mechanisms in the liver. This TF acts primarily by activating genes encoding key enzymes of the lipid and cholesterol biosynthetic pathway (HUA et al., 1995). In relation to the SREBP processing inhibition capacity, long-chain FA, such as eicosapentaenoic acid (EPA), docosahexaenoic acid (DHA), and arachidonic acid (AA), have a larger inhibition capacity in comparison to PUFA with smaller chains, as C18:1, C18:2, and saturated FA practically do not have effects over the SREBP processing (DECKELBAUM; WORGALL; SEO, 2006). The study of Horton et al. (2003) using transgenic mice expressing a dominant positive truncated form of SREBP2 demonstrated that SREBP2 is an activator of cholesterol biosynthesis, with stimulatory effects on genes associated with FA, and in equilibrium with regulatory proteins that limit FA biosynthesis.

In addition, SREBP plays a relevant role in the steroid metabolites, FA cell differentiation, and proliferation of T cells and natural killer (NK) cells. As reported by Kusnadi et al. (2019) SREBP are essential in factor-induced macrophage stimulation of tumor necrosis. The SREBP is associated with the activation of the immune response via the sterol metabolites from the cholesterol pathway involved in T cell proliferation (KUSNADI et al., 2019). Using mice cells induced by interleukin-2 (IL-2) and IL-12, Assman et al. (2017) reported that NK cells utilized glucose for amino acid and FA

biosynthesis at 18 hours post-stimulation (ASSMANN et al., 2017). This incorporation has been associated with the upregulation of SREBP signaling pathways, in which their target genes encode essential molecules for de novo synthesis of FA. Furthermore, SREBP may be involved in IL-8 pathway, a relevant pro-inflammatory cytokine in the modulation of the angiogenic process (WANG et al., 2014). The PUFA may act in the angiogenesis through LOX enzymes, which lead to the formation of leukotrienes (SHAO; ESPENSHADE, 2012).

Hepatic lipid and insulin induce SREBP-related adipogenesis, whereas SREBP promotes inflammatory responses, thus contributing to lipid metabolism and immune responses in the macrophages (SHAO; ESPENSHADE, 2012). The effect of SREBP depends on a variety of environmental signals, including nutritional and inflammatory factors that occur via insulin signaling (ALVES-BEZERRA; COHEN, 2018). There is evidence that liver-specific knockout of the SREBP transport protein SCAP inhibited the activity of SREBP isoforms and prevents steatosis in mice fed high-fat diet (BHATTARAI et al., 2021).

The AACS was identified as participating in the network and may be related to the mechanism of transcription regulation and the activation effect by the SREBP2 precursor TF when pigs were fed the SOY1.5 diet. The AACS plays an important role in the activation of acetoacetate to acetoacetyl-CoA, and hence may be related to the use of ketone body for FA synthesis during adipose tissue development (HASEGAWA et al., 2012). The highest expression level of this gene may be obtained in brown and white adipose tissue (STELZER et al., 2016). The AACS is an acetoacetate-specific ligase. In mice, this gene is regulated in vivo in the liver tissue when induced by hypocholesterolemic agents (HASEGAWA et al., 2012). Hasegawa et al. (2012) studied ketone bodies produced and released in the liver to produce energy in extra liver tissues along with AACS, which could be coordinated by SREBP2.

All DEG identified in the network have relevant functions and relationships with essential mechanisms in the liver. Cholesterol is crucial to the cell membrane, thus contributing to fluidity and permeability, participating in both membrane trafficking and transmembrane signaling (BHATTARAI et al., 2021). Moreover, cholesterol is indirectly related to the control of most biological functions that occur and are facilitated in the membrane. Disturbances of lipid and cholesterol metabolism in the cell are related to diseases, such as cardiovascular and metabolic disorders (BHATTARAI et al., 2021).

Our study corroborates the findings in the literature; in which FA modulate gene expression by key transcription factors in biological processes. However, studies are still limited to pigs and new approaches are needed, this study is the first work that explores the gene network to identify key TF involved in lipid metabolism and inflammatory response by transcriptome analysis from liver samples. The results found, in general, mainly related to differences found regarding the inclusion of soybean oil at different levels, in which the SOY1.5 group showed greater deposition of MUFA and PUFA in the liver compared to SOY3.0, in addition to the difference between albumin and triglycerides. This directly impacts functions associated with the lipid metabolism pathway, such as lipogenesis and adipogenesis, lipid homeostasis, and immune response both negatively and positively as seen with down-regulated and up-regulated DEG.

The liver, as a regulatory and central organ, controls lipid homeostasis through biochemical, cellular, and signaling pathways, endocrine activity, detoxification, and immunomodulation (ALVES-BEZERRA; COHEN, 2018; ZHANG et al., 2018). The detoxifying function is mainly for hazard product degradation and involves β-amyloid peptides (circulating Aβ). Furthermore, some factors such as insulin resistance hinder the detoxification process, leading to an overall increase in the Aβ level (WIĘCKOWSKA-GACEK et al., 2021). One of the first steps in AD progression refers to the appearance of pathological Aβ peptides. The Aβ peptides are related to MAPT deposits, thus causing intracellular tangles and plaque formation in blood vessels. Several physiological mechanisms in the liver regarding the Aβ removal and degradation may be related to AD progression (WIĘCKOWSKA-GACEK et al., 2021).

5.CONCLUSIONS

In this study, we identified the transcription factors RXRA, EGFR, and SREBP2 precursor as key transcription factors linked to lipid homeostasis and inflammatory response from liver transcriptome profile of animal models for human metabolic diseases fed with different levels of dietary soybean oil. The results described herein could contribute to the nutrigenomics research field that aims to elucidate dietary interventions in animal and human health, as well as to drive food technology and science.

REFERENCES

ABBAS, A. K.; LICHTMAN, A. H.; POBER, J. S. **Cellular and Molecular Immunology**. 4th. ed. [s.l.] W.B. Saunders., 2000, 2000.

ALMEIDA, V. V. et al. Effects of increasing dietary oil inclusion from different sources on growth performance, carcass and meat quality traits, and fatty acid profile in genetically lean immunocastrated male pigs. **Livestock Science**, v. 248, p. 104515, 1 jun. 2021.

AOAC. Official Method 963.15. Fat in Cacao Products Soxhlet Extrac tion Method. **AOAC**, 2006.

AOCS. Official approved procedure Am 5-04, Rapid determination of oil/fat utilizing high temperature solvent extraction. **American Oil Chemist's Society**, 2005.

BENJAMINI, Y.; HOCHBERG, Y. Controlling the False Discovery Rate: A Practical and Powerful Approach to Multiple Testing. **Journal of the Royal Statistical Society: Series B (Methodological)**, v. 57, n. 1, 1995.

BLIGH, E. G.; DYER, W. J. A rapid method of total lipid extraction and purification. **Canadian journal of biochemistry and physiology**, v. 37, n. 8, 1959.

BROWN, M. S.; RADHAKRISHNAN, A.; GOLDSTEIN, J. L. **Retrospective on Cholesterol Homeostasis: The Central Role of ScapAnnual Review of Biochemistry**, 2018. .

CALDER, P. C. **ImmunonutritionBritish Medical Journal**, 2003. .

CESAR, A. S. M. et al. Differences in the skeletal muscle transcriptome profile associated with extreme values of fatty acids content. **BMC Genomics**, p. 1–16, 2016. Disponível em: <http://dx.doi.org/10.1186/s12864-016-3306-x>.

FESSLER, M. B. **The Intracellular Cholesterol Landscape: Dynamic Integrator of the Immune ResponseTrends in Immunology**Elsevier Current Trends, , 1 dez. 2016. .

FUJII, J. et al. Identification of a mutation in porcine ryanodine receptor associated with malignant hyperthermia. **Science**, v. 253, n. 5018, 1991.

GORNALL, A. G.; BARDAWILL, C. J.; DAVID, M. M. Determination of serum

proteins by means of the biuret reaction. **The Journal of biological chemistry**, v. 177, n. 2, 1949.

HEGAZI, R. A.; WISCHMEYER, P. E. **Clinical review: Optimizing enteral nutrition for critically ill patients - a simple data-driven formulaCritical Care**, 2011. .

JUMP, D. B. et al. Polyunsaturated fatty acids inhibit S14 gene transcription in rat liver and cultured hepatocytes. **Proceedings of the National Academy of Sciences of the United States of America**, v. 90, n. 18, 1993.

JUMP, D. B. **The biochemistry of n-3 polyunsaturated fatty acidsJournal of Biological Chemistry**, 2002. .

KUSNADI, A. et al. The Cytokine TNF Promotes Transcription Factor SREBP Activity and Binding to Inflammatory Genes to Activate Macrophages and Limit Tissue Repair. **Immunity**, v. 51, n. 2, p. 241- 257.e9, 20 ago. 2019.

LANDS, B. Highly unsaturated fatty acids (HUFA) mediate and monitor food's impact on health. **Prostaglandins & Other Lipid Mediators**, v. 133, p. 4–10, 1 nov. 2017.

LEE, S. H.; LEE, J. H.; IM, S. S. **The cellular function of SCAP in metabolic signalingExperimental and Molecular Medicine**, 2020. .

LOVE, M. I.; HUBER, W.; ANDERS, S. Moderated estimation of fold change and dispersion for RNA-seq data with DESeq2. **Genome Biology**, v. 15, n. 12, 2014.

LUNNEY, J. K. **Advances in swine biomedical model genomicsInternational Journal of Biological Sciences**, 2007. .

MARTIN, C. A. et al. Ácidos graxos poliinsaturados ômega-3 e ômega-6: Importância e ocorrência em alimentos. **Revista de Nutricao**, v. 19, n. 6, 2006.

MATER, M. K. et al. Arachidonic acid inhibits lipogenic gene expression in 3T3-L1 adipocytes through a prostanoid pathway. **Journal of Lipid Research**, v. 39, n. 7, 1998.

MEDZHITOV, R.; JANEWAY, C. A. **Innate immunity: The virtues of a nonclonal system of recognitionCell**, 1997. .

MetaCore (Clarivate Analytics). , 2021. . Disponível em: <portal.genego.com>.

MI, H. et al. The PANTHER database of protein families, subfamilies, functions and pathways. **Nucleic Acids Research**, v. 33, n. DATABASE ISS., 2005.

MOGHADASIAN, M. H.; SHAHIDI, F. Fatty Acids. **International Encyclopedia of Public Health**, p. 114–122, 1 jan. 2017. Disponível em: <https://www.sciencedirect.com/science/article/pii/B9780128036785001570?via%3Dihub>. Acesso em: 2 nov. 2021.

OECD-FAO. OECD-FAO Agricultural Outlook 2021–2030. **OECD-FAO Agricultural Outlook 2021–2030**, p. 163–177, 2021.

PAN, Z. et al. Pig genome functional annotation enhances the biological interpretation of complex traits and human disease. **Nat Commun**, v. 12, 2021.

RADHAKRISHNAN, A. et al. Switch-like Control of SREBP-2 Transport Triggered by Small Changes in ER Cholesterol: A Delicate Balance. **Cell Metabolism**, v. 8, n. 6, p. 512–521, 6 dez. 2008.

ROSTAGNO, H. S. Tabelas brasileiras para aves e suínos: composição de alimentos e exigências nutricionais. **Tabelas brasileiras para aves e suínos: composição de alimentos e exigências nutricionais**, 2011.

SILVA, J. P. M. da et al. Fatty acid profile in brain and hepatic tissues from pigs supplemented with canola oil. **Revista Brasileira de Agrotecnologia**, v. 11, n. 2, 2021.

SIMOPOULOS, A. P. Importance of the omega-6/omega-3 balance in health and disease: Evolutionary aspects of diet. **World Review of Nutrition and Dietetics**, v. 102, 2011.

SUMMERS, K. M. et al. Functional Annotation of the Transcriptome of the Pig, Sus scrofa, Based Upon Network Analysis of an RNAseq Transcriptional Atlas. **Frontiers in Genetics**, v. 10, 2020.

TRINDER, P. Determination of Glucose in Blood Using Glucose Oxidase with an Alternative Oxygen Acceptor. **Annals of Clinical Biochemistry: International Journal of Laboratory Medicine**, v. 6, n. 1, 1969.

WILLIAMS, N. H.; STAHLY, T. S.; ZIMMERMAN, D. R. Effect of Chronic Immune System Activation on the Rate, Efficiency, and Composition of Growth and Lysine

Needs of Pigs Fed from 6 to 27 kg. **Journal of Animal Science**, v. 75, n. 9, 1997.

YATES, C. M.; CALDER, P. C.; ED RAINGER, G. **Pharmacology and therapeutics of omega-3 polyunsaturated fatty acids in chronic inflammatory diseasePharmacology and Therapeutics**, 2014. .

YEHUDA, S.; RABINOVITZ, S.; MOSTOFSKY, D. I. **Essential fatty acids are mediators of brain biochemistry and cognitive functionsJournal of Neuroscience Research**, 1999.

CHAPTER 4: TRANSCRIPTOME PROFILE OF SKELETAL MUSCLE AND LIVER TISSUES USING DIFFERENT SOURCES OF DIETARY FATTY ACIDS IN MALE PIGS

Simara Larissa Fanalli[1], Bruna Pereira Martins da Silva[1], Julia Dezen Gomes[2], Vivian Vezzoni Almeida[3], Felipe André Oliveira Freitas[2], Gabriel Costa Monteiro Moreira[4], Bárbara Silva-Vignato[2], Juliana Afonso[5], James M. Reecy[6], James E. Koltes[6], Dawn Koltes[6], Dorian Garrick[7], Luciana Correia de Almeida Regitano[5], Júlio César de Carvalho Baileiro[8], Flaviana Miranda[9], Luciana Freitas[9], Heidge Fukumasu[1], Gerson Barreto Mourão[2], Luiz Lehmann Coutinho[2], Severino Matias de Alencar[2], Albino Luchiari Filho[2], and Aline Silva Mello Cesar [1,2]*

[1]Faculty of Animal Science and Food Engineering, (FZEA), University of São Paulo, Pirassununga, São Paulo, Brazil

[2]Animal Science Department, Luiz de Queiroz College of Agriculture (ESALQ), University of São Paulo, Piracicaba, Brazil

[3]Department of Animal Science, College of Veterinary Medicine and Animal Science, Goiânia, Goiás, Brazil

[4]University of Liège, GIGA Medical Genomics, Unit of Animal Genomics,

[5]Embrapa Pecuária Sudeste, São Carlos, SP, Brazil

[6]Animal Science Department, Iowa State University, Ames, IA, United States

[7]AL Rae Centre for Genetics and Breeding, Massey University, Hamilton, New Zealand.

[8]College of Veterinary Medicine and Animal Science, University of São Paulo

[9]DB Genética de Suínos, Patos de Minas, MG

ABSTRACT

Pigs (*Sus scrofa*) are an animal model for metabolic diseases in humans. Pork is a source of fatty acids (FA) in the human diet, as they represent one of the most consumed meats in the world. Thus, our objective was to evaluate blood parameters and FA composition, and identify changes in gene expression in skeletal muscle and liver of immunocastrated male pigs fed a diet enriched with different FA profiles, and to identify metabolic pathways and gene networks impacted by the diets, to enlighten the mechanisms underlying this variation involved in metabolic processes and diseases. *Large White* males were randomly divided into three different dietary programs with 18 animals in each: basal diet that consisted mainly corn and soybean meal added 3% of soybean oil (SOY) or 3% canola oil (CO) or 3% fish oil (FO) for a 98-day trial period during the growing and finishing phases. RNA-sequencing was performed from the skeletal muscle and liver samples of each animal by Illumina technology and the differential gene expression analysis was performed by the DESeq2 R package. The FA profile in intramuscular fat and liver were modified by the diet, mainly in relation to polyunsaturated and saturated FA, in addition, we identified the variation in the serum concentration of Cholesterol, HDL, Total Proteins and Albumin. Sixty-five and 148 differentially expressed genes (DEG) were identified in skeletal muscle and liver between CO*vs*SOY, respectively. Pathways related to FA oxidation, regulation of lipid metabolism and pathways related metabolic and neurodegenerative diseases were enriched as being impacted by dietary treatment. Among SOY*vs*FO in skeletal muscle and liver, 531 and 143 DEG were identified respectively, with associated pathways such as, with associated pathways such as metabolic and neurodegenerative diseases, inflammatory processes and immune response networks. Between CO*vs*FO 32 DEG were identified in the skeletal muscle related to metabolism pathways, diseases, and some networks were related to immune response. Our results help to understand the behavior of genes with differential expression in metabolic pathways and gene networks, when comparing the addition of different types of oils in pig diets.

Keywords: pig model, RNA-Seq, metabolic diseases, Large White, differentially expressed genes, soybean oil, canola oil, fish oil, Huntingtin.

1. INTRODUCTION

Pigs (Sus scrofa) are monogastric animals, a widely used scientific animal model, and one of the species with great importance in world meat production (PAN et al., 2021). Pigs produce the second most consumed meat in the world (USDA, 2021). Dietary lipids can influence the quantity and quality of fatty acids (FA) present in pork products (MARTINS et al., 2018). Soybean oil is a primary source of lipids in swine diets and contains unsaturated fat (GOMES et al., 2021; BURNETT et al., 2020).

However, other lipid sources such as canola (CO) and fish oil (FO) are also used in swine diets. Consumption of soybean compared to canola oil leads to significant differences between the FA profiles, mainly for linoleic, linolenic, and oleic acids. Canola oil has approximately 7% of saturated fat content and a high ALA content (11%) (SIERRA et al., 2015), which is reflecte in increase in the ratio of unsaturated and saturated (SFA) FA in pork carcass fat (MYER et al., 1992; SIERRA et al., 2015). Fish oils contain an expected beneficial ratio of n-3 polyunsaturated fatty acids (PUFA) and the benefits involved in inflammation, lipid metabolism, and oxidative stress (ZHANG et al., 2019). Feeding pigs different mixed lipid sources, such as soy, fish, or canola, results in changes in lipid profiles that can lead to high levels of unsaturated fatty acids resulting in healthier products and a softer carcass (MARTINS et al., 2015; BENZ et al., 2011; MITCHAOTHAI et al., 2007). While the use of several different dietary lipids is known to lead to changes in swine carcasses, the optimal lipid sources for swine growth and support of human health is unclear.

The FA composition of foods affects human nutrition by altering the risk for obesity, high plasma cholesterol and cardiovascular disease. Therefore, alterations in the metabolic balance of lipid pathways in the liver and dysregulation of energy control by dietary lipid source could result in pathological conditions such as diabetes, obesity, and metabolic syndrome (SHIMIZU et al., 2015; PARK; HAN, 2019). Monounsaturated (MUFA) and PUFA have appealing functional properties, providing beneficial effects on health, such as the prevention of chronic non-communicable diseases, regulation of the immune response, reduction of the risk of atherosclerosis and reduced occurrence of type 2 diabetes (LOPES, 2010; SALGADO, 2017). Some studies have observed beneficial effects on the inflammatory system caused by the inclusion of lipids in the diet of these animals (DUAN et al., 2014; RAMAYO-CALDAS et al., 2012).

Therefore, scientific studies that allow us to improve our nutrigenomic knowledge about swine and human health through the consumption of pork are of great

importance. In this study, we aimed to evaluate changes in blood biochemical parameters, fatty acid profile in Longissimus lumborum intramuscular fat and liver, and gene expression in skeletal muscle tissue and liver tissue of immunocastrated male pigs fed diets enriched with different fatty acid profiles, and to identify metabolic pathways and process networks.

2. METHODS

All animal procedures were done and are in accord with the requirements of the Animal Care and Use Committee of Luiz de Queiroz College of Agriculture (University of São Paulo, Piracicaba, Brazil, protocol: 2018.5.1787.11.6 and number CEUA 2018-28), and followed ethical principles in animal research, according to the Guide for the Care and Use of Agricultural Animals in Agricultural Research and Teaching (FASS, 2010).

2.1 Animals

In this study, fifty-four genetically lean immunocastrated male pigs (offspring of *Large White* sires x *Large White* dams) with an average age of 71 ± 1.8 days and an average initial body weight (BW) of 28.44 ± 2.95 kg were allocated in one of three treatments in a randomized complete block design with six replicate pens per treatment and three pigs per pen. These animals were housed in an all-in/all-out double-curtain-sided building. Each pen was equipped with a three-hole dry self-feeder and a nipple drinker, allowing pigs ad libitum access to feed and water throughout the experimental period. All the animals were genotyped for the halothane mutation (RYR1 gene) according to Fujii et al. (1991); thus, pigs selected for this trial were all halothane homozygous-negative (NN). The immunocastration of the intact males occurred by the administration of two 2-mL dose of Vivax® (Pfizer Animal Health, Parkville, Australia) on day 56 (127 days of age) and day 70 (141 days of age), in accordance with the manufacturer's recommendations (ALMEIDA et al., 2021).

The experimental diet was used according to the growth and finishing phases: day 0 to 21 for grower I, day 21 to 42 for grower II, day 42 to 56 for finisher I, day 56 to 63 for finisher II, day 63 to 70 for finisher III, and day 70 to 98 for finisher IV. Dietary treatments consisted of corn-soybean meal growing-finishing diets supplemented with 3% canola oil (CO) or 3% fish oil (FO) or 3% soybean oil (SOY) (ALMEIDA et al.,

2021). The diets were formulated to reach or exceed Rostagno et al. (2011) recommendations for growing-finishing pigs. No antibiotic growth promoters were used, and all diets were provided in a meal form.

2.2 Fatty acid profile of samples

Sample collection and fatty acid profile

After 98 days on trial, all pigs were slaughtered (average final body weight of 133.9 ± 9.4 kg), and *Longissimus lumborum* muscle (LL) and liver samples were collected. The tissue samples were quickly excised, snap-frozen in liquid nitrogen, and then stored at -80oC until further analyses.

The FA profile determination was performed from the total lipid isolated from 100 g of the L. lumborum samples and 10 g from liver tissue samples using the cold extraction method by Bligh and Dyer (1959) and methylated according to the procedure outlined by AOCS (2004; Method AM 5-04). A full description of the aforementioned analyses can be found in our previous study (Almeida et al., 2021).

2.3 Blood biochemical parameters

Blood was sampled from the jugular vein four days before slaughter and immediately transferred into non-anticoagulant vacuum tubes for serum separating (Becton Dickinson Vacutainer Systems, Franklin Lakes, NJ, USA) Then, the samples were stored at room temperature for 2 hours to allow for coagulation then centrifuged at 3,000 × g for 10 min to obtain serum that was stored in duplicated 1.5-mL tubes at −20°C. Serum lipid and biochemistries were analyzed by using the Mindray BS-120 chemistry analyzer (Guangdong, China) in the Pathology Laboratory at the University of São Paulo, Pirassununga, SP, Brazil. Blood serum glucose content was quantified by the colorimetric enzymatic method according to Trinder (1969) using commercial kits (VIDA Biotecnologia S/A, Minas Gerais, Brazil), following the manufacturer's protocol. The quantification of total cholesterol and fractions was performed by enzymatic-colorimetric method, but by selective precipitation using commercial kits (Gold Analisa Diagnóstica Ltda, Belo Horizonte, Minas Gerais, Brazil), according to the manufacturer's instructions. The analysis for the determination of total proteins was performed using commercial kits (VIDA Biotecnologia S/A, Lagoa Santa, Minas Gerais, Brazil), following manufacturer's protocol with modifications described by Gornall, Bardawill, David, 1949).

2.4 Statistical analysis

Statistical analyzes to verify the differences in the FA profile of skeletal muscle and liver tissue between the diets were performed using the MIXED procedure of the SAS statistical software (SAS Inst. Inc., Cary, NC, v. 9.4), where a mixed model was adopted using the restricted maximum likelihood (REML) methodology. In the model, the block effects were assumed as a random effects and the dietary treatments as fixed effects. UNIVARIATE procedure (v. 9.4) was used to test for divergence from a normal distribution with homogeneity of residuals for each of the variables. Diagnostics of the density distribution of the Studentized Residual of the model were made with the Shapiro-Wilk test (SAS v.9.4). Significance was declared at $P < 0.05$.

For the statistical analyses to blood biochemical parameters, a mixed model was adopted, using the mixed procedure of the SAS statistical software (v.9.4). In the model, the block effects were declared as a random effect and the dietary treatments as a fixed effect. Fit to normal distribution was verified by the Shapiro-Wilk test of the Studentized residual using the UNIVARIATE procedure (v 9.4). Outliers were removed and a significance of 5% was assumed ($P < 0.05$).

2.5 RNA extraction, library preparation and sequencing

Total RNA was extracted from tissue samples using commercial RNA extraction kits (RNeasy® Mini Kit, Qiagen), according to the manufacturer instructions. With the spectrophotometer Nanodrop 1000 and Bioanalyzer, RNA quantification, purity and integrity were evaluated, respectively. All samples presented an RNA Integrity Number (RIN) higher or equal to seven. From the total RNA from each sample, 2µg were used for library preparation according to the protocol described in the TruSeq RNA Sample Preparation kit v2 guide (Illumina, San Diego, CA). The estimation of libraries average size was made with the Agilent Bioanalyzer 2100 (Agilent, Santa Clara, CA, USA) and the libraries were quantified using quantitative PCR with the KAPA Library Quantification kit (KAPA Biosystems, Foster City, CA, USA). Quantified samples were diluted and pooled (five pools of all 36 samples each), using TruSeq DNA CD Index Plate (96 indexes, 96 samples, Illumina, San Diego, CA, USA). All samples were pooled and sequenced in five lanes of a sequencing flowcell, using the TruSeq PE Cluster kit v4-cBot-HS kit (Illumina, San Diego, CA, USA), and were clustered and sequenced using HiSeq2500 equipment (Illumina, San Diego, CA, USA) with a TruSeq

SBS Kit v4-HS (200 cycles), according to manufacturer instructions. All the sequencing analyses were performed at the Genomics Center at ESALQ, localized in the Animal Biotechnology Laboratory at ESALQ – USP, Piracicaba, São Paulo, Brazil.

2.6 RNA-sequencing, quality control and alignment

Sequencing adaptors and low complexity reads were removed in an initial data filtering step by Trim Galore 0.6.5 software. Reads with Phred score higher than 33 and a length higher than 70 nucleotides were kept after trimming. Quality control and reads statistics were estimated with FASTQC version 0.11.8 software [http://www.bioinformatics.bbsrc.ac.uk/projects/fastqc/]. *Sus Scrofa* 11.1 reference assembly available at Ensembl [http://www.ensembl.org/Sus_scrofa/Info/Index]. The abundance (*read counts*) of mRNAs for all annotated genes was calculated using STAR-2.7.6a [https://currentprotocols.onlinelibrary.wiley.com/doi/abs/10.1002/0471250953.bi1114s51].

2.7 Differentially expressed genes

Differentially expressed genes (DEG) between the comparisons using the two different diets (CO *vs* SOY, SO *vs* FO and CO *vs* FO) from skeletal muscle and liver tissue were identified using the DESeq2, available at Bioconductor open-source software for bioinformatics, using a multi-factor design (LOVE; HUBER; ANDERS, 2014). Prior to statistical analysis the read count data was filtered as follows: i) genes with zero counts for all samples, that is, unexpressed genes, ii) genes with less than one read per sample on average were removed (very lowly expressed); iii) genes that were not present in at least 50% of the samples were removed (rarely expressed). Father was fit as factor in the multi-factor model. The cut-off approach performed to identify the DEG was Benjamini-Hochberg (1995) methodology, used to control false discovery rate (FDR) at 10% (CESAR et al., 2016).

2.8 Functional enrichment analysis

The enrichment analysis was performed by using the MetaCore software (Clarivate analytics). For the muscle tissue, the pathway maps were identified from the lists of 65 DEG (CO*vs*SOY), 531 DEG (SOY*vs*FO), and 32 DEG (CO*vs*FO). For the

liver tissue, the pathway maps were identified from the lists of 148 DEG (COvsSOY) and 143 DEG (SOY*vs*FO).

The functional enrichment analysis of DEG (FDR <0.10) was performed to obtain comparative networks by "analysis of a single experiment" using *Homo sapiens* genome annotation as background reference and a standard parameter of MetaCore software (Clarivate Analytics) v.21.4 build 70700, filtering for the metabolic maps: energy metabolism, lipid metabolism, steroid metabolism; cardiovascular diseases: atherosclerosis; regulation of metabolism; nutritional and metabolic diseases, and nervous system diseases.

3. RESULTS

3.1 Blood parameters and fatty acid profile

We observed that the three different dietary sources of oil altered serum concentrations of total protein (P =0.01), albumin (P <0.01), cholesterol (P =0.04) and HDL (P =0.04). Total protein and albumin levels were lower in pigs fed with SOY compared to CO or FO (P <0.01). Cholesterol and HDL were higher in pigs fed a CO diet compared to soybean or fish oils (P <0.05). Circulating concentrations of glucose, aspartate aminotransferase, globulin, TAG, LDL, and VLDL were similar across dietary treatments (P >0.05; Table 1).

Table 1: Effects of dietary treatments on blood biochemical parameters of immunocastrated male pigs

Variable	Dietary treatment			Pooled SEM[2]	P-value
	CO	FO	SOY		
Glucose (mg/dL)	86.11	89.54	83.40	5.07	0.48
Aspartate Aminotransferase (U/L)	42.72	42.88	38.13	3.01	0.21
TotalProteins (g/dL)	6.84[a]	6.82[a]	6.46[b]	0.14	0.01
Albumin (g/dL)	3.80[a]	3.87[a]	3.46[b]	0.09	<0.01
Globulin (g/dL)	3.04	2.94	3.00	0.13	0.73
Triglycerides (mg/dL)	45.67	39.78	35.70	4.89	0.13
Cholesterol (mg/dL)	99.60[a]	90.34[b]	96.49[b]	3.72	0.04
HDL (mg/dL)	45.59[a]	40.11[b]	43.66[b]	2.21	0.04
LDL (mg/dL)	44.89	42.28	45.71	2.53	0.38
VLDL (mg/dL)	9.11	7.94	7.13	1.00	0.14

[1]Pigs (n = 54) were fed a corn-Soybean meal diet enriched with 3% Soybean oil (SOY), Canola oil (CO), or Fish oil (FO). Values represent the least square means from 18 pigs/treatment.
[2]SEM = standard error of the least square means.
[a–b]Within a row, values without a common superscript differ (P ≤ 0.05) using Tukey's method.

The FA composition was altered (P <0.05) in the LL intramuscular fat and the liver of growing and finishing pigs (Table 2). Concentrations of palmitic acid (P <0.01), stearic acid (P <0.01), oleic acid (P <0.01), docosahexaenoic acid (P <0.01), SFA (P <0.01), MUFA (P <0.01), total n-3 PUFA (P <0.01) and n-6:n-3 PUFA ratio (P <0.01) were different across dietary treatments. Considering all FA, there were differences in the FO treatment compared to either SOY or CO. The FA palmitic acid (P <0.01), stearic acid (P <0.01), eicosapentaenoic acid (P <0.01), docosahexaenoic acid (P <0.01), SFA (P = <0.01) and total n-3 PUFA (P = <0.01) they were elevated in LL considering the FO dietary treatment. The FO dietary treatment decreased oleic acid (P <0.01), MUFA (P = <0.01), and n-6:n-3 PUFA ratio (P <0.01).

Table 2: Effects of dietary treatments on the *Longissimus lumborum* intramuscular FA profile of immunocastrated male pigs.

	Dietary treatment			**Pooled SEM[2]**	***P*-value**
Fatty acid (%)	**CO**	**FO**	**SOY**		
Saturated fatty acid (SFA)					
Myristic acid (C14:0)	1.21	1.24	1.20	0.03	0.64
Palmitic acid (C16:0)	24.95[a]	26.43[b]	25.05[a]	0.35	<0.01
Stearic acid (C18:0)	11.28[a]	12.63[b]	11.83[ab]	0.30	<0.01
Monounsaturated fatty acid (MUFA)					
Palmitoleic acid (C16:1)	3.05	3.22	3.18	0.11	0.48
Oleic acid (C18:1 n-9)	44.95[a]	40.33[b]	44.28[a]	1.04	<0.01
Eicosenoic acid (C20:1 n-9)	0.58	0.56	0.55	0.02	0.52
Polyunsaturated fatty acid (PUFA)					
Linoleic acid (C18:2 n-6)	13.33	14.21	13.14	0.70	0.42
Alpha-linolenic acid (C18:3 n-3)	0.53	0.56	0.57	0.04	0.76
Eicosapentaenoic acid (C20:5 n-3)	0.09[a]	0.46[b]	0.15[a]	0.05	<0.01
Docosahexaenoic acid (C22:6 n-3)	0.11[a]	0.61[b]	0.15[a]	0.05	<0.01
Total SFA	37.44[a]	40.29[b]	38.08[a]	0.59	<0.01
Total MUFA	48.59[a]	44.11[b]	47.84[a]	1.11	<0.01
Total PUFA	14.24	16.61	14.63	1.05	0.15
Total n-3 PUFA[3]	0.68[a]	1.70[b]	0.83[a]	0.12	<0.01

Total n-6 PUFA[4]	13.33	14.21	13.14	0.70	0.42
PUFA:SFA ratio[5]	0.39	0.41	0.38	0.03	0.73
n-6:n-3 PUFA ratio[6]	22.48[a]	8.96[b]	17.19[c]	1.14	<0.01
Atherogenic index[7]	0.48[a]	0.53[b]	0.48[a]	0.01	0.02

[1]Pigs (*n* = 54) were fed a corn-Soybean meal diet enriched with 3% Canola oil or 3% Fish oil or 3% Soybean oil (SOY). Values represent the least square means from 18 pigs/treatment.
[2]SEM = standard error of the least square means.
[3]Total n-3 PUFA = {[C18:3 n-3] + [C20:5 n-3] + [C22:6 n-3]}.
[4]Total n-6 PUFA = C18:2 n-6.
[5]PUFA:SFA ratio = total PUFA/total SFA.
[6]Σ n-6/Σ n-3 PUFA ratio.
[7]Atherogenic index = (4 × [C14:0]) + (C16:0)/(total MUFA] + [total PUFA]), where brackets indicate concentrations (Ulbricht and Southgate, 1991).
[a,b,c]Within a row, values without a common superscript differ (*P ≤ 0.05)* using Tukey's method (Adapted from Almeida et al., 2021).

The composition of the FA profile was also performed in the liver (Table 3). The FA eicosapentaenoic acid (P <0.01), docosahexaenoic acid (P <0.01), and total n-3 PUFA were elevated in liver according to the FO dietary treatment. The FO dietary treatment decreased n-6:n-3 PUFA ratio (P <0.01) as well as, the atherogenic index decreased in CO dietary treatment (P <0.1).

Table 3: Effects of dietary treatments on the liver FA profile of immunocastrated male pigs.

	Dietary treatment			**Pooled**	***P*-**
Fatty acid (%)	**CO**	**FO**	**SOY**	**SEM[2]**	**value**
Saturated fatty acid (SFA)					
Myristic acid (C14:0)	0.91[ab]	0.78[a]	0.98[b]	0.06	0.02
Palmitic acid (C16:0)	21.96	21.61	22.98	0.43	0.06
Stearic acid (C18:0)	23.52	23.92	21.28	1.30	0.28
Monounsaturated fatty acid (MUFA)					
Palmitoleic acid (C16:1)	0.78	0.85	0.93	0.07	0.30
Oleic acid (C18:1 n-9)	24.40[ab]	23.08[a]	27.78[b]	1.27	0.28
Polyunsaturated fatty acid (PUFA)					
Linoleic acid (C18:2 n-6)	24.96	22.76	23.64	0.65	0.06
Alpha-linolenic acid (C18:3 n-3)	1.24	1.05	1.17	0.10	0.36
Eicosapentaenoic acid (C20:5 n-3, EPA)	0.66[a]	1.88[b]	0.27[a]	0.19	<0.01
Docosahexaenoic acid (C22:6 n-3, DHA)	1.69[a]	4.09[b]	0.98[a]	0.39	<0.01
Total SFA	45.14	46.31	45.24	1.14	0.69
Total MUFA	25.17[ab]	23.92[a]	28.71[b]	1.30	0.02
Total PUFA	28.55[a]	29.77[a]	26.06[b]	0.62	<0.01
Total n-3 PUFA[3]	3.59[a]	7.01[b]	2.42[a]	0.53	<0.01

Total n-6 PUFA[4]	24.96	22.76	23.64	0.65	0.06
PUFA:SFA ratio[5]	0.64[ab]	0.65[a]	0.58[b]	0.02	0.03
n-6:n-3 PUFA ratio[6]	8.79[a]	4.67[b]	9.90[a]	0.70	<0.01
Atherogenic index[7]	0.44[a]	0.50 [b]	0.51[b]	0.01	<0.01

[1]Pigs (n = 35) were fed a corn-Soybean meal diet enriched with 3% Canola oil (CO) or 3% Fish oil (FO) or 3% Soybean oil (SOY). Values represent the least square means from 18 pigs/treatment.
[2]SEM = standard error of the least square means.
[3]Total n-3 PUFA = {[C18:3 n-3] + [C20:5 n-3] + [C22:6 n-3]}.
[4]Total n-6 PUFA = C18:2 n-6.
[5]PUFA:SFA ratio = total PUFA/total SFA.
[6]Σ n-6/Σ n-3 PUFA ratio.
[7]Atherogenic index = (4 × [C14:0]) + (C16:0)/(total MUFA] + [total PUFA]), where brackets indicate concentrations (Ulbricht and Southgate, 1991).
[a–b]Within a row, values without a common superscript differ ($P \leq 0.05$) using Tukey's method.

3.2 Sequencing data and differential expression analysis

For the RNA sequencing analysis (RNA-Seq), 54 samples were used for each analyzed tissue. The average numbers of reads sequenced before and after filtering for samples from the skeletal muscle for the CO group were 33,568,010 and 33,085,594; for the SOY group were 31,955,613 and 31,491,236; and, for the FO group were 33,895,987 and 33,393,094. In the liver the CO group presented an average of 35,201,462 and 34,736,732 of reads sequenced before and after filtering; the SOY group presented 34,078,903 and 33,610,858; and, the FO group presented 34,296,605 and 33,801,914. On average 96.33 % of total read pairs were mapped against the *Sscrofa11.1* reference genome assembly (APPENDIX C - Table S1) for the tissues, considering the different diets (CO, SOY, and FO).

A total of 65 DEG (log2 fold change ≥1 or ≤−1; FDR-corrected p-value < 0.1) were identified in skeletal muscle (APPENDIX C - Table S2) between CO*vs*SOY groups, where 47 were down-regulated (log2FC ranging from -5.57 to -0.29) and 18 up-regulated (log2FC ranging 0.22 from to 3.07) in the CO group. For liver tissue (APPENDIX C - Table S2), a total of 148 DEG (log2 fold change ≥1 or ≤−1; FDR-corrected p-value < 0.1) were identified, where 108 were down-regulated (log2FC ranging from -4.71 to -0.29) and 40 up-regulated (log2FC ranging from 0.24 to 2.36) in the CO group. A total of 32 DEG (log2 fold change ≥1 or ≤−1; FDR-corrected p-value < 0.1) were identified in skeletal muscle between CO*vs*FO groups, where 21 were down-regulated (log2FC ranging from -4.84 to -0.47) and 11 up-regulated (log2FC ranging 0.50 from to 2.92) in the CO group. For liver tissue, the CO*vs*FO comparison did not result in DEG. A total of 531 DEG (log2 fold change ≥1 or ≤−1; FDR-corrected p-value < 0.1) were identified in skeletal muscle between SOY*vs*FO groups, where 406

were down-regulated (log2FC ranging from -4.99 to -0.23) and 125 up-regulated (log2FC ranging 0.21 from to 3.52) in the SOY group. For liver tissue, a total of 143 DEG (log2 fold change ≥1 or ≤−1; FDR-corrected p-value < 0.1) were identified, where 87 were down-regulated (log2FC ranging from -3.94 to -0.20) and 56 up-regulated (log2FC ranging from 0.28 to 1.94) in the SOY group. Table 4 presents a summary of the genes and the log2 fold change found between the comparisons.

Table 4. Differentially expressed genes in the skeletal muscle and liver of immunocastrated male pigs

Comparisons	**DEG[1] Down-regulated**	**log2FC[2]**	**DEG[1] Up-regulated**	**log2FC[2]**	**Total DEG[1]**
CO*vs*SOY (skeletal muscle)	47	-5.57 to -0.29	18	0.22 to 3.07	65
COvsSOY (liver)	108	-4.71 to -0.29	40	0.24 to 2.36	148
CO*vs*FO (skeletal muscle)	21	-4.84 to -0.47	11	0.50 to 2.92	32
COvsFO (liver)	-	-	-	-	-
SOY*vs*FO (skeletal muscle)	406	-4.99 to -0.23	125	0.21 to 3.53	531
SOY*vs*FO (liver)	87	-3.94 to -0.20	56	0.28 to 1.94	143

[1]Differentially Expressed Genes; [2]log2 fold change.

Figure 1 shows the Volcano plot of log2 fold change (x-axis) *vs* -log10FDR-corrected p-value (y-axis) from the differential gene expression analysis for the skeletal muscle CO*vs*SOY (A), SOY*vs*FO (B), and CO*vs*FO (C). Figure 2 shows the Volcano plot of log2 fold change (x-axis) *vs* -log10FDR-corrected p-value (y-axis) from the differential gene expression analysis for the liver tissue CO*vs*SOY (A) and SOY*vs*FO (B).

(A)

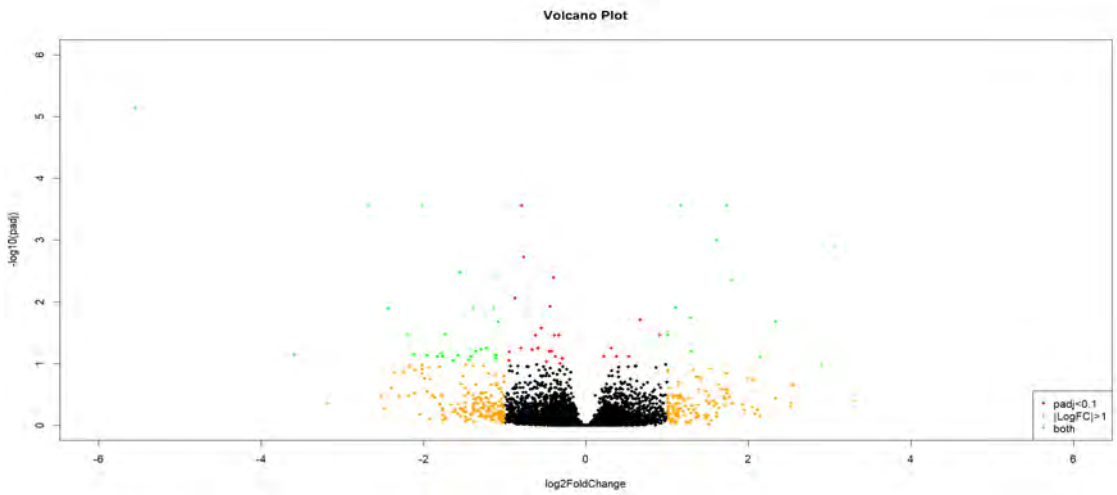

(B)

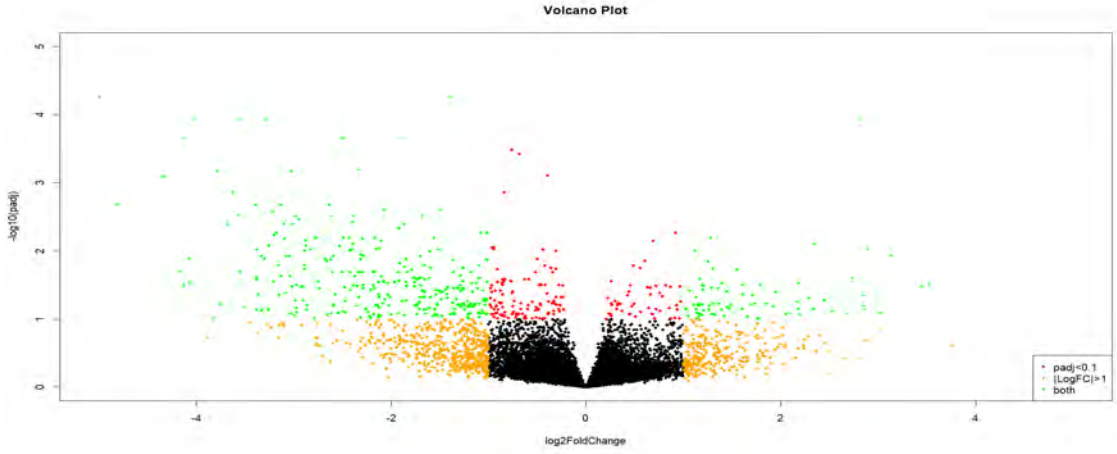

(C)

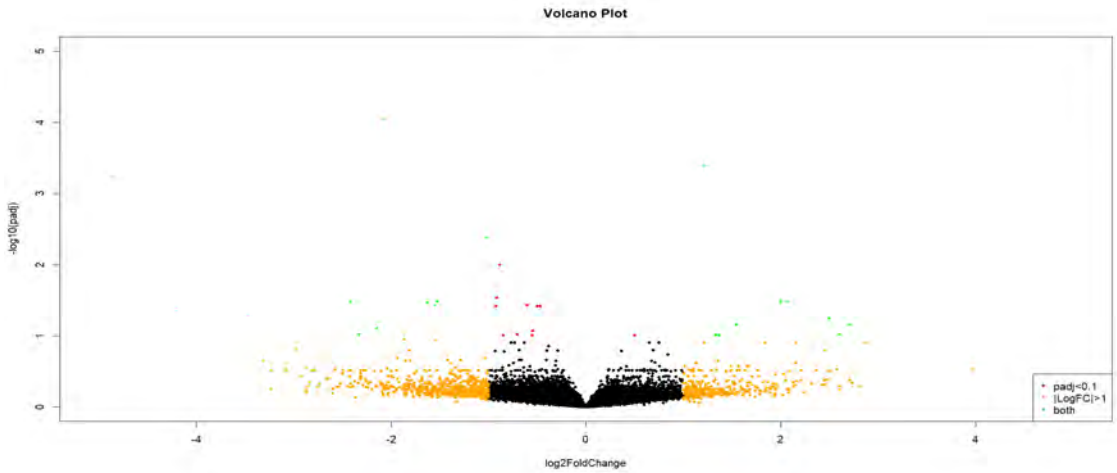

Figure 1: Volcano plot of log2 fold change (x-axis) versus -log10FDR-corrected p-value in RNA-Seq data from muscle tissue (A) CO *vs* SOY, (B) SOY *vs* FO, and (C) CO *vs* FO.

(A)

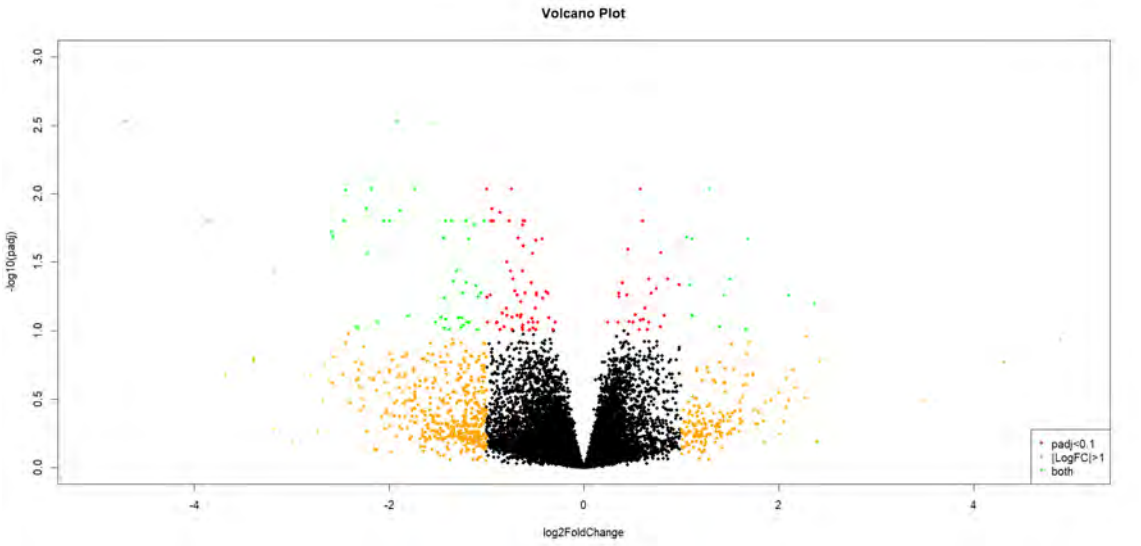

(B)

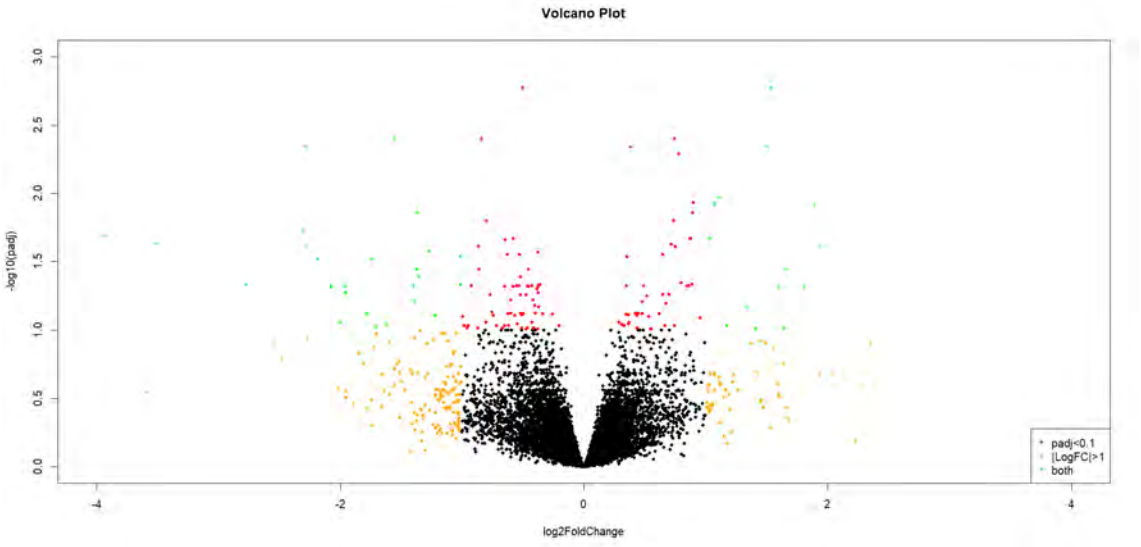

Figure 2: Volcano plot of log2 fold change (x-axis) versus -log10FDR-corrected p-value in RNA-Seq data from liver tissue (A) CO*vs*SOY and (B) SOY*vs*FO.

Twenty DEG were common among the gene expression analysis comparisons within the diets in the liver comparison (CO*vs*SOY and SOY*vs*FO) (Table 5). These results were obtained by using the compare experiments tool from MetaCore software. The comparative analysis demonstrated the majority of common DEG presented in the comparisons between CO*vs*SOY and SOY*vs*FO. In addition, some DEG present log2 fold change with little variation, such as genes belonging to the Cytochrome P450 family (*CYP2B6* -2.45 log2 fold change between CO*vs*SOY and -2.18 log2 fold change

SOvsFO; and *CYP7A1* -2.31 log2 fold change CO*vs*SOY and -2.77 log2 fold change SOY*vs*FO); *CAST* (-0.48 log2 fold change between CO*vs*SOY and -0.52 log2 fold change SOY*vs*FO); and *NGEF (*-0.60 log2 fold change CO*vs*SOY and -0.64 log2 fold change SO*vs*FO*).*

Table 5. Common differentially expressed genes between the comparisons in the liver tissue of immunocastrated male pigs fed with different FA profiles

Gene	**Gene name**	**CO*vs*SOY[1]**	**SOY*vs*FO[1]**
ENSSSCG00000001074	Lysine-specific histone demethylase 1B *(KDM1B)*	-0.48	-0.47
ENSSSCG00000009798	N-acetyllactosaminide beta-1,3-N-acetylglucosaminyltransferase 4 *(B3GNT4)*	-1.91	-1.39
ENSSSCG00000007094	Double zinc ribbon and ankyrin repeat-containing protein 1 *(DZANK1)*	-0.55	-0.55
ENSSSCG00000016957	CD180 antigen *(CD180)*	0.74	0.89
ENSSSCG00000000981	Protein disulfide isomerase *CRELD2 (CRELD2)*	1.05	0.85
ENSSSCG00000013270	Cryptochrome-2 *(CRY2)*	-0.86	-0.67
ENSSSCG00000003006	Cytochrome P450 2B6 *(CYP2B6)*	-2.45	-2.18
ENSSSCG00000006238	Cytochrome P450 7A1*(CYP7A1)*	-2.31	-2.77
ENSSSCG00000014170	Subdomains A and C of human calpastatin domain I *(CAST)*	-0.48	-0.52
ENSSSCG00000003148	D site-binding protein (*DBP*)	-1.57	-1.27
ENSSSCG00000016295	Ephexin-1 *(NGEF)*	-0.60	-0.64
ENSSSCG00000017203	Galactokinase *(GALK1)*	0.68	0.64
ENSSSCG00000016129	G-protein coupled receptor 1 *(CMKLR2)*	-1.20	-0.95
ENSSSCG00000014903	Coiled-coil domain-containing protein 90B, mitochondrial *(CCDC90B)*	-0.42	-0.50
ENSSSCG00000018092	NADH-ubiquinone oxidoreductase chain 6 *(ND6)*	-0.92	-0.92
ENSSSCG00000017781	Peroxisomal sarcosine oxidase *(PIPOX)*	-1.12	-0.98
ENSSSCG00000015243	PR domain zinc finger protein 10 *(PRDM10)*	-0.99	-0.87
ENSSSCG00000004952	Mothers against decapentaplegic homolog 3 *(SMAD3)*	-0.31	-0.37

[1]log2 fold change

In muscle, five DEG were identified as commons between different diets sources, they are the aldehyde dehydrogenase family 3, subfamily A1 (*ALDH3A1* -1.89log2 fold change SOY*vs*FO; -2.01log2 fold change CO*vs*SOY; -2.07log2 fold change CO*vs*FO), aldehyde dehydrogenase family 3 member A2 (*ALDH3A2* -0.69log2 fold change SOY*vs*FO; -0.79log2 fold change CO*vs*SOY; -0.60log2 fold change CO*vs*FO), alpha-1,3-glucosyltransferase, (*ALG6* -0.76log2 fold change SOY*vs*FO; -

0.62log2 fold change CO*vs*SOY; -0.50log2 fold change CO*vs*FO), T-cell surface glycoprotein CD4 (*CD4* -1.36log2 fold change SOY*vs*FO; -1.55log2 fold change CO*vs*SOY; -1.52log2 fold change CO*vs*FO), and lipopolysaccharide-responsive and beige-like anchor protein (*LRBA* -0.45log2 fold change SOY*vs*FO; -0.42log2 fold change CO*vs*SOY; -0.47log2 fold change CO*vs*FO).

When the comparison is between tissues, regardless of the treatment used, an altered expression level was found in two DEG, the first one was the D-box binding PAR bZIP transcription factor (*DBP*) between SOY*vs*FO (-0.98 and -1.27log2 fold change) and CO*vs*SOY (-1.38 and -1.57log2 fold change). The second DEG was the Coiled-coil domain-containing protein 90B, mitochondria (*CCDC90B*) between SOY*vs*FO (-0.36 and -0.50log2 fold change), and CO*vs*SOY (-0.39 and -0.42log2 fold change).

3.3 Functional enrichment analysis for skeletal muscle differential expression (CO*vs*SOY)

Ten different pathway maps (Figure 3) were detected (p-value <0.10), in the functional enrichment analysis between the CO*vs*SOY diets, which are linked to the following DEG, Alcohol Dehydrogenase 7 (Class IV) (*ADH7*): "FA omega oxidation" pathway (Figure 4). Aldehyde Dehydrogenase 3 Family Member A2 (*AL3A2*, *ALDH3A2*): "FA omega oxidation" (Figure 4), "leukotriene 4 biosynthesis and metabolism", "Triacylglycerol metabolism p.1" and "oxidative stress in adipocyte dysfunction in type 2 diabetes and metabolic syndrome X" pathways (Figure 4, 5, 6, 7). The Angiopoietin 1 (*ANGPT1*); "role of adipose tissue hypoxia in obesity and type 2 diabetes" pathway (Figure 8), Nuclear receptor subfamily 0 group B member 2 (*SHP*, *NR0B2*): "Regulation of lipid metabolism RXR-dependent regulation of lipid metabolism via *PPAR, RAR* and *VDR*", "regulation of lipid metabolism FXR-dependent negative-feedback regulation of bile acids concentration", "Selective Insulin resistance in type 2 diabetes in liver", "regulation of metabolism_bile acids regulation of glucose and lipid metabolism via *FXR*" pathways (Figure 9, 10, 11, 12), and, T-Cell Surface Glycoprotein (*CD4*) DEG related to "breakdown of *CD4*+ T cell peripheral tolerance in type 1 diabetes mellitus" (Figure 11).

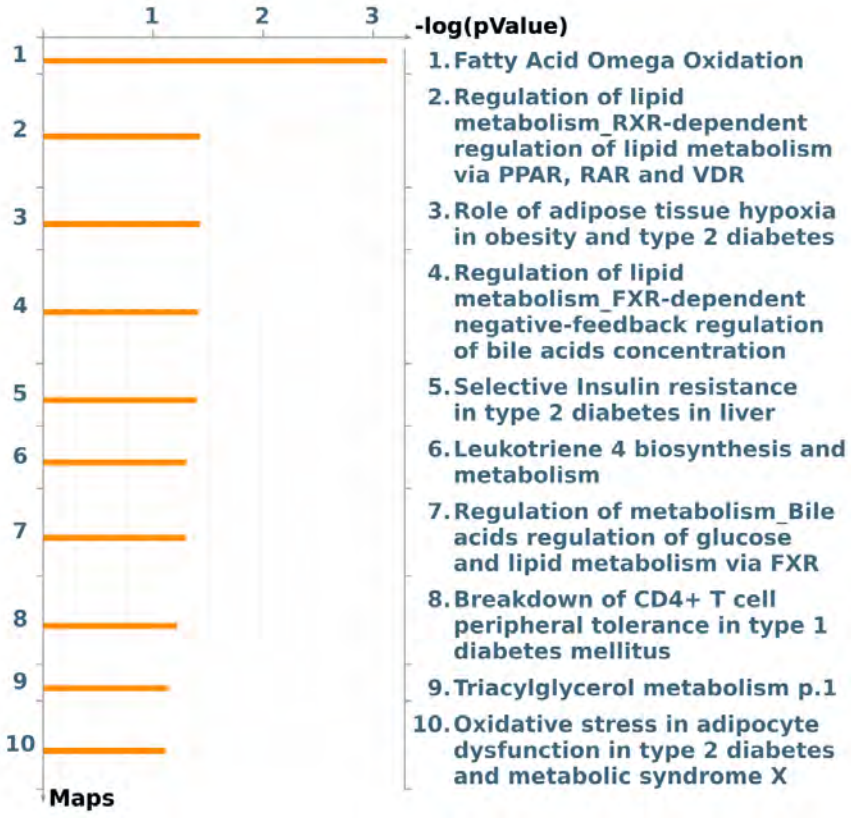

Figure 3: Pathway maps by MetaCore software (p-value < 0.1) from the list of differentially expressed genes (FDR 10%) in the skeletal muscle of immunocastrated male pigs fed with two different oil (3.0 % canola oil *vs* 3.0% soybean oil).

In our study, several DEG were identified, such as *ADH7* in skeletal muscle of pigs fed with different oils (CO*vs*SOY), which was more expressed in the CO group (log2 fold change +2.34). Another gene identified as DEG in the muscle of pigs fed different types of oil (CO*vs*SOY) was *AL3A2* (log2 fold change -0.79) less expressed in the CO group, participating in the "FA omega oxidation" ($p < 0.10$) (Figure 4) and "leukotriene 4 biosynthesis and metabolism" pathway (Figure 5). The *AL3A2* DEG was further enriched ($p<0.10$) for the "triacylglycerol metabolism" pathway (Figure 6) and identified in the "oxidative stress in adipocyte dysfunction in type 2 diabetes and metabolic syndrome X" pathway (Figure 7).

The DEG angiopoietin-1 gene *(Ang-1, ANGPT1)* was identified in our findings as less expressed (log2 fold change -1.22) in the group of animals fed CO. The enrichment analysis demonstrated its relation with the "role of adipose tissue hypoxia in obesity and type 2 diabetes" pathway (Figure 8). Another DEG was the nuclear receptor subfamily gene 0 group B member 2 (*NR0B2*) or *SHP*. Nuclear receptors (*NRs*) are a family of TF that play a critical role in different aspects in mammals as can be seen in

the pathways enriched by MetaCore analysis in Figure 9, 10, 11 and 12. In our study, *SHP* was more expressed in the CO group (log2 fold change +2.15).

Fundamental in the immune response, *CD4* was identified as DEG in the muscle of pigs fed different types of oil (CO*vs*SOY), less expressed (log2 fold change -1.55) in the CO group. It is involved in "breakdown of *CD4*+ T cell peripheral tolerance in type 1 diabetes mellitus" (Figure 13) pathway map, enriched by MetaCore.

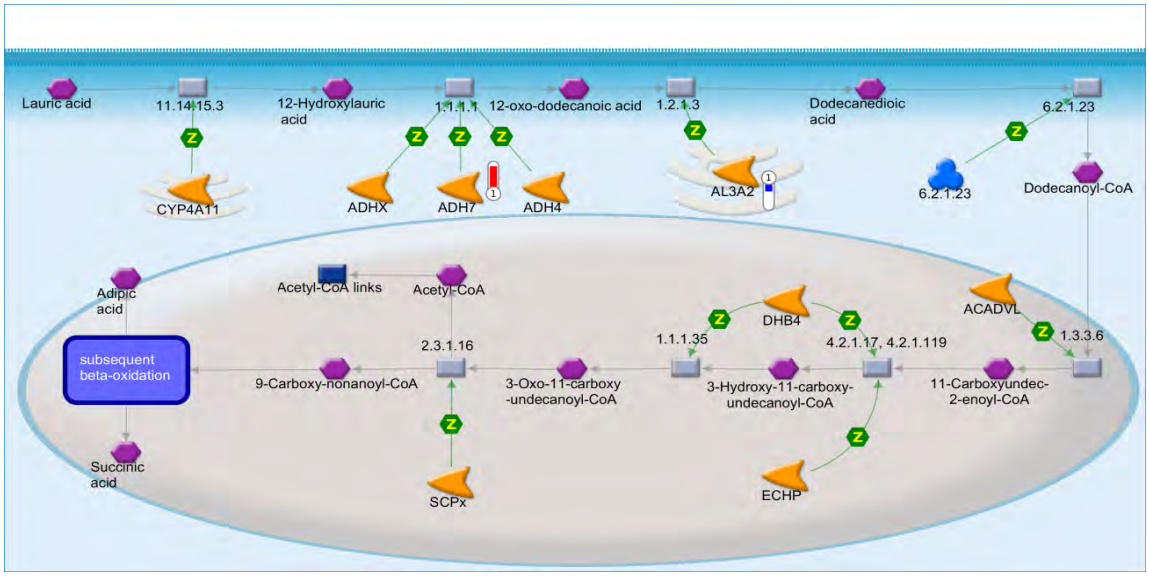

Figure 4: Fatty Acid Omega Oxidation pathway map by MetaCore software (p-value < 0.1) from the list of differentially expressed genes (FDR 10%) in the skeletal muscle immunocastrated male pigs fed with two different oil in the diet (3.0 % canola oil and 3.0 % soybean oil). The blue thermometer indicate that the DEG is downregulated (log2 fold change -0.79) and red thermometer indicate that the DEG is up-regulated (log2 fold change +2.37) in the diet with 3.0 % of canola oil (CO). Green arrows indicate positive interaction and gray arrows indicate unspecified interaction. For a detailed definition, see https://portal.genego.com/legends/MetaCoreQuickReferenceGuide.pdf.

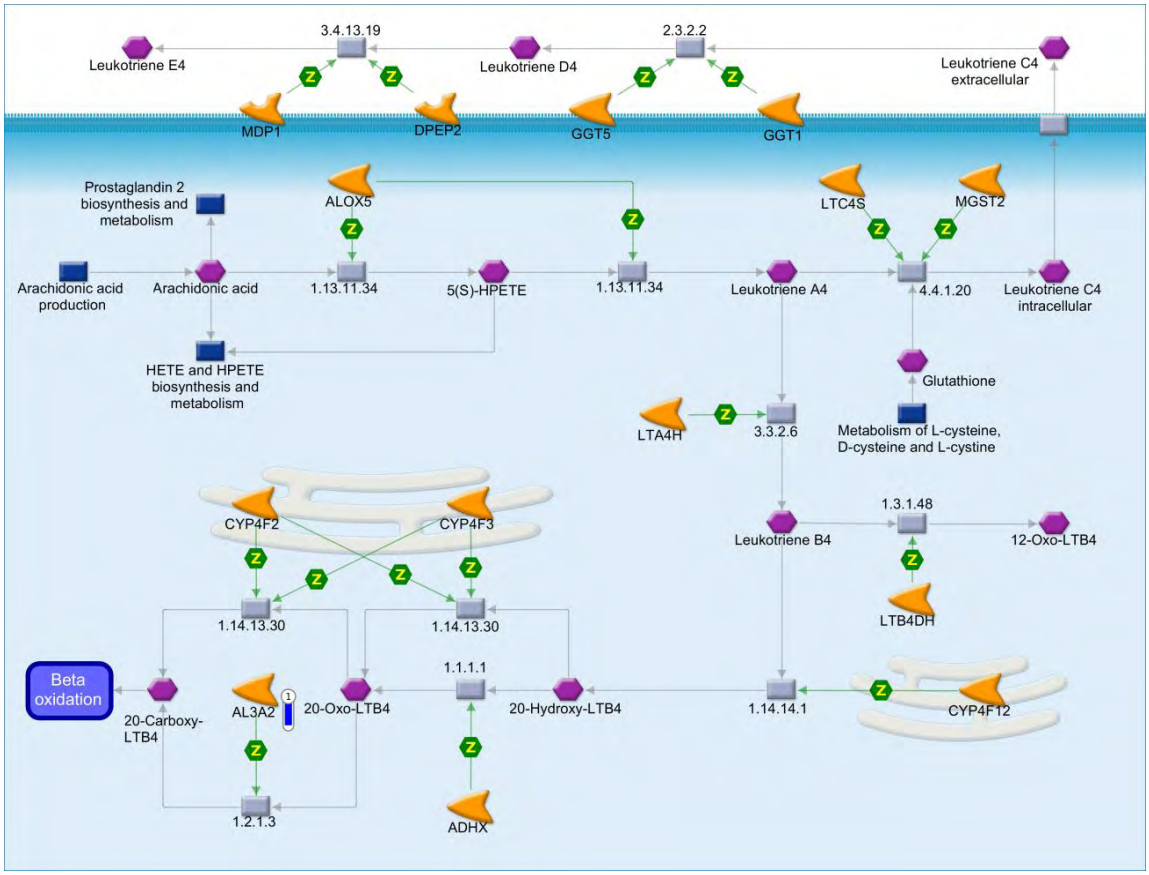

Figure 5. Leukotriene 4 biosynthesis and metabolism pathway map by MetaCore software (p-value < 0.1) from the list of differentially expressed genes (FDR 10%) in the skeletal muscle immunocastrated male pigs fed with two different oils in the diet (3.0 % canola oil and 3.0 % soybean oil). The blue thermometer indicates that the DEG is down-regulated (log2 fold change -0.79) in the diet with 3.0 % of canola oil (CO). Green arrows indicate positive interaction and gray arrows indicate unspecified interaction. For a detailed definition, see https://portal.genego.com/legends/MetaCoreQuickReferenceGuide.pdf.

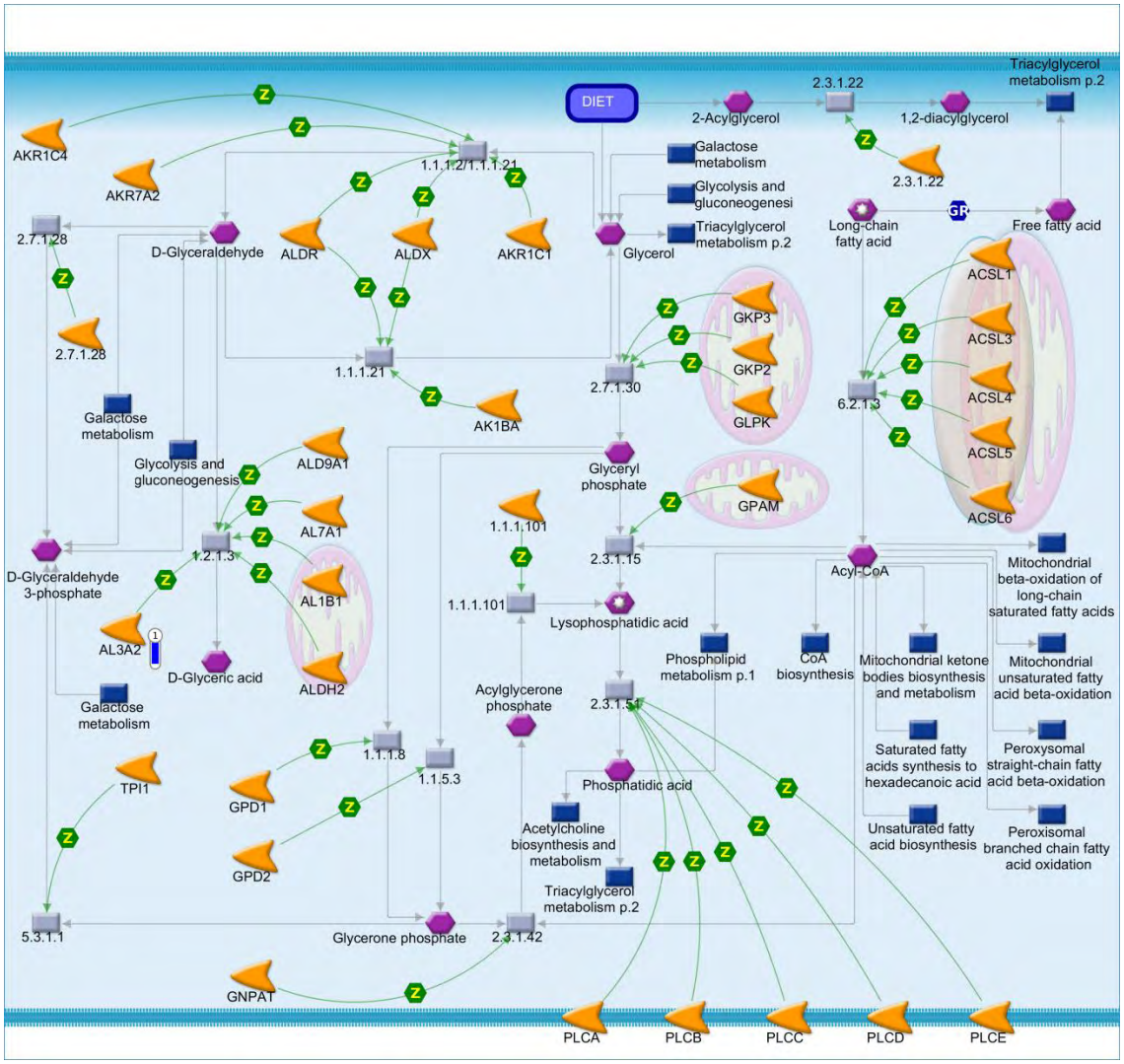

Figure 6. Triacylglycerol metabolism p.1 pathway map by MetaCore software (p-value < 0.0.101) from the list of differentially expressed genes (FDR 10%) in the skeletal muscle immunocastrated male pigs fed with two different oils in the diet (3.0 % canola oil and 3.0 % soybean oil). The blue thermometer indicates that the DEG is down-regulated (log2 fold change -0.79) in the diet with 3.0 % of canola oil (CO). Green arrows indicate positive interaction and gray arrows indicate unspecified interaction. For a detailed definition, see https://portal.genego.com/legends/MetaCoreQuickReferenceGuide.pdf.

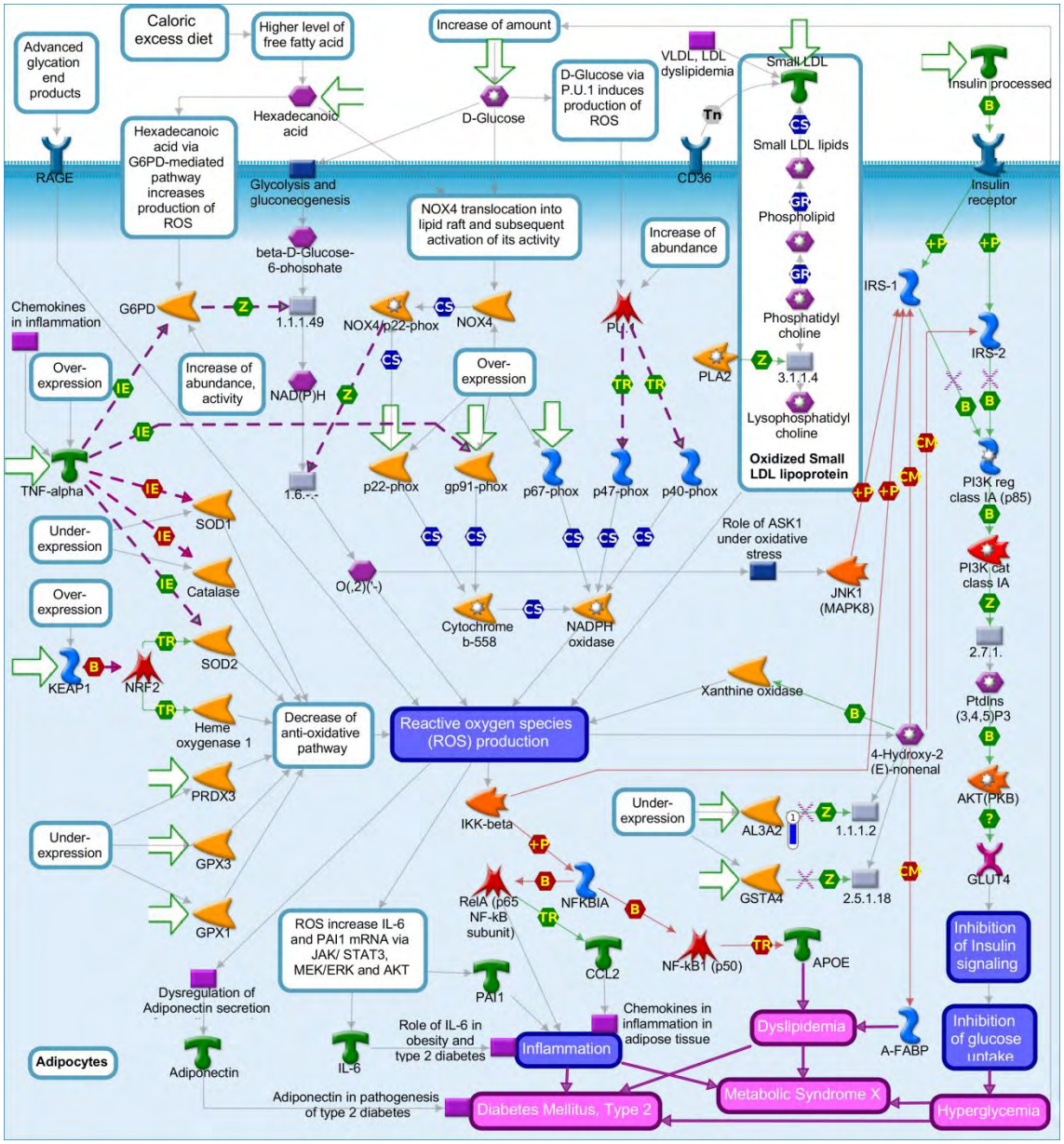

Figure 7: Oxidative stress in adipocyte dysfunction in type 2 diabetes and metabolic syndrome X pathway map by MetaCore software (p-value <0.10) from the list of differentially expressed genes (FDR 10%) in the skeletal muscle immunocastrated male pigs fed with two different oil in the diet (3.0 % canola oil and 3.0 % soybean oil). The blue thermometer indicates that the DEG is down-regulated (log2 fold change -0.79) in the diet with 3.0 % of canola oil (CO). Purple lines indicates enhancement in diseases and purple dotted line emerges in diseases. Green arrows indicate positive interaction and gray arrows indicate unspecified interaction. For a detailed definition, see https://portal.genego.com/legends/MetaCoreQuickReferenceGuide.pdf.

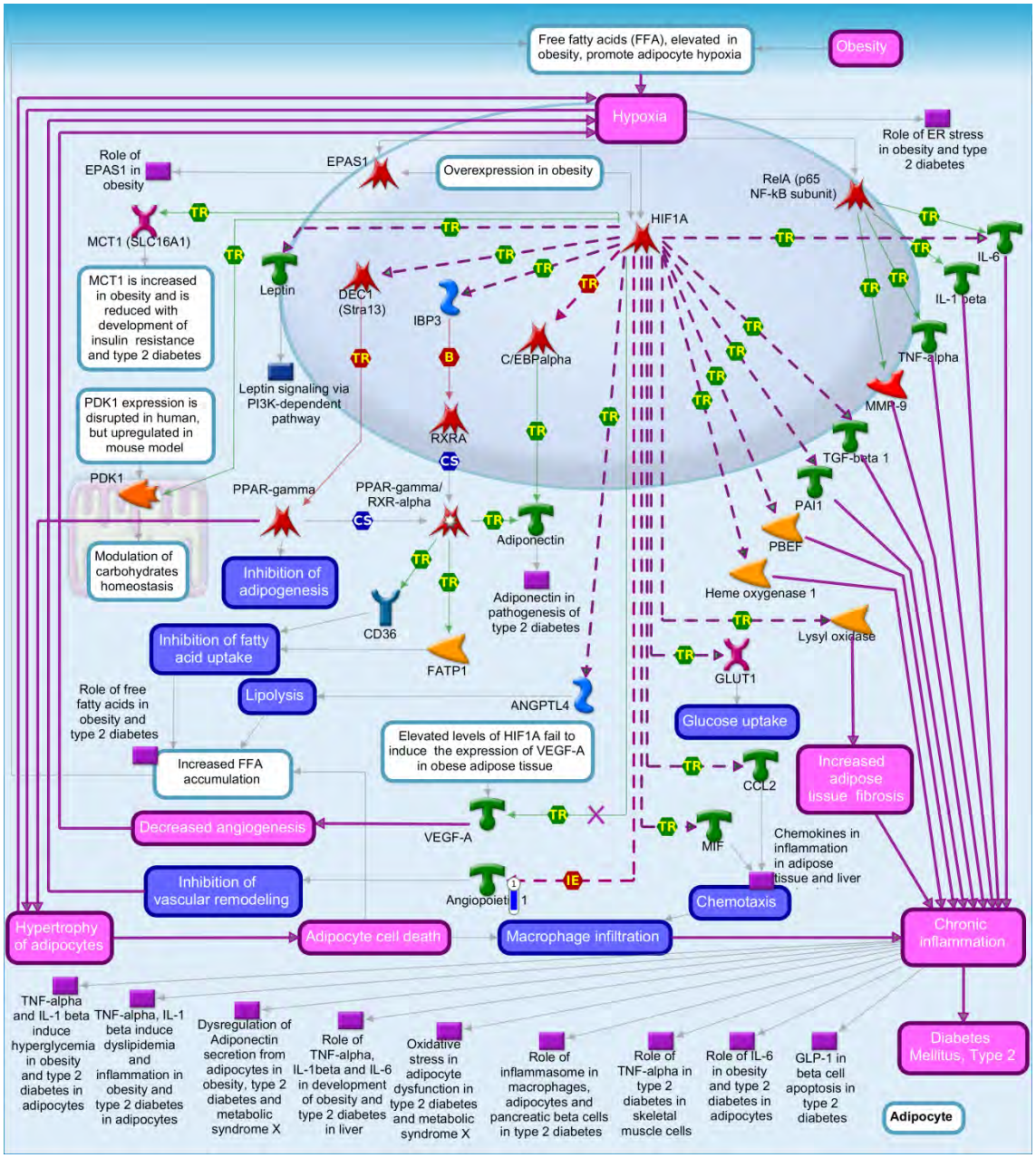

Figure 8. Role of adipose tissue hypoxia in obesity and type 2 diabetes pathway map by MetaCore software (p-value < 0.10) from the list of differentially expressed genes (FDR 10%) in the skeletal muscle immunocastrated male pigs fed with two different oil in the diet (3.0 % canola oil and 3.0 % soybean oil). The blue thermometer indicates that the DEG is down-regulated (log2 fold change -1.22) in the diet with 3.0 % of canola oil (CO). Purple lines indicates enhancement in diseases and purple dotted line emerges in diseases. Green arrows indicate positive interactions, red arrows indicate negative interaction and gray arrows indicate unspecified interaction. For a detailed definition, see https://portal.genego.com/legends/MetaCoreQuickReferenceGuide.pdf.

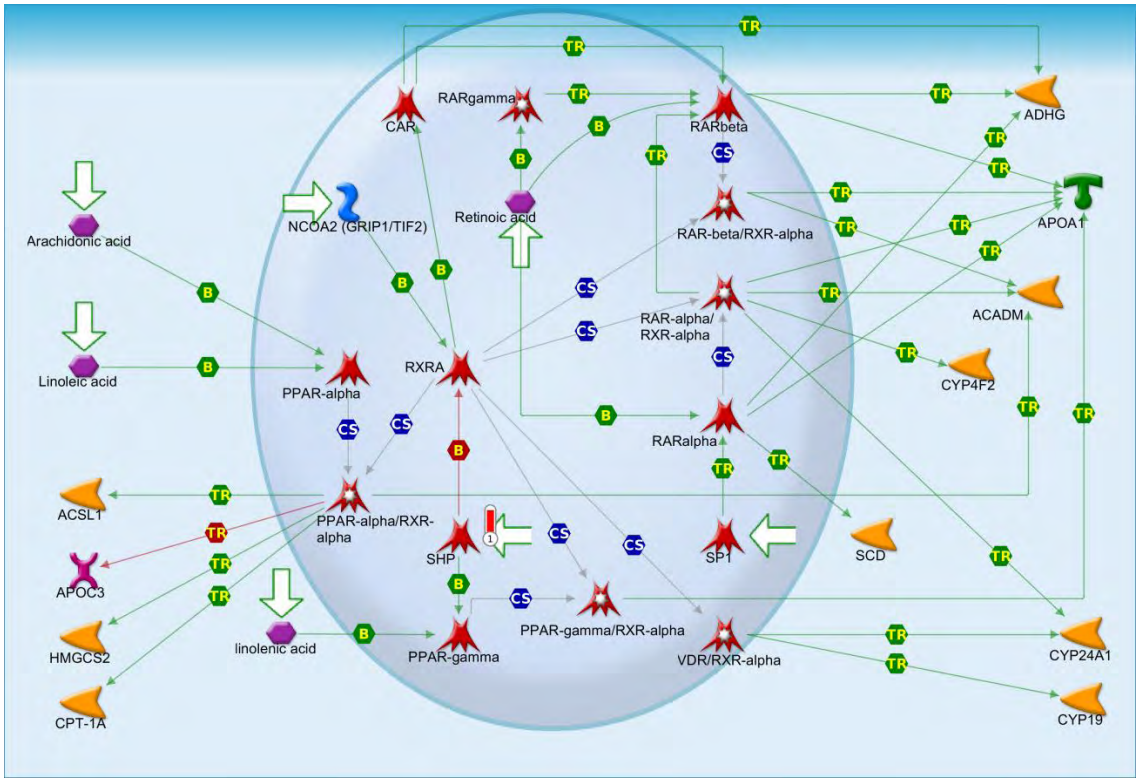

Figure 9: Regulation of lipid metabolism_RXR-dependent regulation of lipid metabolism via PPAR, RAR and VDR pathway map by MetaCore software (p-value <0.10) from the list of differentially expressed genes (FDR 10%) in the skeletal muscle immunocastrated male pigs fed with two different oil in the diet (3.0 % canola oil and 3.0 % soybean oil). The red thermometer indicate that the DEG is up-regulated (log2 fold change +2.15) in the diet with 3.0 % of canola oil (CO). Green arrows indicate positive interaction and gray arrows indicate unspecified interaction. For a detailed definition, see https://portal.genego.com/legends/MetaCoreQuickReferenceGuide.pdf.

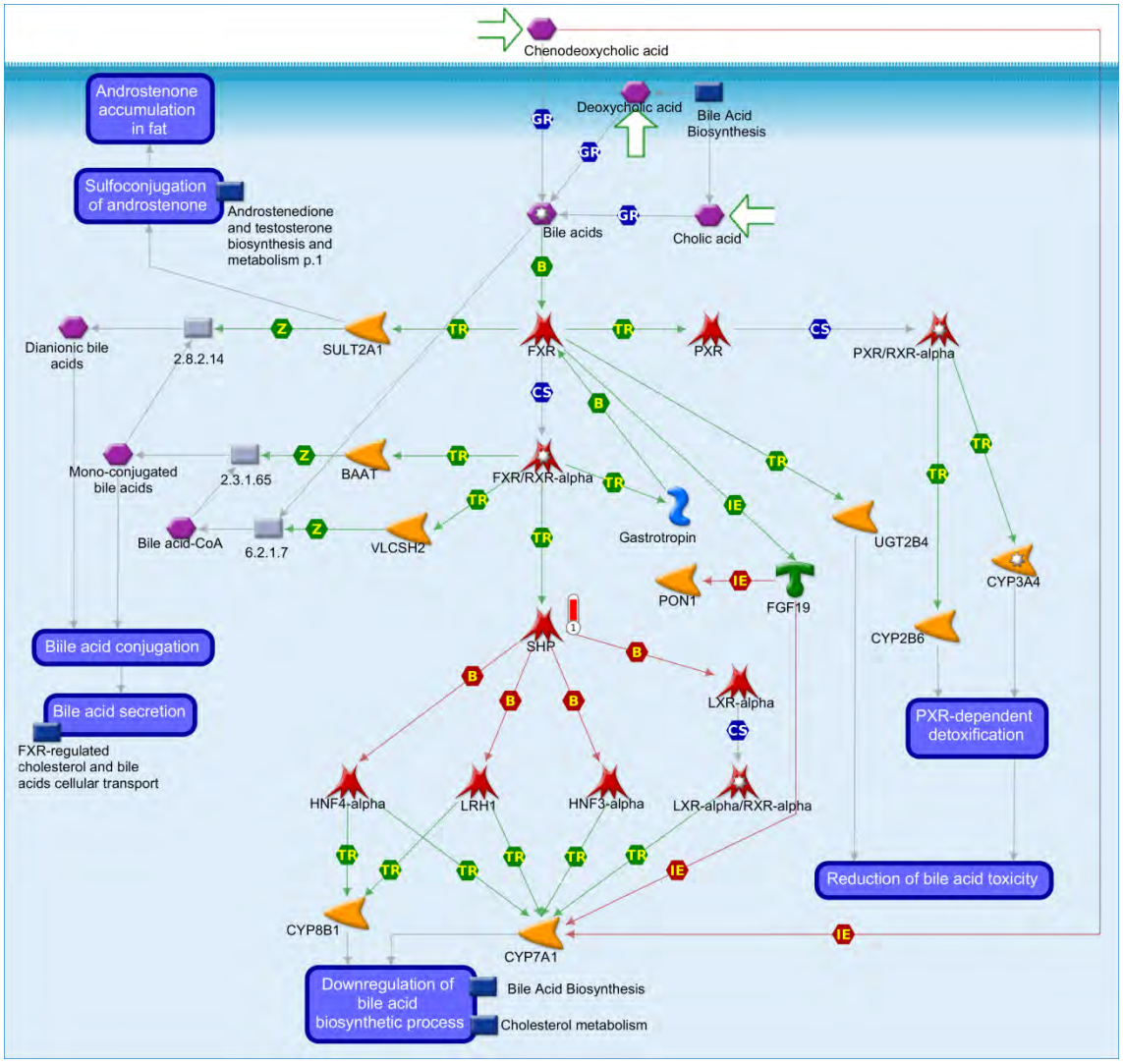

Figure 10: Regulation of lipid metabolism_FXR-dependent negative-feedback regulation of bile acids concentration pathway map by MetaCore software (p-value < 0.10) from the list of differentially expressed genes (FDR 10%) in the skeletal muscle immunocastrated male pigs fed with two different oil in the diet (3.0 % canola oil and 3.0 % soybean oil). The red thermometer indicate that the DEG is up-regulated (log2 fold change +2.15) in the diet with 3.0 % of canola oil (CO). Green arrows indicate positive interaction and gray arrows indicate unspecified interaction. For a detailed definition, see https://portal.genego.com/legends/MetaCoreQuickReferenceGuide.pdf.

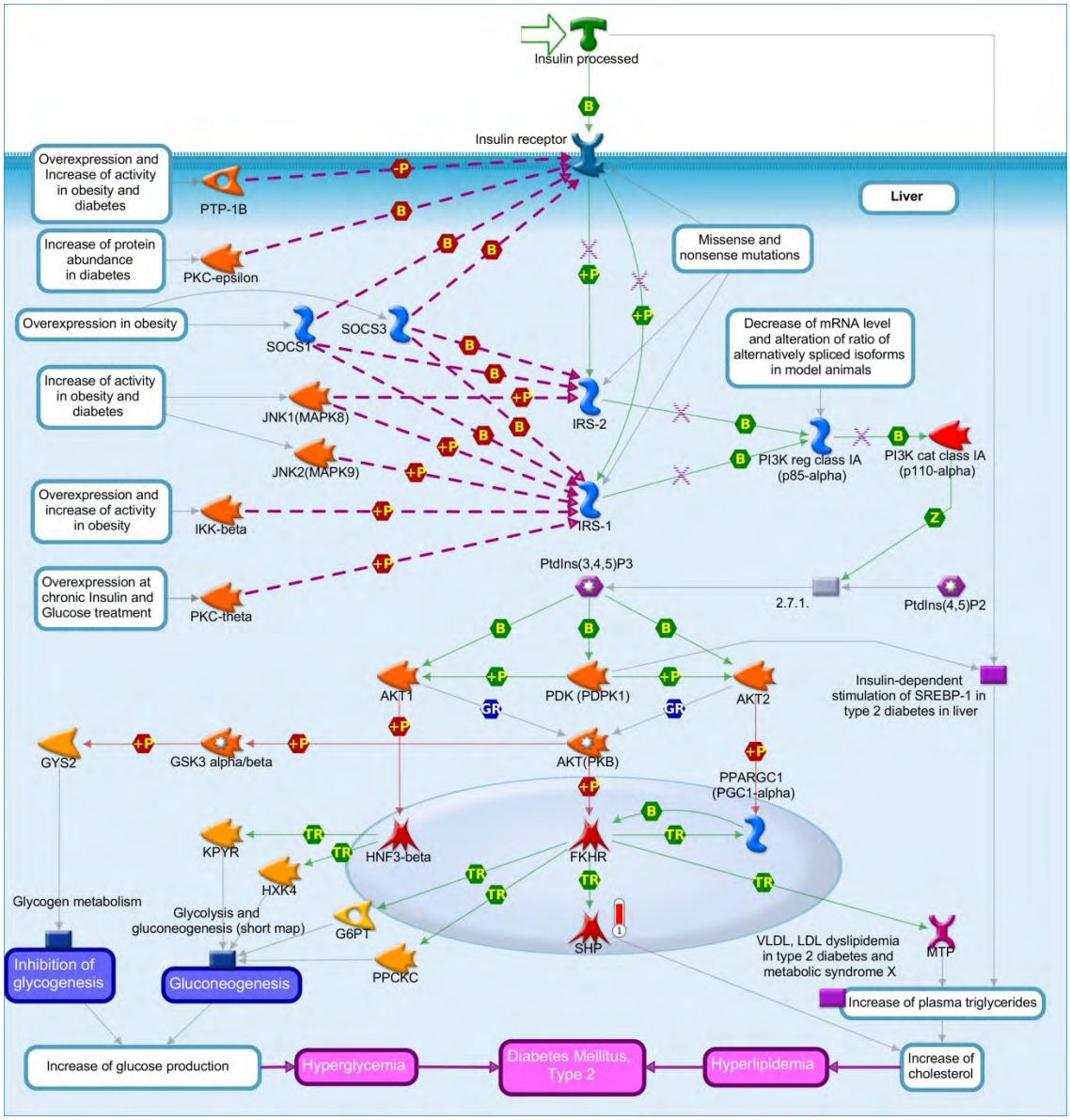

Figure 11. Selective Insulin resistance in type 2 diabetes in liver pathway map by MetaCore software (p-value < 0.10) from the list of differentially expressed genes (FDR 10%) in the skeletal muscle immunocastrated male pigs fed with two different oil in the diet (3.0 % canola oil and 3.0 % soybean oil). The red thermometer indicate that the DEG is up-regulated (log2 fold change +2.15) in the diet with 3.0 % of canola oil (CO). Purple lines indicates enhancement in diseases and purple dotted line emerges in diseases. Green arrows indicate positive interactions, red arrows indicate negative interaction and gray arrows indicate unspecified interaction. For a detailed definition, see https://portal.genego.com/legends/MetaCoreQuickReferenceGuide.pdf.

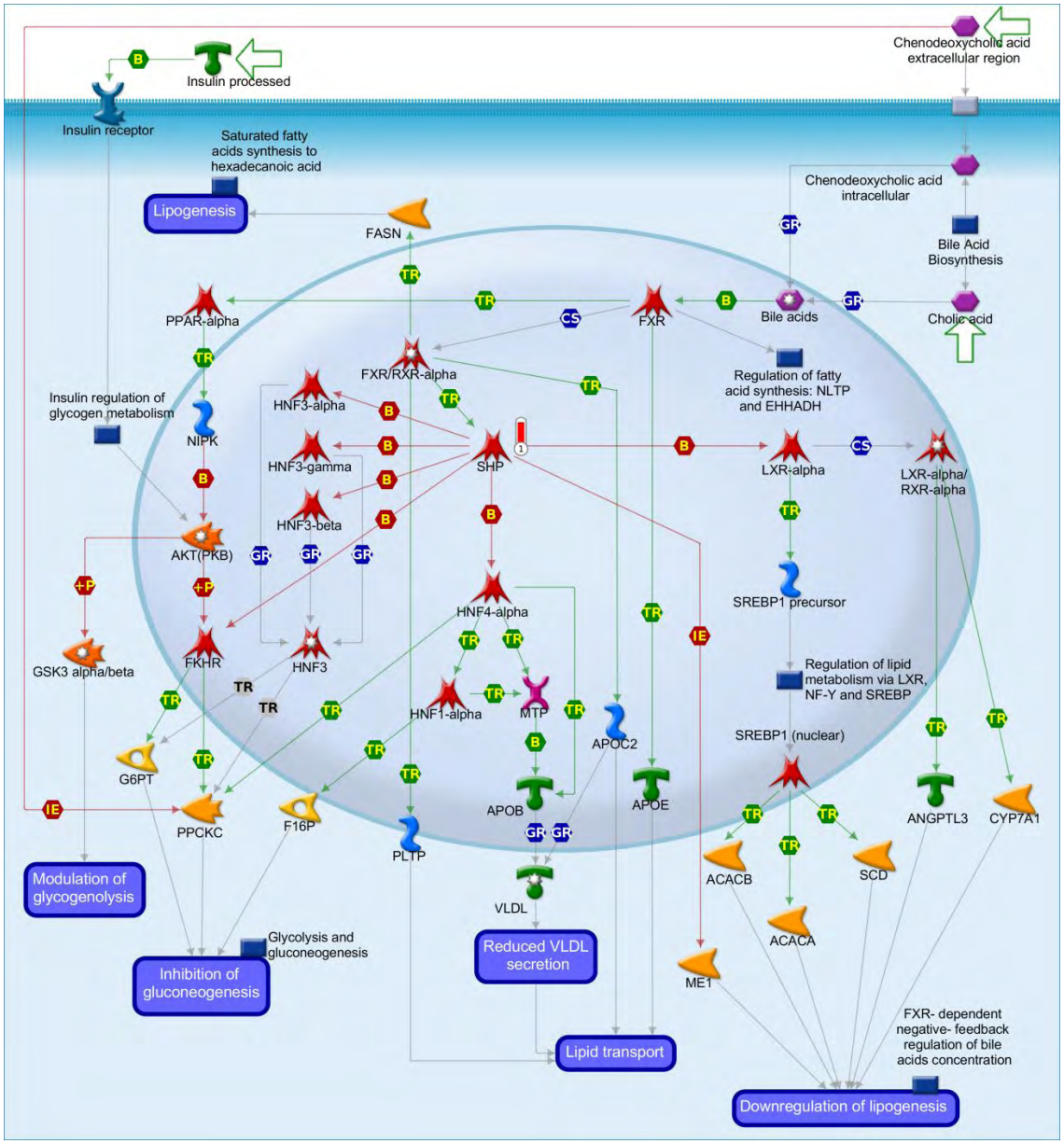

Figure 12. Regulation of metabolism_Bile acids regulation of glucose and lipid metabolism via FXR pathway map by MetaCore software (p-value < 0.10) from the list of differentially expressed genes (FDR 10%) in the skeletal muscle immunocastrated male pigs fed with two different oil in the diet (3.0 % canola oil and 3.0 % soybean oil). The red thermometer indicate that the DEG is up-regulated (log2 fold change +2.15) in the diet with 3.0 % of canola oil (CO). Green arrows indicate positive interaction and gray arrows indicate unspecified interaction. For a detailed definition, see https://portal.genego.com/legends/MetaCoreQuickReferenceGuide.pdf.

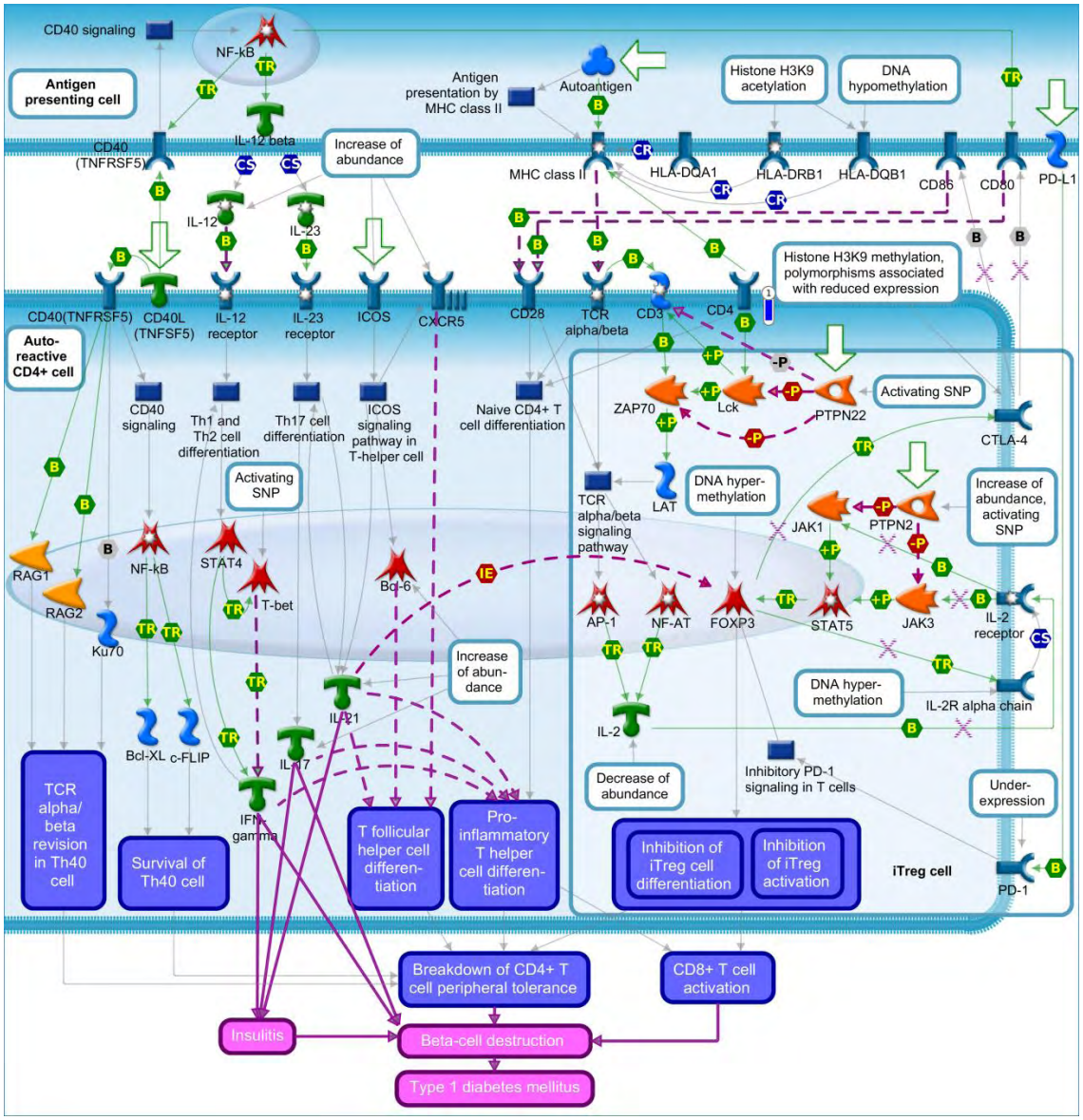

Figure 13. Breakdown of CD4+ T cell peripheral tolerance in type 1 diabetes mellitus pathway map by MetaCore software (p-value < 0.10) from the list of differentially expressed genes (FDR 10%) in the skeletal muscle immunocastrated male pigs fed with two different oil in the diet (3.0 % canola oil and 3.0 % soybean oil). The blue thermometer indicate that the DEG is down-regulated (log2 fold change -1.55) in the diet with 3.0 % of canola oil (CO). Purple lines indicates enhancement in diseases and purple dotted line emerges in diseases. Green arrows indicate positive interaction and gray arrows indicate unspecified interaction. For a detailed definition, see https://portal.genego.com/legends/MetaCoreQuickReferenceGuide.pdf.

To observe the interactions of DEG in gene networks, the analysis of process networks was performed using MetaCore software (Table 6), identifying networks related (p value <0.1) to the immune response, metabolism regulation and signal transduction. The identified immune response networks “antigen presentation” was enriched for the *CD4* DEG (log2 fold change -1.55); the “transport bile acids transport and its regulation”, “regulation of bile acid metabolism and negative *FXR*-dependent regulation of bile acids concentration”, and “signal transduction_ESR2” pathways were

enriched for the nuclear receptor subfamily 0 group B member 2 (*SHP*, *NR0B2*; log2 fold change +2.15) DEG.

Table 6. Processes networks by MetaCore software (p-value <0.10) from the list of differentially expressed genes (FDR 10%) in the skeletal muscle of immunocastrated male pigs fed with different oil sources (Canola oil and Soybean oil CO*vs*SOY)

Process Networks	**P-value**	**DEG[1]**
Immune response_Antigen presentation	0.01	*CD4*
Transport_Bile acids transport and its regulation	0.07	*SHP*
Regulation of metabolism_Bile acid regulation of lipid metabolism and negative FXR-dependent regulation of bile acids concentration	0.07	*SHP*
Signal transduction_ESR2 pathway	0.08	*SHP*

[1] Differentially Expressed Genes

3.4 Functional enrichment analysis for liver differential expression (CO*vs*SOY)

In the enriched signaling pathways (p <0.10) (Table 7) we identified genes such as mitochondrial encoded *NADH* dehydrogenase 5 (*ND5 MT – ND5*) and mitochondrial encoded *NADH* dehydrogenase 6 (*MT - ND6*), present in the "*CREB1*-dependent transcription deregulation pathway in Huntington's Disease" (Figure 14); cytochrome P450 family 7 subfamily A member 1 (*CYP7A1*) and cytochrome *P450* family 2 subfamily B member 6 (*CYP2B6*) related to "regulation of lipid metabolism *FXR*-dependent negative-feedback regulation of bile acids concentration" (Figure 15), monoacylglycerol O-acyltransferase 2 (*MOGAT2*) in "triacylglycerol biosynthesis in obesity and diabetes mellitus, type II" pathway (Figure 16), the neuronal guanine nucleotide exchange factor *NGEF/Ephexin* gene in the "Huntingtin-dependent transcription deregulation pathway in Huntington's Disease" (Figure 17), the cytochrome *P450* family 4 subfamily A member 11 (*CYP4A11*) in "FA omega oxidation" (Figure 18), and platelet glycoprotein 4 *CD36* that participates in putative pathways of "oleic acid sensing in ventromedial hypothalamus in obesity (rodent model)" (Figure 19), and "role of adipose tissue hypoxia in obesity and type 2 diabetes" (Figure 20).

Table 7: Pathway maps by MetaCore software (p-value <0.1) from the list of differentially expressed genes (FDR 10%) in the liver of immunocastrated male pigs fed with different oil sources

Pathway maps	***P-value***	**DEG[1]**
"CREB1-dependent transcription deregulation in Huntington's Disease"	0.01	*MT-ND6, MT-ND5*
"Regulation of lipid metabolism_FXR-dependent negative-feedback regulation of bile acids concentration"	0.01	*CYP2B6, CYP7A1*
"Triacylglycerol biosynthesis in obesity and diabetes mellitus, type II"	0.07	*MOGAT2*
"Huntingtin-depended transcription deregulation in Huntington's Disease"	0.08	*Ephexin*
"Fatty Acid Omega Oxidation"	0.09	*CYP4A11*
"Putative pathways of Oleic acid sensing in ventromedial hypothalamus in obesity (rodent model)"	0.09	*CD36*
"Role of adipose tissue hypoxia in obesity and type 2 diabetes"	0.09	*CD36*

[1]Differentially Expressed Genes

The genes *NADH* dehydrogenase 5 (*ND5*) and *NADH* dehydrogenase *(ND6)* were identified as DEG in the liver of pigs fed different oil sources with lower expression (log2 fold change -1 and -0.93) in the CO group, and were involved in the "*CREB1* - dependent transcription deregulation in Huntington's Diseases" pathway.

The cytochrome *P450* family 7 subfamily A member 1 *(CYP7A1)* and cytochrome P450 family 2 subfamily B member 6 *(CYP2B6)* genes are members of the cytochrome P450 superfamily of enzymes. Herein, they were identified as DEG in the liver of pigs fed different sources of oil (CO*vs*SOY), with lower expression (log2 fold change -2.31 and -2.45) in pigs of the CO group, and enriched in the "lipid metabolism FXR dependent negative-feedback regulation of bile acids concentration" pathway. *MOGAT2* was identified as the lowest expressed liver DEG (log2 fold change -4.72) in pigs of the CO group. The cytochrome P450 family 4 subfamily A member 11 gene *(CYP4A11)* was identified with lower expression in diets containing CO (log2 fold change -1.25) and enriched in the "FA omega oxidation" pathway. The "FA omega oxidation" pathway was also enriched in the CO*vs*SOY comparison in the muscle tissue, presenting the *ADH7* and the *AL3A2* as DEG.

The neuronal gene guanine nucleotide exchange factor *(NGEF)* was identified as a down-regulated gene (log2 fold change -0.6) in the CO group. *NGEF* appears as *Ephexin* in the "Huntingtin-dependent transcription deregulation in Huntington's

Disease" pathway. The *CD36* gene was identified as the lowest expression DEG (log2 fold change -0.48) in a group receiving a diet with CO, and enriched in the "putative pathways of oleic acid sensing in ventromedial hypothalamus in obesity (rodent model)", and "role of adipose tissue hypoxia in obesity and type 2 diabetes" pathways.

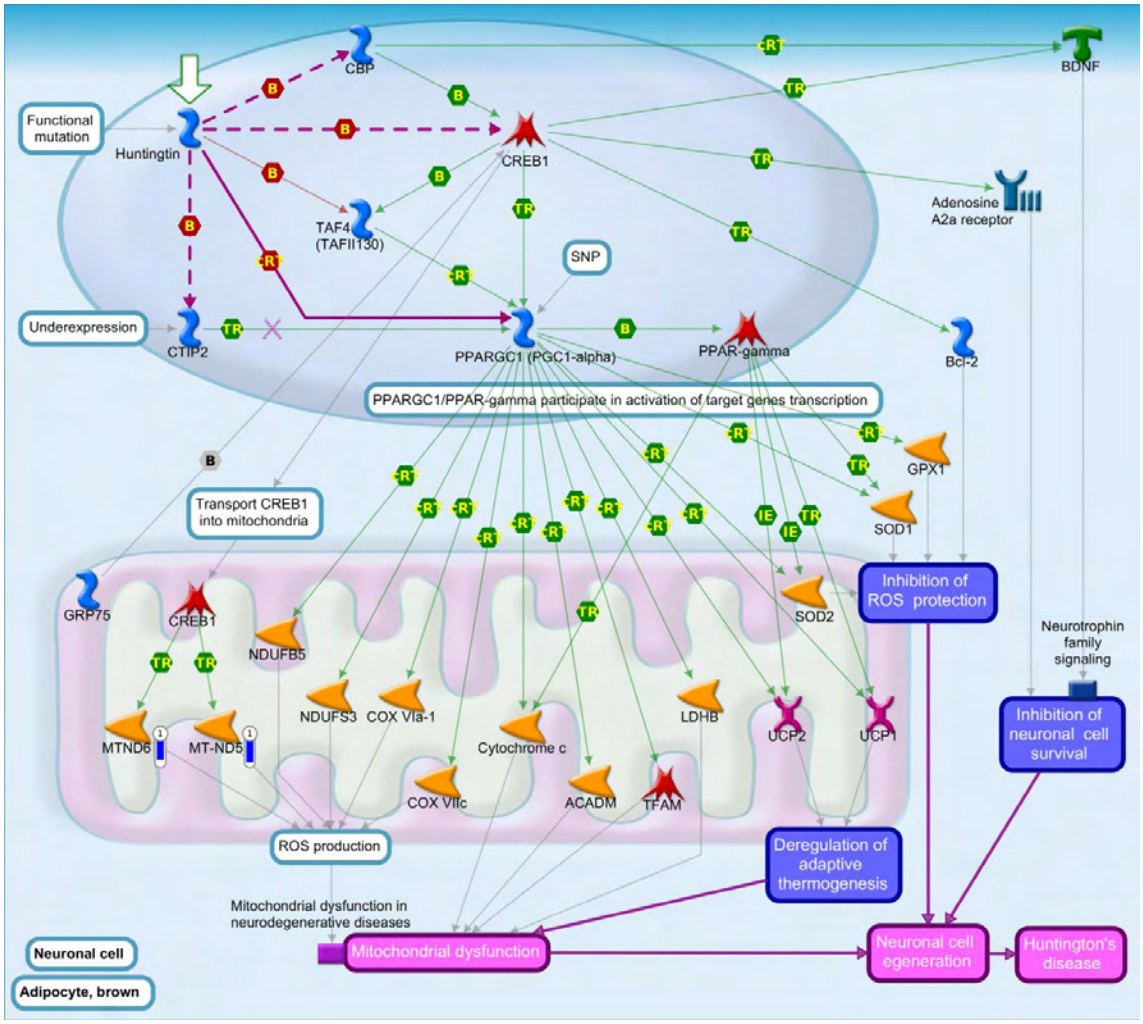

Figure 14. CREB1-dependent transcription deregulation in Huntington's Diseases pathway map by MetaCore software (p-value < 0.1) from the list of differentially expressed genes (FDR 10%) in the liver immunocastrated male pigs fed with two different oils in the diet (3.0 % canola oil and 3.0 % soybean oil). The blue thermometer indicates that the DEG is down-regulated (log2 fold change -1 and log2 fold change -0.93) in the diet with 3.0 % of canola oil (CO). Purple lines indicate enhancement in diseases and purple dotted line emerges in diseases. Green arrows indicate positive interaction and gray arrows indicate unspecified interaction. For a detailed definition, see https://portal.genego.com/legends/MetaCoreQuickReferenceGuide.pdf.

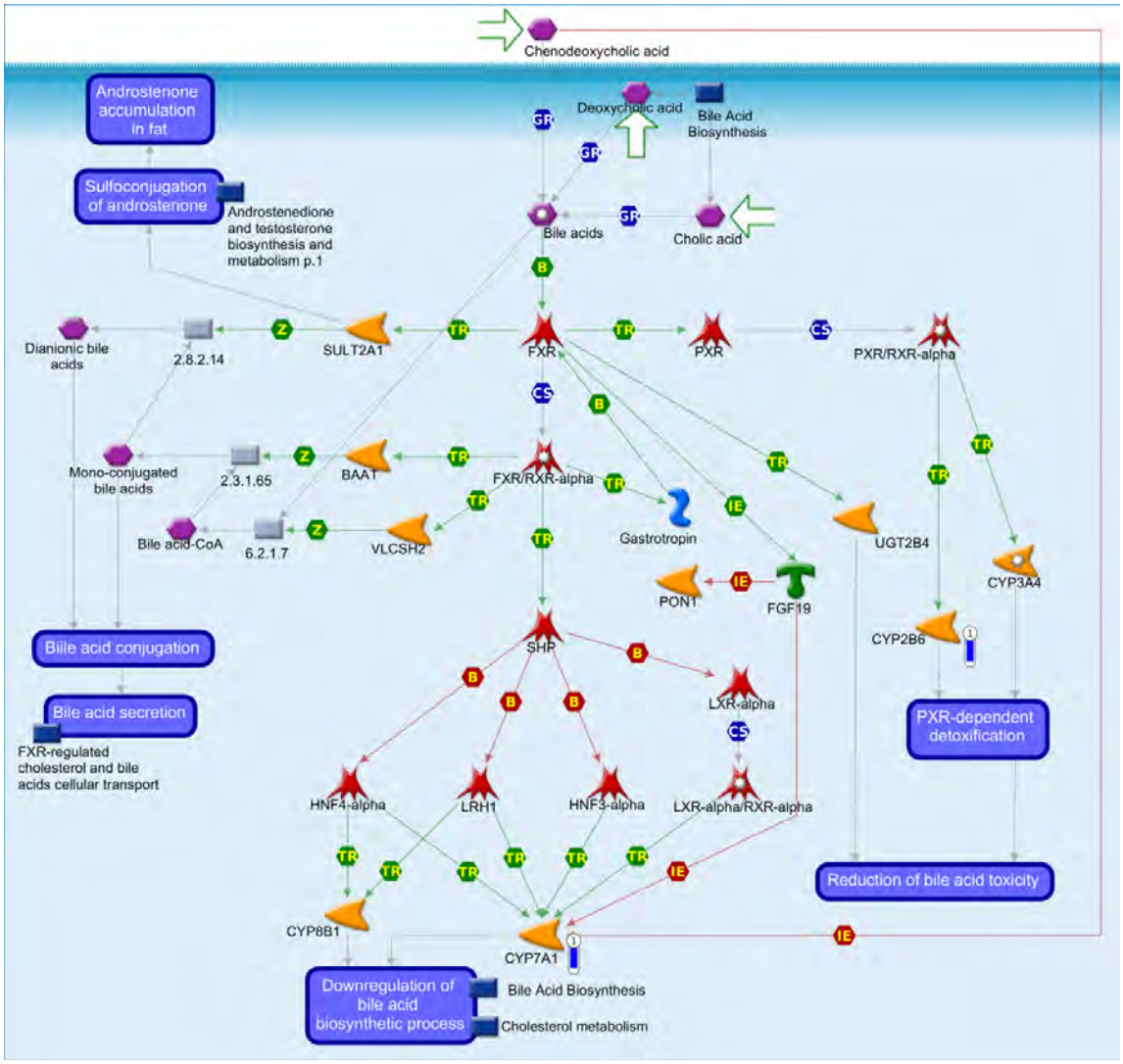

Figure 15. Regulation of lipid metabolism_FXR-dependent negative-feedback regulation of bile acids concentration pathway map by MetaCore software (p-value < 0.10) from the list of differentially expressed genes (FDR 10%) in the liver tissue immunocastrated male pigs fed with two different oils in the diet (3.0 % canola oil and 3.0 % soybean oil). The blue thermometer indicates that the DEG is down-regulated (log2 fold change -2.31 and -2.45) in the diet with 3.0 % of canola oil (CO). Green arrows indicate positive interaction and gray arrows indicate unspecified interaction. For a detailed definition, see https://portal.genego.com/legends/MetaCoreQuickReferenceGuide.pdf.

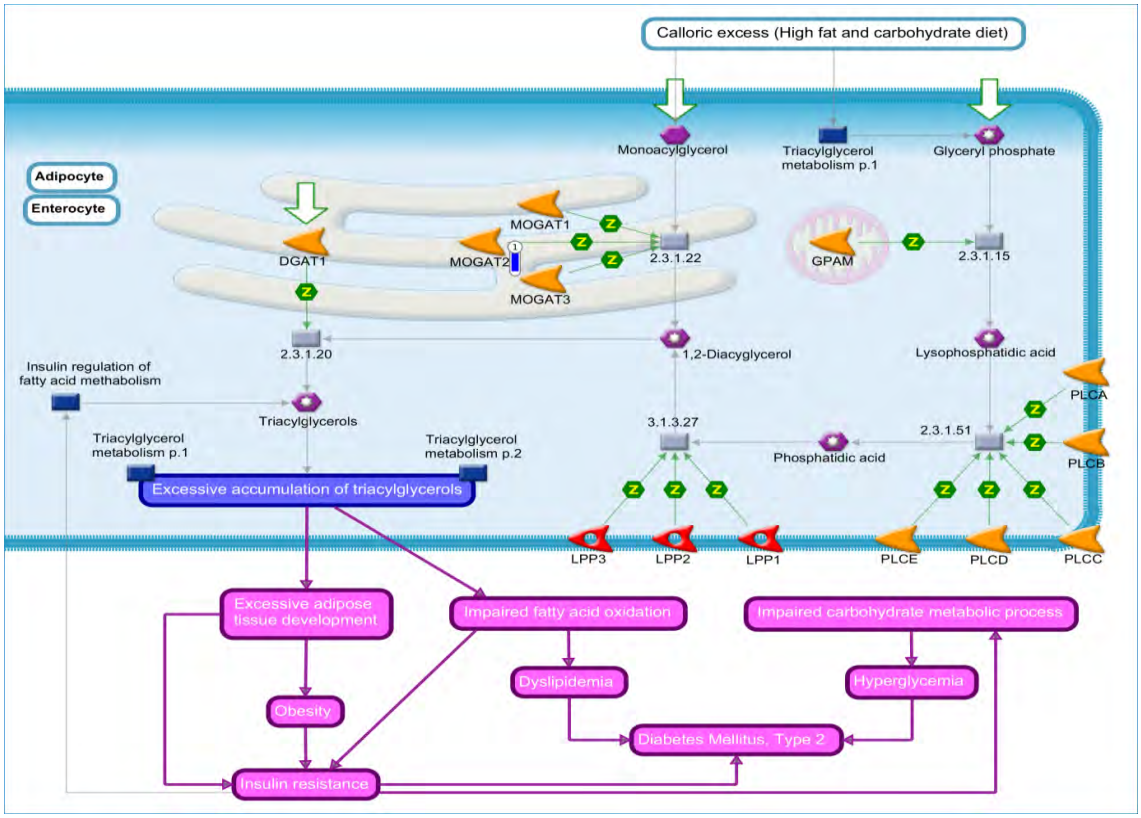

Figure 16. Triacylglycerol biosynthesis in obesity and diabetes mellitus type II pathway map by MetaCore software (p-value < 0.10) from the list of differentially expressed genes (FDR 10%) in the liver tissue immunocastrated male pigs fed with two different oil in the diet (3.0 % canola oil and 3.0 % soybean oil). The blue thermometer indicate that the DEG is down-regulated (log2 fold change -4.72) in the diet with 3.0 % of canola oil (CO). Purple lines indicates enhancement in diseases. Green arrows indicate positive interaction and gray arrows indicate unspecified interaction. For a detailed definition, see https://portal.genego.com/legends/MetaCoreQuickReferenceGuide.pdf

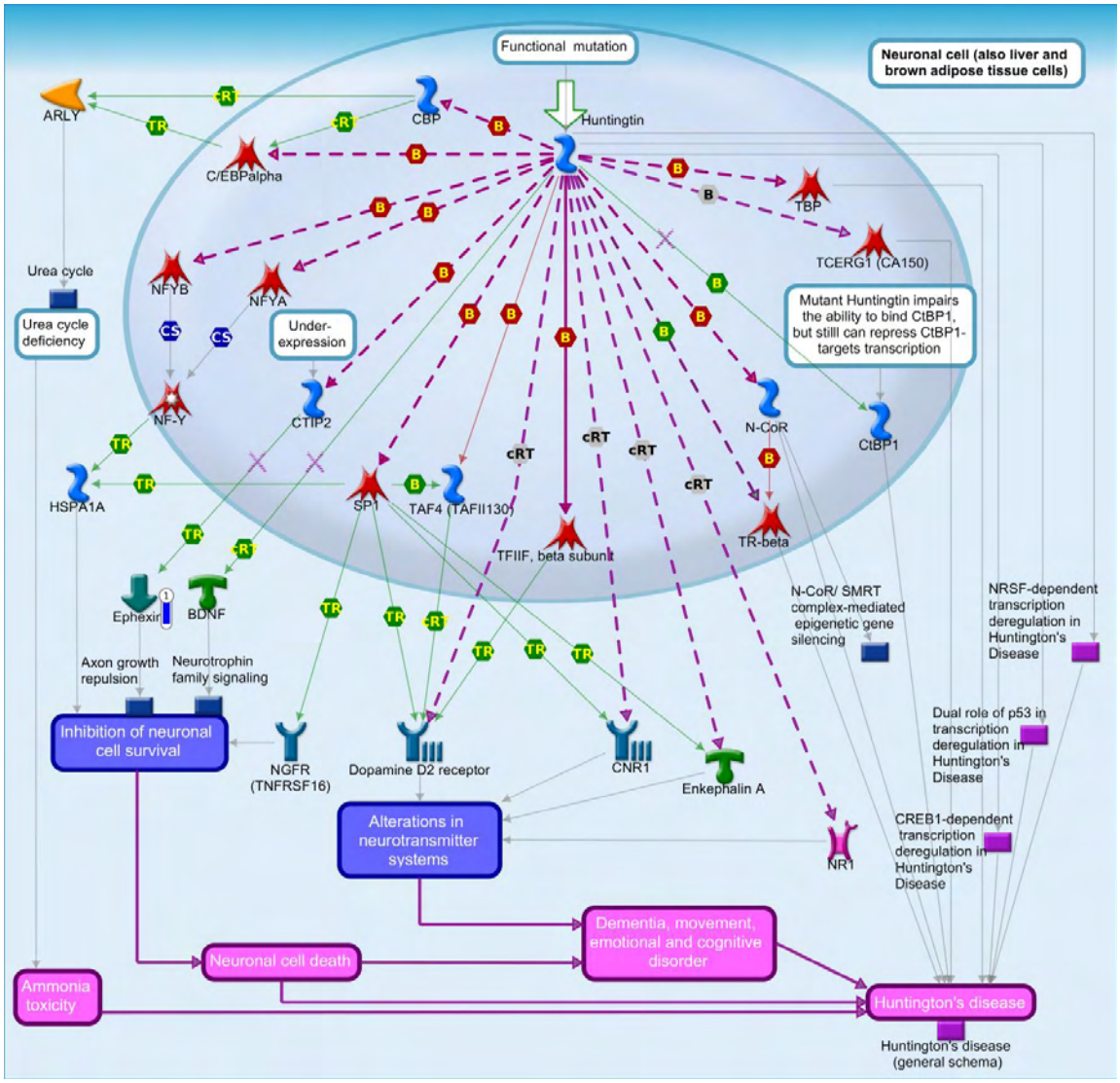

Figure 17. Huntingtin-depended transcription deregulation in Huntington's Disease pathway map by MetaCore software (p-value < 0.10) from the list of differentially expressed genes (FDR 10%) in the liver tissue immunocastrated male pigs fed with two different oils in the diet (3.0 % canola oil and 3.0 % soybean oil). The blue thermometer indicates that the DEG is down-regulated (log2 fold change -0.6) in the diet with 3.0 % of canola oil (CO). Purple lines indicate enhancement in diseases and purple dotted line emerges in diseases. Green arrows indicate positive interaction and gray arrows indicate unspecified interaction. For a detailed definition, see https://portal.genego.com/legends/MetaCoreQuickReferenceGuide.pdf.

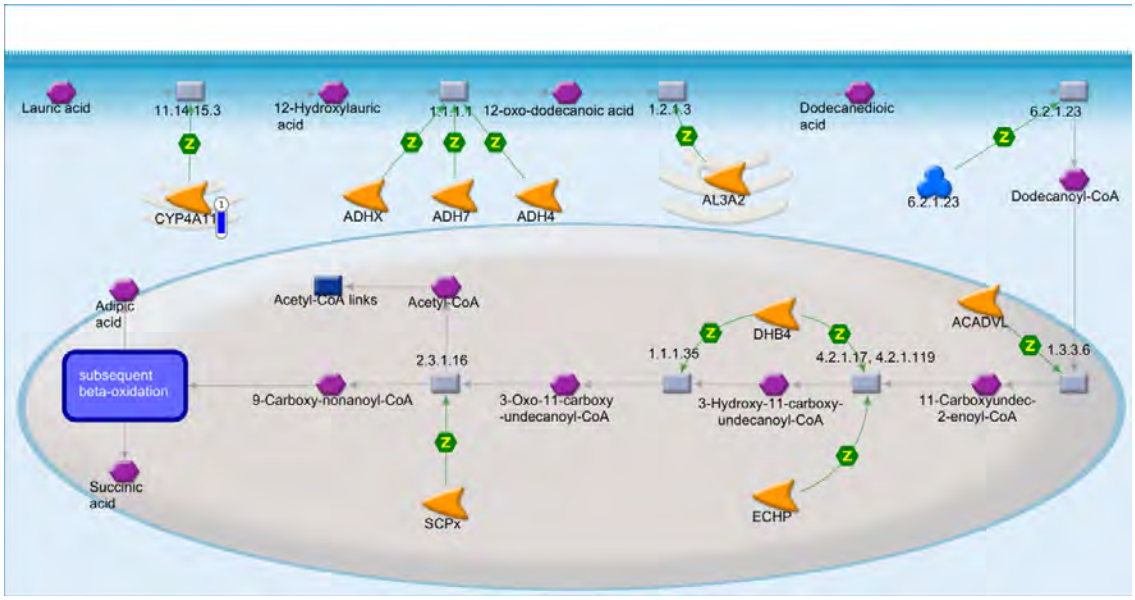

Figure 18. Fatty Acid Omega Oxidation pathway map by MetaCore software (p-value < 0.10) from the list of differentially expressed genes (FDR 10%) in the liver tissue immunocastrated male pigs fed with two different oils in the diet (3.0 % canola oil and 3.0 % soybean oil). The blue thermometer indicates that the DEG is down-regulated (log2 fold change -1.25) in the diet with 3.0 % of canola oil (CO). Green arrows indicate positive interaction and gray arrows indicate unspecified interaction. For a detailed definition, see https://portal.genego.com/legends/MetaCoreQuickReferenceGuide.pdf.

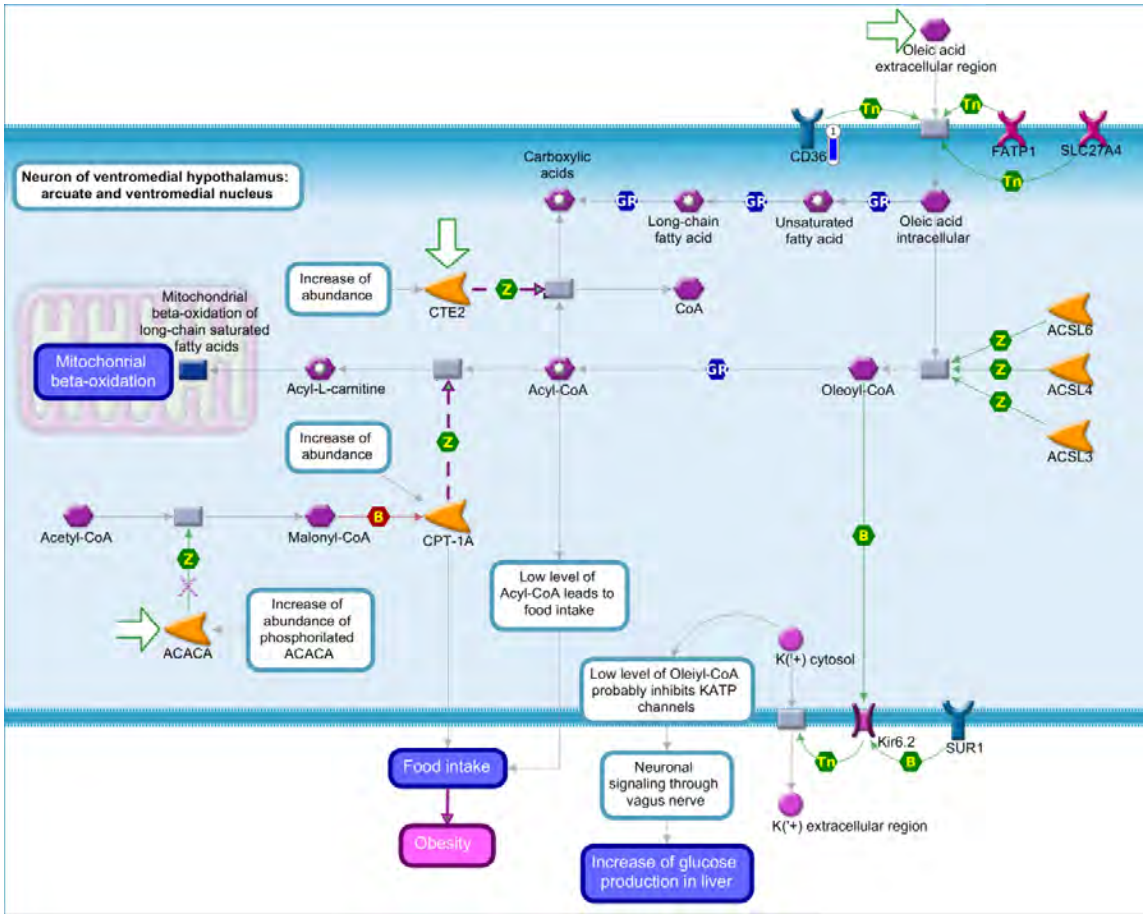

Figure 19. Putative pathways of Oleic acid sensing in ventromedial hypothalamus in obesity (rodent model) pathway map by MetaCore software (p-value < 0.10) from the list of differentially expressed genes (FDR 10%) in the liver tissue immunocastrated male pigs fed with two different oils in the diet (3.0 % canola oil and 3.0 % soybean oil). The blue thermometer indicates that the DEG is down-regulated

(log2 fold change -0.48) in the diet with 3.0 % of canola oil (CO). Purple lines indicate enhancement in diseases and purple dotted line emerges in diseases. Green arrows indicate positive interaction and gray arrows indicate unspecified interaction. For a detailed definition, see https://portal.genego.com/legends/MetaCoreQuickReferenceGuide.pdf.

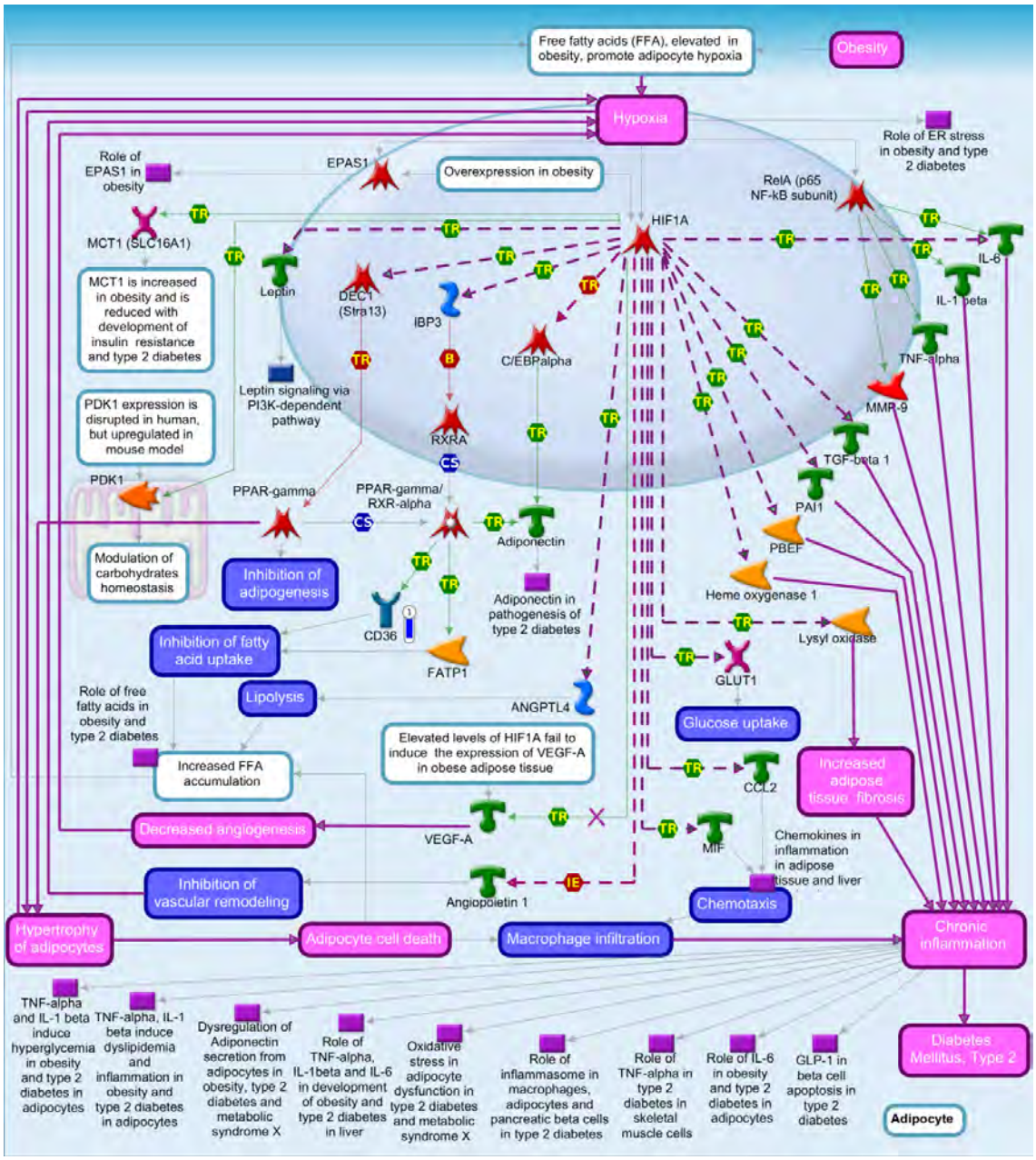

Figure 20. Role of adipose tissue hypoxia in obesity and type 2 diabetes) pathway map by MetaCore software (p-value < 0.10) from the list of differentially expressed genes (FDR 10%) in the liver tissue immunocastrated male pigs fed with two different oils in the diet (3.0 % canola oil and 3.0 % soybean oil). The blue thermometer indicates that the DEG is down-regulated (log2 fold change -0.48) in the diet with 3.0 % of canola oil (CO). Purple lines indicate enhancement in diseases and purple dotted line emerges in diseases. Green arrows indicate positive interaction and gray arrows indicate unspecified interaction. For a detailed definition, see https://portal.genego.com/legends/MetaCoreQuickReferenceGuide.pdf.

To observe the interactions of DEG in gene networks, an analysis of process networks was performed in the MetaCore software (Figure 21). The identified networks were related to inflammatory processes, metabolism and neuropeptide signaling. Among the networks obtained were identified (p-value <0.1) the "inflammation_Kallikrein-kinin system" (p-value 7.143E-04) presenting the DEG kininogen 1 (*KNG1*) (log2 fold change -0.65); the "signal transduction_Neuropeptide signaling" pathway (p-value 2.230e-2), that presented some DEG in the Galpha(i)-specific peptide GPCRs group: neuropeptide Y receptor Y1 (*NPY1R*) (log2 fold change -1.09); and, the "development/regulation of angiogenesis" pathway (p-value 5.475e-2), presenting the DEG *SMAD* family member 3 (*SMAD3*) (log2 fold change -0.32), Galpha(i)-specific peptide GPCRs: *NPY1R* (log2 fold change -1.09).

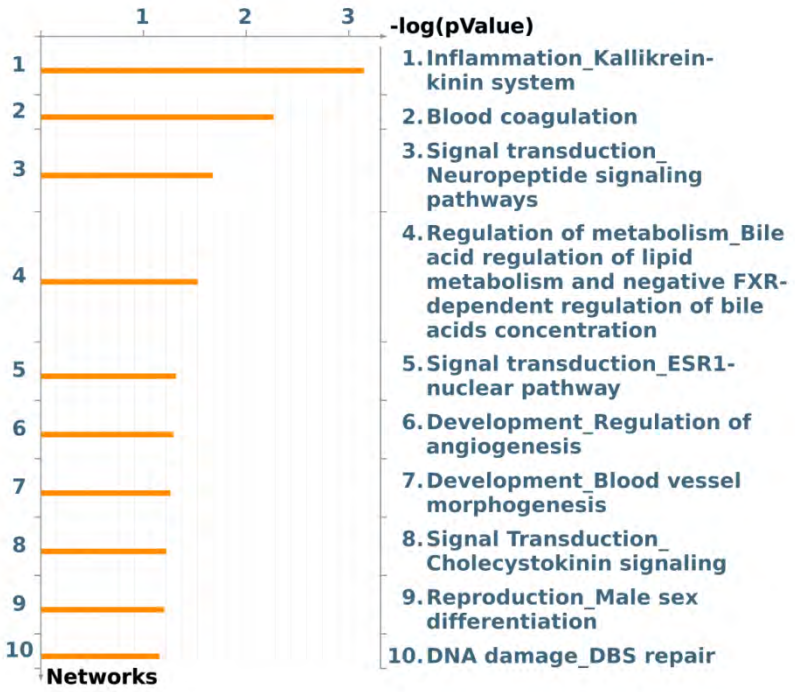

Figure 21. Top 10 enriched networks identified by MetaCore software from the list of differentially expressed genes (FDR 10%) in the liver tissue immunocastrated male pigs fed with different oils (3.0 % canola oil and 3.0 % of soybean oil).

3.5 Functional enrichment analysis for skeletal muscle differential expression (SOY*vs*FO)

Some pathway maps detected (p-value <0.10) are shown in Table 8 with the corresponding p-value and DEG. The complete list of enriched pathway maps can be found in the APPENDIX C (Table S3).

When the comparison was related to SOY and FO we identified the highest amount of total DEG, in skeletal muscle it was the highest amount of both down-regulated and up-regulated DEG.

Table 8: Pathway maps enriched by MetaCore software (p-value <0.10) from the list of differentially expressed genes (FDR 10%) in the liver of immunocastrated male pigs fed with different oil sources

Pathway Maps	**p-value**	**DEG[1]**
TNF-alpha, IL-1 beta induce dyslipidemia and inflammation in obesity and type 2 diabetes in adipocytes	1,165E-04	*AZGP1, PDE3B, APOE, Perilipin, LIPS*
Putative pathways for stimulation of fat cell differentiation by Bisphenol A	4,803E-04	*PPAR-gamma, TCF7L2 (TCF4), SCD, C/EBPalpha*
Signal transduction_WNT/Beta-catenin signaling in tissue homeostasi	1,367E-03	*TCF7L2 (TCF4), Tcf(Lef), WNT, PPCKC*
Adiponectin in pathogenesis of type 2 diabetes	4,446E-03	*SCD, PPCKC, ACOX1*
Role of IL-6 in obesity and type 2 diabetes in adipocytes	5,884E-03	*PPAR-gamma, Perilipin, LIPS*
Dysregulation of Adiponectin secretion from adipocytes in obesity, type 2 diabetes and metabolic syndrome X	9,516E-03	*PPAR-gamma, IL-18, C/EBPalpha*
Regulation of metabolism_Bile acids regulation of glucose and lipid metabolism via FXR"	1,173E-02	*APOE, SCD, PPCKC*
Transport_HDL-mediated reverse cholesterol transport	1,252E-02	*APOE, CES1, SR-BI*

The genes zinc alpha-2-glycoprotein 1 (*AZGP1*), phosphodiesterase 3B (*PDE3B*), apolipoprotein E (*APOE*), Perilipin 1 (*PLIN1*), and lipase E hormone sensitive type (*LIPS*) were identified as DEG in the skeletal. The *AZGP1* gene, a lipid-mobilizing adipokine, was identified with lower expression (log2 fold change -3.79) in the muscle of pigs from the SOY group. In addition, were enriched in the "*TNF-alpha* pathway, *IL-1* beta induces dyslipidemia and inflammation in obesity and type 2 diabetes in adipocytes" pathway (Figure 22). *APOE* was enriched in "regulation of metabolism_bile acids regulation of glucose and lipid metabolism via FXR" (Figure 23), and "transport_HDL-mediated reverse cholesterol transport" (Figure 24).

Another DEG that can be inhibited by *TNF-alpha* is *Perilipin 1*, which has lower expression (log2 fold change -2.99) in the SOY group. This DEG showed lower expression (log2 fold change -2.10) in groups fed a diet containing SOY. The DEG

LIPS was identified with lower expression (log2 fold change -1.30) in groups of animals fed with SOY. *PPARG* was identified as DEG in the muscle of pigs fed different oils; *PPARG* showed lower expression (log2 fold change -1.92) in the group of pigs fed with soybean oil. The first enriched pathway that presents *PPARG* was the "putative pathways for stimulation of fat cell differentiation by Bisphenol A" (Figure 25). Moreover, *PPARG* participate in other enriched pathways such as the "role of IL-6 in obesity and type 2 diabetes in adipocytes" (Figure 26), and "dysregulation of adiponectin secretion from adipocytes in obesity, type 2 diabetes and metabolic syndrome X" (Figure 27), together with the CCAAT enhancer binding protein alpha (*C/EBP-alpha*).

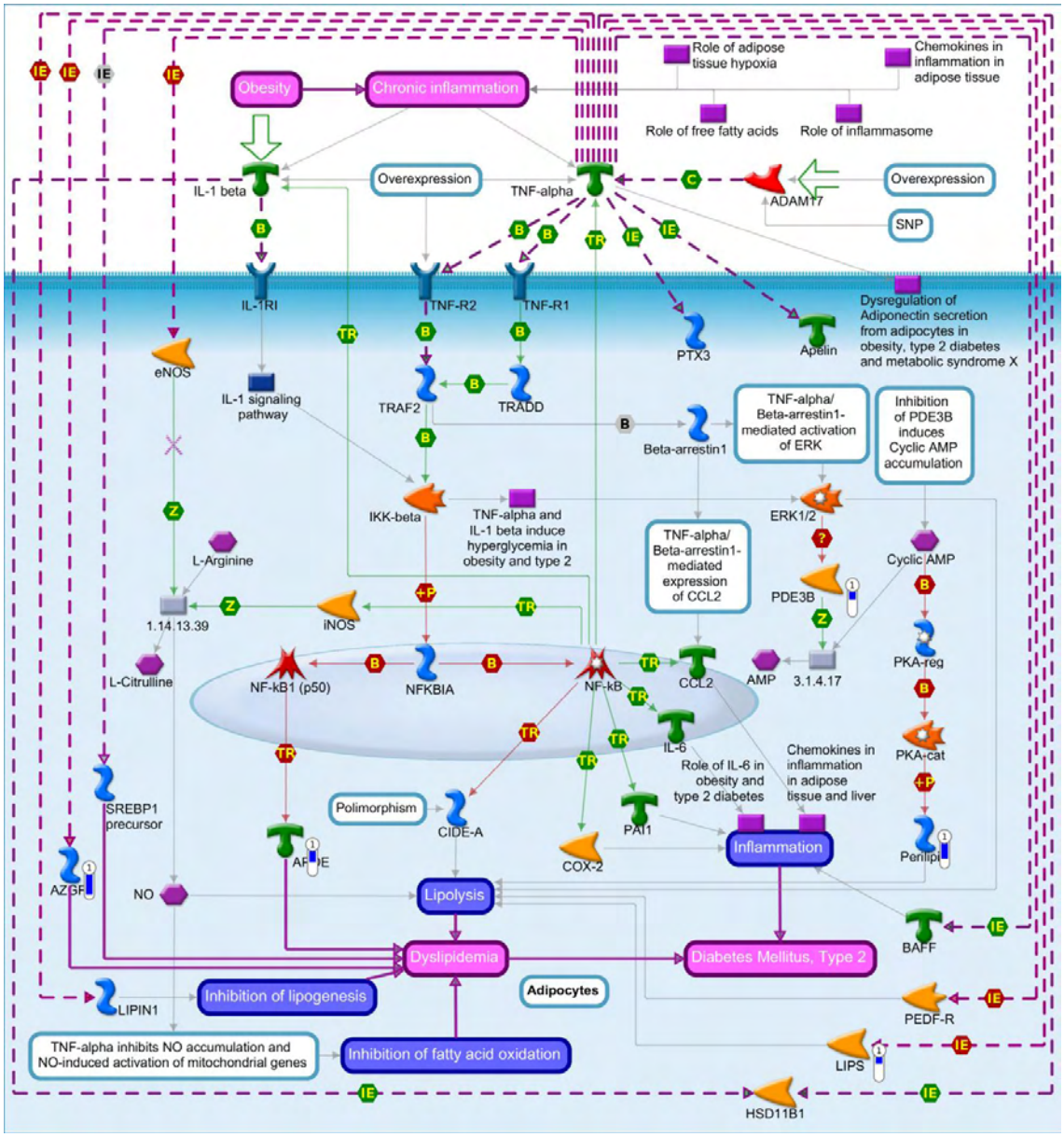

Figure 22. TNF-alpha, IL-1 beta induce dyslipidemia and inflammation in obesity and type 2 diabetes in adipocytes pathway map by MetaCore software (p-value < 0.10) from the list of differentially expressed genes (FDR 10%) in the skeletal muscle tissue immunocastrated male pigs fed with two different oil in the diet (3.0 % soybean oil and 3.0% fish oil). The blue thermometer indicates that the DEG is down-regulated in the diet with 3.0 % of soybean oil (SOY). Purple lines indicate enhancement in diseases and purple dotted line emerges in diseases. Green arrows indicate positive interaction and gray arrows indicate unspecified interaction. For a detailed definition, see https://portal.genego.com/legends/MetaCoreQuickReferenceGuide.pdf.

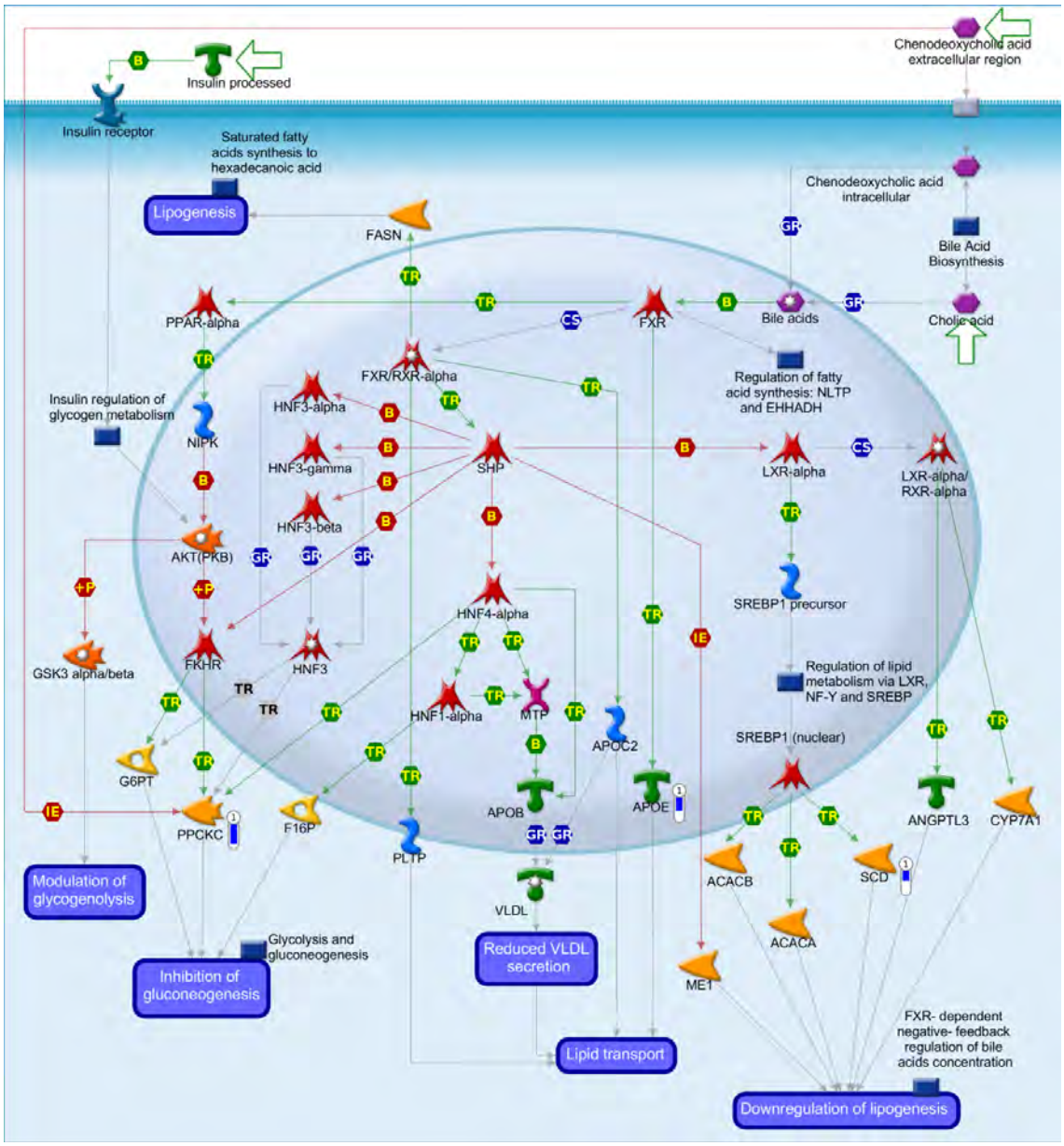

Figure 23. Regulation of metabolism_Bile acids regulation of glucose and lipid metabolism via FXR pathway map by MetaCore software (p-value < 0.10) from the list of differentially expressed genes (FDR 10%) in the skeletal muscle tissue immunocastrated male pigs fed with two different oils in the diet (3.0 % soybean oil and 3.0 % fish oil). The blue thermometer indicates that the DEG is down-regulated in the diet with 3.0 % of soybean oil (SOY). Green arrows indicate positive interaction and gray arrows indicate unspecified interaction. For a detailed definition, see https://portal.genego.com/legends/MetaCoreQuickReferenceGuide.pdf

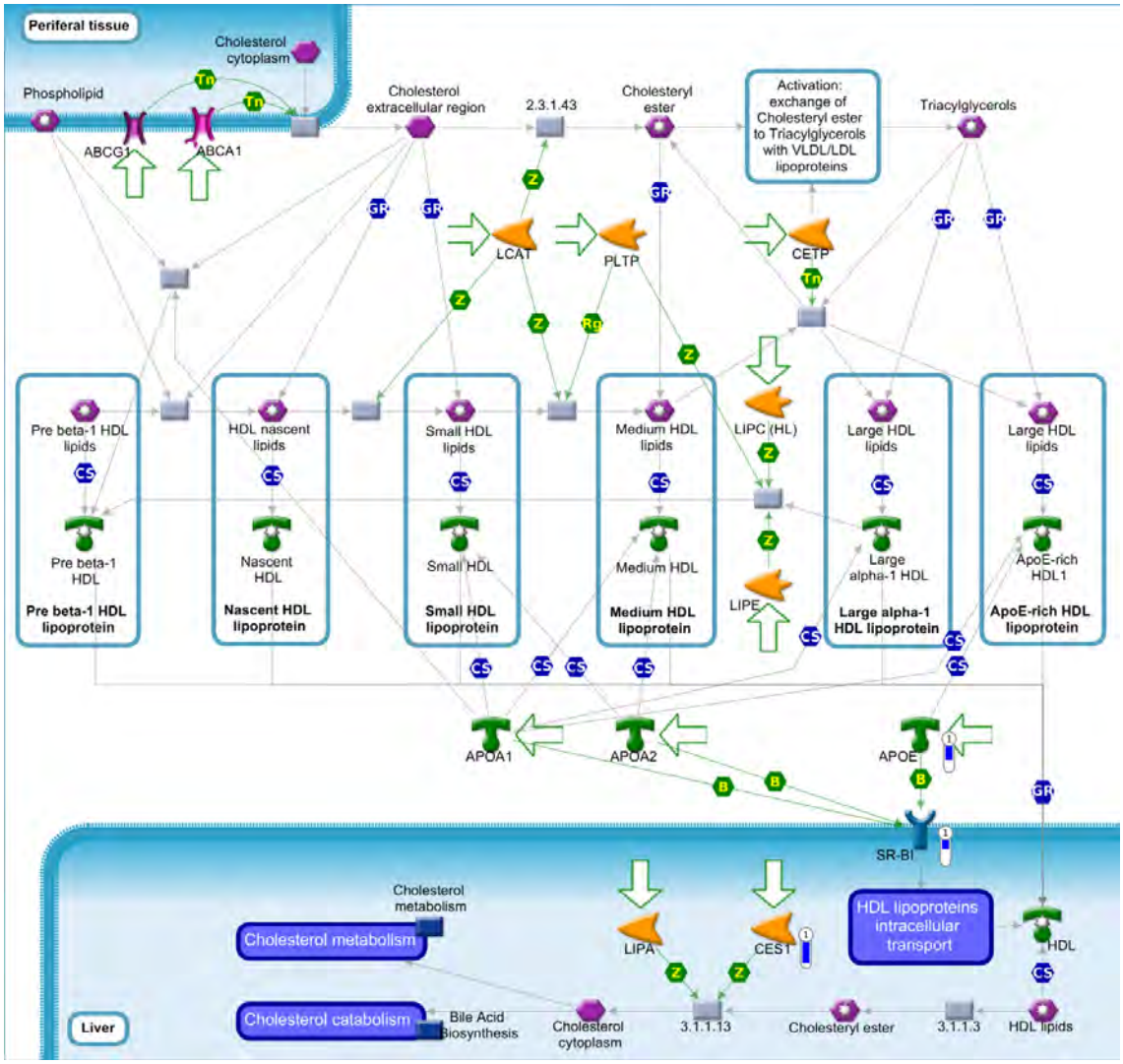

Figure 24. Transport_HDL-mediated reverse cholesterol transport pathway map by MetaCore software (p-value < 0.10) from the list of differentially expressed genes (FDR 10%) in the skeletal muscle tissue immunocastrated male pigs fed with two different oils in the diet (3.0 % soybean oil and 3.0 % fish oil). The blue thermometer indicates that the DEG is down-regulated in the diet with 3.0 % of soybean oil (SOY). Green arrows indicate positive interaction and gray arrows indicate unspecified interaction. For a detailed definition, see https://portal.genego.com/legends/MetaCoreQuickReferenceGuide.pdf

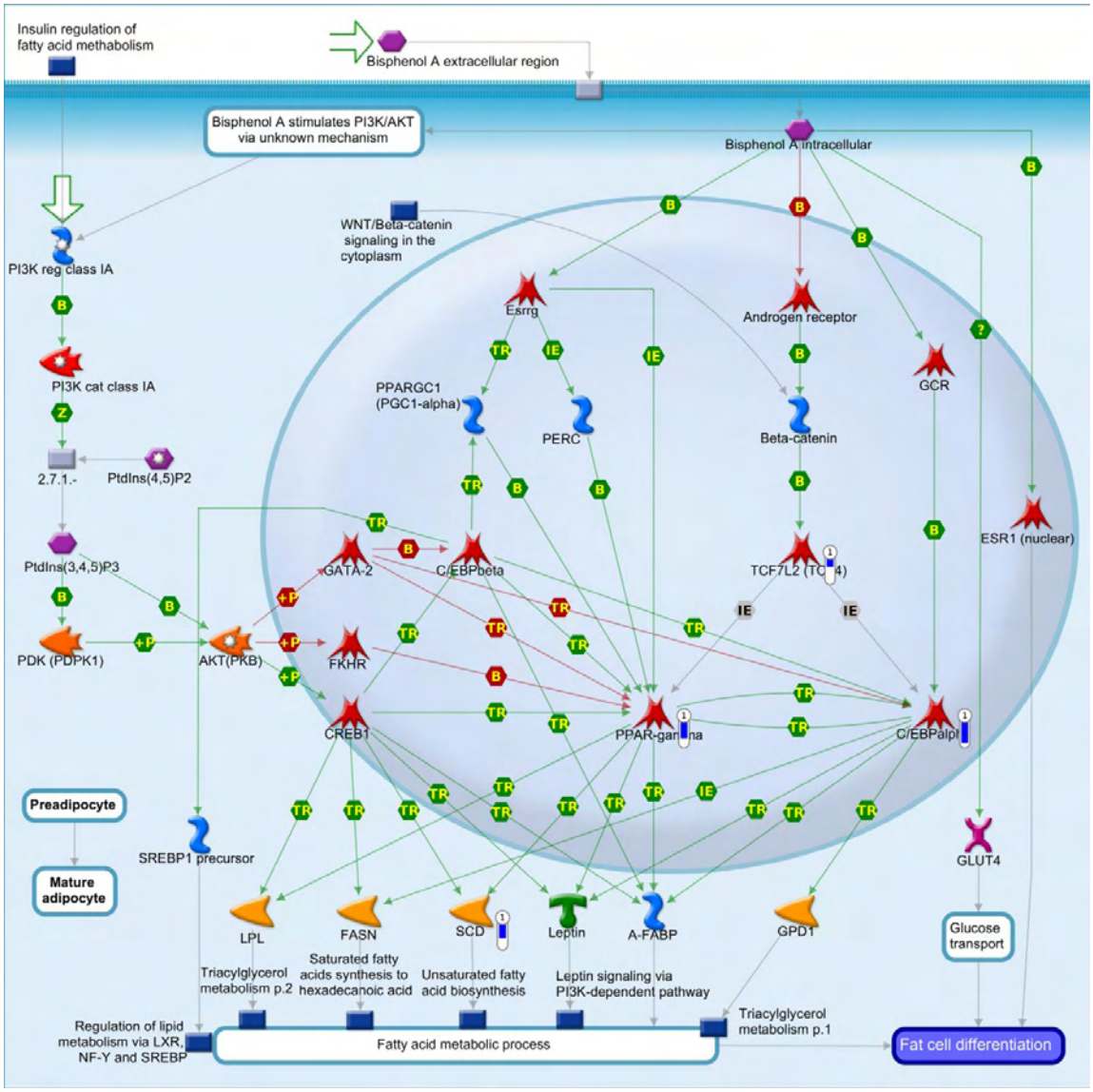

Figure 25. Putative pathways for stimulation of fat cell differentiation by Bisphenol A pathway map by MetaCore software (p-value < 0.10) from the list of differentially expressed genes (FDR 10%) in the skeletal muscle tissue immunocastrated male pigs fed with two different oils in the diet (3.0 % soybean oil and 3.0 % fish oil). The blue thermometer indicates that the DEG is down-regulated in the diet with 3.0 % of soybean oil (SOY). Green arrows indicate positive interaction and gray arrows indicate unspecified interaction. For a detailed definition, see https://portal.genego.com/legends/MetaCoreQuickReferenceGuide.pdf

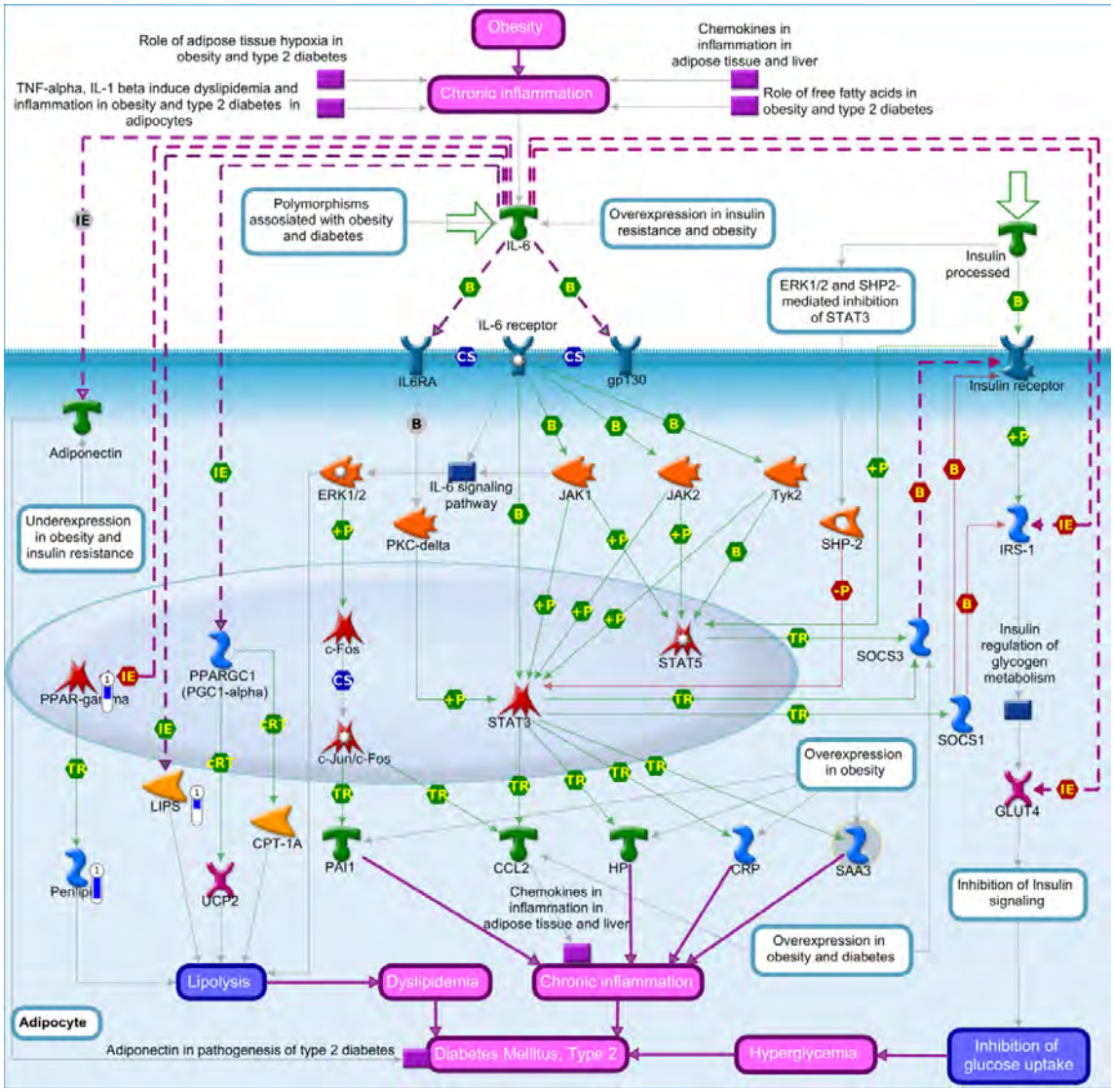

Figure 26. Role of IL-6 in obesity and type 2 diabetes in adipocytes pathway map by MetaCore software (p-value < 0.10) from the list of differentially expressed genes (FDR 10%) in the skeletal muscle tissue immunocastrated male pigs fed with two different oils in the diet (3.0 % soybean oil and 3.0 % fish oil). The blue thermometer indicates that the DEG is down-regulated in the diet with 3.0 % of soybean oil (SOY). Purple lines indicate enhancement in diseases and purple dotted line emerges in diseases. Green arrows indicate positive interaction and gray arrows indicate unspecified interaction. For a detailed definition, see https://portal.genego.com/legends/MetaCoreQuickReferenceGuide.pdf.

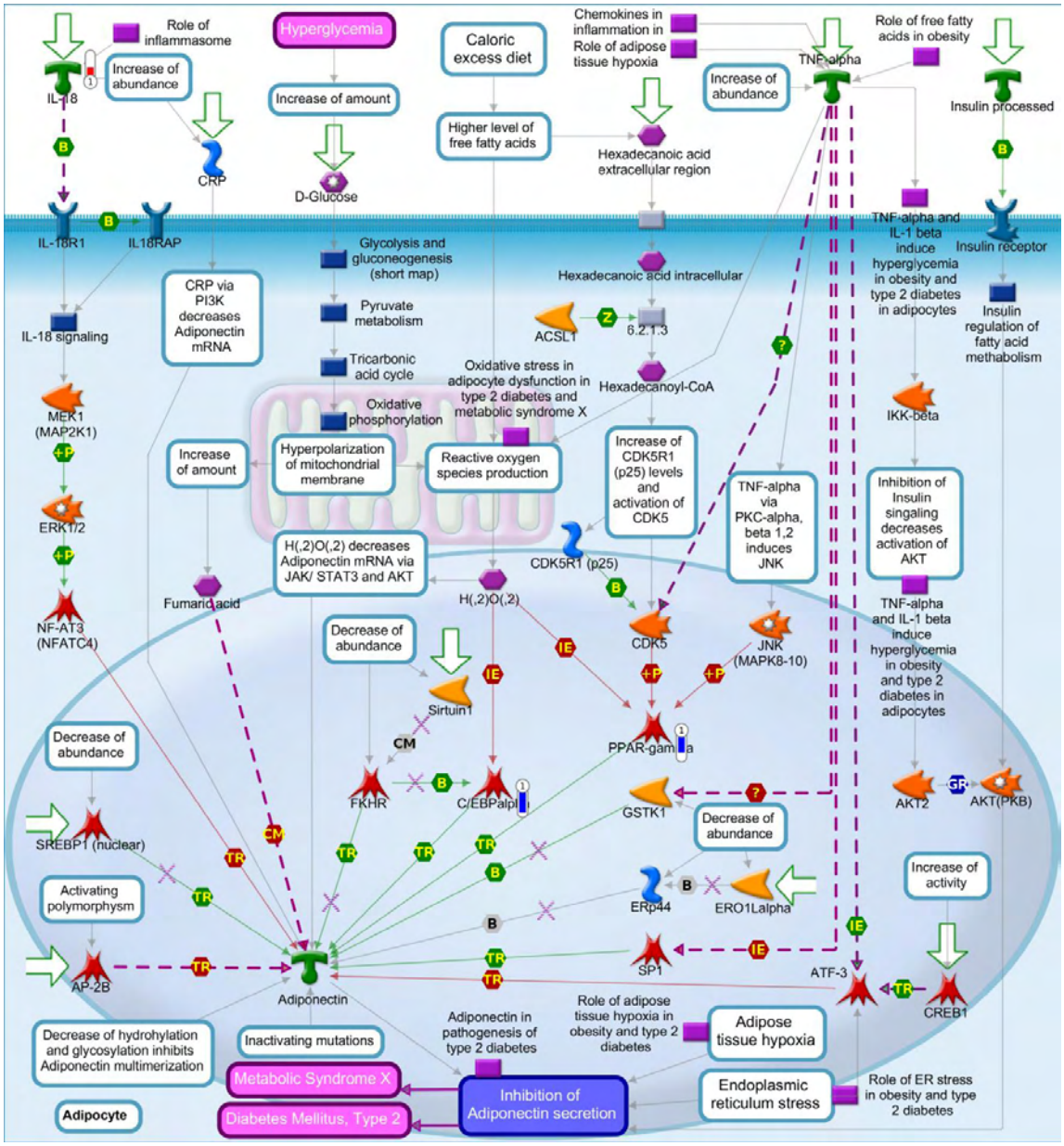

Figure 27. Dysregulation of Adiponectin secretion from adipocytes in obesity, type 2 diabetes and metabolic syndrome X pathway map by MetaCore software (p-value < 0.10) from the list of differentially expressed genes (FDR 10%) in the skeletal muscle tissue immunocastrated male pigs fed with two different oils in the diet (3.0 % soybean oil and 3.0 % fish oil). The blue thermometer indicates that the DEG is down-regulated in the diet with 3.0 % of soybean oil (SOY). Green arrows indicate positive interaction and gray arrows indicate unspecified interaction. For a detailed definition, see https://portal.genego.com/legends/MetaCoreQuickReferenceGuide.pdf.

The *SCD* gene was identified as the DEG with the lower expression (log2 fold change -1.6) in the SOY group, and was enriched in the "putative pathways for stimulation of fat cell differentiation by Bisphenol A", "adiponectin in pathogenesis of type 2 diabetes" and "regulation of metabolism_bile acids regulation of glucose and lipid metabolism via FXR" pathways (Figure 28 and 29). The transcription factor 7 like 2 (*TCF7L2*) was identified as the DEG with a lowest expression (-0.96log2 fold change) in the SOY group. In addition, *TCF7L2* participates in the "signal transduction_*WNT/Beta-catenin* signaling in tissue homeostasis" pathway (Figure 29) activating *c-Myc* transcription, which positively regulates cell population proliferation, among other effects, like activating and inhibiting genes and transcription factors. *C/EBP-alpha* was identified as DEG in our study with the smaller expression (log2 fold change -2.4) related to the group of pigs that received soybean oil. *C/EBP-alpha* transcription factor is an enriched in the "putative pathways for stimulation of fat cell differentiation by Bisphenol A" pathway (Figure 25).

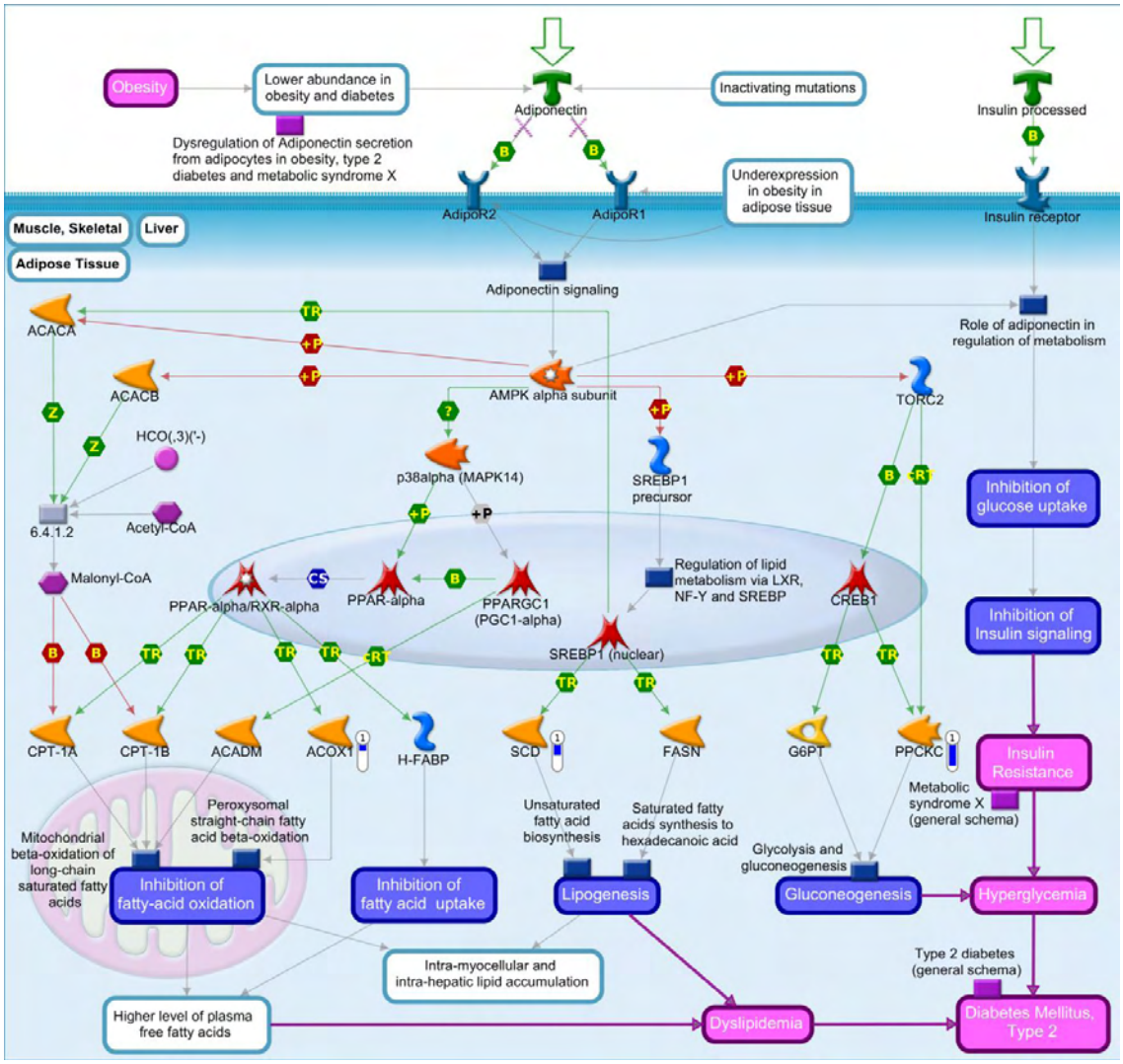

Figure 28. Adiponectin in pathogenesis of type 2 diabetes pathway map by MetaCore software (p-value < 0.10) from the list of differentially expressed genes (FDR 10%) in the skeletal muscle tissue immunocastrated male pigs fed with two different oils in the diet (3.0 % soybean oil and 3.0 % fish oil). The blue thermometer indicates that the DEG is down-regulated in the diet with 3.0 % of soybean oil (SOY). Green arrows indicate positive interaction and gray arrows indicate unspecified interaction. For a detailed definition, see https://portal.genego.com/legends/MetaCoreQuickReferenceGuide.pdf.

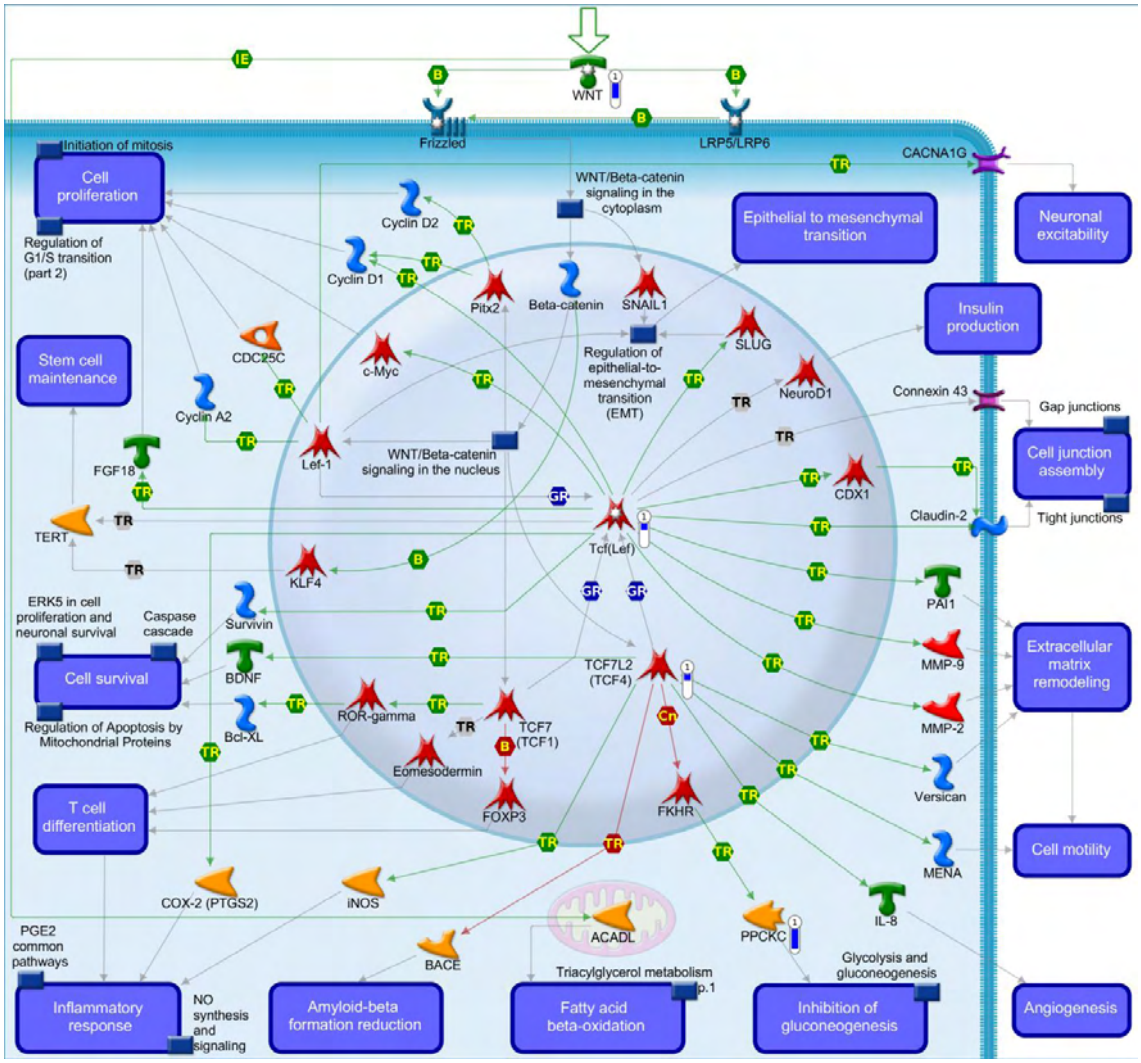

Figure 29. signal transduction_WNT/Beta-catenin signaling in tissue homeostasis pathway map by MetaCore software (p-value < 0.10) from the list of differentially expressed genes (FDR 10%) in the skeletal muscle tissue immunocastrated male pigs fed with two different oils in the diet (3.0 % soybean oil and 3.0 % fish oil). The blue thermometer indicates that the DEG is down-regulated in the diet with 3.0 % of soybean oil (SOY). Green arrows indicate positive interaction and gray arrows indicate unspecified interaction. For a detailed definition, see https://portal.genego.com/legends/MetaCoreQuickReferenceGuide.pdf.

To better understand the observed interactions of DEG in gene networks, the analysis of process networks was performed using MetaCore software (Figure 30). Networks related (p value <0.1) to muscle contraction (p-value 2.429E-06), “regulation of angiogenesis” (p-value 7.863E-03), “transmission of nerve impulse”, and “immune response” (p-value 1.878E-02) were identified herein. Some DEG were identified enriched in the networks like the *GPCR* in the “chemostaxis” network; *PPARG, APOE, MELC, PACAP* receptor 1 in the “development neurogenesis axonal guidance” network, and *APOE, MELC, Actin, C/EBP, SR-BI,* among others, in the “immune response phagocytosis” network.

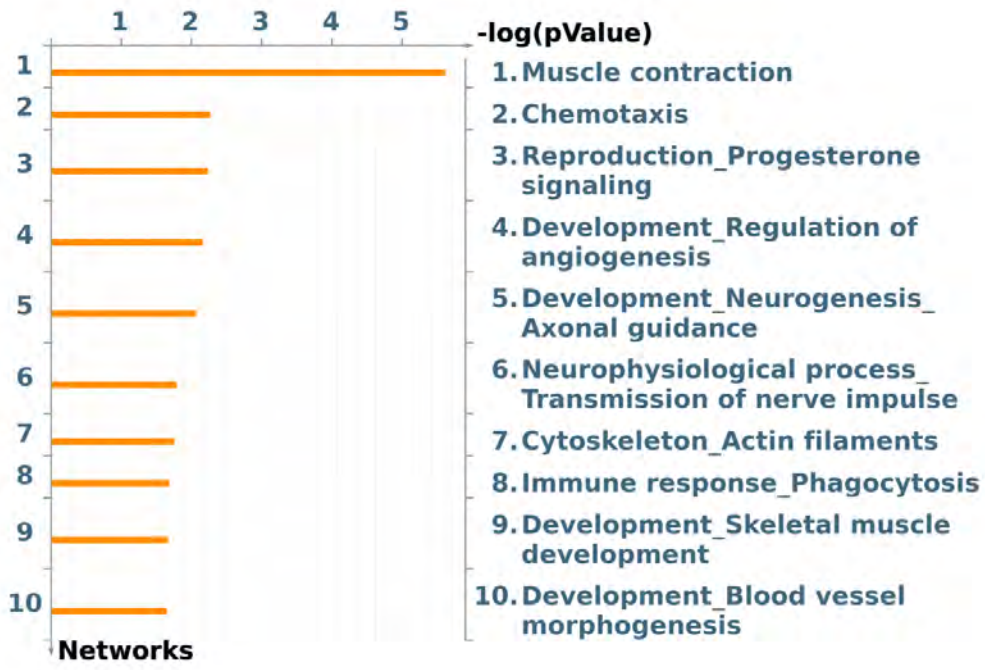

Figure 30. Top 10 enriched networks identified by MetaCore software from the list of differentially expressed genes (FDR 10%) in the skeletal muscle tissue immunocastrated male pigs fed with different oils (3.0 % canola oil and 3.0 % of soybean oil).

3.6 Functional enrichment analysis for liver differential expression (SOY*vs*FO)

The enriched pathway maps (Figure 31) were obtained (p-value <0.10), were "regulation of lipid metabolism FXR-dependent negative-feedback regulation of bile acids concentration" (Figure 32) (*CYP2B6* and *CYP7A1* DEG), "cholesterol metabolism" (Figure 33) (*ACOX2* and *CYP7A1* DEG); "bile acid biosynthesis" (Figure 34) (*ACOX2* and *CYP7A1* DEG);" role of inflammasome in macrophages, adipocytes and pancreatic beta cells in type 2 diabetes and Role of IFN-beta in inhibition of Th1 cell differentiation in multiple sclerosis" (Figure 35 and 36) (*IL-18* DEG); "Huntingtin-dependent transcription deregulation in Huntington's disease" (Figure 37) (*Ephexin* DEG), among others (Figure 38, 40, and 41).

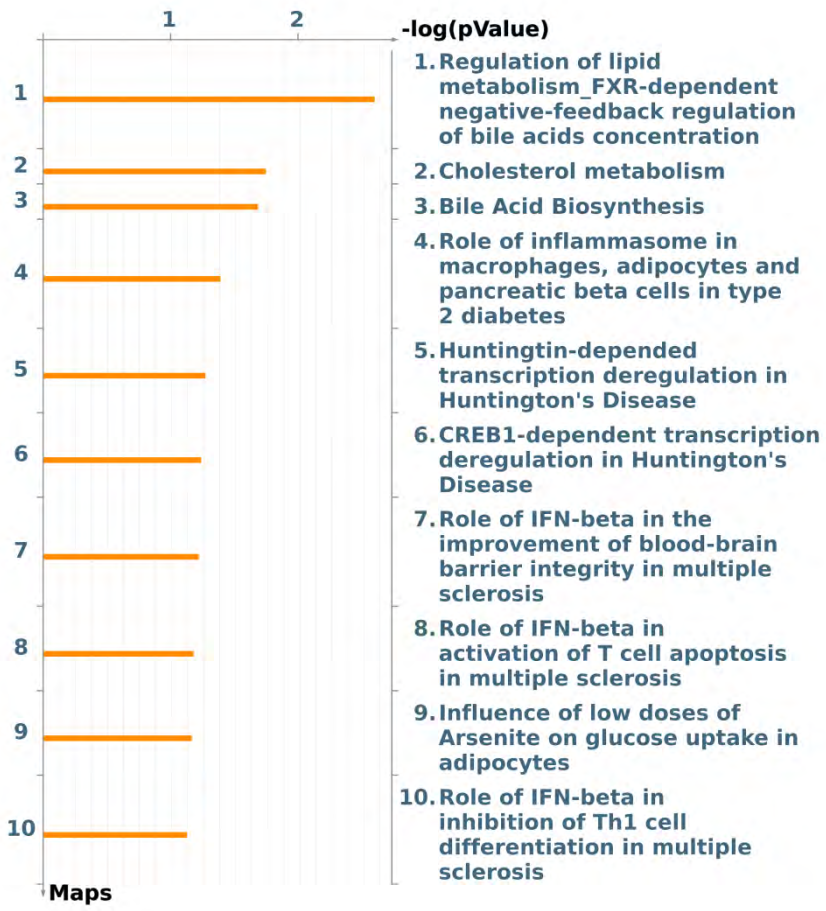

Figure 31: Pathway maps by MetaCore software (p-value < 0.1) from the list of differentially expressed genes (FDR 10%) in the liver immunocastrated male pigs fed two oil (3.0 % canola oil vs 3.0% soybean oil).

The *CYP7A1* is enriched in other pathways with the gene acyl-CoA oxidase 2 *ACOX2*, which was identified as DEG and has lower expression (log2 fold change -0.37) in the group fed with a diet enriched with soybean oil. The *CYP7A1* and *ACOX*2 DEG were enriched in the "cholesterol metabolism" and the "bile acid biosynthesis" pathways, highlighting the importance of their relationship to bile acids.

The *IL-18* showed higher expression (log2 fold change +0.49) in the liver of pigs fed SOY diet and was enriched in the "role of inflammasome pathway in macrophages, adipocytes and pancreatic beta cells in type 2 diabetes". Another enriched pathway that *IL-18* may be involved in is the "role of *IFN-beta* in inhibition of Th1 cell differentiation in multiple sclerosis". Moreover, the DEG neural guanine nucleotide exchange factor (NGEF) identified in the liver of pigs fed diets with the addition of different oils was previously identified as DEG in other comparisons, and a common gene among all diets (Table 5). The *NEGF* showed lower expression (log2 fold change -

0.65) in pigs fed the SOY diet, and was enriched within the “Huntingtin-dependent transcription deregulation pathway in Huntington's Disease” as *Ephexin*.

The *MTND6* presented a lower expression (log2 fold change -0.92) in the SOY group, in addition it was enriched in the “*CREB1*-dependent transcription deregulation pathway in Huntington's Disease” pathway.

The *KIF3B* was identified in our study with lower expression (log2 fold change -0.53) in the liver of pigs fed with SOY. It participates in the “influence of low doses of arsenite on glucose uptake in adipocytes” pathway.

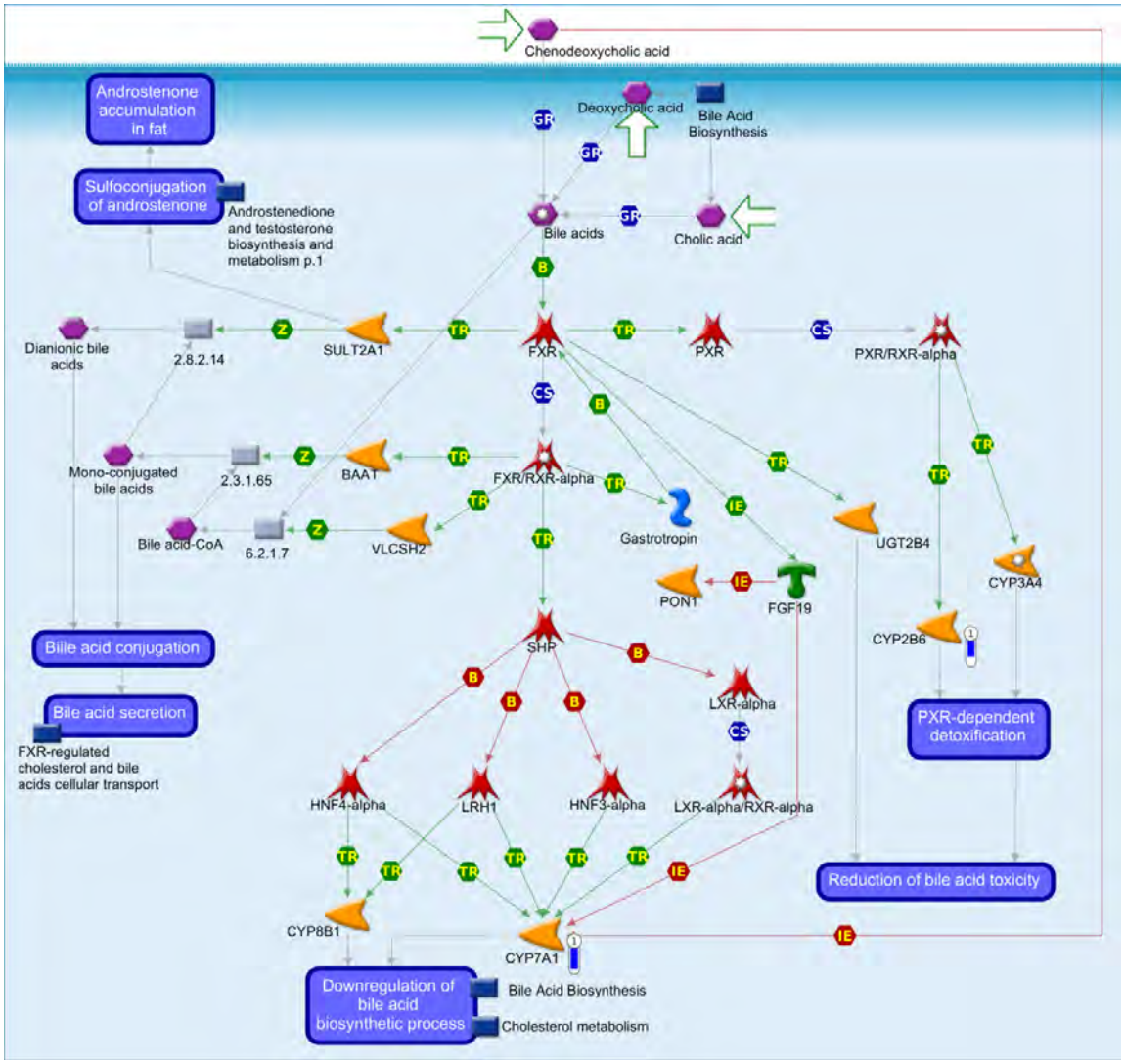

Figure 32. Regulation of lipid metabolismo FXR-dependent negative-feedback regulation of bile acids concentration. pathway map by MetaCore software (p-value < 0.10) from the list of differentially expressed genes (FDR 10%) in the liver tissue immunocastrated male pigs fed with two different oils in the diet (3.0 % soybean oil and 3.0 % fish oil). The blue thermometer indicates that the DEG is down-regulated in the diet with 3.0 % of soybean oil (SOY). Green arrows indicate positive interaction and gray

arrows indicate unspecified interaction. For a detailed definition, see https://portal.genego.com/legends/MetaCoreQuickReferenceGuide.pdf.

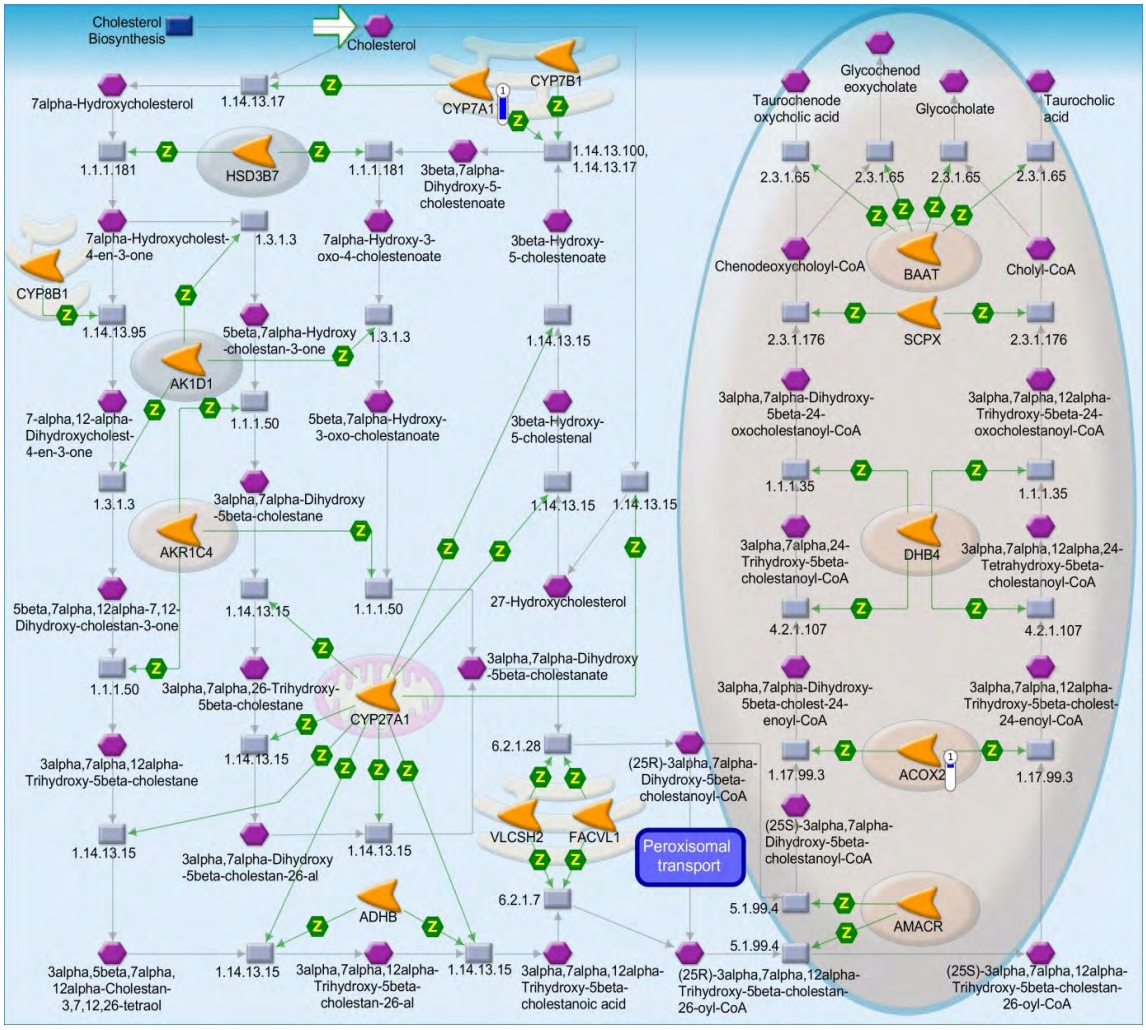

Figure 33. Cholesterol metabolism pathway map by MetaCore software (p-value < 0.10) from the list of differentially expressed genes (FDR 10%) in the liver tissue immunocastrated male pigs fed with two different oils in the diet (3.0 % soybean oil and 3.0 % fish oil). The blue thermometer indicates that the DEG is down-regulated in the diet with 3.0 % of soybean oil (SOY). Green arrows indicate positive interaction and gray arrows indicate unspecified interaction. For a detailed definition, see https://portal.genego.com/legends/MetaCoreQuickReferenceGuide.pdf.

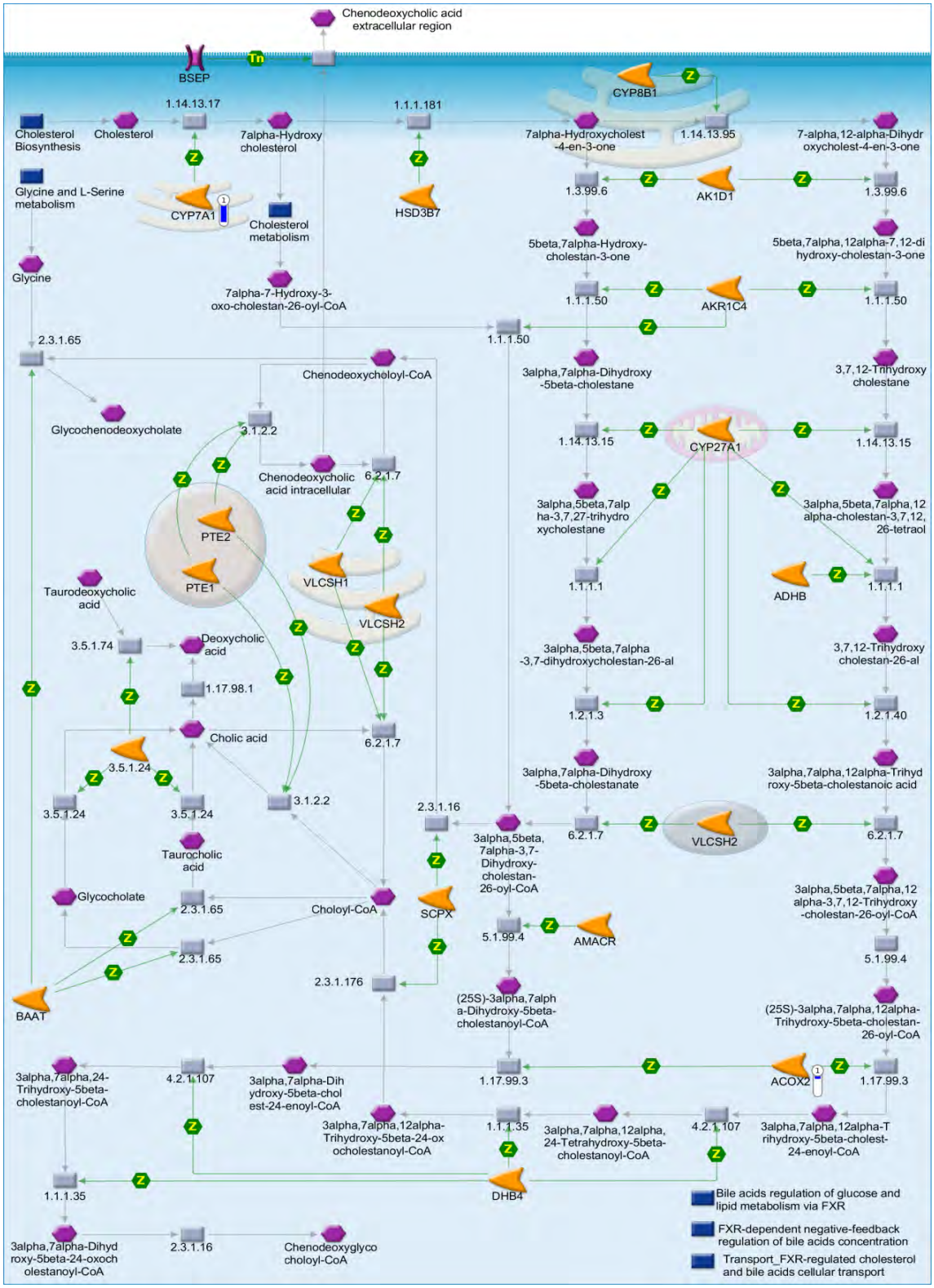

Figure 34. Bile Acid Biosynthesis pathway map by MetaCore software (p-value < 0.10) from the list of differentially expressed genes (FDR 10%) in the liver tissue immunocastrated male pigs fed with two different oils in the diet (3.0 % soybean oil and 3.0 % fish oil). The blue thermometer indicates that the DEG is down-regulated in the diet with 3.0 % of soybean oil (SOY). Green arrows indicate positive interaction and gray arrows indicate unspecified interaction. For a detailed definition, see https://portal.genego.com/legends/MetaCoreQuickReferenceGuide.pdf

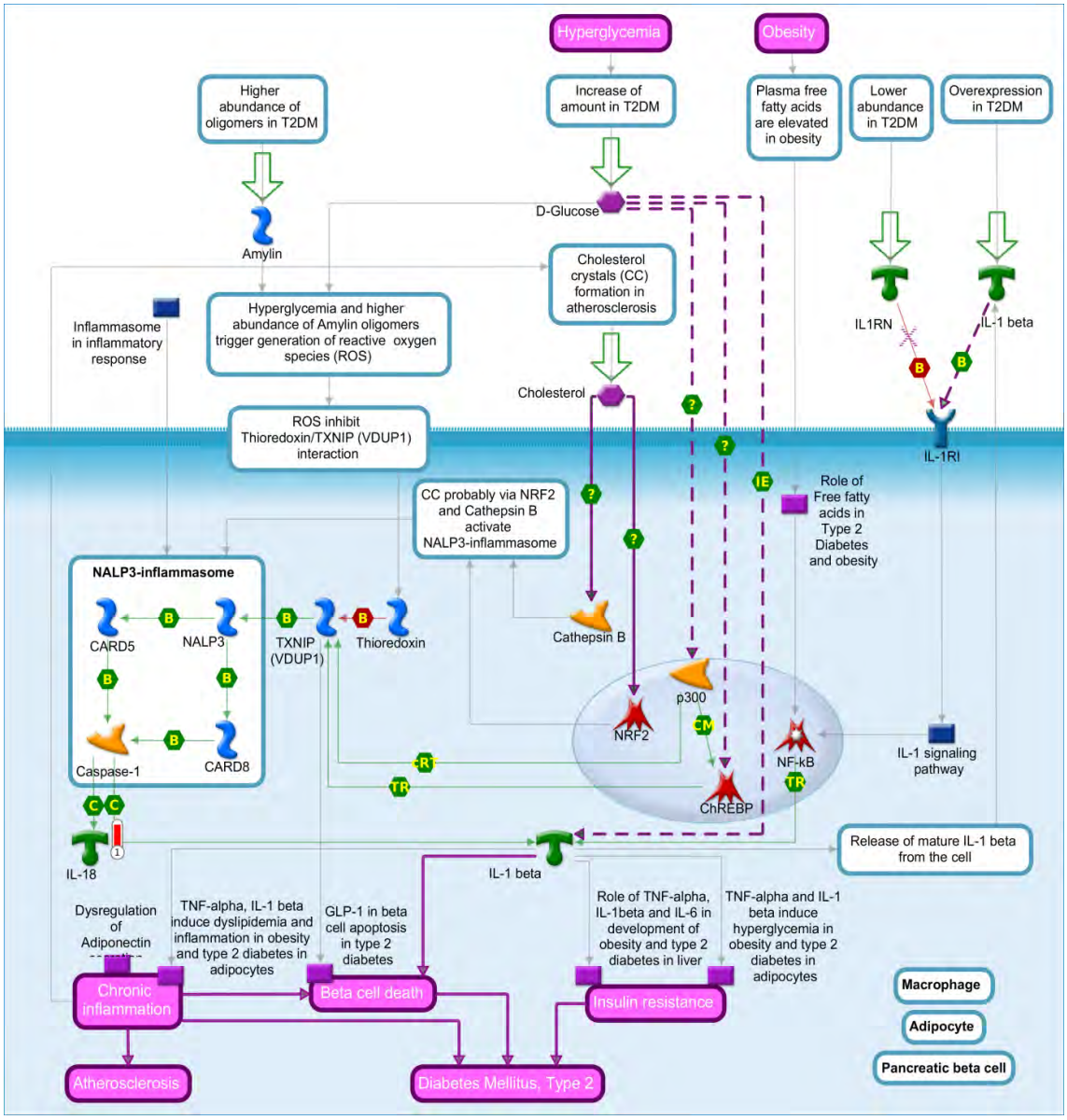

Figure 35. Role of inflammasome in macrophages, adipocytes and pancreatic beta cells in type 2 diabetes pathway map by MetaCore software (p-value < 0.10) from the list of differentially expressed genes (FDR 10%) in the liver tissue immunocastrated male pigs fed with two different oils in the diet (3.0 % soybean oil and 3.0 % fish oil). The blue thermometer indicates that the DEG is down-regulated in the diet with 3.0 % of soybean oil (SOY). Green arrows indicate positive interaction and gray arrows indicate unspecified interaction. For a detailed definition, see https://portal.genego.com/legends/MetaCoreQuickReferenceGuide.pdf

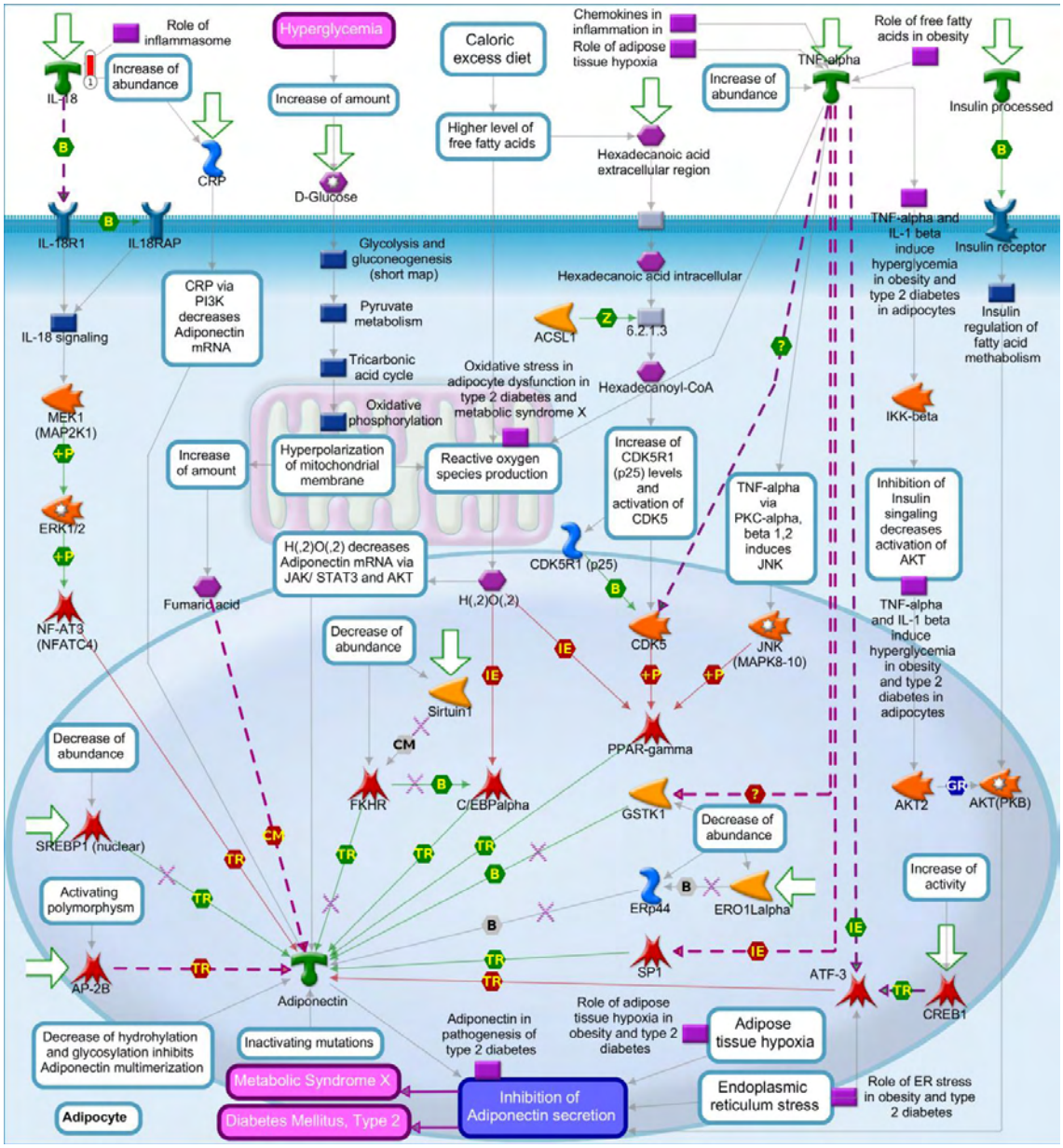

Figure 36. Role of IFN-beta in inhibition of Th1 cell differentiation in multiple sclerosis pathway map by MetaCore software (p-value < 0.10) from the list of differentially expressed genes (FDR 10%) in the liver tissue immunocastrated male pigs fed with two different oils in the diet (3.0 % soybean oil and 3.0 % fish oil). The blue thermometer indicates that the DEG is down-regulated in the diet with 3.0 % of soybean oil (SOY). Green arrows indicate positive interaction and gray arrows indicate unspecified interaction. For a detailed definition, see https://portal.genego.com/legends/MetaCoreQuickReferenceGuide.pdf

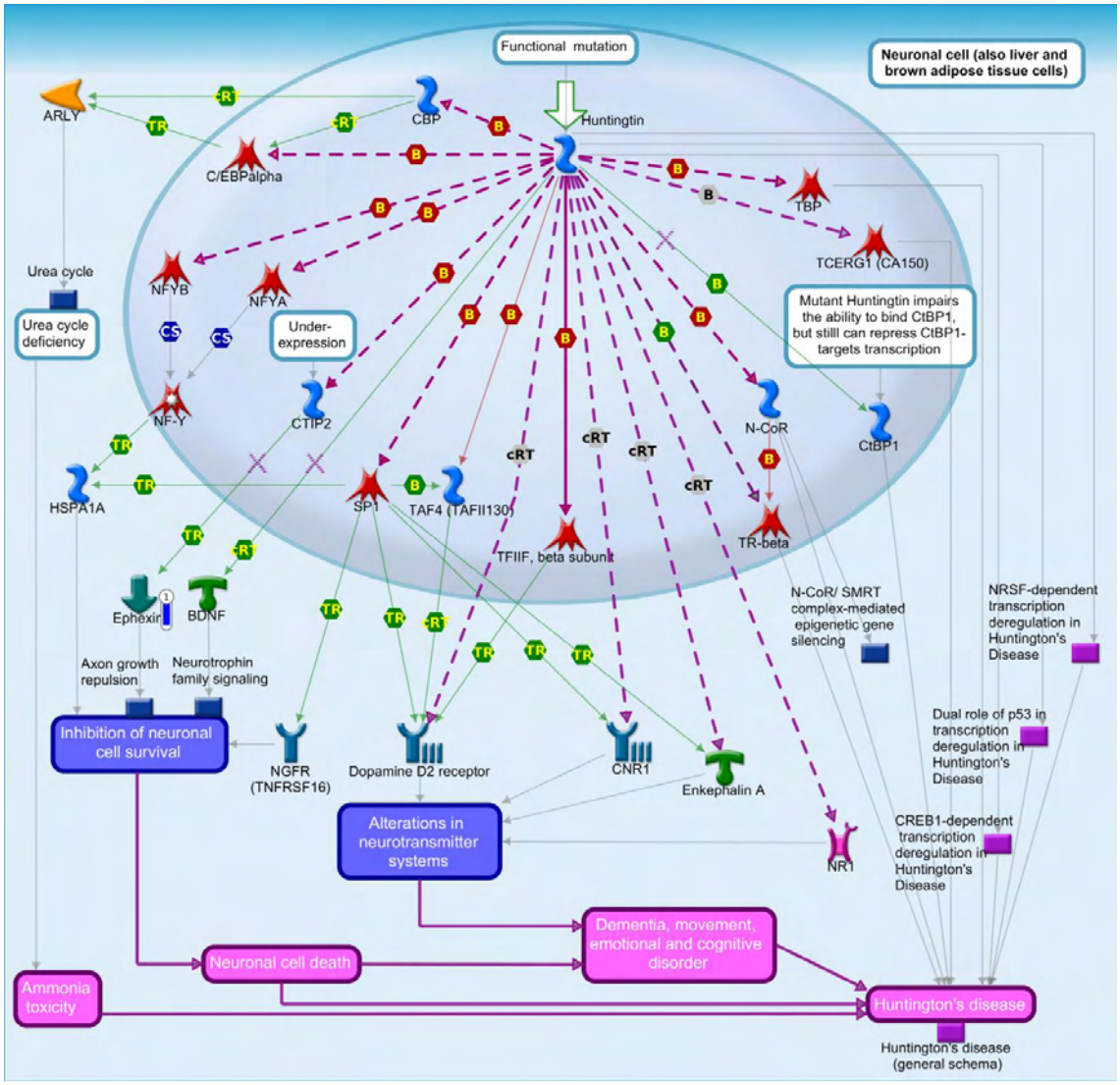

Figure 37. Huntingtin-depended transcription deregulation in Huntington's Disease pathway map by MetaCore software (p-value < 0.10) from the list of differentially expressed genes (FDR 10%) in the liver tissue immunocastrated male pigs fed with two different oils in the diet (3.0 % soybean oil and 3.0 % fish oil). The blue thermometer indicates that the DEG is down-regulated in the diet with 3.0 % of soybean oil (SOY). Green arrows indicate positive interaction and gray arrows indicate unspecified interaction. For a detailed definition, see https://portal.genego.com/legends/MetaCoreQuickReferenceGuide.pdf.

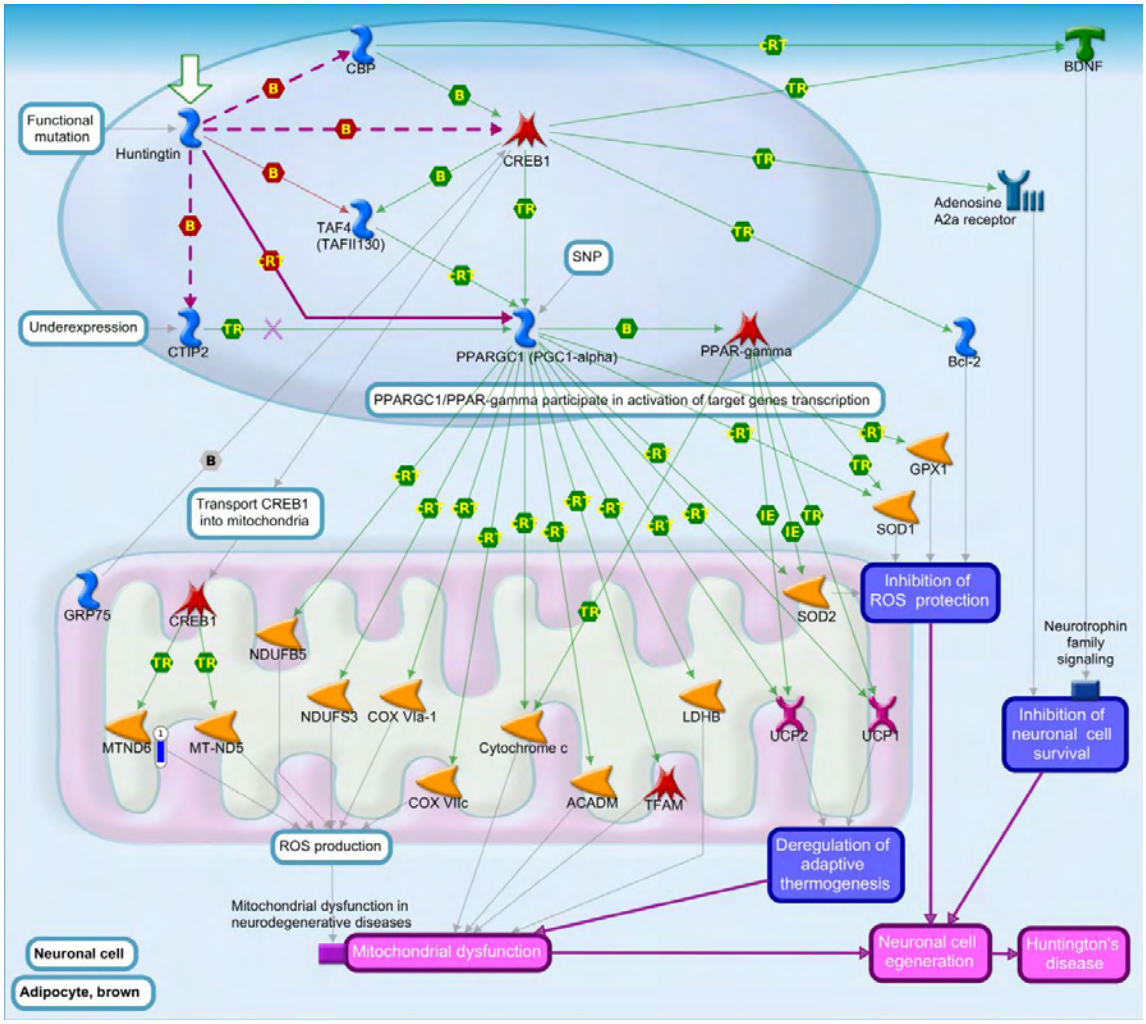

Figure 38. CREB1-dependent transcription deregulation in Huntington's Disease pathway map by MetaCore software (p-value < 0.10) from the list of differentially expressed genes (FDR 10%) in the liver tissue immunocastrated male pigs fed with two different oils in the diet (3.0 % soybean oil and 3.0 % fish oil). The blue thermometer indicates that the DEG is down-regulated in the diet with 3.0 % of soybean oil (SOY). Green arrows indicate positive interaction and gray arrows indicate unspecified interaction. For a detailed definition, see https://portal.genego.com/legends/MetaCoreQuickReferenceGuide.pdf

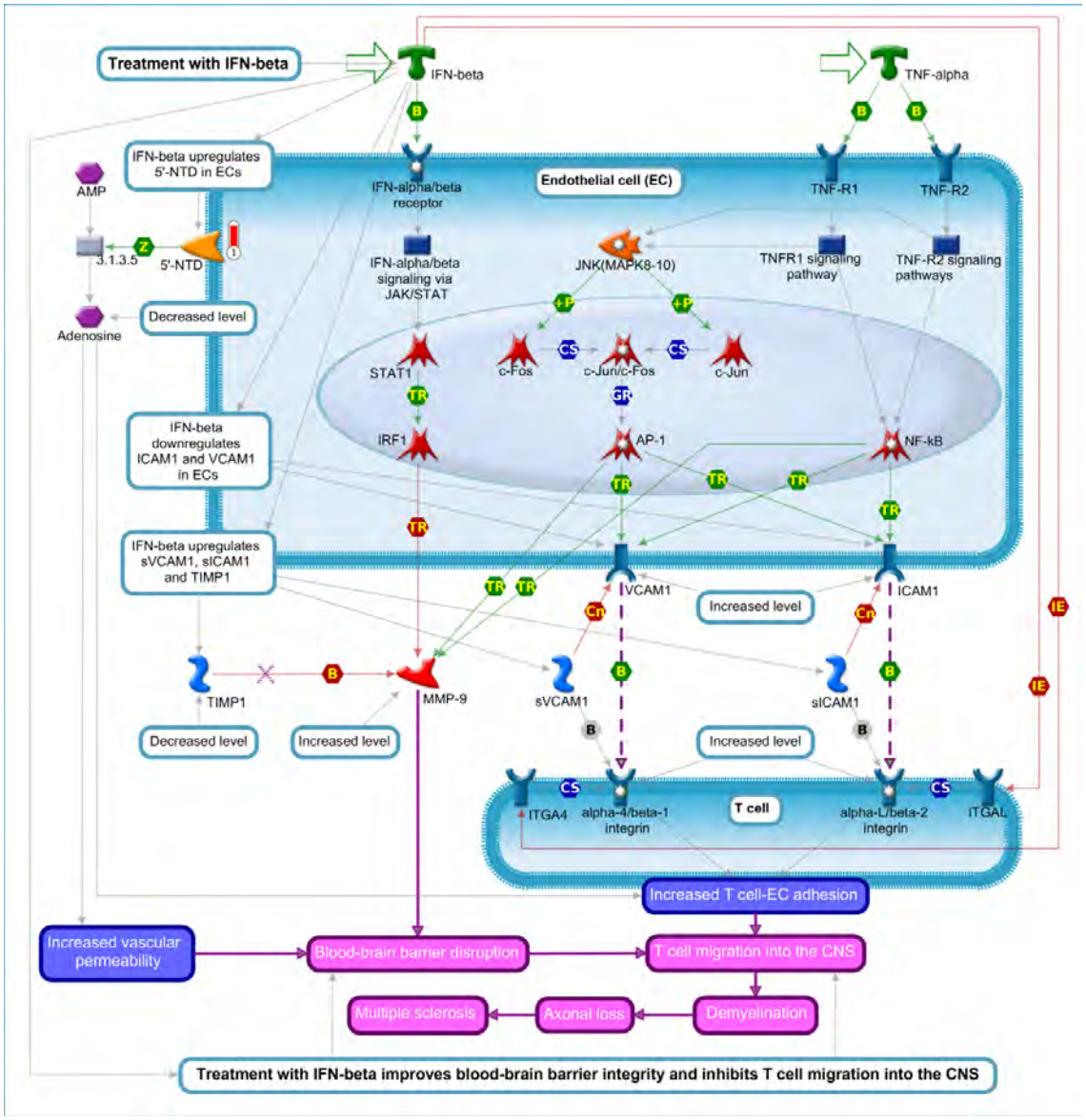

Figure 39. Role of IFN-beta in the improvement of blood-brain barrier integrity in multiple sclerosis pathway map by MetaCore software (p-value < 0.10) from the list of differentially expressed genes (FDR 10%) in the liver tissue immunocastrated male pigs fed with two different oils in the diet (3.0 % soybean oil and 3.0 % fish oil). The blue thermometer indicates that the DEG is down-regulated in the diet with 3.0 % of soybean oil (SOY). Green arrows indicate positive interaction and gray arrows indicate unspecified interaction. For a detailed definition, see https://portal.genego.com/legends/MetaCoreQuickReferenceGuide.pdf

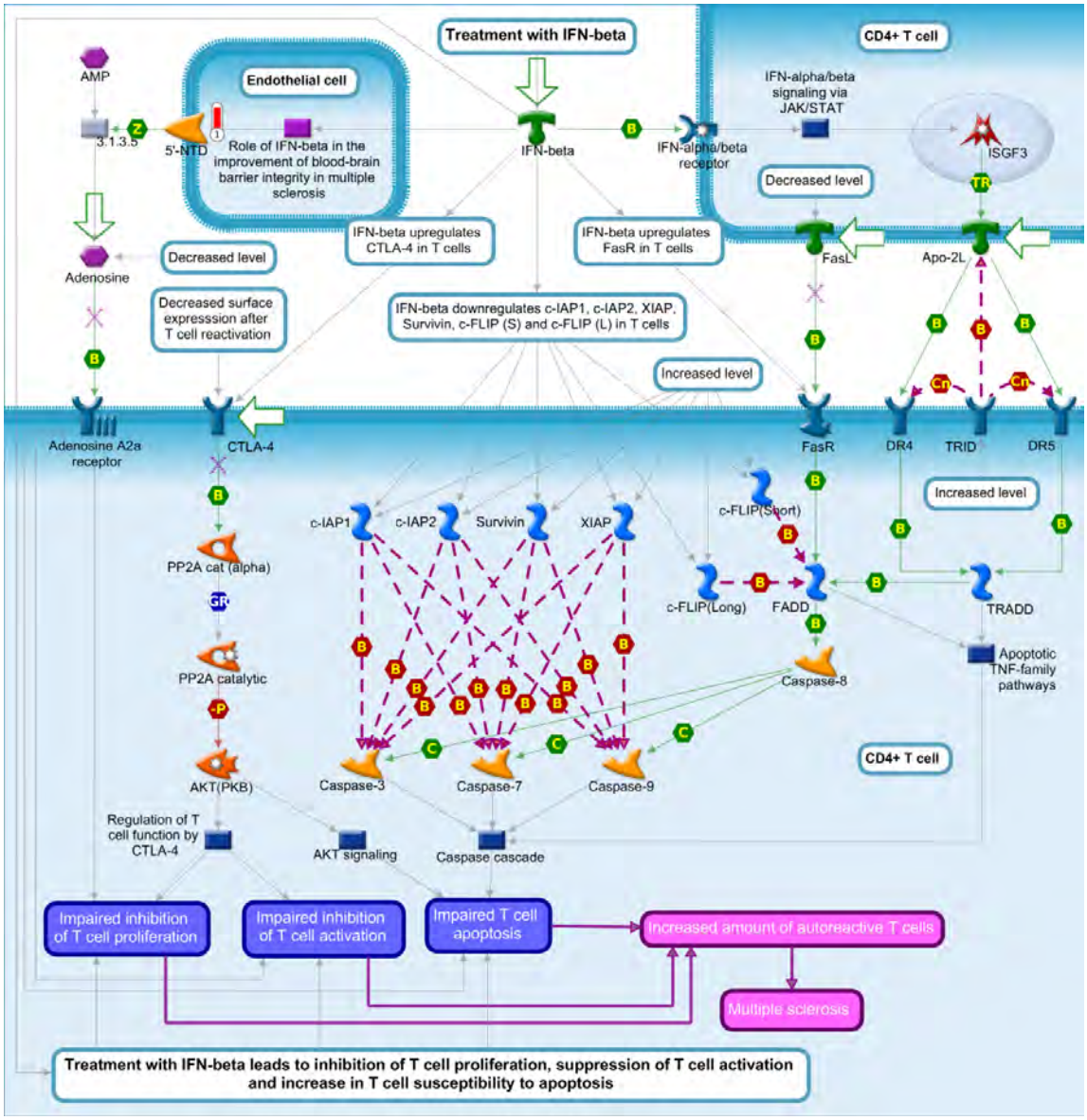

Figure 40. Role of IFN-beta in activation of T cell apoptosis in multiple sclerosis pathway map by MetaCore software (p-value < 0.10) from the list of differentially expressed genes (FDR 10%) in the liver tissue immunocastrated male pigs fed with two different oils in the diet (3.0 % soybean oil and 3.0 % fish oil). The blue thermometer indicates that the DEG is down-regulated in the diet with 3.0 % of soybean oil (SOY). Green arrows indicate positive interaction and gray arrows indicate unspecified interaction. For a detailed definition, see https://portal.genego.com/legends/MetaCoreQuickReferenceGuide.pdf

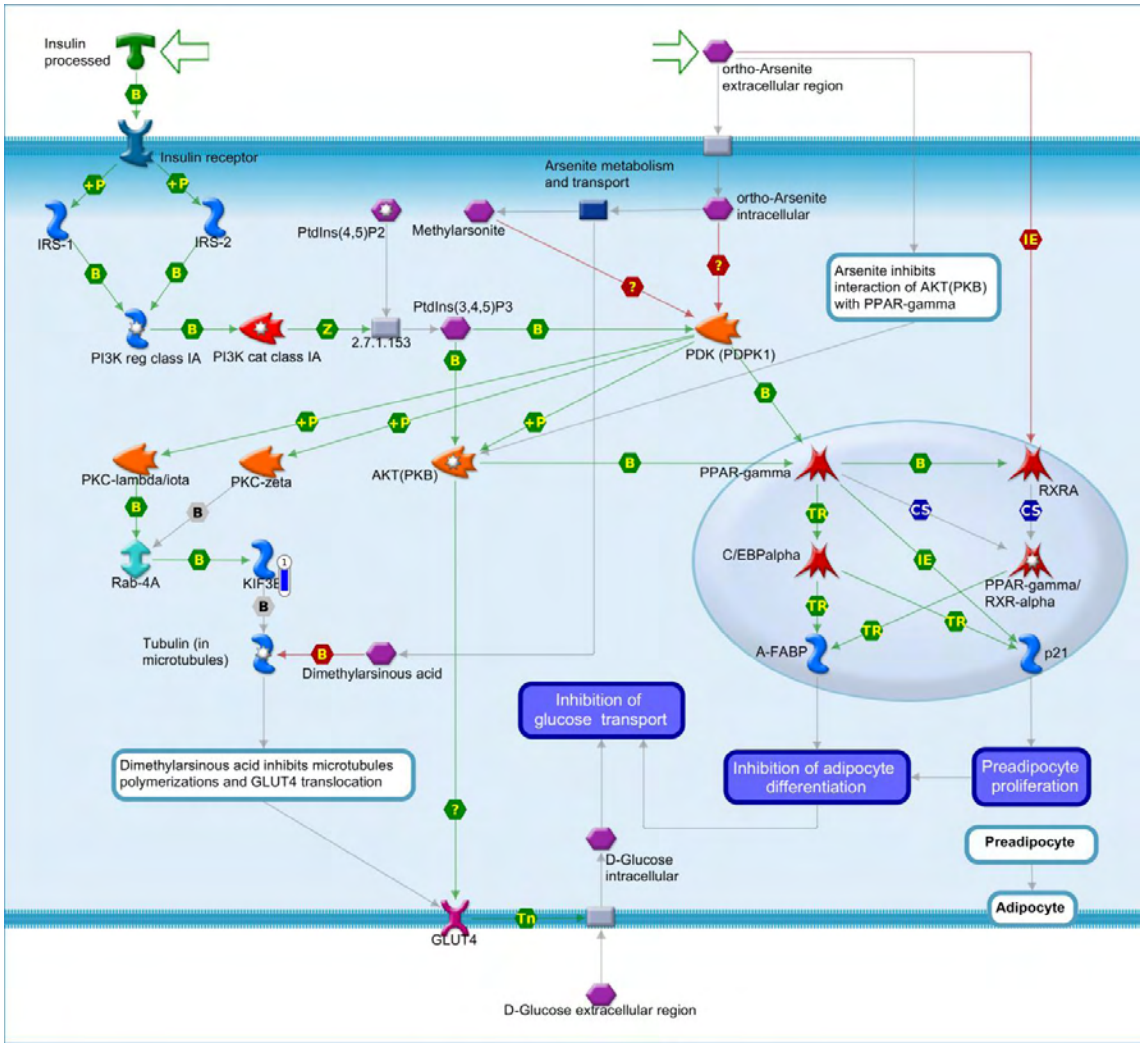

Figure 41. Influence of low doses of arsenite on glucose uptake in adipocytes pathway map by MetaCore software (p-value < 0.10) from the list of differentially expressed genes (FDR 10%) in the liver tissue immunocastrated male pigs fed with two different oils in the diet (3.0 % soybean oil and 3.0 % fish oil). The blue thermometer indicates that the DEG is down-regulated in the diet with 3.0 % of soybean oil (SOY). Green arrows indicate positive interaction and gray arrows indicate unspecified interaction. For a detailed definition, see https://portal.genego.com/legends/MetaCoreQuickReferenceGuide.pdf.

In addition to these analyses, a process networks analysis (Table 9) was obtained to assist in the understanding of the enriched pathways through interactions by gene networks that are related to the change of oil in the diet. Emphasizing the pathways of "regulation of bile acid metabolism", "regulation of lipid metabolism", and "negative *FXR* dependent regulation of bile acids concentration", as well as, pathways related to signal transduction, sodium transport, and neurophysiological process.

Table 8: Processes networks by MetaCore software (p-value <0.1) from the list of differentially expressed genes (FDR 10%) in the liver tissue immunocastrated male pigs fed between two different oil sources (SOY*vs*FO)

Process Networks	p-value	DEG
Signal transduction_ESR1-nuclear pathway	1.081E-02	*BCAS3, SMAD3, CYP7A1, DLC1 (Dynein LC8a)*
Regulation of metabolism_Bile acid regulation of lipid metabolism and negative FXR-dependent regulation of bile acids concentration"	3.351E-02	*CYP2B6, CYP7A1*
Transport_Sodium transport	6.506E-02	*SLC5A9, SN1, SN2*
Reproduction_Male sex differentiation	7.348E-02	*Olfactory receptor, SMAD3, Calpastatin*
Neurophysiological process_Olfactory transduction	7.476E-02	*Olfactory receptor*
Cytoskeleton_Cytoplasmic microtubules	7.926E-02	*KIF3B, DLC1 (Dynein LC8a)*
Cardiac development_BMP_TGF_beta_signaling	8.165E-02	*MSX1, SMAD3*
Signal transduction_Androgen receptor nuclear signaling	9.267E-02	*SMAD3, NRIP*

3.7 Functional enrichment analysis for skeletal muscle differential expression (COvsFO)

Different pathway maps were detected (p-value <0.10) (Figure 42), most of the pathways presented the stearoyl-CoA desaturase *(SCD)* DEG, such as "adiponectin in pathogenesis of type 2 diabetes" (Figure 43); "regulation of lipid metabolism *RXR*-dependent regulation of lipid metabolism via *PPAR, RAR and VDR*" (Figure 44); "putative pathways for stimulation of fat cell differentiation by Bisphenol A" (Figure 45); "regulation of lipid metabolism Regulation of lipid metabolism via *LXR, NF-Y,* and *SREBP" (*Figuree 46); and, "regulation of metabolism Bile acids regulation of glucose and lipid metabolism via *FXR* and Role of ER stress in obesity and type 2 diabetes" (Figure 47). We also detected pathways presenting the DEG aldehyde dehydrogenase 3 family member A2 *(AL3A2*), like the "FA omega oxidation" (Figure 48), "leukotriene 4 biosynthesis and metabolism" (Figure 49), "triacylglycerol metabolism (Figure 50), and some presenting the DEG *CD4,* as the "breakdown of *CD4+ T* cell peripheral tolerance in type 1 diabetes mellitus" (Figure 51).

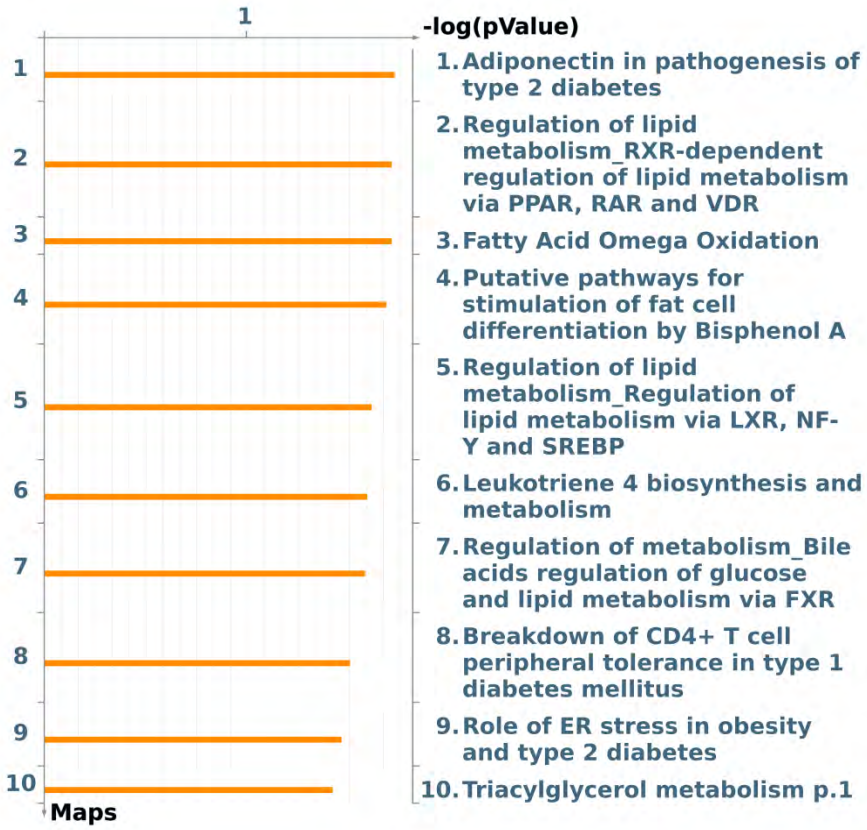

Figure 42. Pathway maps by MetaCore software (p-value < 0.1) from the list of differentially expressed genes (FDR 10%) in the skeletal muscle immunocastrated male pigs fed with two different oil (3.0 % canola oil vs 3.0% fish oil).

In our study, *SCD* expression was lower (log2 fold change -1.62) in the group of pigs fed with the canola oil diet. The *SCD*-enriched pathways were "adiponectin in pathogenesis of type 2 diabetes", "regulation of lipid metabolism *RXR*-dependent regulation of lipid metabolism via *PPAR, RAR and VDR"*, "putative pathways for stimulation of fat cell differentiation by Bisphenol A", and "regulation of lipid metabolism regulation of lipid metabolism via *LXR, NF-Y and SREBP*".

The *AL3A2* gene was identified as DEG between CO*vs*FO, the expression of *AL3A2* was lower in the CO group. This gene has MetaCore enriched pathways related to "FA omega oxidation", "leukotriene 4 biosynthesis and metabolism", and "triacylglycerol metabolism p.1". Lastly, T-cell surface glycoprotein *CD4 (CD4)* was enriched in pathways related to the "Breakdown of CD4+ T cell peripheral tolerance in type 1 diabetes mellitus".

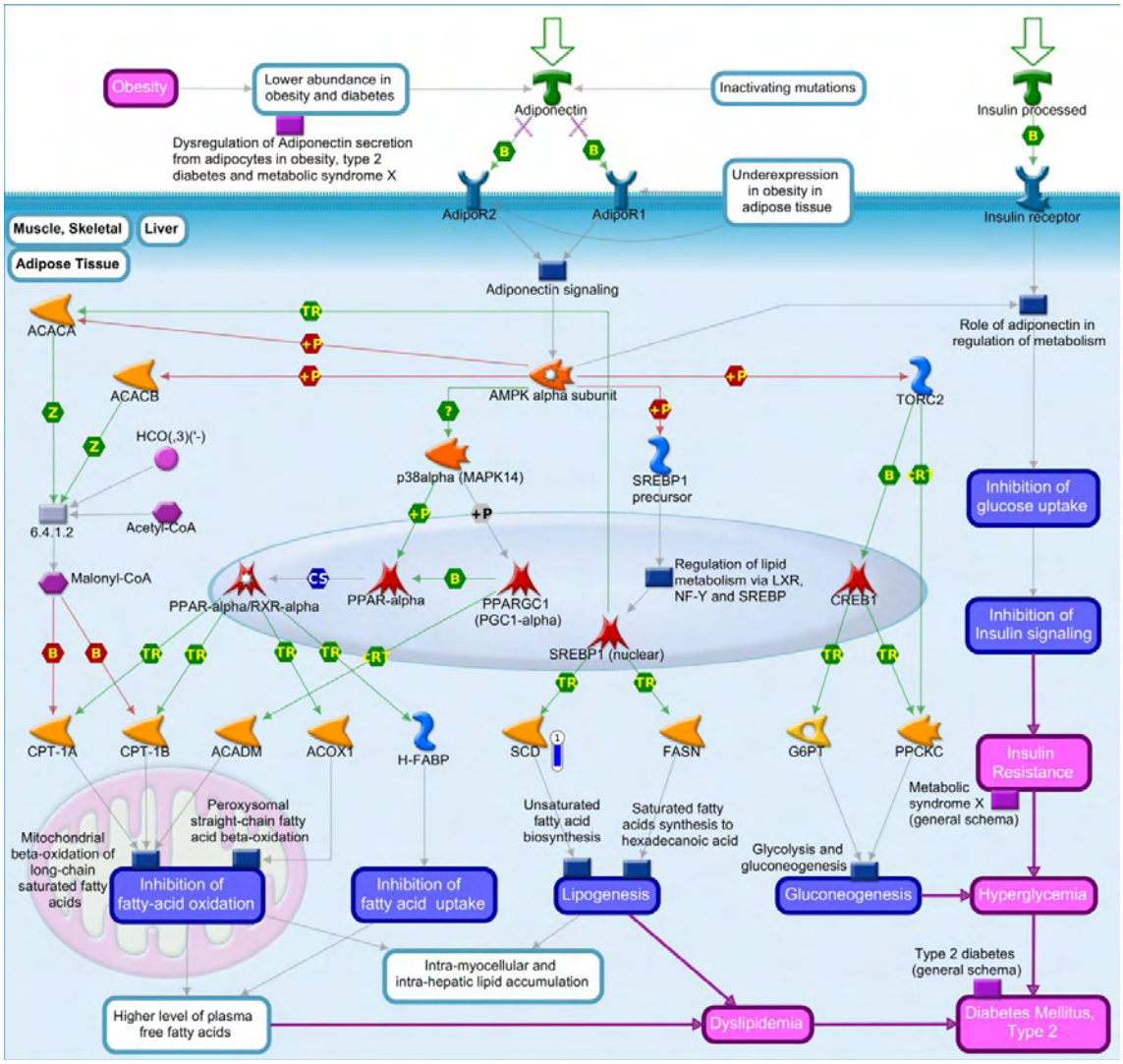

Figure 43. Adiponectin in pathogenesis of type 2 diabetes pathway map by MetaCore software (p-value < 0.10) from the list of differentially expressed genes (FDR 10%) in the skeletal muscle immunocastrated male pigs fed with two different oils in the diet (3.0 % canola oil and 3.0 % fish oil). The blue thermometer indicates that the DEG is down-regulated in the diet with 3.0 % of canola oil (CO). Green arrows indicate positive interaction and gray arrows indicate unspecified interaction. For a detailed definition, see https://portal.genego.com/legends/MetaCoreQuickReferenceGuide.pdf.

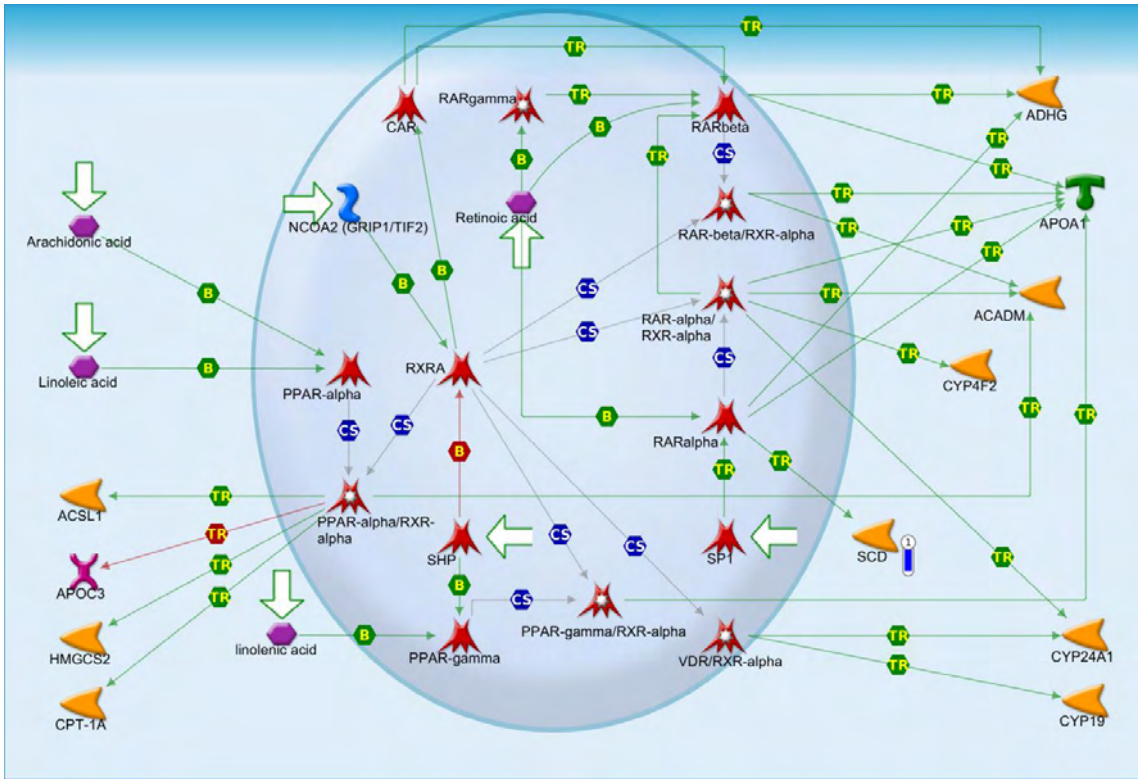

Figure 44. Regulation of lipid metabolism_RXR-dependent regulation of lipid metabolism via PPAR, RAR and VDR pathway map by MetaCore software (p-value < 0.10) from the list of differentially expressed genes (FDR 10%) in the skeletal muscle immunocastrated male pigs fed with two different oils in the diet (3.0 % canola oil and 3.0 % fish oil). The blue thermometer indicates that the DEG is down-regulated in the diet with 3.0 % of canola oil (CO). Green arrows indicate positive interaction and gray arrows indicate unspecified interaction. For a detailed definition, see https://portal.genego.com/legends/MetaCoreQuickReferenceGuide.pdf.

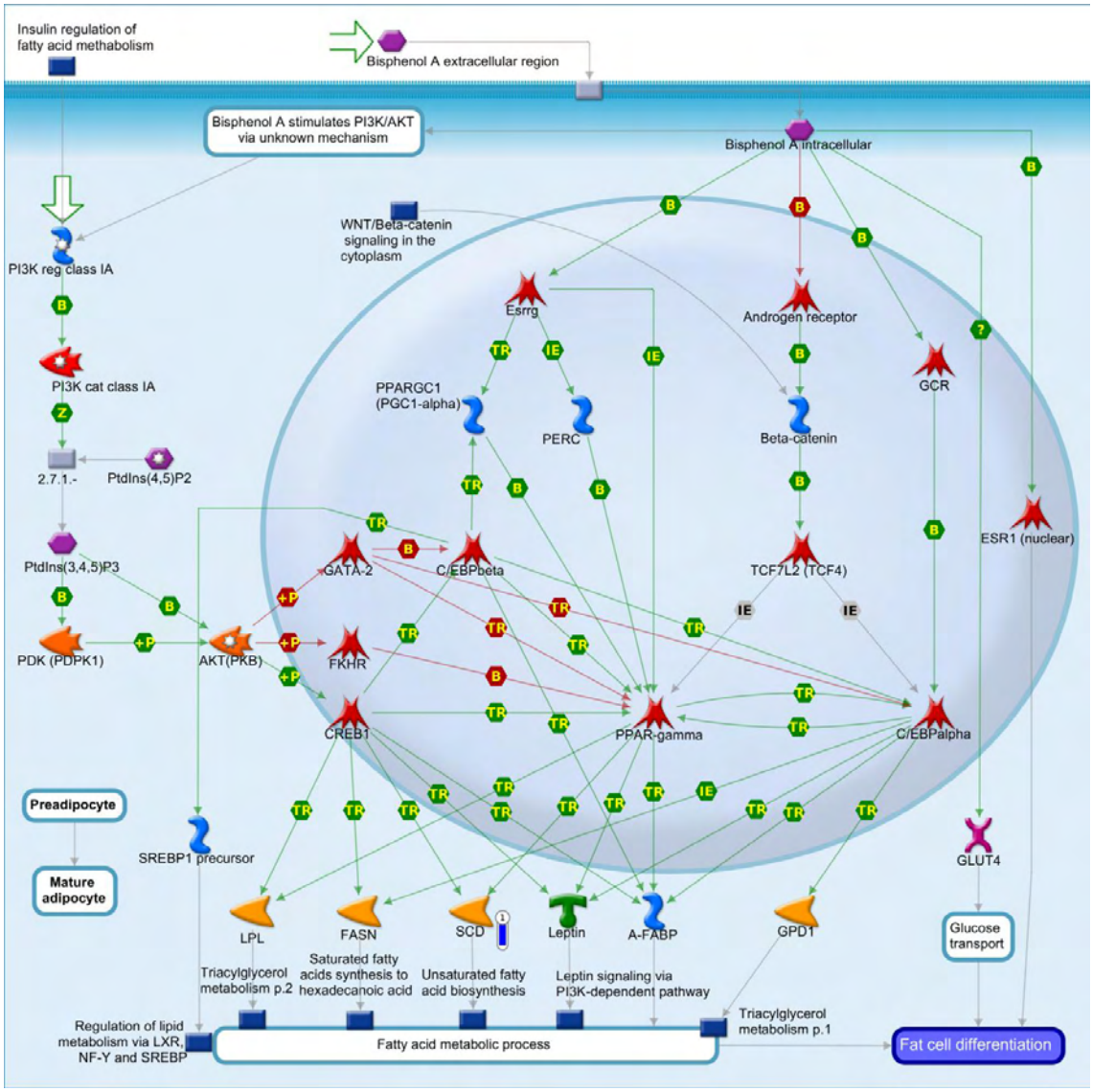

Figure 45. Putative pathways for stimulation of fat cell differentiation by Bisphenol A pathway map by MetaCore software (p-value < 0.10) from the list of differentially expressed genes (FDR 10%) in the skeletal muscle immunocastrated male pigs fed with two different oils in the diet (3.0 % canola oil and 3.0 % fish oil). The blue thermometer indicates that the DEG is down-regulated in the diet with 3.0 % of canola oil (CO). Green arrows indicate positive interaction and gray arrows indicate unspecified interaction. For a detailed definition, see https://portal.genego.com/legends/MetaCoreQuickReferenceGuide.pdf.

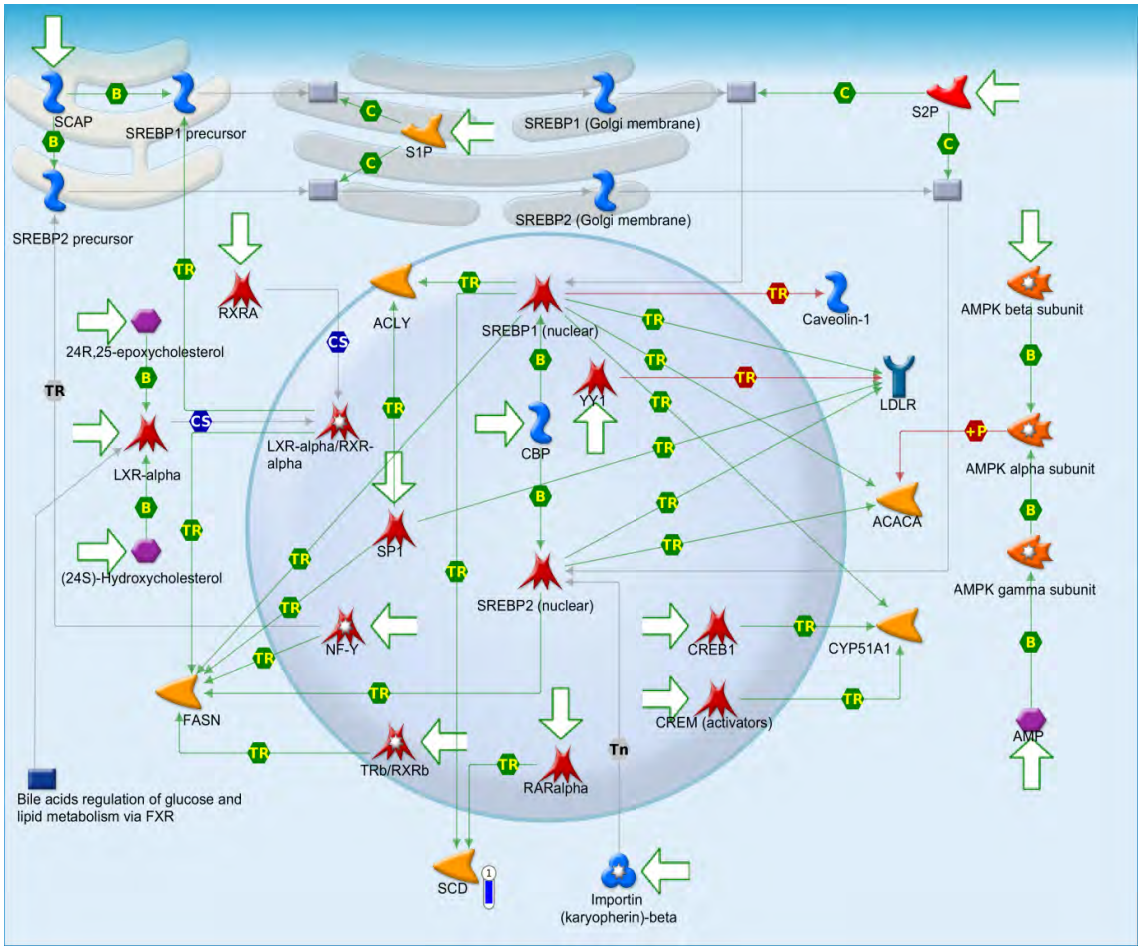

Figure 46. Regulation of lipid metabolism_Regulation of lipid metabolism via LXR, NF-Y and SREBP pathway map by MetaCore software (p-value < 0.10) from the list of differentially expressed genes (FDR 10%) in the skeletal muscle immunocastrated male pigs fed with two different oils in the diet (3.0 % canola oil and 3.0 % fish oil). The blue thermometer indicates that the DEG is down-regulated in the diet with 3.0 % of canola oil (CO). Green arrows indicate positive interaction and gray arrows indicate unspecified interaction. For a detailed definition, see https://portal.genego.com/legends/MetaCoreQuickReferenceGuide.pdf.

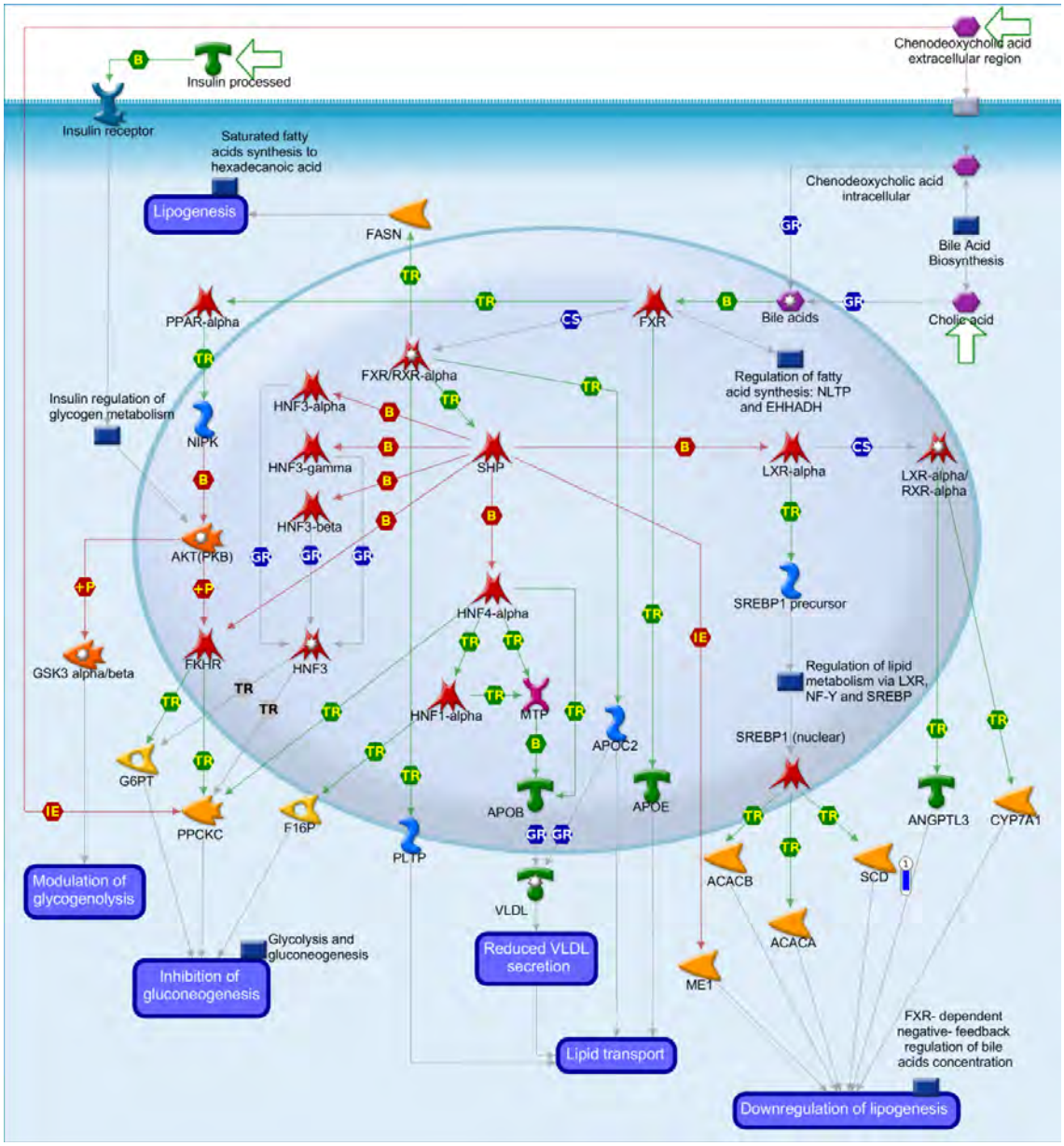

Figure 47. Regulation of metabolism_Bile acids regulation of glucose and lipid metabolism via FXR pathway map by MetaCore software (p-value < 0.10) from the list of differentially expressed genes (FDR 10%) in the skeletal muscle immunocastrated male pigs fed with two different oils in the diet (3.0 % canola oil and 3.0 % fish oil). The blue thermometer indicates that the DEG is down-regulated in the diet with 3.0 % of canola oil. (CO). Green arrows indicate positive interaction and gray arrows indicate unspecified interaction. For a detailed definition, see https://portal.genego.com/legends/MetaCoreQuickReferenceGuide.pdf.

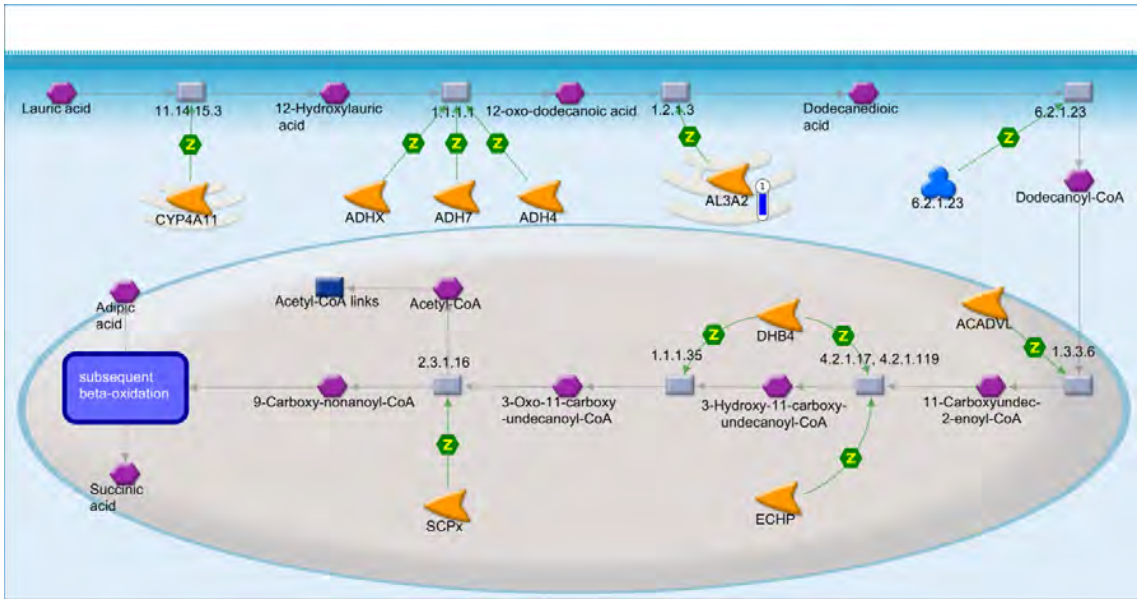

Figure 48. Fatty Acid Omega Oxidation pathway map by MetaCore software (p-value < 0.10) from the list of differentially expressed genes (FDR 10%) in the skeletal muscle immunocastrated male pigs fed with two different oils in the diet (3.0 % canola oil and 3.0 % fish oil). The blue thermometer indicates that the DEG is down-regulated in the diet with 3.0 % of canola oil (CO). Green arrows indicate positive interaction and gray arrows indicate unspecified interaction. For a detailed definition, see https://portal.genego.com/legends/MetaCoreQuickReferenceGuide.pdf.

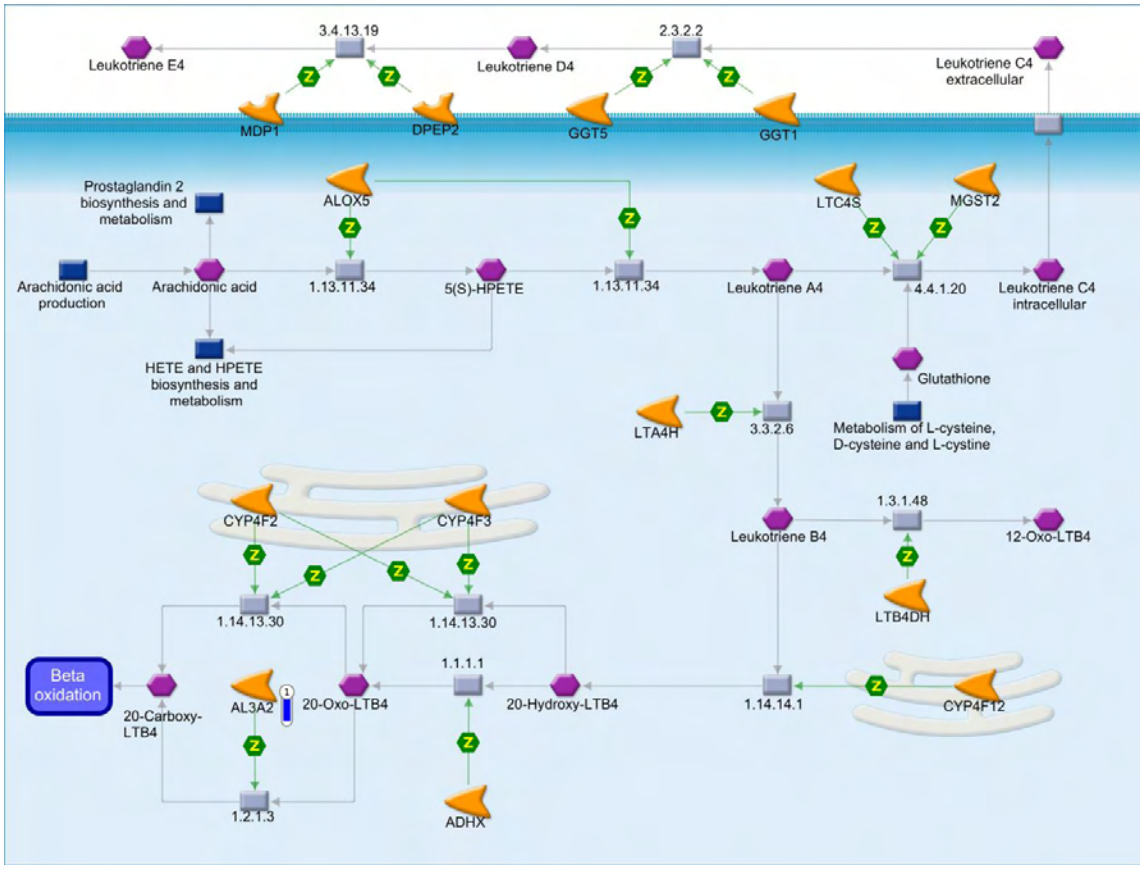

Figure 49. Leukotriene 4 biosynthesis and metabolism pathway map by MetaCore software (p-value < 0.10) from the list of differentially expressed genes (FDR 10%) in the skeletal muscle immunocastrated male pigs fed with two different oils in the diet (3.0 % canola oil and 3.0 % fish oil). The blue thermometer indicates that the DEG is down-regulated in the diet with 3.0 % of canola oil (CO). Green

arrows indicate positive interaction and gray arrows indicate unspecified interaction. For a detailed definition, see https://portal.genego.com/legends/MetaCoreQuickReferenceGuide.pdf.

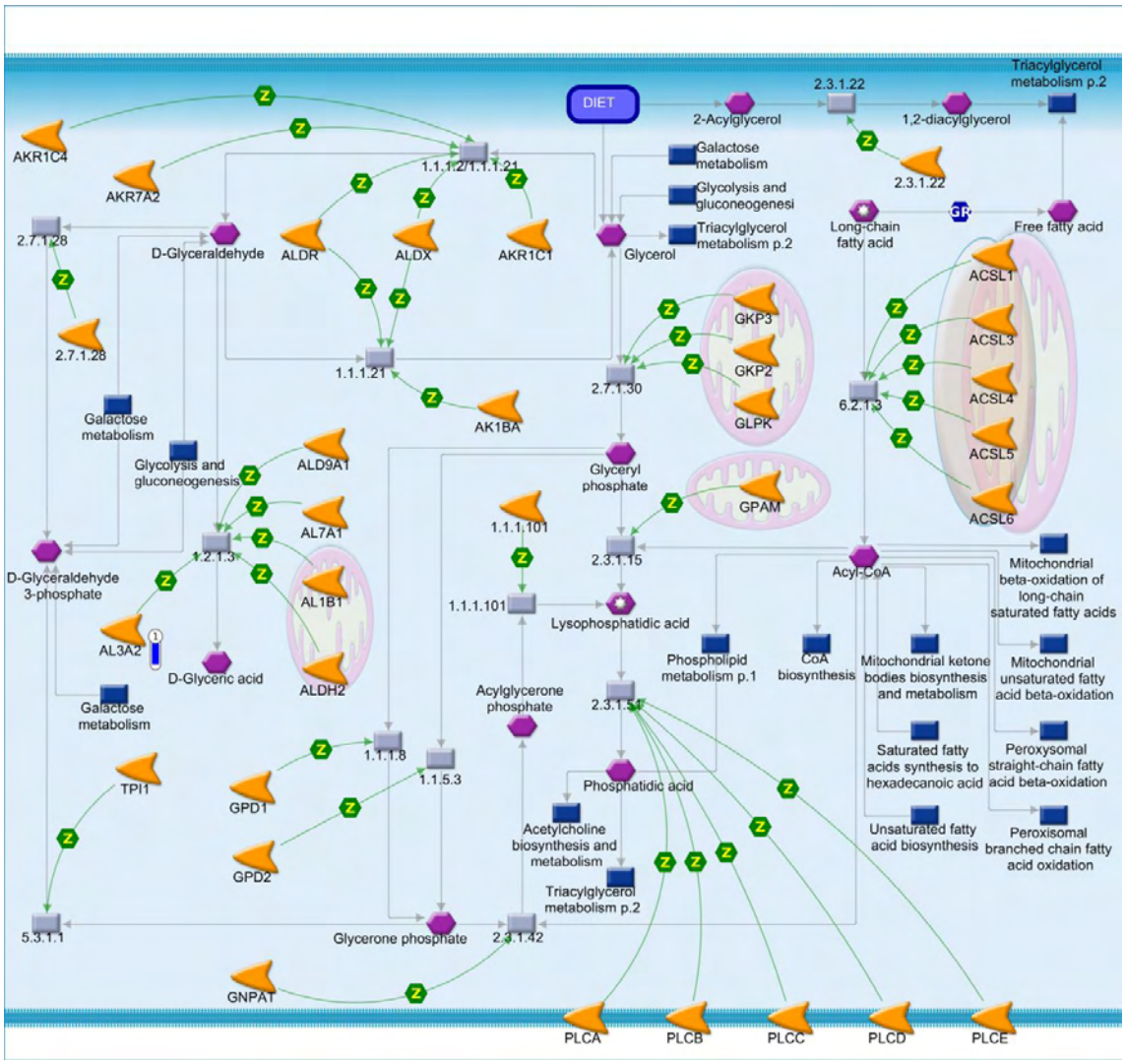

Figure 50. Triacylglycerol metabolism p.1 pathway map by MetaCore software (p-value < 0.10) from the list of differentially expressed genes (FDR 10%) in the skeletal muscle immunocastrated male pigs fed with two different oils in the diet (3.0 % canola oil and 3.0 % fish oil). The blue thermometer indicates that the DEG is down-regulated in the diet with 3.0 % of canola oil (CO). Green arrows indicate positive interaction and gray arrows indicate unspecified interaction. For a detailed definition, see https://portal.genego.com/legends/MetaCoreQuickReferenceGuide.pdf.

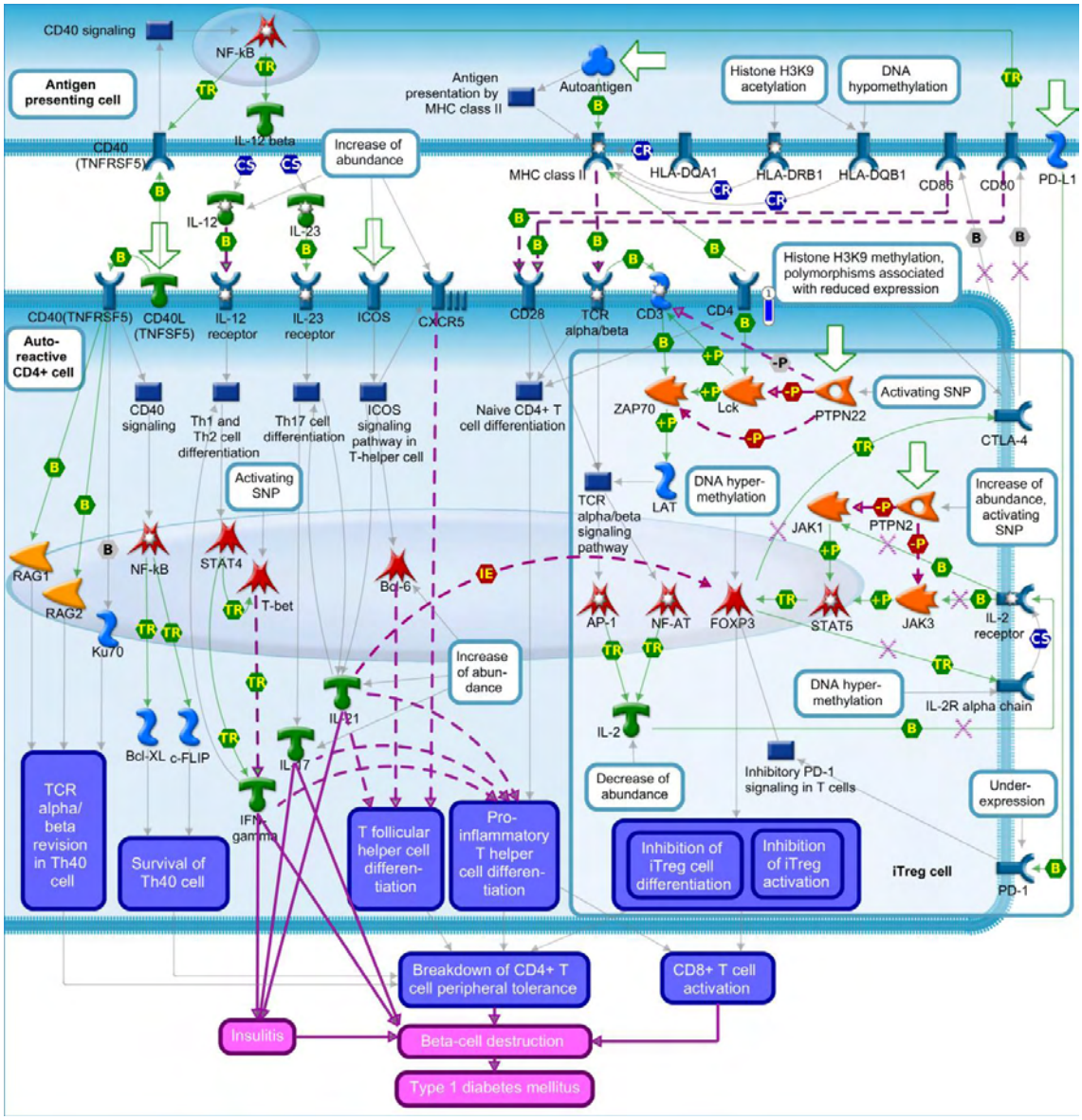

Figure 51. Breakdown of CD4+ T cell peripheral tolerance in type 1 diabetes mellitus pathway map by MetaCore software (p-value < 0.10) from the list of differentially expressed genes (FDR 10%) in the skeletal muscle immunocastrated male pigs fed with two different oil in the diet (3.0 % canola oil and 3.0 % fish oil). The blue thermometer indicates that the DEG is down-regulated in the diet with 3.0 % of canola oil (CO). Green arrows indicate positive interaction and gray arrows indicate unspecified interaction. For a detailed definition, see https://portal.genego.com/legends/MetaCoreQuickReferenceGuide.pdf.

A process networks analysis was performed to help understanding the enriched pathways through interactions by gene networks that are related to dietary oil change. Emphasizing the pathways regulation of bile acid metabolism and negative *FXR* dependent regulation of bile acid concentration, signal transduction, inflammation amphoterin signaling, chemotaxis, development skeletal muscle with the genes *SCD*, *AKAP3*, *Myosin heavy chain (MyHC)*, and *CD4* (Figure 52).

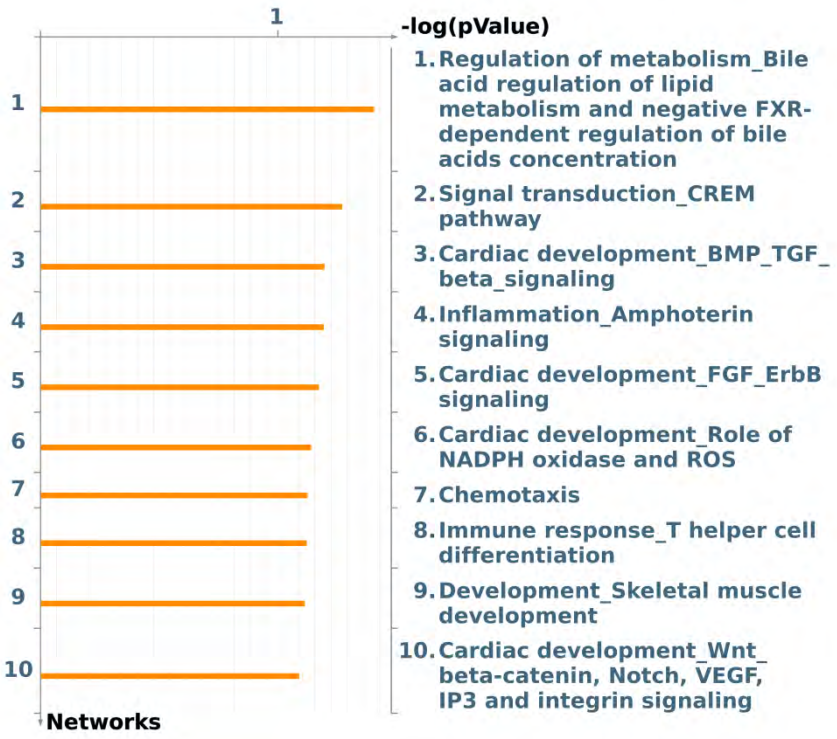

Figure 52. Top 10 enriched networks identified by MetaCore software from the list of differentially expressed genes (FDR 10%) in the skeletal muscle immunocastrated male pigs fed with different oils (3.0 % canola oil and 3.0 % of soybean oil).

4.DISCUSSION

Fatty acid profile and blood biochemical parameters: We observed with the analysis of the intramuscular lipid composition, that the addition of FO in the diet of growing and finishing pigs showed a higher FA profile composition of eicosapentaenoic acid (C20:5 n-3), docosahexaenoic acid (C22:6 n-3), and SFA as palmitic acid (C16:0) and stearic acid (C18:0). According to Jeromson et al. (2015), diets rich in saturated fat may be associated with the onset of obesity and type 2 diabetes. In the other hand, the pigs fed with fish oil showed the lowest n-6:n-3 PUFA ratio, showing the potential of the diet in modifying pork composition through FA modulation in the animals' diet (MA; JIANG; LAI, 2016). Our findings corroborate with Jeromson et al. (2015), which stated that the skeletal muscle can be manipulated according to changes in the animal diet.

Omega 3 PUFA has been linked to protection against chronic and metabolic diseases, whereas n-6 PUFA may be related to inflammation, blood vessel constriction, and aggregation. Thus, the proportion of these PUFA and the dietary LA and ALA content may be relevant to the regulation of body homeostasis inflammation and anti-inflammatory effect (SAINI; KEUM, 2018). The modification of pork FA can show us

pathways and networks related to both inflammation and relevant diseases and metabolic processes. Moreover, the amount and source of fat plays a key role in regulating the metabolic health of the whole body, FA are components of cell membranes, act as signaling molecules, and may change related to the muscle lipid pool, thus modifying both metabolic and physical functions of the skeletal muscle (JEROMSON et al., 2015).

According to Saini and Keum (2018), n−3 and n−6 PUFA have opposite effects on the metabolic functions of the body, so they are important to be analyzed. The myristic acid, involved in the increase in plasma cholesterol concentration has a harmful cardiovascular effect in humans (KASPRZYK; TYRA; BABICZ, 2015). Herein, the liver composition of animals receiving diets with FO and CO ($P < 0.05$) was lower for this SFA compared to pigs fed diets containing SOY.

According to Corominas et al. (2013) modifications related to the replacement of SFA by MUFA or PUFA decreases serum LDL-cholesterol and total Cholesterol, in our study we did not observe a difference in serum LDL-cholesterol and total cholesterol was lower in the groups fed with FO and SOY compared to the CO group. In FO we observed higher total PUFA composition in the liver and in LL intramuscular FA, with higher deposition of total n-3 PUFA as well as in the liver.

A lower atherogenic index ($P < 0.05$) - which is related to the general dietary quality of lipids (ALMEIDA et al., 2021) and a greater amount of total PUFA, EPA and DHA compared to other types of oils. The atherogenic index is related to predicting the risk of developing atherosclerosis and coronary heart disease; in addition, it is related to dyslipidemia, which is characterized by high plasma concentration of triglycerides and total cholesterol, HDL, LDL (NIROUMAND et al., 2015). In our results the highest serum concentration of cholesterol was found in the CO group.

Genes common to dietary treatments: CO*vs*SOY and SOY*vs*FO showed a higher ratio of common DEG expressed in the diets, showing little variation in the log2 fold change. These genes were modified independently of the source among the FA profiles of the diets in the liver. The DEG *CAST* was identified between comparisons showing little variation in expression, the protein encoded by the gene is a *Calpain* inhibitor and the system between *Calpain* and *Calpastatin* is related to membrane fusion events (STELZER, G. et al, 2016). Together with calcium, it regulates the activity of *Calpain* (RAMI, et al., 2003). Another DEG identified in the liver independent of diet was *CYP7A1* which plays an important role in cholesterol and FA metabolism. The *CYP7A1*

can be inhibited by feedback from hydrophobic bile acids, as bile acids are physiological ligands for the farnesoid X receptor (*FXR*), which when activated indirectly can repress *CYP7A1* through small heterodimer protein (*SHP-1*) induction. Furthermore, *CYP7A1* can be repressed via *JNK* which is activated by *TNF-alpha* in primary cultures of rat hepatocytes (Gupta et al., 2001). In addition, the *CYP7A1* was already considered a putative gene related to FA metabolism in the liver, and was associated with the composition profile of intramuscular FA in a GWAS study conducted by Ramayo-Caldas et al. (2012).

Regarding the common DEG in skeletal muscle, regardless of diet (soybean oil, fish oil, or canola oil), most of them were down-regulated. As an example, the *ALG6* involved in the catalysis of the precursor related to the regulation of lipid metabolism (STELZER, G. et al, 2016). Another DEG identified in the muscle was *CD4* that is related to immune responses and function and is regulated by related signaling pathways. Hypercholesterolemia can mediate the inflammatory response of CD4+ T cells, but this is not completely established in the literature (CAI; JIN and CHEIN, 2021).

The common DEG identified both in the skeletal muscle and liver are related in the regulation of some circadian rhythm genes (*DBP*), and Ca^{+}, cAMP, and lipid signaling pathways (*CCDC90B*) (STELZER, G. et al, 2016). These results demonstrate that modifying the diet profile using different oil sources in distinct tissues impact the gene expression profile, regardless of the dietary treatment having a direct relation to FA.

Functional enrichment analysis in the skeletal muscle and liver tissue with differential expression for the COvsSOY and COvsFO comparisons: Between CO*vs*SOY we identified *AL3A2* and *CD4* DEG in significant pathways maps, the same happened between the comparison of CO*vs*FO diets and in the process networks comparisons. The enzyme *AL3A2* participates in the oxidation of long-chain aliphatic aldehydes to FA (STELZER, G. et al, 2016), possibly being related to the oxidation of 12-oxo-dodecanoic acid to dodecanedioic acid. Furthermore, the aldehyde dehydrogenase *(ALDH)* family, play a relevant role in the function and induction of regulatory T cells, cellular detoxification, and amino acid metabolism (BAZEWICZ et al., 2019). Also, this gene family is important to the detoxifying role in ethanol-caused accumulation of free FA and triacylglycerol, ethanol inhibits lipoprotein export, and increases FA uptake and lipid peroxidation (GALLI; PRICE; CRABB, 1999). Thus, the

consumption of SOY may be related to the improvement of lipid oxidation rate. Similar results were observed in previous work comparing different proportions of soybean oil in which the increase of soybean oil in the pig diet (3.0% of soybean) resulted in a possible improvement in the lipid oxidation rate (Chapter 2). The *AL3A2* was also enriched in the "leukotriene 4 biosynthesis and metabolism" pathway (CO*vs*SOY). Leukotrienes (LTs) are pro-inflammatory mediators. Leukotriene B4 (LBT4) is a lipid mediator derived from arachidonic acid (AA) and plays a relevant role in chronic inflammatory diseases; such as arthritis, cardiovascular diseases, cancer, and metabolic disorders. In studies using fibroblasts, LBT4 showed high levels in obese adipose tissue, contributing to obesity (CHAKRABARTI et al., 2011; Mothe-Satney et al., 2012; Wan et al., 2017). Leukotriene B4 (20-Carboxy-LTB4) can undergo more beta oxidation, which can be directly impacted by the enzyme *AL3A2*, which in the CO group has lower expression, thus causing a decrease in the oxidation process of 20-Oxo-LTB4 to 20-Carboxy-leukotriene B4 in the final step in which the enzyme participates.

The *AL3A2* was enriched in the "triacylglycerol metabolism" pathway. In muscle, FA are a substrate for oxidation and in the liver, which is involved in reesterification, producing triacylglycerol that will later be secreted as very low-density lipoprotein. There is cooperation between tissues, mainly the adipose, liver, and skeletal muscle tissues, so if there is an accumulation of triacylglycerol in skeletal muscle and liver it will probably result in insulin resistance (FRAYN; ARNER; YKI-JÄRVINEN, 2006). Furthermore, *AL3A2* has been linked to Sjögren-Larsson syndrome, since an interruption of *AL3A2* function causes fat accumulation in cells, underscoring the importance of this enzyme in detoxification in various lipid degradation pathways (KUMAR et al., 2020) which is committed to the decrease in expression with CO group. Studies are still needed to understand the specific functions of the *AL3A2* gene (KUMAR et al., 2020).

Finally, *AL3A2* was identified in the "oxidative stress in adipocyte dysfunction in type 2 diabetes and metabolic syndrome X" pathway. Underexpression of *AL3A2* and *GSTA4* may result in attenuation of the lipid peroxide elimination system in obese and insulin-resistant humans, increasing the levels of 4-Hydroxy-2(E)-nonenal, which, when binding xanthine oxidase, increases oxidative activity, and consequently, the additional generation of intracellular reactive oxygen species (ROS) (CURTIS et al., 2010; GRIMSRUD et al., 2007; UNOKI et al., 2007). When the animals were fed soybean oil,

there was a higher expression of *AL3A2*, which may be involved in the increase of the lipid peroxide elimination system.

Another noteworthy gene is *CD4*, it acts as a co-receptor with the T cell receptor on T lymphocytes and on B cells, macrophages, granulocytes, and in several brain regions (STELZER, G. et al, 2016). In "breakdown of *CD4+ T* cell peripheral tolerance in type 1 diabetes mellitus" pathway map, we can see *CD4* through different mechanisms of APC activation, cytokine secretion and direct cell-cell interactions, CD4+ T cells participate in the activation of diabetogenic *CD8+ T* cells, and when activated, autoreactive CD8+ T cells are related to the cytotoxic destruction of pancreatic beta cells (BAKER et al., 2012; PEAKMAN, 2008). In a study evaluating whether n-3 PUFA can alter T cell motility, Cucchi et al (2020) used cells from mice fed a diet enriched with *EPA* and *DHA* for 3 weeks. The authors demonstrated that n-3 PUFA has anti-inflammatory activity, that can be at the systemic level, in which there is a modification of the network of lipid mediators in lymphoid and adipose tissues, and consequent redistribution of *CD4* + T cells in favor of an anti-inflammatory phenotype affecting related cytoskeletal rearrangements migration of activated *CD4 + T* cells (CUCCHI et al., 2020). In our study, the modification of FA profiles by supplying different oils resulted in a decrease of *CD4* in the muscle of pigs fed canola oil. The *CD4* acts as a co-receptor with the T cell receptor on T lymphocytes and on B cells, macrophages, granulocytes and in several brain regions (Stelzer, G. et al, 2016).

Another enriched gene of fundamental importance in several processes is the angiopoietin-1 gene *(Ang-1, ANGPT1).* The *ANGPT1* has a fundamental role in angiogenesis (a process essential for the growth and expansion of adipose tissue) that encompasses signaling mechanisms coordinated with angiopoietins-1 and -2 *(Ang-1, Ang-2)* and TEK tyrosine kinase (*Tie-2*) that is its receptor. In addition, it has an anti-apoptotic function, although its specific role in adipocyte physiology remains unknown (SON et al., 2020). In our study, even the canola oil group showed lower expression of *Ang-1*, the composition of linoleic acid and alpha linolenic acid did not show any difference between the diets. In a study with 3T3-L1 pre- and mature adipocytes cells treated with linoleic acid (18: 2n6) for four, eight, and 16 hours the gene expression of *Ang-1*, *Ang-2,* and *Tie-2* in response to PUFA treatment was determined in mature adipocytes resulting in a decrease in *Ang-1* of 60% from four to eight hours; a decrease in *Ang-2* about 30% in the same period; and, a decrease in *Tie-2* of 72%, 49% and 35% at 4, 8 and 16 hours (SON et al., 2020). The *Ang-1/Tie*-2 pathway is known to be related

to the ability to suppress apoptosis and caspase activation in endothelial cells, improving vascular integrity (SON et al., 2020). In obesity, *HIF1A*-induced transcription of VEGF-A inhibits angiogenesis due to its interruption and hypoxia-activated *HIF1A* inhibiting the expression of *Angiopoietin 1*, which can result in inhibition of vascular remodeling, finally, this increase in adipose tissue mass in obesity without adequate vascularization support leads to hypoxia (PASARICA et al., 2009).

The small heterodimer partner *(SHP, NR0B2)* is a single NR that performs its regulatory function through protein-protein interactions with each other and with TFs, being a transcriptional repressor of gene expression (ZHANGDOWN, YUXIA; HAGEDORN; WANG, 2011). In addition to regulating gene expression related to bile acid transport, lipid metabolism and gluconeogenesis, SHP is also important in the down-regulation of the conversion of cholesterol to bile acids, and can induce apoptosis in liver and cancer cells (ZHANG, Yuxia; Hagedorn; Wang, 2011). The *SHP* was enriched via Regulation of metabolism_Bile acids regulation of glucose and lipid metabolism via FXR. The farnesoid X receptor (FXR) modulates lipogenic processes and bile acid biosynthesis, and in the pathway map the FXR together with the *SHP* are the main metabolism regulators (Mathur et al., 2021). In the CO group the *SHP* is up-regulated and related in pathway it inhibits transcription factors, that is, with the increase of *SHP* there is an accentuation of the final processes impacting processes such as the reduction of very low density lipoprotein (VLDL) secretion; negative regulation of lipid biosynthetic process, and negative regulation of gluconeogenesis, in addition to impacting genes related to FA biosynthesis. In the pathway “Insulin resistance in type 2 diabetes in liver”, the *SHP* is a target of the forkhead box O1 (FKHR) and is related to type 2 diabetes. In a study with mice, the high-fat diet mice overexpressed *SHP* while *SHP* deficiency in another group of mice was related to the prevention of fatty liver, also showed a reduced expression of FA uptake and de novo FA synthesis genes (HUANG et al. , 2007; DUFOUR and Claviem 2010). According to Huang et al. (2007) an overexpression of *SHP* in cultured hepatocytes increases the accumulation of lipids, in our results there was an increase in Cholesterol (mg/dL) in the CO group both in relation to SOY and FO.

Despite the similarities in FA composition of CO*vs*SOY, such as the composition of OA, EPA, Total SFA, and Total MUFA, several important genes and pathways were enriched. The identification in the liver of Myristic acid, OA, EPA, total DHA MUFA, Total n-3 and the ratio between n-6:n-3 was equal in the CO and SOY

group revealing in genes and pathways important to lipid processes and diseases. In the liver, when comparing the CO*vs*SOY diets, we found the cAMP Response Element Binding Protein 1 *(CREB1),* a widely expressed TF (LEE et al., 2005), critical for lipid synthesis and triacylglycerol accumulation (YAO et al., 2020). This TF is involved in the regulation of adipocyte differentiation, lipogenesis, and insulin activity in adipose tissues (Klemm et al., 2001). Heat shock protein 9 70kDa *(GRP75)* is involved in the delivery of *CREB1* to mitochondria. Interruption of *CREB1* activity in mitochondria leads to decreased expression of mitochondrial encoded *MTND6* and *MTND5*, down-regulation complex I-dependent mitochondrial respiration and consequent mitochondrial dysfunction and neuronal cell death in Huntington's disease (LEE et al., 2005). In this study, *MTND5* and *MTND6* showed lower expression in animals fed with CO in the diet, which may result in an accentuation of the mitochondrial dysfunction process. Mitochondria utilize FA from *PER1/2* clock proteins, regardless of feeding time, which may occur through carnitine transport and through mitochondrial pyruvate metabolism, nutrient regulation by mitochondria may occur due to the circadian clock regulation which may optimize the mitochondrial response to dietary changes (Neufeld-COHEN et al., 2016). *MTND5* and *MTND6* are related to Leigh syndrome, which is related to a dysfunctional response to the mitochondrial oxidative phosphorylation system (OXPHOS) and a low generation of ATP, resulting in neurons with high energy demand and low ATP that trigger a stress cascade culminating in gliosis and vacuolization of neuronal tissue over time (SCHUBERT; VILARINHO, 2020).

Another gene enriched between the comparison CO*vs*SOY was *CYP7A1*. This gene can act catalyzing the first reaction in the cholesterol pathway in the liver, i.e., it participates in the conversion of cholesterol to bile acids, which is the main mechanism for removing cholesterol from the body, which may be related to the higher serum concentration of cholesterol found in CO group. Moreover, the *CYP2B6* gene is involved in the oxidative metabolism of xenobiotics, such as plant lipids (STELZER, G. et al, 2016). Additionally, the *CYP2B6* gene, enriched by the CO*vs*SOY comparison, is involved in the oxidative metabolism of xenobiotics, such as plant lipids (STELZER, G. et al, 2016). The *CYP7A1* and *CYP2B6* are members of the cytochrome P450 superfamily of enzymes and play an important role in the synthesis of cholesterol, steroids and other lipids (Stelzer, G. et al, 2016). The *CYP7A1* and *CYP2B6* were enriched for the regulation of “lipid metabolism FXR dependent negative – feedback regulation of bile acids concentration” pathway map, in which a negative regulation of

sterol 12 alpha-hydroxylase *(CYP8B1*) and *CYP7A1* results in a decrease in the biosynthesis of bile acids. In our study, the different oil sources added to the diet resulted in a decreased expression of *CYP7A1* and *CYP2B6* genes in the CO group. The farnesoid nuclear receptor X (*FXR)* activates the transcription of member 2 of group I of the nuclear receptor (*PXR*) subfamily 1, resulting in an increase in *PXR*-dependent processes and detoxification by *CYP2B6* (CASTILLO-OLIVARES; GIL, 2000; Jahan; Chiang, 2005). Bile acids are end products of cholesterol catabolism, they are related to the regulation of hepatic lipid, glucose, and energy homeostasis, in addition to the maintenance of metabolic homeostasis through the activation of nuclear receptors and G protein-coupled receptor (*GPCR)* signaling, as they are signaling molecules (CHIANG, 2013; JUNG; MANGELSDORF; MEYER, 2006). The bile acid-mediated FXR activation lowers HDL-cholesterol, while *FXR* deactivation increases HDL-cholesterol levels, this is due to bile acids via structural apolipoprotein (apoA-I) (Dufour and CLAVIEN, 2007). Our findings show that the CO group has a higher serum concentration of HDL and Cholesterol, which may be related to the genes that were expressed in lower amounts by the CO group.

Another member of the P450 family, the *CYP4A11* DEG catalyzes the ω-hydroxylation of saturated, branched-chain, and unsaturated fatty acids. In addition, *CYP4A* and *CYP4F* (which ω-hydroxylate a variety of long-chain and very long-chain SFA) have a role in hepatic FA metabolism. *CYP4A* main function in the liver is to metabolize medium-chain FA (MCFA, C:10 –C:16) with importance related to caloric restriction and in animals fed a high-fat diet, which mimics induced lipolysis by starvation and excessive transport of FA to the liver (HARDWICK, 2008). In the "FA omega oxidation" pathway, *CYP4A11* omega-hydroxylates lauric acid. Thus, we observed that the modification of the oil in pig diets modified the expression of the *CYP4A11* gene, being down-regulated in the CO group, negatively impacting the end products of the pathway.

The monoacylglycerol O-acyltransferase 2 *(MOGAT2),* gene participates in the catalysis of diacylglycerol synthesis from 2-monoacylglycerol and fatty acyl-CoA, with the power to form a complex involved in the resynthesis of digested triacylglycerol. Triacylglycerol plays a key role in the absorption of dietary fat by the small intestine and is expressed mainly in the intestine and liver (STELZER, G. et al, 2016). Studies with male mice with deletion of the gene encoding this enzyme (Mogat2 −/−) showed that it can consume and absorb normal amounts of dietary fat. In addition. *MOGAT2*

was linked with deficiency to a protective relationship to obesity, metabolic disorders, intolerance to glucose, hypercholesterolemia and hepatic steatosis induced by a high dietary fat intake and showed lower fasting insulin concentrations and better glucose tolerance (YEN et al., 2009). Thus, *MOGAT* has an important relation with the regulation of triacylglycerol homeostasis in response to diet and studies related to this gene are relevant to human obesity (NELSON et al., 2014; YANG; NICKELS, 2015). The *MOGAT2* was enriched in the “triacylglycerol biosynthesis pathway in obesity and diabetes mellitus, type II”. The acylation pathway of Monoacylglycerol with a fatty acyl-CoA is carried out by *MOGAT2*, being important in enterocytes after feeding, in which large amounts of monoacylglycerols and FA are released from the digestion of dietary lipids. Our findings confirm the results of other studies that show its importance and relation to obesity, mainly; in pathways that plays a predominant role in enterocytes after feeding (SHI; CHENG, 2009).

The *NGEF (Ephexin)* was enriched in the "Huntingtin-dependent transcription deregulation in Huntington's Disease” pathway, in this neurodegenerative disorder the mutant Huntingtin inhibits *BAF* cell CLL/lymphoma Chromatin Remodeling Complex Subunit *Bcl11B (CTIP2)* (Desplats; Lambert; Thomas, 2008). Thus, inhibiting transcription of the *NGEF (Ephexin)* and *CTIP2* underexpression can inhibit *Ephexin* transcription, leading to inhibition of neuronal cell survival. In addition, *Bcl11B* is related to the control of T cell subtype specification in the immune system (Desplats; Lambert; Thomas, 2008). By modifying the source of oil in the diet of pigs in the growth and finishing phases, we identified the difference in the expression of the *NGEF* gene between canola oil and soybean oil, with lower expression in the CO group. *NGEF* is a guanine nucleotide exchange factor *(GEF)* that differentially activates *GTPases* (*RHOA, RAC1* and *CDC42*) and is associated with *EPH-Ephrin* signaling pathway (STELZER, G. et al, 2016).

The platelet glycoprotein 4 gene *(CD36)* binds to long-chain FA and can function in the transport and/or as a regulator of FA transport (STELZER, G. et al, 2016) and a negative regulator of angiogenesis and inflammation. *CD36* is ubiquitously expressed, being present in cells such as hepatocytes; adipocytes; cardiac and skeletal myocytes; and specialized epithelia of the breast, kidney, and intestine (Silverstein; Febbraio, 2009). According to Silverstein and Febbraio (2009), *CD36* is related to the pathogenesis of diseases such as atherosclerosis and Alzheimer's disease. Long-chain fatty acids (LCFA) circulate in the blood and small portions of LCFA enter the brain

where FA metabolism within the ventromedial hypothalamic region (VHM) can function as a sensor for nutrient availability (LE FOLL et al., 2009). LCFA (in particular, oleic acid) enter HMV neuronal cells probably via FA transport protein 1 (FATP1), *SLC27A4*, and *CD36* (LE FOLL et al., 2009; LEVIN et al., 2011). In summary, the detection of hypothalamic oleic acid is impaired in animal models for obesity, as the increase in proteins that reverse the esterification of oleic acid and other effects that can decrease Acyl-CoA (Oleoyl-CoA) contributing to an increase in food intake and glucose production (LANE et al., 2008). *CD36* was also enriched in the "role of adipose tissue hypoxia in obesity and type 2 diabetes" pathway, and it is a shared target of *LXR, PXR,* and *PPAR-gamma* (YIN et al., 2009). Decreased expression of *FATP1* and *CD36* may result in inhibition of FA absorption and increased accumulation of free FA. The mechanisms and effects of this pathway result in a decrease in adiponectin and an underexpression in obesity leads to insulin resistance (CHEN, BAOYING et al., 2006; YIN et al., 2009). In addition to hypertrophy and adipocyte death, that can be caused by inhibition linked to PPAR-gamma, and consequently this increase in apoptosis of adipose tissue leads to macrophage infiltration in adipose tissue and a release of stored FA (LEVIN et al., 2011; WEISBERG et al., 2003). The modification of the diets with the oils resulted in changes in *CD36* gene expression, which may be involved in relevant pathways, related to inflammatory processes.

The "regulation of metabolism_bile acid regulation of lipid metabolism and negative FXR-dependent regulation of bile acids concentration" process network was enriched in both skeletal muscle (*SHP*) and liver (*CYP2B6* and *CYP7A1*). Again, the importance of enriched DEG that are involved in regulatory pathways and networks related to bile acids that regulate glucose and lipid metabolism in hepatocytes is noted. Through the MetaCore enrichment results we observed the difference between the pathways and the networks enriched in the skeletal muscle and liver, as well as we observed differences between depositions of FA within the tissues.

Functional enrichment analysis for skeletal muscle and liver differential expression SOYvsFO: Obesity predisposes to insulin resistance, type 2 diabetes, and cardiovascular problems (MRACEK et al., 2010), in obese tissue overexpression of tumor necrosis factor-α *(TNF-alpha)* and interleukin-1β *(IL1b)* activates related pathways *NF-KB* and *EKR,* causing impaired expression of genes related to inflammation, lipolysis, and FA oxidation (ALEXANDRAKI et al., 2006. The cytokines *TNF-alpha, IL1b,* and *IL6* are considered the main regulators of inflammation

involved in the pathogenesis of type 2 diabetes mellitus (ALEXANDRAKI et al., 2006). *AZGP1*, as well as *APOE, Perilipin*, *LIPS* and *PDE3B* were enriched in the "TNF-alpha pathway, IL-1 beta induce dyslipidemia and inflammation in obesity and type 2 diabetes in adipocytes". This signaling pathway is related to the overexpression of *TNF-alpha* and *IL-1 beta*, which in obese adipose tissue activate *NF-KB* and *EKR*, impairing genes with important functions. *TNF-alpha* inhibits *PDE3B* leading to the accumulation of Cyclic AMP (ZHANG et al., 2002), moreover, in this pathway, *TNF-alpha* also inhibits both *LIPS* inducing lipolysis, as well as *AZGP1* and *APOE* that are underexpressed in obese tissue and may promote the development of dyslipidemia (HUANG et al., 2007; MRACEK et al., 2010).

The *AZGP1* was identified as DEG and is related to the stimulation of lipid degradation in adipocytes, in addition to being related to extensive fat loss in some advanced cancers (STELZER, G. et al, 2016). The *PLIN1* belongs to the *Perilipin* protein family and was differentially expressed in L*ongissimus* muscle regulating the deposition of the intramuscular fat content of commercial hybrids (Pietrain × Duroc) × (Landrace × Yorkshire) (LI et al., 2018). In the study performed by Li et al. (2018), the authors suggested that a *PLIN1* knockdown can decrease the level of triglycerides and lipid droplet size in adipocytes (LI et al., 2018). In Gandolfi et al. (2011) study, *Perilipin 1* and *Perilipin 2* were expressed in the semimembranosus muscle of commercial crossbred male castrated pigs and the specificity of the antibodies was confirmed by Western blot analysis (GANDOLFI et al., 2011). In the enriched pathway "TNF-alpha, IL-1 beta induces dyslipidemia and inflammation in obesity and type 2 diabetes in adipocytes", *TNF-alpha PKA-cat (cAMP-dependent)* phosphorylates *Perilipin A* and decreases its activity resulting in stimulation of lipolysis (ZHANG, HUI H. et al., 2002). In addition, it participates in the "role of IL-6 in obesity and type 2 diabetes in adipocytes pathway" (Table 7). *Perilipin* coats the lipid storage droplets in adipocytes and participates in the inhibition of lipolysis (STELZER, G. et al, 2016).

Another DEG identified was *APOE*, a protein associated with lipid particles that is essential for the normal catabolism of the constituents of triglyceride-rich lipoproteins, and is involved in the immune innate adaptive responses. In addition, it participates in the biosynthesis of VLDLs by the liver (STELZER, G. et al, 2016). Dysfunctions in *APOE* protein can result in familial dysbetalipoproteinemia (type III hyperlipoproteinemia), and consequently, atherosclerosis. Using the CRISPR/Cas9 technique, Fang et al. (2018), interrupted *APOE* expression in miniature pigs fed an

induction diet high in fat and cholesterol, revealing that the animals had severe hypercholesterolemia and developed progressive atherosclerotic lesions (FANG et al., 2018). *APOE* in our study was enriched in the “regulation of metabolism_bile acids regulation of glucose and lipid metabolism via *FXR”,* in which *APOE* is positively regulated by *FXR* that may be involved in lipid transport (MAK et al., 2002). Additionally, *APOE* may be involved in the "transport HDL-mediated reverse cholesterol transport" pathway, in which *APOE* increases HDL binding to SRBI and selective cholesteryl ester uptake (VAN DER VELDE, 2010). Finally, in a study performed by Song et al. (2020), in which the animals were fed a diet with an n-6:n-3 ratio of 4:1 or 2:1, *LIPS/HSL* showed a higher relative gene expression compared to the control group with an 18:1 ratio. In our study, the pattern obtained was similar, in which the FO diet showed a lower n-6:n-3 ratio (8.96) and consecutively higher expression of *LIPS/HSL* when compared to SOY in skeletal muscle. The DEG *LIPS,* which is related to the conversion of cholesterol esters into free cholesterol to produce steroid hormones (STELZER, G. et al, 2016),

In addition, *PPARG* regulating adipocyte differentiation, regulates insulin sensitivity, is related to diseases, including obesity, diabetes, atherosclerosis, and cancer (STELZER, G. et al, 2016). In our study *PPARG* was enriched in "putative pathways for stimulation of fat cell differentiation by Bisphenol A", "Role of IL-6 in obesity and type 2 diabetes in adipocytes", and "dysregulation of Adiponectin secretion from adipocytes in obesity, type 2 diabetes and metabolic syndrome X". Studies have identified the relationship of *PPAR* to nutrition and involvement in skeletal muscle, such as the study from Yu et al. (2011) evaluating a diet high in saturated fat (beef tallow) or high in unsaturated fat (fish oil) in transgenic mice, which resulted in the decreased deposition of lipids in the liver by PUFA, and the ability to stimulate the expression of adipogenic genes and glucose metabolism genes in *PPARG* transgenic mice when fed fish oil. Another study in mice identified that *PPARG* knockout in muscle affected insulin sensitivity in skeletal muscle (HEVENER et al., 2003). Furthermore, there is an important involvement of *PPARG* in the direct regulation of lipid metabolism in immune cells (WELCH et al., 2003). *PPAR* form heterodimers with retinoid X receptors (*RXRs*) and these heterodimers regulate the transcription of several genes (STELZER, G. et al, 2016).

In the “putative pathways for stimulation of fat cell differentiation by Bisphenol A” other DEG were enriched for SOY*vs*FO and may be related to a direct effect or

mechanism on *PPARG*, such as the effect of *PPARG* activation on the increase in mRNA expression of the stearoyl-CoA desaturase (*SCD*) gene. The *SCD* gene is related to the biosynthesis of FA, mainly the synthesis of oleic acid, fundamental in the regulation of the expression of genes that are involved in lipogenesis. It participates in the body's energy homeostasis, involved to the biosynthesis of membrane phospholipids, cholesteryl esters, and triglycerides (STELZER, G. et al, 2016). In a study evaluating some candidate genes from commercial crossbred pigs (Shanzhu × Duroc), *PPAR* was correlated with carcass characteristics and muscle meat quality and did not present a relationship with intramuscular fat content. On the other hand, *SCD* expression levels showed a correlation (Pearson $P<0.05$) with intramuscular fat content, indicating that genes involved in the PPAR signaling pathway are important for pork meat quality traits (WANG et al., 2016). Furthermore, *SCD* was enriched in the "adiponectin pathway in the pathogenesis of type 2 diabetes" to adiponectin inhibits *SREBP1* or that ends up decreasing SCD that was down-regulated in SOY, decreasing in liver lipogenesis (AWAZAWA et al., 2009).

The *TCFL2* identified as DEG between SOY*vs*FO in skeletal muscle is a TF essential in the *Wnt* signaling pathway, it is related to the pathogenesis of human diseases, has a strong genetic association with type 2 diabetes mellitus (DEL BOSQUE-PLATA et al., 2021). Findings by Geoghegan et. al. (2019), in a study with adipose tissue cells from mice fed a high-fat diet, portrayed the direct role of *TCF7L2* in the regulation of gene expression of metabolic pathways (GEOGHEGAN et al., 2019). In our study the enriched pathway "putative pathways for stimulation of fat cell, differentiation by bisphenol A" it presents a transcriptional regulatory relationship to *PPARG* (CHEN, Xi et al., 2018) and C/EBP-alpha. *C/EBPalpha* modulate the expression of genes involved in cell cycle regulation and interact with the *PPARG* promoter and stimulate *PPARG* expression (BRUN et al., 1996).

In relation to the network of processes enriched for the skeletal muscle, we identified networks related to muscle contraction with DEG down-regulated from the SOY group, demonstrating that SOY negatively regulated muscle contraction genes compared to animals from the FO group.

In the liver, between SOY*vs*FO DEG were enriched in important signaling pathways. The liver is the organ that expresses all the enzymes necessary for the synthesis of bile acids, the pathway from cholesterol is catalyzed by *CYP7A1*, this enzyme catalyzes cholesterol hydroxylation at 7th position (CHIANG; FERRELL,

2020). The degradation of cholesterol to form bile acids can be through *CYP7A1* of the classical pathway or through the mitochondrial *CYP7A1* of the alternative pathway (NORLIN et al., 2000). In the cholesterol metabolism pathway, *ACOX2* also participates through the activating effect on the catalysis mechanism of a bile acid intermediate (VELDHOVEN et al., 1994). Thus, cholesterol metabolism can be decreased with the expression of *CYP7A1* and *ACOX2* in the SOY group. In the study of the muscle transcriptome of pigs with extreme values of FA composition by Puig-Oliveras et al., (2014) *ACOX2* was enriched related to lipid metabolism with functions related to oxidation, synthesis, and insulin resistance.

Another gene *CYP2B6* was identified as DEG when comparing SOY*vs*FO diets, with negative regulation in the SOY group, *CYP2B6* and *CYP7A1* were previously shown as DEG between CO*vs*SOY down-regulated in the CO group. Interactions between constitutive androstane receptors can affect the expression of the *CYP2B6* gene *(CAR, NR1i3)* and the pregnane X receptor *(PXR, NR1i2) CAR/PXR*, and of liver-enriched transcription factors (LETFs), such as hepatic nuclear 4α (*HNF4α*) and CCAAT/enhancer binding protein α *(C/EBPalpha*) (LI, LINHAO et al., 2016).

The DEG identified in the liver *IL-18* is a pro-inflammatory, pro-atherogenic cytokine, high levels of this cytokine were identified in a study with individuals presenting type 2 diabetes mellitus (ASO et al., 2003), showing possible participation in the development of the disease (THORAND et al., 2005). IL-18 was enriched in "role of inflammasome in macrophages, adipocytes and pancreatic beta cells in type 2 diabetes" pathway by MetaCore. *IL-18* may be related to metabolic syndrome and its consequences, that is, it may be involved in the set of risk factors that identify a population at increased risk for developing metabolic syndrome, which encompasses type 2 diabetes mellitus and cardiovascular diseases (CVD) (TRØSEID; SELJEFLOT; ARNESEN, 2010). In addition, IL-18 has atherogenic properties through effects on *IL-6, TNF-α* and interferon-γ, thus dietary interventions have been proposed to decrease *IL-18* levels in obese women resulting in weight loss such as an important intervention to reduce *IL-18* levels (ESPOSITO et al., 2002). In our study, IL-18 is also enriched in the "role of *IFN-beta* in inhibition of Th1 cell differentiation in multiple sclerosis" pathway, in this pathway the *IL-18* plays a fundamental role in the differentiation of T-helper cells 1, and plays a fundamental role in the differentiation of T-helper cells 1, which initiate signaling pathways that lead to T-helper 1 cell differentiation and *IFN-gamma* production (DINARELLO, 1999; CODARRI et al., 2010). The multiple sclerosis is an

autoimmune disease mediated by autoreactive T helper 1 cells (Th1) that, upon entering the central nervous system, can cause damage to the myelin sheath (HEMMER et al., 2002). *IL18* was up-regulated in SOY group with possible relation to a pro-inflammatory condition, in other hand the atherogenic index showed no difference between the diets in liver.

The *MTND6* gene previously reported as DEG in the liver is related to Leigh syndrome and catalyzes the electron transfer from NADH through the respiratory chain (STELZER, G. et al, 2016). *MTND6* gene may be related to ROS production and transcriptional regulation of *CREB1* directly, in which mitochondrial *CREB1* binds to the promoter of the *MTND6* gene and promotes its expression (LEE et al., 2005). Additionally, this gene was enriched for "CREB1-dependent transcription deregulation in Huntington's Disease" pathway, MTND6 is down-regulated in the SOY group in the liver, in which a reduced expression of MTND6 down-regulated complex I-dependent mitochondrial respiration impacting dysfunction mitochondrial and cell death in Huntington's Disease (LEE et al., 2005).

A study investigating the role of high-fat diets in Alzheimer's disease in the brain of young rats resulted in decreased activities of *NTPDase*, 5'nucleotidase and the neurotransmitter Acetylcholine *AChE,* causing cognitive impairment characteristic of Alzheimer's disease (KAIZER et al., 2018). The *NTSE* was up-regulated in the group SOY, related to increased conversion of extracellular AMP to adenosine, resulting in reduced vascular permeability and inhibition of leukocyte cell-cell adhesion and transmigration across the endothelial cell barrier (HUNSUCKER et al., 2005) in the enriched pathway “role of IFN-beta in the improvement of blood-brain barrier integrity in multiple sclerosis”. *NTSE* is also enriched in “role of *IFN-beta* inactivation of T cell apoptosis in multiple sclerosis”, as well as, on AMP hydrolysis to produce adenosine which can result in modulation of the frequency, rate, or extent of T cell proliferation leading to T cell inactivation (apoptotic process) in treatment with *IFN-beta* affecting multiple sclerosis (KIZAKI et al., 1990).

In addition, to these discussed analyses, a process networks analysis was performed to help the understanding of the enriched pathways, through interactions by gene networks that are related to the change of oil in the diet. The enriched process networks emphasize the pathways maps found between SOY*vs*FO, with DEG participating in networks of regulation of bile acid metabolism, regulation of lipid metabolism, and negative FXR dependent regulation of bile acids concentration, as well

as pathways related to signal transduction, sodium transport, and neurophysiological process. In both skeletal muscle and liver, we observed biochemical parameters and FA composition being modulated according to soy and fish oil exchange, in addition to signaling pathways and gene networks of important processes and diseases.

Functional enrichment analysis for skeletal muscle differential expression for the COvsFO comparison: The *SCD* gene was identified in the CO*vs*FO comparison performed with skeletal muscle, and has been enriched in several pathway maps (Table 7). *SCD* expression has already been documented regulated by diet and environmental temperatures (HSIEH et al., 2007; NTAMBI; SESSLER; TAKOVA, 1996). Furthermore, in PUFA studies in diabetic mice, hepatic *SCD* was inhibited (WATERS; Ntambi, 1996). The *SCD* was enriched in the pathways "adiponectin in pathogenesis of type 2 diabetes", which is related to adiponectin secreted by white adipose tissue with a relevant role in energy homeostasis control in insulin sensitive tissues, regulation of glucose and lipid metabolism (LENNON et al., 1998), and SCD negatively impacts the lipid biosynthetic process in the CO group where it was identified down-regulated. Moreover, *SCD* was enriched in the "regulation of lipid metabolism *RXR*-dependent regulation of lipid metabolism via *PPAR, RAR and VDR"*, in which the transcription factor *RARα* can bind to the *SCD* gene promoter and activate *SCD* expression (SAMUEL et al., 2001); "putative pathways for stimulation of fat cell differentiation by Bisphenol A", in which the adipogenic TF *C/EBPbeta* can increase *SCD* expression (Tang; Zhang; Lane, 2004) and can impact the process of FA metabolism; "regulation of lipid metabolism regulation of lipid metabolism via *LXR, NF-Y and SREBP*", in which transcriptional regulation of *SREBP1a* and *SREBP1*c can occur promoting *SCD-1* expression (LENNON et al., 1998); and, in the "regulation pathway of metabolism bile acids regulation of glucose and lipid metabolism via *FXR* and Role of ER stress in obesity and type 2 diabetes", related to transcriptional regulation of different enzymes and transporters that modulate glycolysis, lipogenic processes and bile acid biosynthesis (LENNON et al., 1998). In the study conducted by Puig-Oliveras et al. (2014), *SCD* was enriched in FA divergent pigs related to oxidation, accumulation, concentration, and lipid homeostasis. The authors also found this gene identified as down-regulated in the adipose tissue of animals with higher PUFA content in Iberian pigs x Landrace and with greater expression in animals showing higher values of intramuscular fat content.

Another DEG enriched in some pathway maps between CO*vs*FO was *AL3A2.* It is related to the oxidation of long-chain aliphatic aldehydes to FA (Stelzer, G. et al,

2016). Furthermore, there is a relationship of the aldehyde dehydrogenase *(ALDH)* family in the induction, function, and resistance of regulatory T cells (Tregs) to cytotoxic therapy. When the animals were fed fish oil, there was a higher expression of *AL3A2*, which may be involved in the increase in lipid peroxide elimination system. *AL3A2* was enriched in our study between CO*vs*SOY comparisons in muscle as previously noted.

The *CD4+* T cell is related to the induction and maintenance of chronic inflammation in several human inflammatory diseases (FAN et al., 2018). A study by Fan et al. (2018) with *CD4+* T cells isolated from buffy-coat leukocytes with doses of LA, EPA, and DHA, resulted in *in vitro* alterations of phospholipid FA profiles of the *CD4* + T cell membrane. In our results, the FA profile was modified in the muscle and a higher level of n-3 was found in fish oil, which may be related to the modification of CD4 expression, with a decrease in expression when the pigs were fed with canola oil. As previously described, the *CD4* was also identified and enriched in the "breakdown of CD4+ T cell peripheral tolerance in type 1 diabetes mellitus" pathway in our study when considering the CO*vs*SOY comparison.

The *SCD*, *MyHC*, *AKAP3*, and *CD4* DEG were enriched in the networks of processes between CO*vs*FO related to metabolism regulation, highlighting the importance of the identified DEG in metabolism and inflammation regulation. Among CO*vs*FO even with few DEG identified important pathways and networks of relevant processes were enriched, the main difference observed between diets in relation to FA composition was the n-6:n-3 PUFA ratio in which CO presented the highest relationship and that have been a key point for DEG related to inflammation and metabolism.

In summary, most of the common down-regulated DEG were identified in more than one diet, resulting in the reduction of essential product in normal metabolic pathways, or even the gene with low expression in the disease pathway, improving the inflammatory process depending on of its function within the track, therefore, an individual analysis of each process is necessary.

Studies are still limited in pigs and new approaches are needed. The results found, in general, mainly related to neurological diseases, obesity, and metabolism, and of great relevance in humans. Thus, the pigs are presented as a suitable animal model for the study of FA (LUNNEY, 2007; PUIG-OLIVERAS et al., 2014).

5.CONCLUSIONS

The enrichment of the basal diet with oil sources containing different FA profiles influenced the composition of the FA profile, the blood parameters and the gene expression in metabolic pathways and networks processes in both skeletal muscle and liver tissues of immunocastrated male pigs during growth-finishing phases. Our results gathered information about the relationships between tissues and the broad functioning of the body, providing an important contribution for animal health and production, as well as offering insight to improve human health, as the pig is an excellent animal model. Moreover, our results demonstrated different biological mechanisms helping us to understand gene behavior regulated by the FA profile.

REFERENCES

ABBAS, A. K.; LICHTMAN, A. H.; POBER, J. S. **Cellular and Molecular Immunology**. 4th. ed. [s.l.] W.B. Saunders., 2000, 2000.

ALMEIDA, V. V. et al. Effects of increasing dietary oil inclusion from different sources on growth performance, carcass and meat quality traits, and fatty acid profile in genetically lean immunocastrated male pigs. **Livestock Science**, v. 248, p. 104515, 1 jun. 2021.

AOAC. Official Method 963.15. Fat in Cacao Products Soxhlet Extrac tion Method. **AOAC**, 2006.

AOCS. Official approved procedure Am 5-04, Rapid determination of oil/fat utilizing high temperature solvent extraction. **American Oil Chemist's Society**, 2005.

BENJAMINI, Y.; HOCHBERG, Y. Controlling the False Discovery Rate: A Practical and Powerful Approach to Multiple Testing. **Journal of the Royal Statistical Society: Series B (Methodological)**, v. 57, n. 1, 1995.

BLIGH, E. G.; DYER, W. J. A rapid method of total lipid extraction and purification. **Canadian journal of biochemistry and physiology**, v. 37, n. 8, 1959.

BROWN, M. S.; RADHAKRISHNAN, A.; GOLDSTEIN, J. L. **Retrospective on Cholesterol Homeostasis: The Central Role of ScapAnnual Review of Biochemistry**, 2018. .

CALDER, P. C. **ImmunonutritionBritish Medical Journal**, 2003. .

CESAR, A. S. M. et al. Differences in the skeletal muscle transcriptome profile associated with extreme values of fatty acids content. **BMC Genomics**, p. 1–16, 2016. Disponível em: <http://dx.doi.org/10.1186/s12864-016-3306-x>.

FESSLER, M. B. **The Intracellular Cholesterol Landscape: Dynamic Integrator of the Immune ResponseTrends in Immunology**Elsevier Current Trends, , 1 dez. 2016. .

FUJII, J. et al. Identification of a mutation in porcine ryanodine receptor associated with malignant hyperthermia. **Science**, v. 253, n. 5018, 1991.

GORNALL, A. G.; BARDAWILL, C. J.; DAVID, M. M. Determination of serum proteins by means of the biuret reaction. **The Journal of biological chemistry**, v. 177, n. 2, 1949.

HEGAZI, R. A.; WISCHMEYER, P. E. **Clinical review: Optimizing enteral nutrition for critically ill patients - a simple data-driven formulaCritical Care**, 2011. .

JUMP, D. B. et al. Polyunsaturated fatty acids inhibit S14 gene transcription in rat liver and cultured hepatocytes. **Proceedings of the National Academy of Sciences of the United States of America**, v. 90, n. 18, 1993.

JUMP, D. B. **The biochemistry of n-3 polyunsaturated fatty acidsJournal of Biological Chemistry**, 2002. .

KUSNADI, A. et al. The Cytokine TNF Promotes Transcription Factor SREBP Activity and Binding to Inflammatory Genes to Activate Macrophages and Limit Tissue Repair. **Immunity**, v. 51, n. 2, p. 241- 257.e9, 20 ago. 2019.

LANDS, B. Highly unsaturated fatty acids (HUFA) mediate and monitor food's impact on health. **Prostaglandins & Other Lipid Mediators**, v. 133, p. 4–10, 1 nov. 2017.

LEE, S. H.; LEE, J. H.; IM, S. S. **The cellular function of SCAP in metabolic signalingExperimental and Molecular Medicine**, 2020. .

LOVE, M. I.; HUBER, W.; ANDERS, S. Moderated estimation of fold change and dispersion for RNA-seq data with DESeq2. **Genome Biology**, v. 15, n. 12, 2014.

LUNNEY, J. K. **Advances in swine biomedical model genomicsInternational Journal of Biological Sciences**, 2007. .

MARTIN, C. A. et al. Ácidos graxos poliinsaturados ômega-3 e ômega-6: Importância e ocorrência em alimentos. **Revista de Nutricao**, v. 19, n. 6, 2006.

MATER, M. K. et al. Arachidonic acid inhibits lipogenic gene expression in 3T3-L1 adipocytes through a prostanoid pathway. **Journal of Lipid Research**, v. 39, n. 7, 1998.

MEDZHITOV, R.; JANEWAY, C. A. **Innate immunity: The virtues of a nonclonal system of recognitionCell**, 1997. .

MetaCore (Clarivate Analytics). , 2021. . Disponível em: <portal.genego.com>.

MI, H. et al. The PANTHER database of protein families, subfamilies, functions and pathways. **Nucleic Acids Research**, v. 33, n. DATABASE ISS., 2005.

MOGHADASIAN, M. H.; SHAHIDI, F. Fatty Acids. **International Encyclopedia of**

Public Health, p. 114–122, 1 jan. 2017. Disponível em: <https://www.sciencedirect.com/science/article/pii/B9780128036785001570?via%3Dihub>. Acesso em: 2 nov. 2021.

OECD-FAO. OECD-FAO Agricultural Outlook 2021–2030. **OECD-FAO Agricultural Outlook 2021–2030**, p. 163–177, 2021.

PAN, Z. et al. Pig genome functional annotation enhances the biological interpretation of complex traits and human disease. **Nat Commun**, v. 12, 2021.

RADHAKRISHNAN, A. et al. Switch-like Control of SREBP-2 Transport Triggered by Small Changes in ER Cholesterol: A Delicate Balance. **Cell Metabolism**, v. 8, n. 6, p. 512–521, 6 dez. 2008.

ROSTAGNO, H. S. Tabelas brasileiras para aves e suínos: composição de alimentos e exigências nutricionais. **Tabelas brasileiras para aves e suínos: composição de alimentos e exigências nutricionais**, 2011.

SILVA, J. P. M. da et al. Fatty acid profile in brain and hepatic tissues from pigs supplemented with canola oil. **Revista Brasileira de Agrotecnologia**, v. 11, n. 2, 2021.

SIMOPOULOS, A. P. Importance of the omega-6/omega-3 balance in health and disease: Evolutionary aspects of diet. **World Review of Nutrition and Dietetics**, v. 102, 2011.

SUMMERS, K. M. et al. Functional Annotation of the Transcriptome of the Pig, Sus scrofa, Based Upon Network Analysis of an RNAseq Transcriptional Atlas. **Frontiers in Genetics**, v. 10, 2020.

TRINDER, P. Determination of Glucose in Blood Using Glucose Oxidase with an Alternative Oxygen Acceptor. **Annals of Clinical Biochemistry: International Journal of Laboratory Medicine**, v. 6, n. 1, 1969.

WILLIAMS, N. H.; STAHLY, T. S.; ZIMMERMAN, D. R. Effect of Chronic Immune System Activation on the Rate, Efficiency, and Composition of Growth and Lysine Needs of Pigs Fed from 6 to 27 kg. **Journal of Animal Science**, v. 75, n. 9, 1997.

YATES, C. M.; CALDER, P. C.; ED RAINGER, G. **Pharmacology and therapeutics of omega-3 polyunsaturated fatty acids in chronic inflammatory diseasePharmacology and Therapeutics**, 2014. .

YEHUDA, S.; RABINOVITZ, S.; MOSTOFSKY, D. I. **Essential fatty acids are mediators of brain biochemistry and cognitive functionsJournal of Neuroscience Research**, 1999. .

OVERVIEW

We observed that the modification of the oil level in pig diets modified the expression of some genes. Among the SOY1.5*vs*SOY3.0 diets, we observed a better relationship when using SOY3.0 associated with the enriched pathways presented and the association with gene function. In diets with SOY1.5 pathways were identified related to metabolic and neurodegenerative diseases and inflammatory processes were enriched.

When evaluating the different sources of oil, our findings show that the CO group has a higher serum concentration of HDL and Cholesterol, which may be related to the genes that were expressed in lower amounts by the CO group or related to important inhibits transcription factors such as *SHP* impacting VLDL secretion; negative regulation of lipid biosynthetic process and is up-regulated in CO group.

The SOY, CO and FO showed more related biochemical parameters and while the FA profile SOY and CO group showed more similar FA deposition in the tissues, but that did not impact equally when the gene expression analysis was performed. The analysis of the intramuscular lipid composition, that the addition of FO in the diet of growing and finishing pigs showed a higher FA profile composition of EPA, DHA, and SFA as palmitic acid and stearic acid. The liver composition of animals fed diets with FO and CO was lower for this SFA compared to pigs fed diets containing SOY.

Among SOY*vs*FO the highest amount of DEG was observed in muscle with important genes and networks, involved in dyslipidemia and inflammation in obesity and type 2 diabetes, and atherosclerosis. In addition, SOY appears negatively regulated muscle contraction genes compared to animals from the FO group. Already in the liver DEG involved in cholesterol metabolism and, consequently, bile acids.

Furthermore, the most of the common down-regulated DEG was identified in more than one diet, resulting in the reduction of essential product in normal metabolic pathways, or even the gene with low expression in the disease pathway, improving the inflammatory process depending on of its function within the road, therefore, an individual analysis of each process is necessary. In both skeletal muscle and liver, we observed biochemical parameters and FA composition being modulated according to diet, as well as signaling pathways and gene networks.

APPENDIX A: SUPPLEMENTARY FILE
CHAPTER 2

Table S1: Number of reads (*paired-end*) mapped in skeletal muscle and liver of pigs fed diets containing different levels of soybean oil (SOY1.5: 1.5% and SOY3.0: 3.0% soybean oil).

Samples (liver – 1.5%)	Reads strandR1	Reads strandR2	Total reads	Trimmed readsR1	Trimmed readsR2	Total trimmed	unmapped (%)	multimapping (%)	noFeature (%)	ambiguous (%)
L4	16976486	16976486	33952972	16763079	16763079	33526158	1.49	9.56	6.31	6.3
L7	23406368	23406368	46812736	23157593	23157593	46315186	1.56	10.54	7.3	5.58
L13	16285871	16285871	32571742	15974514	15974514	31949028	2.94	46.41	21.89	2.41
L14	17569096	17569096	35138192	17291477	17291477	34582954	2.17	13.23	8.76	5.75
L16	19341857	19341857	38683714	19070176	19070176	38140352	2.72	16.24	8.26	5.33
L28	17127166	17127166	34254332	16802121	16802121	33604242	4.9	30.28	12.18	4.5
L32	18474696	18474696	36949392	18219469	18219469	36438938	2.99	12.77	6.65	5.39
L33	16073495	16073495	32146990	15820698	15820698	31641396	2.64	13.57	9.9	6.08
L34	16827574	16827574	33655148	16591270	16591270	33182540	2.63	22.68	19.33	4.17
L35	15873423	15873423	31746846	15628724	15628724	31257448	2.83	21.11	8.84	6.22
L41	14053129	14053129	28106258	13812926	13812926	27625852	3.24	13.31	6.97	5.47
L43	14976488	14976488	29952976	14750942	14750942	29501884	2	11.09	7.1	6.29
L47	15428890	15428890	30857780	15196845	15196845	30393690	2.66	12.43	7.14	5.86
L49	14756528	14756528	29513056	14514882	14514882	29029764	2.46	39.57	16.33	2.82
L56	14250075	14250075	28500150	14017456	14017456	28034912	2.97	32.35	14.02	3.81
L62	17292555	17292555	34585110	17118909	17118909	34237818	1.98	12.73	8.22	5.79
L66	16560931	16560931	33121862	16388636	16388636	32777272	1.99	12	10.16	6.32
Total	285274628	285274628	570549256	281119717	281119717	562239434			-	
Average	16780860	16780860	**33561721**	16536454	16536454	**33072908**			-	

ummapped	7222473
mapped pairs	273897244
uniquely mapped	220645398
% mapped	97.43
% uniquely mapped	78.49

Samples (liver – 3.0%)	**Reads strandR1**	**Reads strandR2**	**Total reads**	**Trimmed readsR1**	**Trimmed readsR2**	**Total trimmed**	**unmapped (%)**	**multimapping (%)**	**noFeature (%)**	**ambiguous (%)**
L3	17396801	17396801	34793602	17189863	17189863	34379726	1.46	9.4	6.87	6.15
L10	20704172	20704172	41408344	20449667	20449667	40899334	2.68	10.03	8.13	5.71
L11	15858812	15858812	31717624	15683401	15683401	31366802	1.87	13.15	6.65	5.94
L12	17957727	17957727	35915454	17714575	17714575	35429150	1.84	11.79	8.07	5.94
L18	16192070	16192070	32384140	15975133	15975133	31950266	2.72	16.35	8.33	6.51
L19	15751527	15751527	31503054	15526082	15526082	31052164	2.56	14.23	8.24	5.38
L26	16829185	16829185	33658370	16590646	16590646	33181292	2.24	14.84	7.7	6.2
L46	15265575	15265575	30531150	15009755	15009755	30019510	2.72	47.27	20.6	2.34
L53	14581821	14581821	29163642	14334854	14334854	28669708	2.64	21.17	9.94	6.03
L54	15593189	15593189	31186378	15384127	15384127	30768254	2.39	21.97	11.33	5.52
L55	18872901	18872901	37745802	18594669	18594669	37189338	2.51	17.98	9.45	5.48
L59	16293809	16293809	32587618	16054665	16054665	32109330	3.51	14.36	7.84	6.12
L61	16259565	16259565	32519130	15989887	15989887	31979774	2.91	50.46	20.61	2.2
L63	17530152	17530152	35060304	17310788	17310788	34621576	2.24	13.66	8.79	5.69
L68	18432836	18432836	36865672	18212361	18212361	36424722	2.33	22.78	10.58	5.3
L69	16561309	16561309	33122618	16355205	16355205	32710410	2.22	9.32	7.58	6.03
L70	17487210	17487210	34974420	17248945	17248945	34497890	2.96	17.34	8.84	5.13
L72	19141470	19141470	38282940	18873100	18873100	37746200	2.76	19.24	7.55	6.2

Total	306710131	306710131	613420262	302497723	302497723	604995446
Average	17039452	17039452	**34078903**	16805429	16805429	**33610858**
mapped pairs	295016291					
uniquely mapped	238028576					
% mapped	97.53					
% uniquely mapped	78.69					

Samples (liver – 1.5%)	**Reads strandR1**	**Reads strandR2**	**Total reads**	**Trimmed readsR1**	**Trimmed readsR2**	**Total trimmed**	**unmapped (%)**	**multimapping (%)**	**noFeature (%)**	**ambiguous (%)**
M4	17267556	17267556	34535112	16937791	16937791	33875582	4.13	2.96	11.62	6.34
M7	15768590	15768590	31537180	15473109	15473109	30946218	3.13	2.93	10.75	7.96
M13	15147254	15147254	30294508	14928139	14928139	29856278	2.31	2.91	9.21	8.87
M14	14953433	14953433	29906866	14708222	14708222	29416444	3.45	3.01	10.37	7.04
M16	15040352	15040352	30080704	14832612	14832612	29665224	3.26	2.58	7.88	8.24
M28	19113774	19113774	38227548	18808021	18808021	37616042	2.92	3.18	9.58	8.79
M32	18292938	18292938	36585876	18074419	18074419	36148838	2.76	3.11	10.44	8.37
M33	18785249	18785249	37570498	18531101	18531101	37062202	3.18	2.86	8.20	9.37
M34	17881329	17881329	35762658	17644950	17644950	35289900	2.99	2.74	6.18	9.95
M35	17165144	17165144	34330288	16948708	16948708	33897416	2.73	2.94	11.61	6.68
M37	17432175	17432175	34864350	17162089	17162089	34324178	2.23	3.05	9.29	9.37

M41	17482308	17482308	34964616	17223676	17223676	34447352	3.53	2.56	13.30	5.33
M43	15007205	15007205	30014410	14798993	14798993	29597986	4.57	3.11	8.95	8.25
M47	13841460	13841460	27682920	13664442	13664442	27328884	2.92	2.80	10.22	7.52
M49	17707101	17707101	35414202	17467077	17467077	34934154	2.22	2.89	7.82	10.65
M56	16316156	16316156	32632312	16108973	16108973	32217946	4.72	2.91	11.99	6.29
M62	16595573	16595573	33191146	16319678	16319678	32639356	3.20	2.40	9.68	7.02
M66	17334677	17334677	34669354	17060580	17060580	34121160	4.14	2.93	9.79	7.05
Total	301132274	301132274	602264548	296692580	296692580	593385160	8879388	278540259	-	
Average	16729571	16729571	**33459142**	16482921	16482921	**32965842**	493299	15474459	-	
mapped pairs	**287099577**									
uniquely mapped	**278540259**									
% mapped	**96.77**									
% uniquely mapped	**93.88**									

Samples (liver – 3.0%)	**Reads strandR1**	**Reads strandR2**	**Total reads**	**Trimmed readsR1**	**Trimmed readsR2**	**Total trimmed**	**unmapped (%)**	**multimapping (%)**	**noFeature (%)**	**ambiguous (%)**
M3	15646435	15646435	31292870	15396193	15396193	30792386	4.22	2.90	9.46	6.77
M10	13575043	13575043	27150086	13337731	13337731	26675462	2.29	2.80	13.14	6.46
M11	14777149	14777149	29554298	14513593	14513593	29027186	2.49	2.25	13.31	4.62
M12	16505168	16505168	33010336	16114942	16114942	32229884	2.60	2.75	8.20	8.91
M18	15403431	15403431	30806862	15179363	15179363	30358726	2.15	2.79	10.35	7.31
M19	14791761	14791761	29583522	14615040	14615040	29230080	3.16	2.70	11.68	7.85

M26	18888244	18888244	37776488	18587847	18587847	37175694	2.37	3.01	9.34	7.54
M46	14178120	14178120	28356240	14002783	14002783	28005566	1.67	2.17	13.98	5.14
M53	17380539	17380539	34761078	17151536	17151536	34303072	4.17	2.71	8.78	8.43
M54	17007569	17007569	34015138	16748500	16748500	33497000	3.78	3.09	10.33	7.87
M55	16423107	16423107	32846214	16211289	16211289	32422578	3.97	2.97	11.18	6.31
M59	15764683	15764683	31529366	15577575	15577575	31155150	2.89	3.00	8.85	6.94
M61	15556503	15556503	31113006	15332622	15332622	30665244	2.58	3.02	8.73	7.34
M63	16554614	16554614	33109228	16359501	16359501	32719002	3.09	2.71	6.96	8.57
M68	16181956	16181956	32363912	15955270	15955270	31910540	3.93	2.82	9.93	7.56
M69	16575604	16575604	33151208	16368158	16368158	32736316	3.01	2.61	9.86	7.59
M70	15648586	15648586	31297172	15462025	15462025	30924050	3.08	2.72	9.56	7.54
M72	16742006	16742006	33484012	16507152	16507152	33014304	3.44	2.82	9.73	7.81
Total	**287600518**	287600518	575201036	283421120	283421120	566842240	8358796	266846154	-	
Average	**15977807**	15977807	**31955613**	15745618	15745618	**31491236**	464378	14824786	-	
mapped pairs	**274717524**									
uniquely mapped	**266846154**									
% mapped	**96.93**									
% uniquely mapped	**94.15**									

Table S2a: Differently expressed genes of skeletal muscle from immunocastrated male pigs fed diets containing different levels of soybean oil (SOY1.5: 1.5% and SOY3.0: 3.0% soybean oil).

Gene	Gene name	Gene description	log2 fold change	p-value	padj
ENSSSCG00000051166	*0*	0	-5.808032302	8.28E-11	1.44E-06
ENSSSCG00000018044	*ALDH3A1*	aldehyde dehydrogenase 3 family member A1 [Source:VGNC Symbol;Acc:VGNC:85238]	-2.214350354	2.02E-08	0.0001751036689
ENSSSCG00000050531	*0*	0	-2.857981431	6.27E-08	0.0003623295477
ENSSSCG00000009578	*Novel gene*	cyclin dependent kinase 20 [Source:NCBI gene (formerly Entrezgene);Acc:100157041]	1.043406601	1.62E-07	0.0007038375919
ENSSSCG00000017884	*TEKT1*	tektin 1 [Source:VGNC Symbol;Acc:VGNC:93867]	-2.686760932	9.04E-07	0.003063425464
ENSSSCG00000018041	*ALDH3A2*	aldehyde dehydrogenase 3 family member A2 [Source:VGNC Symbol;Acc:VGNC:85239]	-0.7725978417	1.06E-06	0.003063425464
ENSSSCG00000011195	*GALNT15*	polypeptide N-acetylgalactosaminyltransferase 15 [Source:VGNC Symbol;Acc:VGNC:88331]	1.743580561	1.44E-06	0.003337811781
ENSSSCG00000007033	*AP3M2*	adaptor related protein complex 3 subunit mu 2 [Source:VGNC Symbol;Acc:VGNC:96369]	-1.057992302	1.54E-06	0.003337811781
ENSSSCG00000000687	*CD4*	CD4 molecule [Source:VGNC Symbol;Acc:VGNC:86417]	-1.571429473	1.80E-06	0.003460511486
ENSSSCG00000017383	*Novel gene*	membrane primary amine oxidase-like [Source:NCBI gene (formerly Entrezgene);Acc:110256000]	-2.38907725	2.21E-06	0.003826708065
ENSSSCG00000051302	*0*	0	-4.903832177	7.65E-06	0.01205847736
ENSSSCG00000009523	*Novel gene*	gamma-glutamylamine cyclotransferase [Source:VGNC Symbol;Acc:VGNC:88434]	-1.095640915	1.10E-05	0.01593042843
ENSSSCG00000014903	*CCDC90B*	coiled-coil domain containing 90B [Source:VGNC Symbol;Acc:VGNC:86328]	-0.4136992218	1.72E-05	0.02287066575
ENSSSCG00000022842	*0*	0	-1.908517749	2.11E-05	0.02611694993
ENSSSCG00000011186	*COL6A5*	collagen type VI alpha 5 chain [Source:VGNC Symbol;Acc:VGNC:86879]	-3.315042353	2.82E-05	0.03072422499
ENSSSCG00000003815	*ALG6*	ALG6 alpha-1.3-glucosyltransferase [Source:VGNC Symbol;Acc:VGNC:85253]	-0.6812533567	2.84E-05	0.03072422499
ENSSSCG00000016334	*SCLY*	selenocysteine lyase [Source:VGNC Symbol;Acc:VGNC:98302]	1.119705678	3.02E-05	0.03075470242

ENSSSCG00000024860	*Novel gene*	sodium/glucose cotransporter 1-like [Source:NCBI gene (formerly Entrezgene);Acc:102159834]	-1.552752046	3.96E-05	0.0360860446
ENSSSCG00000017914	*GLTPD2*	glycolipid transfer protein domain containing 2 [Source:VGNC Symbol;Acc:VGNC:88502]	1.409092907	3.81E-05	0.0360860446
ENSSSCG00000047596	*0*	0	-1.356318157	4.34E-05	0.03757770537
ENSSSCG00000049049	*0*	0	2.323458046	4.95E-05	0.04083759732
ENSSSCG00000031442	*CLP1*	cleavage factor polyribonucleotide kinase subunit 1 [Source:VGNC Symbol;Acc:VGNC:86775]	0.5279530375	5.29E-05	0.04165485363
ENSSSCG00000031274	*F12*	coagulation factor XII [Source:VGNC Symbol;Acc:VGNC:99647]	-3.037305113	5.64E-05	0.04247399486
ENSSSCG00000001612	*Novel gene*	adenylate cyclase type 10 [Source:NCBI gene (formerly Entrezgene);Acc:100737927]	-1.373001245	6.53E-05	0.04523513456
ENSSSCG00000049866	*0*	0	-2.94543778	6.42E-05	0.04523513456
ENSSSCG00000051428	*0*	0	-1.290252039	6.96E-05	0.04636188598
ENSSSCG00000006852	*NTNG1*	netrin G1 [Source:VGNC Symbol;Acc:VGNC:90935]	-3.052870533	8.09E-05	0.05066128809
ENSSSCG00000017392	*CCR10*	C-C motif chemokine receptor 10 [Source:VGNC Symbol;Acc:VGNC:86369]	-1.401022198	8.19E-05	0.05066128809
ENSSSCG00000024671	*WNT9A*	Wnt family member 9A [Source:VGNC Symbol;Acc:VGNC:94978]	0.9869047129	9.21E-05	0.05150486767
ENSSSCG00000032849	*MLPH*	melanophilin [Source:VGNC Symbol;Acc:VGNC:96225]	1.222281538	9.37E-05	0.05150486767
ENSSSCG00000047413	*OTOS*	otospiralin [Source:NCBI gene (formerly Entrezgene);Acc:100525436]	-2.24308749	9.05E-05	0.05150486767
ENSSSCG00000016519	*AKR1D1*	aldo-keto reductase family 1 member D1 [Source:VGNC Symbol;Acc:VGNC:85230]	-2.375990401	9.51E-05	0.05150486767
ENSSSCG00000005840	*C8G*	complement C8 gamma chain [Source:VGNC Symbol;Acc:VGNC:86078]	-1.625800408	0.0001023352144	0.05373839182
ENSSSCG00000000720	*AKAP3*	A-kinase anchoring protein 3 [Source:VGNC Symbol;Acc:VGNC:85218]	-0.7665318991	0.0001291958176	0.06245445951
ENSSSCG00000025130	*KLF12*	Kruppel like factor 12 [Source:VGNC Symbol;Acc:VGNC:89492]	-0.6217220571	0.0001297455446	0.06245445951
ENSSSCG00000011141	*CALML5*	calmodulin like 5 [Source:VGNC Symbol;Acc:VGNC:95874]	-2.166181674	0.0001235811742	0.06245445951
ENSSSCG00000010039	*SLC5A4*	solute carrier family 5 member 4 [Source:NCBI gene (formerly	1.342238969	0.0001592671372	0.07459297894

		Entrezgene);Acc:397376]			
ENSSSCG00000036851	*Novel gene*	granulocyte-macrophage colony-stimulating factor receptor subunit alpha [Source:NCBI gene (formerly Entrezgene);Acc:102161330]	-2.621882224	0.0001753086104	0.07994533971
ENSSSCG00000037652	*0*	0	-0.7675202402	0.0001838484963	0.0816900152
ENSSSCG00000000660	*A2M*	alpha-2-macroglobulin [Source:NCBI gene (formerly Entrezgene);Acc:403166]	-1.794910267	0.0002056122517	0.08690377339
ENSSSCG00000051557	*0*	0	1.278729883	0.0002053765648	0.08690377339
ENSSSCG00000030026	*SORCS1*	sortilin related VPS10 domain containing receptor 1 [Source:VGNC Symbol;Acc:VGNC:93339]	-1.347857428	0.0002149211551	0.08761806329
ENSSSCG00000007642	*Novel gene*	alpha-2-glycoprotein 1. zinc-binding [Source:VGNC Symbol;Acc:VGNC:85710]	-2.670567878	0.0002174145491	0.08761806329
ENSSSCG00000000856	*PAH*	phenylalanine hydroxylase [Source:VGNC Symbol;Acc:VGNC:91155]	-2.390264546	0.0002264859506	0.08919943268
ENSSSCG00000049474	*0*	0	-2.088920688	0.0002549455868	0.09817671274

Table S2b. Differently expressed genes of liver from immunocastrated male pigs fed diets containing different levels of soybean oil (SOY1.5: 1.5% and SOY3.0: 3.0% soybean oil).

Gene	Gene name	Gene description	log2 fold change	p-value	padj
ENSSSCG00000010495	*ALDH18A1*	aldehyde dehydrogenase 18 family member A1 [Source:VGNC Symbol;Acc:VGNC:85237]	1.228170453	7.74E-17	1.14E-12
ENSSSCG00000006821	*GSTM3*	glutathione S-transferase mu 3 [Source:VGNC Symbol;Acc:VGNC:88726]	3.030939403	6.86E-08	0.000504642
ENSSSCG00000038171	*Novel gene*	acyl-coenzyme A amino acid N-acyltransferase 2 [Source:NCBI gene (formerly Entrezgene);Acc:100515185]	-2.595455208	1.25E-07	0.000613114
ENSSSCG00000017203	*GALK1*	galactokinase 1 [Source:VGNC Symbol;Acc:VGNC:88326]	0.848319954	2.09E-07	0.00064627
ENSSSCG00000017311	*MAPT*	microtubule associated protein tau [Source:VGNC Symbol;Acc:VGNC:90016]	-1.184806057	2.20E-07	0.00064627
ENSSSCG00000031106	*PLA2G2D*	phospholipase A2 group IID [Source:VGNC Symbol;Acc:VGNC:91491]	1.891406481	3.26E-07	0.000799206
ENSSSCG00000000867	*SPIC*	Spi-C transcription factor [Source:NCBI gene (formerly Entrezgene);Acc:102164462]	1.174206043	4.17E-07	0.000877077
ENSSSCG00000011970	*CMSS1*	cms1 ribosomal small subunit homolog [Source:VGNC Symbol;Acc:VGNC:96723]	-0.68726484	6.92E-07	0.00127316
ENSSSCG00000010593	*CNNM2*	cyclin and CBS domain divalent metal cation transport mediator 2 [Source:VGNC Symbol;Acc:VGNC:86828]	-0.933271692	8.91E-07	0.001457637
ENSSSCG00000051557	*0*	0	1.362072581	1.06E-06	0.001561504
ENSSSCG00000029449	*Novel gene*	proteoglycan 4 [Source:NCBI gene (formerly Entrezgene);Acc:100518683]	1.123914163	1.94E-06	0.002594773
ENSSSCG00000009831	*CUX2*	cut like homeobox 2 [Source:VGNC Symbol;Acc:VGNC:87094]	-1.301360454	4.39E-06	0.005340179
ENSSSCG00000034360	*CELSR2*	cadherin EGF LAG seven-pass G-type receptor 2 [Source:VGNC Symbol;Acc:VGNC:98748]	-1.278325946	4.72E-06	0.005340179
ENSSSCG00000041289	*IL10RB*	interleukin 10 receptor subunit beta [Source:NCBI gene (formerly Entrezgene);Acc:396657]	0.524887589	5.62E-06	0.005835676
ENSSSCG00000022842	*0*	0	-2.096314873	6.44E-06	0.005835676
ENSSSCG00000028124	*SNRPN*	small nuclear ribonucleoprotein polypeptide N [Source:NCBI gene (formerly Entrezgene);Acc:100626432]	0.714687266	6.51E-06	0.005835676

ENSSSCG00000038869	*APLNR*	apelin receptor [Source:VGNC Symbol;Acc:VGNC:85412]	-1.45150965	6.74E-06	0.005835676
ENSSSCG00000036265	*0*	0	0.746821892	7.44E-06	0.006082801
ENSSSCG00000013270	*CRY2*	cryptochrome circadian regulator 2 [Source:VGNC Symbol;Acc:VGNC:87012]	-0.921854835	8.78E-06	0.00680139
ENSSSCG00000035344	*UBE2S*	ubiquitin conjugating enzyme E2 S [Source:VGNC Symbol;Acc:VGNC:94651]	0.800535434	9.41E-06	0.006928273
ENSSSCG00000004919	*NEDD4L*	NEDD4 like E3 ubiquitin protein ligase [Source:VGNC Symbol;Acc:VGNC:90667]	-0.476841346	1.24E-05	0.007274222
ENSSSCG00000014110	*DMGDH*	dimethylglycine dehydrogenase [Source:VGNC Symbol;Acc:VGNC:87347]	-0.793381624	1.25E-05	0.007274222
ENSSSCG00000045982	*0*	0	3.103149102	1.13E-05	0.007274222
ENSSSCG00000001565	*CDKN1A*	cyclin dependent kinase inhibitor 1A [Source:VGNC Symbol;Acc:VGNC:86514]	0.809252815	1.15E-05	0.007274222
ENSSSCG00000000130	*CYTH4*	cytohesin 4 [Source:VGNC Symbol;Acc:VGNC:87137]	-1.235385958	1.28E-05	0.007274222
ENSSSCG00000039102	*0*	0	1.426169974	1.16E-05	0.007274222
ENSSSCG00000006620	*TUFT1*	tuftelin 1 [Source:VGNC Symbol;Acc:VGNC:98886]	0.7136153	1.48E-05	0.007804823
ENSSSCG00000010829	*Novel gene*	mitochondrial amidoxime reducing component 1 [Source:NCBI gene (formerly Entrezgene);Acc:100516871]	-1.327379259	1.45E-05	0.007804823
ENSSSCG00000003006	*CYP2B22*	cytochrome P450 2B4-like [Source:NCBI gene (formerly Entrezgene);Acc:102165015]	-2.558340514	1.95E-05	0.009919037
ENSSSCG00000004392	*AMD1*	adenosylmethionine decarboxylase 1 [Source:NCBI gene (formerly Entrezgene);Acc:100155925]	0.72176522	2.15E-05	0.010228021
ENSSSCG00000014314	*Novel gene*	F-box and leucine rich repeat protein 21. pseudogene [Source:NCBI gene (formerly Entrezgene);Acc:100517085]	-2.060872565	2.18E-05	0.010228021
ENSSSCG00000045889	*0*	0	-1.481033351	2.22E-05	0.010228021
ENSSSCG00000028464	*TMEM170A*	transmembrane protein 170A [Source:VGNC Symbol;Acc:VGNC:98659]	0.690687724	2.56E-05	0.010839685
ENSSSCG00000014903	*CCDC90B*	coiled-coil domain containing 90B [Source:VGNC Symbol;Acc:VGNC:86328]	-0.499695943	2.44E-05	0.010839685
ENSSSCG00000007636	*GJC3*	gap junction protein gamma 3 [Source:VGNC Symbol;Acc:VGNC:88470]	-0.802078521	2.65E-05	0.010839685
ENSSSCG00000029790	*PCYOX1*	prenylcysteine oxidase 1 [Source:VGNC Symbol;Acc:VGNC:91235]	1.446786119	2.62E-05	0.010839685

ENSSSCG00000014170	*CAST*	calpastatin [Source:VGNC Symbol;Acc:VGNC:99603]	-0.578249602	3.11E-05	0.012062628
ENSSSCG00000043197	*0*	0	-2.195985819	3.06E-05	0.012062628
ENSSSCG00000024158	*ANO1*	anoctamin 1 [Source:VGNC Symbol;Acc:VGNC:85354]	-0.634201169	3.32E-05	0.01208406
ENSSSCG00000046214	*IFT22*	intraflagellar transport 22 [Source:NCBI gene (formerly Entrezgene);Acc:100519188]	-0.750343186	3.35E-05	0.01208406
ENSSSCG00000017251	*SOX9*	SRY-box transcription factor 9 [Source:VGNC Symbol;Acc:VGNC:99053]	-1.020096875	3.37E-05	0.01208406
ENSSSCG00000030677	*GART*	phosphoribosylglycinamide formyltransferase. phosphoribosylglycinamide synthetase. phosphoribosylaminoimidazole synthetase [Source:VGNC Symbol;Acc:VGNC:88353]	0.647739876	3.55E-05	0.012442145
ENSSSCG00000033189	*Novel gene*	FAM3 metabolism regulating signaling molecule D [Source:NCBI gene (formerly Entrezgene);Acc:100621654]	-1.124766188	3.64E-05	0.012452594
ENSSSCG00000021161	*CKS2*	CDC28 protein kinase regulatory subunit 2 [Source:NCBI gene (formerly Entrezgene);Acc:100520933]	1.215088133	4.16E-05	0.013925615
ENSSSCG00000012621	*UBE2A*	ubiquitin conjugating enzyme E2 A [Source:VGNC Symbol;Acc:VGNC:94639]	0.43027832	4.30E-05	0.014050515
ENSSSCG00000003815	*ALG6*	ALG6 alpha-1.3-glucosyltransferase [Source:VGNC Symbol;Acc:VGNC:85253]	-0.737649912	4.66E-05	0.01465718
ENSSSCG00000016322	*ACKR3*	atypical chemokine receptor 3 [Source:VGNC Symbol;Acc:VGNC:96017]	0.890815037	4.68E-05	0.01465718
ENSSSCG00000038719	*0*	0	3.064228736	5.05E-05	0.015174358
ENSSSCG00000037478	*Novel gene*	proline rich 29 [Source:VGNC Symbol;Acc:VGNC:91857]	1.277823564	5.00E-05	0.015174358
ENSSSCG00000004520	*MAPK4*	mitogen-activated protein kinase 4 [Source:VGNC Symbol;Acc:VGNC:90004]	-2.362938567	5.20E-05	0.015323159
ENSSSCG00000017885	*SMTNL2*	smoothelin like 2 [Source:VGNC Symbol;Acc:VGNC:93268]	1.760205609	6.16E-05	0.017787694
ENSSSCG00000050735	*0*	0	-2.130715892	6.33E-05	0.017924513
ENSSSCG00000006761	*DCLRE1B*	DNA cross-link repair 1B [Source:VGNC Symbol;Acc:VGNC:87186]	0.892836353	6.55E-05	0.018199032
ENSSSCG00000003148	*DBP*	D-box binding PAR bZIP transcription factor [Source:VGNC Symbol;Acc:VGNC:87167]	-1.411584769	6.71E-05	0.018282894
ENSSSCG00000037954	*CAVIN4*	caveolae associated protein 4 [Source:VGNC Symbol;Acc:VGNC:86219]	-3.002814976	7.85E-05	0.019652375

ENSSSCG00000025830	*NUP93*	nucleoporin 93 [Source:VGNC Symbol;Acc:VGNC:90987]	0.42256335	7.93E-05	0.019652375
ENSSSCG00000029097	*RCC1*	regulator of chromosome condensation 1 [Source:VGNC Symbol;Acc:VGNC:92175]	0.768883916	7.76E-05	0.019652375
ENSSSCG00000050649	*0*	0	0.927383422	8.01E-05	0.019652375
ENSSSCG00000039626	*DERL3*	derlin 3 [Source:VGNC Symbol;Acc:VGNC:87262]	1.039467205	7.76E-05	0.019652375
ENSSSCG00000006538	*FLAD1*	flavin adenine dinucleotide synthetase 1 [Source:NCBI gene (formerly Entrezgene);Acc:100153896]	0.435943304	7.86E-05	0.019652375
ENSSSCG00000048848	*Novel gene*	0	3.635942766	8.22E-05	0.019836902
ENSSSCG00000004861	*TSHZ1*	teashirt zinc finger homeobox 1 [Source:VGNC Symbol;Acc:VGNC:94492]	-0.450855146	9.58E-05	0.020636096
ENSSSCG00000041880	*Novel gene*	0	1.061391008	9.67E-05	0.020636096
ENSSSCG00000041295	*Novel gene*	0	2.01143876	9.47E-05	0.020636096
ENSSSCG00000014924	*CTSC*	cathepsin C [Source:VGNC Symbol;Acc:VGNC:87075]	0.33998948	9.16E-05	0.020636096
ENSSSCG00000008712	*PPP2R2C*	protein phosphatase 2 regulatory subunit Bgamma [Source:VGNC Symbol;Acc:VGNC:91749]	1.360903088	9.36E-05	0.020636096
ENSSSCG00000046072	*0*	0	-1.040114668	9.15E-05	0.020636096
ENSSSCG00000017446	*0*	0	1.605637691	8.93E-05	0.020636096
ENSSSCG00000017914	*GLTPD2*	glycolipid transfer protein domain containing 2 [Source:VGNC Symbol;Acc:VGNC:88502]	1.360216766	9.22E-05	0.020636096
ENSSSCG00000004181	*VNN1*	vanin 1 [Source:NCBI gene (formerly Entrezgene);Acc:397246]	-0.91708414	0.000105896	0.021353371
ENSSSCG00000013397	*ARNTL*	aryl hydrocarbon receptor nuclear translocator like [Source:VGNC Symbol;Acc:VGNC:96796]	0.991356761	0.000104988	0.021353371
ENSSSCG00000010330	*PPIF*	peptidylprolyl isomerase F [Source:VGNC Symbol;Acc:VGNC:98213]	0.811822638	0.000103295	0.021353371
ENSSSCG00000010664	*ENO4*	enolase 4 [Source:VGNC Symbol;Acc:VGNC:87704]	-1.15995899	0.0001027	0.021353371
ENSSSCG00000031741	*Novel gene*	ribonucleotide reductase regulatory subunit M2 [Source:NCBI gene (formerly Entrezgene);Acc:100316853]	1.032013439	0.000119215	0.023714078
ENSSSCG00000050714	*0*	0	-2.35605963	0.000135889	0.026670406
ENSSSCG00000036359	*SLC43A1*	solute carrier family 43 member 1 [Source:VGNC Symbol;Acc:VGNC:93116]	-1.661658371	0.000141319	0.027015764
ENSSSCG00000051637	*0*	0	-1.469795879	0.000139643	0.027015764
ENSSSCG00000010079	*PPM1F*	protein phosphatase. Mg2+/Mn2+ dependent 1F [Source:VGNC	0.417176978	0.000167284	0.031569402

		Symbol;Acc:VGNC:91706]			
ENSSSCG00000026473	*ABCA8*	ATP-binding cassette sub-family A member 8 [Source:NCBI gene (formerly Entrezgene);Acc:100520512]	-0.768374163	0.000178474	0.033254968
ENSSSCG00000026981	*Novel gene*	mitochondrial ribosomal protein S6 [Source:VGNC Symbol;Acc:VGNC:90399]	0.516699456	0.000184404	0.033511383
ENSSSCG00000043669	*0*	0	-1.3329421	0.000184332	0.033511383
ENSSSCG00000009824	*RAD9B*	RAD9 checkpoint clamp component B [Source:VGNC Symbol;Acc:VGNC:92063]	-1.199530919	0.000190786	0.034248489
ENSSSCG00000011925	*CD200R1*	CD200 receptor 1 [Source:NCBI gene (formerly Entrezgene);Acc:100155169]	-0.789479141	0.000203717	0.03448138
ENSSSCG00000013176	*TMX2*	thioredoxin related transmembrane protein 2 [Source:VGNC Symbol;Acc:VGNC:98379]	0.481687905	0.000195107	0.03448138
ENSSSCG00000050685	*0*	0	5.926102529	0.000206978	0.03448138
ENSSSCG00000038234	*TMEM175*	transmembrane protein 175 [Source:VGNC Symbol;Acc:VGNC:94111]	0.720771095	0.000201982	0.03448138
ENSSSCG00000008383	*Novel gene*	activator of HSP90 ATPase homolog 2. pseudogene [Source:NCBI gene (formerly Entrezgene);Acc:110260004]	0.655487295	0.000208481	0.03448138
ENSSSCG00000039272	*IP6K3*	inositol hexakisphosphate kinase 3 [Source:VGNC Symbol;Acc:VGNC:89174]	1.84521056	0.000200437	0.03448138
ENSSSCG00000000038	*CYB5R3*	NADH-cytochrome b5 reductase 3-like [Source:NCBI gene (formerly Entrezgene);Acc:100524254]	-0.626338706	0.000207209	0.03448138
ENSSSCG00000049683	*0*	0	1.081218416	0.000221558	0.036115359
ENSSSCG00000017635	*MKS1*	MKS transition zone complex subunit 1 [Source:VGNC Symbol;Acc:VGNC:96589]	-0.911186079	0.000223268	0.036115359
ENSSSCG00000004554	*PCLAF*	PCNA clamp associated factor [Source:NCBI gene (formerly Entrezgene);Acc:100514810]	1.264458095	0.000225784	0.0361255
ENSSSCG00000014070	*ANKRA2*	ankyrin repeat family A member 2 [Source:VGNC Symbol;Acc:VGNC:85320]	-0.462576626	0.000229408	0.036226198
ENSSSCG00000001863	*TMEM266*	transmembrane protein 266 [Source:VGNC Symbol;Acc:VGNC:94166]	-1.571486788	0.000231336	0.036226198
ENSSSCG00000002762	*TERF2*	telomeric repeat binding factor 2 [Source:VGNC Symbol;Acc:VGNC:93882]	-0.522057382	0.000233949	0.036249738
ENSSSCG00000028794	*Novel gene*	transmembrane protein 91 [Source:NCBI gene (formerly	-0.77091119	0.000237925	0.036481843

		Entrezgene);Acc:100511932]			
ENSSSCG00000004291	*NT5E*	5'-nucleotidase ecto [Source:VGNC Symbol;Acc:VGNC:90925]	0.781373422	0.00025318	0.037980039
ENSSSCG00000009798	*B3GNT4*	UDP-GlcNAc:betaGal beta-1.3-N-acetylglucosaminyltransferase 4 [Source:VGNC Symbol;Acc:VGNC:85725]	-1.521042459	0.000253388	0.037980039
ENSSSCG00000010632	*TECTB*	tectorin beta [Source:VGNC Symbol;Acc:VGNC:93860]	-2.199103244	0.00025615	0.037980039
ENSSSCG00000022011	*NMI*	N-myc and STAT interactor [Source:VGNC Symbol;Acc:VGNC:96447]	0.494779165	0.000264817	0.037980039
ENSSSCG00000008727	*MSX1*	msh homeobox 1 [Source:VGNC Symbol;Acc:VGNC:90431]	0.749762452	0.000263041	0.037980039
ENSSSCG00000025698	*SERPINE1*	serpin family E member 1 [Source:VGNC Symbol;Acc:VGNC:98310]	0.888460384	0.00026451	0.037980039
ENSSSCG00000017605	*MMD*	monocyte to macrophage differentiation associated [Source:VGNC Symbol;Acc:VGNC:90264]	0.907669689	0.000265757	0.037980039
ENSSSCG00000039013	*NOTUM*	notum. palmitoleoyl-protein carboxylesterase [Source:VGNC Symbol;Acc:VGNC:90826]	-0.479168552	0.000279729	0.039592427
ENSSSCG00000008298	*DUSP11*	dual specificity phosphatase 11 [Source:VGNC Symbol;Acc:VGNC:87477]	0.517016575	0.000282796	0.039645248
ENSSSCG00000036095	*ACOT12*	acyl-CoA thioesterase 12 [Source:VGNC Symbol;Acc:VGNC:85017]	-0.897569474	0.000293415	0.040710191
ENSSSCG00000000808	*SLC38A2*	solute carrier family 38 member 2 [Source:VGNC Symbol;Acc:VGNC:93094]	0.756211864	0.000298196	0.040710191
ENSSSCG00000017913	*Novel gene*	proteasome 20S subunit beta 6 [Source:VGNC Symbol;Acc:VGNC:91908]	0.55236465	0.000298689	0.040710191
ENSSSCG00000043977	*Novel gene*	cytochrome c oxidase subunit 6B1-like [Source:NCBI gene (formerly Entrezgene);Acc:100519366]	-0.648902961	0.000322141	0.041963825
ENSSSCG00000003478	*CROCC*	ciliary rootlet coiled-coil. rootletin [Source:VGNC Symbol;Acc:VGNC:97946]	-0.781228328	0.000321653	0.041963825
ENSSSCG00000003861	*ORC1*	origin recognition complex subunit 1 [Source:VGNC Symbol;Acc:VGNC:91060]	1.023905687	0.000318467	0.041963825
ENSSSCG00000027903	*Novel gene*	phylloquinone omega-hydroxylase CYP4F2-like [Source:NCBI gene (formerly Entrezgene);Acc:110259328]	-0.633412934	0.000313094	0.041963825
ENSSSCG00000034829	*0*	0	2.208820878	0.000315877	0.041963825
ENSSSCG00000013842	*CYP4F3*	docosahexaenoic acid omega-hydroxylase CYP4F3-like [Source:NCBI gene (formerly Entrezgene);Acc:110259329]	-1.102417942	0.000326851	0.042203887

ENSSSCG00000004702	*STRC*	stereocilin [Source:NCBI gene (formerly Entrezgene);Acc:100519812]	1.640069058	0.000338467	0.042222263
ENSSSCG00000021738	*PTPN2*	protein tyrosine phosphatase non-receptor type 2 [Source:VGNC Symbol;Acc:VGNC:98545]	0.307904222	0.00033724	0.042222263
ENSSSCG00000015398	*SEMA3A*	semaphorin 3A [Source:VGNC Symbol;Acc:VGNC:92693]	2.273019945	0.000338342	0.042222263
ENSSSCG00000006090	*MTERF3*	mitochondrial transcription termination factor 3 [Source:VGNC Symbol;Acc:VGNC:90442]	0.468972878	0.000332635	0.042222263
ENSSSCG00000024802	*MACC1*	MET transcriptional regulator MACC1 [Source:VGNC Symbol;Acc:VGNC:89935]	-1.361082221	0.000345485	0.042704544
ENSSSCG00000010954	*Novel gene*	iron-sulfur cluster assembly 1 [Source:NCBI gene (formerly Entrezgene);Acc:100516824]	0.433675705	0.000348135	0.042704544
ENSSSCG00000016668	*PDE1C*	phosphodiesterase 1C [Source:VGNC Symbol;Acc:VGNC:91250]	2.26214859	0.000352217	0.042848277
ENSSSCG00000044227	*NRG4*	neuregulin 4 [Source:NCBI gene (formerly Entrezgene);Acc:100516621]	-0.631932926	0.000356895	0.043061404
ENSSSCG00000050723	*0*	0	-0.779701198	0.000360365	0.043126552
ENSSSCG00000051421	*0*	0	-2.093680369	0.000371279	0.043953523
ENSSSCG00000032473	*NYNRIN*	NYN domain and retroviral integrase containing [Source:VGNC Symbol;Acc:VGNC:91003]	-0.817681692	0.000373247	0.043953523
ENSSSCG00000044746	*0*	0	-1.012517463	0.000380991	0.044509374
ENSSSCG00000003891	*CYP4A24*	cytochrome P450 4A24 [Source:NCBI gene (formerly Entrezgene);Acc:403326]	-1.274774884	0.000396819	0.044849535
ENSSSCG00000009755	*AACS*	acetoacetyl-CoA synthetase [Source:VGNC Symbol;Acc:VGNC:84937]	-0.753273771	0.000399136	0.044849535
ENSSSCG00000042325	*0*	0	-2.565182431	0.000393078	0.044849535
ENSSSCG00000008414	*ERLEC1*	endoplasmic reticulum lectin 1 [Source:VGNC Symbol;Acc:VGNC:87775]	0.339602459	0.000393639	0.044849535
ENSSSCG00000010885	*TLR5*	toll like receptor 5 [Source:NCBI gene (formerly Entrezgene);Acc:100144476]	-0.864821728	0.000397643	0.044849535
ENSSSCG00000050646	*0*	0	-1.919783139	0.00041106	0.045258743
ENSSSCG00000005488	*Novel gene*	orosomucoid 1 [Source:NCBI gene (formerly Entrezgene);Acc:396901]	1.05647224	0.000412706	0.045258743
ENSSSCG00000046729	*0*	0	-0.874469599	0.000415077	0.045258743

ENSSSCG00000015604	*NEK2*	NIMA related kinase 2 [Source:VGNC Symbol;Acc:VGNC:90675]	1.60571251	0.000408558	0.045258743
ENSSSCG00000022353	*RAP1GDS1*	Rap1 GTPase-GDP dissociation stimulator 1 [Source:VGNC Symbol;Acc:VGNC:92087]	0.380821231	0.000421011	0.045355545
ENSSSCG00000035867	*GFOD1*	glucose-fructose oxidoreductase domain containing 1 [Source:VGNC Symbol;Acc:VGNC:88424]	0.627316647	0.000422127	0.045355545
ENSSSCG00000003882	*SLC5A9*	solute carrier family 5 member 9 [Source:VGNC Symbol;Acc:VGNC:93149]	-1.33920632	0.000432453	0.045469342
ENSSSCG00000026367	*IFT172*	intraflagellar transport 172 [Source:VGNC Symbol;Acc:VGNC:89046]	-0.433384435	0.000429716	0.045469342
ENSSSCG00000000259	*CSAD*	cysteine sulfinic acid decarboxylase [Source:VGNC Symbol;Acc:VGNC:87027]	0.734733743	0.000428472	0.045469342
ENSSSCG00000011477	*ACOX2*	acyl-CoA oxidase 2 [Source:VGNC Symbol;Acc:VGNC:85021]	-0.393312766	0.000435788	0.045495027
ENSSSCG00000012376	*GDPD2*	glycerophosphodiester phosphodiesterase domain containing 2 [Source:VGNC Symbol;Acc:VGNC:88407]	1.052301696	0.000449323	0.046252022
ENSSSCG00000002529	*0*	0	1.439686788	0.000447513	0.046252022
ENSSSCG00000032452	*WFS1*	wolframin ER transmembrane glycoprotein [Source:VGNC Symbol;Acc:VGNC:94955]	0.733009562	0.000459734	0.046995038
ENSSSCG00000021041	*Novel gene*	peptidase M20 domain containing 1 [Source:NCBI gene (formerly Entrezgene);Acc:100627595]	1.355994255	0.000470886	0.047803043
ENSSSCG00000009215	*ABCG2*	ATP-binding cassette. sub-family G (WHITE). member 2 [Source:NCBI gene (formerly Entrezgene);Acc:397073]	0.592831252	0.000485212	0.048920006
ENSSSCG00000005610	*SLC2A8*	solute carrier family 2 member 8 [Source:VGNC Symbol;Acc:VGNC:93053]	0.973851585	0.000490883	0.049155089
ENSSSCG00000010996	*BAG1*	BAG cochaperone 1 [Source:VGNC Symbol;Acc:VGNC:96502]	0.348931081	0.000504325	0.050159874
ENSSSCG00000005082	*PCNX4*	pecanex 4 [Source:HGNC Symbol;Acc:HGNC:20349]	-0.52862047	0.000531683	0.051877563
ENSSSCG00000012074	*BACE2*	beta-secretase 2 [Source:NCBI gene (formerly Entrezgene);Acc:100517374]	0.380431366	0.000528392	0.051877563
ENSSSCG00000021597	*PHLDA2*	pleckstrin homology like domain family A member 2 [Source:VGNC Symbol;Acc:VGNC:91397]	1.201675359	0.000535355	0.051877563
ENSSSCG00000025564	*GAS2L1*	growth arrest specific 2 like 1 [Source:VGNC Symbol;Acc:VGNC:88355]	0.553699772	0.000536309	0.051877563
ENSSSCG00000038489	*BHLHA15*	basic helix-loop-helix family member a15 [Source:VGNC	0.862673804	0.000546265	0.051877563

		Symbol;Acc:VGNC:85812]			
ENSSSCG00000006939	*ZNHIT6*	zinc finger HIT-type containing 6 [Source:VGNC Symbol;Acc:VGNC:98909]	0.361274726	0.000541793	0.051877563
ENSSSCG00000039553	*ASPG*	asparaginase [Source:VGNC Symbol;Acc:VGNC:85583]	0.88068487	0.000544495	0.051877563
ENSSSCG00000035243	*RAB27B*	RAB27B. member RAS oncogene family [Source:VGNC Symbol;Acc:VGNC:98250]	1.526943033	0.000559345	0.05277921
ENSSSCG00000000071	*ST13*	ST13 Hsp70 interacting protein [Source:NCBI gene (formerly Entrezgene);Acc:100624451]	-0.349973011	0.000571771	0.053608114
ENSSSCG00000012597	*PLS3*	plastin 3 [Source:VGNC Symbol;Acc:VGNC:91573]	-0.496508492	0.000584207	0.054427348
ENSSSCG00000012653	*ZDHHC9*	zinc finger DHHC-type palmitoyltransferase 9 [Source:VGNC Symbol;Acc:VGNC:95131]	0.422630229	0.000588244	0.054458854
ENSSSCG00000003729	*RNF125*	ring finger protein 125 [Source:VGNC Symbol;Acc:VGNC:92352]	0.996330575	0.000616817	0.056394724
ENSSSCG00000006023	*SYBU*	syntabulin [Source:VGNC Symbol;Acc:VGNC:93649]	-0.783521698	0.000615921	0.056394724
ENSSSCG00000009853	*WSB2*	WD repeat and SOCS box containing 2 [Source:VGNC Symbol;Acc:VGNC:94982]	0.24360142	0.000622203	0.056535989
ENSSSCG00000016216	*TUBA4A*	tubulin alpha 4a [Source:VGNC Symbol;Acc:VGNC:95557]	0.855202297	0.000638304	0.057643167
ENSSSCG00000015405	*CD36*	CD36 molecule [Source:NCBI gene (formerly Entrezgene);Acc:733702]	-0.517319333	0.000647154	0.058085974
ENSSSCG00000005391	*MSANTD3-TMEFF1*	Myb/SANT DNA binding domain containing 3 [Source:NCBI gene (formerly Entrezgene);Acc:100513775]	-0.889969873	0.00067234	0.059672651
ENSSSCG00000006155	*ZBTB10*	zinc finger and BTB domain containing 10 [Source:VGNC Symbol;Acc:VGNC:95058]	-0.920263847	0.000672939	0.059672651
ENSSSCG00000005057	*FBXO34*	F-box protein 34 [Source:VGNC Symbol;Acc:VGNC:88041]	0.713856942	0.000701511	0.060733666
ENSSSCG00000011325	*MYL3*	myosin light chain 3 [Source:VGNC Symbol;Acc:VGNC:90515]	-1.36812861	0.000694821	0.060733666
ENSSSCG00000016314	*TRPM8*	transient receptor potential cation channel subfamily M member 8 [Source:VGNC Symbol;Acc:VGNC:95867]	1.115163799	0.000705534	0.060733666
ENSSSCG00000037845	*YEATS4*	YEATS domain containing 4 [Source:NCBI gene (formerly Entrezgene);Acc:100739489]	0.607943517	0.000691257	0.060733666
ENSSSCG00000010879	*KIF26B*	kinesin family member 26B [Source:VGNC Symbol;Acc:VGNC:96087]	-0.781925282	0.000700606	0.060733666
ENSSSCG00000037268	*APCS*	amyloid P component. serum [Source:VGNC Symbol;Acc:VGNC:85407]	0.7134869	0.000766375	0.065587454

ENSSSCG00000007235	*TPX2*	TPX2 microtubule nucleation factor [Source:VGNC Symbol;Acc:VGNC:95559]	0.833253578	0.000776255	0.066048953
ENSSSCG00000016295	*NGEF*	neuronal guanine nucleotide exchange factor [Source:VGNC Symbol;Acc:VGNC:96443]	-0.557395545	0.000789713	0.066807877
ENSSSCG00000002645	*GALNS*	galactosamine (N-acetyl)-6-sulfatase [Source:VGNC Symbol;Acc:VGNC:97061]	-0.476559511	0.000798953	0.067203362
ENSSSCG00000010947	*FBP2*	fructose-bisphosphatase 2 [Source:NCBI gene (formerly Entrezgene);Acc:100134828]	-1.267698089	0.00080615	0.067423456
ENSSSCG00000014060	*KIAA1191*	KIAA1191 [Source:VGNC Symbol;Acc:VGNC:99783]	0.462641317	0.000822406	0.067950934
ENSSSCG00000038801	*NPNT*	nephronectin [Source:VGNC Symbol;Acc:VGNC:90855]	-0.833218212	0.000826306	0.067950934
ENSSSCG00000024679	*UPF3A*	UPF3A regulator of nonsense mediated mRNA decay [Source:VGNC Symbol;Acc:VGNC:94719]	-0.654137554	0.000820709	0.067950934
ENSSSCG00000031736	*MGST2*	microsomal glutathione S-transferase 2 [Source:VGNC Symbol;Acc:VGNC:90203]	0.716140152	0.000849692	0.069485937
ENSSSCG00000005494	*TNC*	tenascin C [Source:NCBI gene (formerly Entrezgene);Acc:397460]	1.253119099	0.000876881	0.070827989
ENSSSCG00000011849	*TNK2*	tyrosine kinase non receptor 2 [Source:VGNC Symbol;Acc:VGNC:94279]	-0.573591187	0.000877743	0.070827989
ENSSSCG00000014141	*RFESD*	Rieske Fe-S domain containing [Source:VGNC Symbol;Acc:VGNC:92236]	0.636540729	0.000880538	0.070827989
ENSSSCG00000041180	*0*	0	-0.92244208	0.000889756	0.071180466
ENSSSCG00000011802	*KNG1*	kininogen 1 [Source:VGNC Symbol;Acc:VGNC:89557]	-0.674900878	0.000896771	0.071353883
ENSSSCG00000010036	*SLC5A1*	solute carrier family 5 member 1 [Source:VGNC Symbol;Acc:VGNC:93140]	-0.547852624	0.000906181	0.071715004
ENSSSCG00000015387	*TRA2A*	transformer 2 alpha homolog [Source:VGNC Symbol;Acc:VGNC:94353]	0.376263962	0.000913507	0.071821505
ENSSSCG00000017673	*INTS2*	integrator complex subunit 2 [Source:VGNC Symbol;Acc:VGNC:89162]	0.556263914	0.000917286	0.071821505
ENSSSCG00000032657	*RPL3L*	ribosomal protein L3 like [Source:VGNC Symbol;Acc:VGNC:92428]	-0.714916811	0.000929611	0.072401488
ENSSSCG00000022891	*MYMK*	myomaker. myoblast fusion factor [Source:NCBI gene (formerly Entrezgene);Acc:100627299]	-1.363723566	0.000946522	0.072601362
ENSSSCG00000015120	*USP2*	ubiquitin specific peptidase 2 [Source:VGNC	-0.810639247	0.000941637	0.072601362

		Symbol;Acc:VGNC:94751]			
ENSSSCG00000007909	*ABAT*	4-aminobutyrate aminotransferase [Source:VGNC Symbol;Acc:VGNC:96910]	-0.508370361	0.000946974	0.072601362
ENSSSCG00000000951	*CSRP2*	cysteine and glycine rich protein 2 [Source:NCBI gene (formerly Entrezgene);Acc:100153630]	0.73645108	0.00096933	0.073549186
ENSSSCG00000038322	*Novel gene*	diacylglycerol O-acyltransferase 2-like [Source:NCBI gene (formerly Entrezgene);Acc:110259135]	-1.78235937	0.000966228	0.073549186
ENSSSCG00000004478	*MYO6*	myosin VI [Source:NCBI gene (formerly Entrezgene);Acc:397085]	-0.802251345	0.000981932	0.073745089
ENSSSCG00000009211	*0*	0	0.45598236	0.000979445	0.073745089
ENSSSCG00000002475	*SERPINA6*	serpin family A member 6 [Source:NCBI gene (formerly Entrezgene);Acc:396736]	-1.376836118	0.000999674	0.074379877
ENSSSCG00000037046	*TUBB4B*	tubulin beta 4B class IVb [Source:VGNC Symbol;Acc:VGNC:94580]	0.585766005	0.00100049	0.074379877
ENSSSCG00000002368	*LTBP2*	latent transforming growth factor beta binding protein 2 [Source:VGNC Symbol;Acc:VGNC:89886]	-0.879040525	0.001010974	0.07454989
ENSSSCG00000030511	*LGR5*	leucine rich repeat containing G protein-coupled receptor 5 [Source:NCBI gene (formerly Entrezgene);Acc:100151994]	-1.076109186	0.001012906	0.07454989
ENSSSCG00000003554	*Novel gene*	selenoprotein N [Source:VGNC Symbol;Acc:VGNC:98611]	0.304225896	0.001020362	0.074725025
ENSSSCG00000013102	*MS4A7*	membrane spanning 4-domains A7 [Source:VGNC Symbol;Acc:VGNC:90413]	-1.597781843	0.001061867	0.076995416
ENSSSCG00000010475	*CYP26A1*	cytochrome P450. family 26. subfamily A. polypeptide 1 [Source:NCBI gene (formerly Entrezgene);Acc:100124374]	-1.948084935	0.001065223	0.076995416
ENSSSCG00000045759	*0*	0	1.436584532	0.001067056	0.076995416
ENSSSCG00000039188	*AK8*	adenylate kinase 8 [Source:VGNC Symbol;Acc:VGNC:85213]	-0.919807475	0.001112052	0.078030467
ENSSSCG00000027689	*SRM*	spermidine synthase [Source:VGNC Symbol;Acc:VGNC:98623]	0.775530263	0.001123808	0.078030467
ENSSSCG00000009758	*DHX37*	DEAH-box helicase 37 [Source:VGNC Symbol;Acc:VGNC:87293]	0.372790383	0.001122698	0.078030467
ENSSSCG00000012623	*SLC25A5*	solute carrier family 25 member 5 [Source:VGNC Symbol;Acc:VGNC:93022]	0.573332102	0.0011052	0.078030467
ENSSSCG00000000419	*RDH16*	retinol dehydrogenase 16 [Source:NCBI gene (formerly Entrezgene);Acc:100626199]	-0.626711809	0.001109613	0.078030467
ENSSSCG00000031716	*PTPRQ*	protein tyrosine phosphatase receptor type Q [Source:NCBI gene	2.401321664	0.0011165	0.078030467

		(formerly Entrezgene);Acc:102166132]			
ENSSSCG00000050092	*0*	0	1.707526977	0.001105297	0.078030467
ENSSSCG00000040003	*UAP1L1*	UDP-N-acetylglucosamine pyrophosphorylase 1 like 1 [Source:VGNC Symbol;Acc:VGNC:94627]	-0.432509172	0.001120486	0.078030467
ENSSSCG00000005636	*SLC25A25*	solute carrier family 25 member 25 [Source:VGNC Symbol;Acc:VGNC:93002]	1.061325213	0.001157397	0.078353785
ENSSSCG00000026532	*DNASE2B*	deoxyribonuclease 2 beta [Source:VGNC Symbol;Acc:VGNC:96980]	-0.768214097	0.001155811	0.078353785
ENSSSCG00000014100	*TBCA*	tubulin folding cofactor A [Source:VGNC Symbol;Acc:VGNC:93783]	0.433333926	0.001137105	0.078353785
ENSSSCG00000033822	*THRSP*	thyroid hormone responsive [Source:NCBI gene (formerly Entrezgene);Acc:100512730]	-2.934995084	0.001171048	0.078353785
ENSSSCG00000008996	*PLRG1*	pleiotropic regulator 1 [Source:NCBI gene (formerly Entrezgene);Acc:100514171]	0.391736308	0.001160488	0.078353785
ENSSSCG00000048115	*0*	0	1.586578494	0.001150909	0.078353785
ENSSSCG00000017754	*Novel gene*	galectin 9 [Source:NCBI gene (formerly Entrezgene);Acc:396972]	0.622523786	0.001151568	0.078353785
ENSSSCG00000017915	*VMO1*	vitelline membrane outer layer 1 homolog [Source:VGNC Symbol;Acc:VGNC:94833]	-0.965440403	0.001166677	0.078353785
ENSSSCG00000034733	*CMAS*	cytidine monophosphate N-acetylneuraminic acid synthetase [Source:VGNC Symbol;Acc:VGNC:86797]	0.288806915	0.001182468	0.078759828
ENSSSCG00000046688	*0*	0	-1.632740768	0.001208298	0.080117797
ENSSSCG00000010027	*PATZ1*	POZ/BTB and AT hook containing zinc finger 1 [Source:VGNC Symbol;Acc:VGNC:91190]	-0.390229422	0.001234749	0.08042262
ENSSSCG00000020750	*0*	0	4.856267333	0.001228667	0.08042262
ENSSSCG00000045281	*0*	0	-1.229050046	0.001226126	0.08042262
ENSSSCG00000000500	*Novel gene*	RAB3A interacting protein [Source:NCBI gene (formerly Entrezgene);Acc:100152578]	0.490723852	0.001229844	0.08042262
ENSSSCG00000009578	*Novel gene*	cyclin dependent kinase 20 [Source:NCBI gene (formerly Entrezgene);Acc:100157041]	0.989286887	0.001262175	0.081487759
ENSSSCG00000016050	*INPP1*	inositol polyphosphate-1-phosphatase [Source:VGNC Symbol;Acc:VGNC:96373]	0.485156215	0.001259437	0.081487759
ENSSSCG00000039573	*SLPI*	secretory leukocyte peptidase inhibitor [Source:NCBI gene	0.865079526	0.001283127	0.082478714

		(formerly Entrezgene);Acc:396886]			
ENSSSCG00000003489	*EMC1*	ER membrane protein complex subunit 1 [Source:VGNC Symbol;Acc:VGNC:97050]	0.345774007	0.001306661	0.083626292
ENSSSCG00000033842	*CFDP1*	craniofacial development protein 1 [Source:VGNC Symbol;Acc:VGNC:86610]	0.335555685	0.001319858	0.083742704
ENSSSCG00000035238	*ELOVL1*	ELOVL fatty acid elongase 1 [Source:VGNC Symbol;Acc:VGNC:87657]	0.480646213	0.001315126	0.083742704
ENSSSCG00000028287	*C2orf68*	chromosome 3 C2orf68 homolog [Source:VGNC Symbol;Acc:VGNC:86023]	-0.195279441	0.001336354	0.084425451
ENSSSCG00000008966	*PARM1*	prostate androgen-regulated mucin-like protein 1 [Source:VGNC Symbol;Acc:VGNC:91182]	0.837573571	0.001345084	0.084613805
ENSSSCG00000013057	*Novel gene*	solute carrier family 22 member 9-like [Source:NCBI gene (formerly Entrezgene);Acc:110255291]	-0.633024679	0.001413301	0.088526752
ENSSSCG00000014950	*VSTM5*	V-set and transmembrane domain containing 5 [Source:VGNC Symbol;Acc:VGNC:94875]	1.445306967	0.001438141	0.089701011
ENSSSCG00000017118	*TERT*	telomerase reverse transcriptase [Source:VGNC Symbol;Acc:VGNC:93883]	1.023990018	0.001465316	0.091010352
ENSSSCG00000005930	*SLC45A4*	solute carrier family 45 member 4 [Source:VGNC Symbol;Acc:VGNC:93125]	0.507846233	0.00147244	0.091068579
ENSSSCG00000008484	*SRSF7*	serine and arginine rich splicing factor 7 [Source:VGNC Symbol;Acc:VGNC:93477]	0.464648986	0.001492073	0.091548273
ENSSSCG00000012380	*P2RY4*	pyrimidinergic receptor P2Y4 [Source:VGNC Symbol;Acc:VGNC:91127]	-0.835455469	0.001492635	0.091548273
ENSSSCG00000009874	*RASAL1*	RAS protein activator like 1 [Source:VGNC Symbol;Acc:VGNC:92104]	-1.031991881	0.001500245	0.091633208
ENSSSCG00000024570	*KDM4B*	lysine demethylase 4B [Source:VGNC Symbol;Acc:VGNC:89413]	-0.349193148	0.001525831	0.092567677
ENSSSCG00000048536	*0*	0	-2.483177313	0.001528121	0.092567677
ENSSSCG00000031851	*CBR2*	carbonyl reductase 2 [Source:NCBI gene (formerly Entrezgene);Acc:396780]	-1.701423375	0.001565807	0.09446181
ENSSSCG00000002620	*EFHC1*	EF-hand domain containing 1 [Source:VGNC Symbol;Acc:VGNC:87570]	-1.121960572	0.001582518	0.094706065
ENSSSCG00000007046	*TRMT6*	tRNA methyltransferase 6 [Source:VGNC	0.335891458	0.001582724	0.094706065

		Symbol;Acc:VGNC:95956]			
ENSSSCG00000026784	*LMNB2*	lamin B2 [Source:VGNC Symbol;Acc:VGNC:89761]	0.512496505	0.001614986	0.094711537
ENSSSCG00000015756	*XKR5*	XK related 5 [Source:VGNC Symbol;Acc:VGNC:95946]	1.226490326	0.001606498	0.094711537
ENSSSCG00000007955	*CLUAP1*	clusterin associated protein 1 [Source:VGNC Symbol;Acc:VGNC:86791]	-0.401691286	0.001608954	0.094711537
ENSSSCG00000028509	*RBM8A*	RNA binding motif protein 8A [Source:VGNC Symbol;Acc:VGNC:92162]	0.335854621	0.001595909	0.094711537
ENSSSCG00000000738	*RHNO1*	RAD9-HUS1-RAD1 interacting nuclear orphan 1 [Source:VGNC Symbol;Acc:VGNC:92282]	1.07498257	0.001595429	0.094711537
ENSSSCG00000020872	*Novel gene*	PDZK1 interacting protein 1 [Source:NCBI gene (formerly Entrezgene);Acc:100626400]	1.659249735	0.001629094	0.09515979
ENSSSCG00000004751	*CHP1*	calcineurin like EF-hand protein 1 [Source:VGNC Symbol;Acc:VGNC:86657]	0.293884712	0.001636223	0.095198442
ENSSSCG00000004225	*TPD52L1*	TPD52 like 1 [Source:VGNC Symbol;Acc:VGNC:94334]	1.437230783	0.001656563	0.095252373
ENSSSCG00000013366	*Novel gene*	lactate dehydrogenase A [Source:VGNC Symbol;Acc:VGNC:99784]	0.453194498	0.001653995	0.095252373
ENSSSCG00000001746	*PKHD1*	PKHD1 ciliary IPT domain containing fibrocystin/polyductin [Source:VGNC Symbol;Acc:VGNC:91476]	-1.035714114	0.001651128	0.095252373
ENSSSCG00000037430	*COL6A6*	collagen type VI alpha 6 chain [Source:NCBI gene (formerly Entrezgene);Acc:100516642]	-1.441172126	0.001671233	0.095721987
ENSSSCG00000026425	*ADAMTSL2*	ADAMTS like 2 [Source:VGNC Symbol;Acc:VGNC:85091]	-0.615021404	0.001688615	0.096342686
ENSSSCG00000012174	*APOO*	apolipoprotein O [Source:NCBI gene (formerly Entrezgene);Acc:100525438]	0.671705556	0.001702345	0.096751015
ENSSSCG00000002004	*PSME2*	proteasome activator subunit 2 [Source:NCBI gene (formerly Entrezgene);Acc:397522]	0.601998471	0.001713451	0.09700767
ENSSSCG00000003419	*MAD2L2*	mitotic arrest deficient 2 like 2 [Source:VGNC Symbol;Acc:VGNC:89941]	0.46731087	0.001736182	0.097917994
ENSSSCG00000028977	*DOK6*	docking protein 6 [Source:VGNC Symbol;Acc:VGNC:87404]	-1.041124802	0.001756407	0.098680564
ENSSSCG00000008878	*PPID*	peptidylprolyl isomerase D [Source:VGNC Symbol;Acc:VGNC:98212]	0.48033967	0.001782828	0.098807505
ENSSSCG00000034776	*TAFA5*	TAFA chemokine like family member 5 [Source:VGNC Symbol;Acc:VGNC:93728]	1.196245048	0.001784791	0.098807505
ENSSSCG00000032028	*0*	0	-0.412051568	0.001785516	0.098807505

ENSSSCG00000026043	*Novel gene*	transglutaminase 3 [Source:NCBI gene (formerly Entrezgene);Acc:100153042]	1.647098945	0.001773465	0.098807505
ENSSSCG00000032403	*Novel gene*	t-complex 10 like 2. pseudogene [Source:NCBI gene (formerly Entrezgene);Acc:102162648]	1.073137536	0.001799684	0.099004076
ENSSSCG00000006830	*PSMA5*	proteasome 20S subunit alpha 5 [Source:VGNC Symbol;Acc:VGNC:98838]	0.524429625	0.00180252	0.099004076
ENSSSCG00000030682	*MACO1*	macoilin 1 [Source:VGNC Symbol;Acc:VGNC:98497]	-0.369921925	0.001853548	0.099698224
ENSSSCG00000009852	*VSIG10*	V-set and immunoglobulin domain containing 10 [Source:NCBI gene (formerly Entrezgene);Acc:100153531]	-0.524982139	0.001855345	0.099698224
ENSSSCG00000010261	*PPA1*	inorganic pyrophosphatase 1 [Source:VGNC Symbol;Acc:VGNC:96757]	0.603373104	0.001841954	0.099698224
ENSSSCG00000006213	*Novel gene*	alcohol dehydrogenase iron containing 1 [Source:VGNC Symbol;Acc:VGNC:98730]	-0.722566714	0.001855796	0.099698224
ENSSSCG00000040334	*CBX6*	chromobox 6 [Source:VGNC Symbol;Acc:VGNC:97915]	-0.459596538	0.001832267	0.099698224
ENSSSCG00000009334	*HSPH1*	heat shock protein family H (Hsp110) member 1 [Source:NCBI gene (formerly Entrezgene);Acc:100048931]	0.833600703	0.001855475	0.099698224
ENSSSCG00000043973	*Novel gene*	0	1.057496419	0.001905553	0.099859664
ENSSSCG00000013751	*NACC1*	nucleus accumbens associated 1 [Source:VGNC Symbol;Acc:VGNC:90563]	0.487549957	0.001899087	0.099859664
ENSSSCG00000035025	*ADGRV1*	adhesion G protein-coupled receptor V1 [Source:VGNC Symbol;Acc:VGNC:96788]	-0.83790941	0.00189962	0.099859664
ENSSSCG00000010532	*LOXL4*	lysyl oxidase like 4 [Source:VGNC Symbol;Acc:VGNC:89783]	1.10869009	0.001899493	0.099859664
ENSSSCG00000022797	*PPP1R3B*	protein phosphatase 1 regulatory subunit 3B [Source:VGNC Symbol;Acc:VGNC:95636]	-0.942698221	0.001890111	0.099859664
ENSSSCG00000009085	*NUDT6*	nudix hydrolase 6 [Source:VGNC Symbol;Acc:VGNC:90963]	-0.607769702	0.001897132	0.099859664
ENSSSCG00000039681	*B9D1*	B9 domain containing 1 [Source:VGNC Symbol;Acc:VGNC:85737]	-0.61054856	0.001906288	0.099859664

APPENDIX B: SUPPLEMENTARY FILE
CHAPTER 3.

Table S1: Effect of the diets on blood biochemical parameters and fatty acid profile of liver from immunocastrated male pigs fed diets containing different levels of soybean oil (SOY1.5: 1.5% and SOY3.0: 3.0% soybean oil).

Variable	Treatments		Pooled SEM[1]	P-value
	SOY1.5	SOY3.0		
Glucose(mg/dL)	81.85	82.85	4.17	0.81
Aspartataminotransferase (U/L)	40.35	38.13	2.42	0.37
TotalProteins (g/dL)	6.69	6.47	0.13	0.11
Albumin(g/dL)	3.70a	3.46b	0.11	<0.05
Globulin(g/dL)	2.996	2.999	0.12	0.98
Triglycerides(mg/dL)	44.48a	35.70b	4	<0.05
Cholesterol(mg/dL)	99.34	96.55	4.58	0.55
HDL(mg/dL)	44.34	43.72	2.06	0.77
LDL(mg/dL)	45.99	45.71	2.91	0.92
VLDL(mg/dL)	9.00a	7.13b	0.81	<0.05
Body weight (kg)	130.61	131.17	3.0430	0.86
Intramuscular fat (%)	1.94	2.63	0.35	0.06
Liver fat (%)	2.6750	3.1878	0.6520	0.44
Total SFA (%)	46.69	45.24	1.03	0.31
Total MUFA (%)	22.01a	28.78b	1.04	<0.01
Total PUFA (%)	30.79a	26.06b	0.55	<0.01
Total n-3 PUFA (%)[2]	3.75a	2.42b	0.37	<0.01
Total n-6 PUFA (%)[3]	27.02a	23.64b	0.67	<0.01
PUFA:SFA ratio (%)[4]	0.67a	0.58b	0.02	<0.01
n-6:n-3 PUFA ratio[5]	8.51a	9.9b	0.5	<0.05
Atherogenic index[6]	0.45a	0.49b	0.18	<0.01

[1] SEM = standard error of the least square means.
[2] Total n-3 PUFA = {[C18:3 n-3] + [C20:5 n-3] + [C22:6 n-3]}.
[3] Total n-6 PUFA = C18:2 n-6.
[5]4PUFA:SFA ratio = total PUFA/total SFA.
[5] Σ n-6/Σ n-3 PUFA ratio.
[6] Atherogenic index = (4 × [C14:0]) + (C16:0)/(total MUFA] + [total PUFA]). where brackets indicate concentrations (Ulbricht and Southgate. 1991).
a-b Within a row. values without a common superscript differ ($P \leq 0.05$) or tended to differ ($0.05 < P \leq 0.10$) using Student's t test.

Table S2. Differently expressed genes of liver from immunocastrated male pigs fed diets containing different levels of soybean oil (SOY1.5: 1.5% and SOY3.0: 3.0% soybean oil).

(see in APPENDIX A - Chapter 2 Table S2b)

Table S3. Enrichment for GO terms by PANTHER Overrepresentation Test of liver from immunocastrated male pigs fed diets containing different levels of soybean oil (SOY1.5: 1.5% and SOY3.0: 3.0% soybean oil).

Analysis Type:	PANTHER Overrepresentation Test (Released 20220202)	
Annotation Version and Release Date:	PANTHER version 17.0 Released 2022-02-22	
Analyzed List:	Client Text Box Input (Sus scrofa)	
Reference List:	*Sus scrofa* (all genes in database)	
Test Type:	PANTHER Overrepresentation Test. Type: FISHER	
Correction:	FDR	
PANTHER GO-Slim Biological Process	Sus scrofa - REFLIST (22162)	(FDR)
glucose metabolic process (GO:0006006)	*CBR2. PPP1R3B. FBP2*	3.23E-02
negative regulation of endopeptidase activity (GO:0010951)	*CAST. SERPINA6. KNG1*	3.77E-02
negative regulation of peptidase activity (GO:0010466)	*CAST. SERPINA6. KNG1*	2.33E-02
negative regulation of proteolysis (GO:0045861)	*CAST. SERPINA6. KNG1*	1.91E-02
hexose metabolic process (GO:0019318)	*CBR2. PPP1R3B. FBP2*	4.86E-02
negative regulation of hydrolase activity (GO:0051346)	*CAST. SERPINA6. KNG1*	2.10E-02
regulation of endopeptidase activity (GO:0052548)	*CAST. SERPINA6. KNG1*	3.39E-02
regulation of peptidase activity (GO:0052547)	*CAST. SERPINA6. KNG1*	2.95E-02
negative regulation of molecular function (GO:0044092)	*CAST. SERPINA6. KNG1. NEDD4L*	3.23E-02
cytoskeleton-dependent intracellular transport (GO:0030705)	*MYO6. SYBU. CLUAP1. MKS1. IFT172. B9D1*	2.61E-02

Table S4. Transcription factors associated identified from the functional annotation analysis by MetaCore (Clarivate Analytics) [https://portal.genego.com/] from the list of differentially expressed genes of liver tissue of immunocastrated male pigs fed with two different soybean oil proportions in the diet (SOY1.5: 1.5 % and SOY3.0: 3.0 % of soybean oil).

Transcription factor	Description	Reference
T3Rbeta / RXR-alpha. RXRA retinoid X receptor alpha	Along with *PPARα.* it represses the transcriptional activity of *HNF4α.*	10.1016/j.metabol.2021.154705
HNF1-beta HNF1 homeobox B	It may be involved in the inhibition of canonical Wnt signaling as it competes with the binding of β-catenin/LEF complexes. It is also related to the regulation of liver. kidney. pancreas and other epithelial organs.	10.1073 / pnas.1909452116
E2F1 - E2F1/DP1 complex E2F transcription factor 1	Important in lipogenesis. it is also the progression of the cell cycle and induction of apoptosis in case of DNA damage. During the initial phase of adipogenesis. it can trigger *PPARγ* expression. When dysregulated. it activates cytoplasmic Ras/mitogen-activated protein *(MAPK)* signaling cascades.	(1)10.1016/j.anndiagpath.2019.01.002 (2)10.1016/S1534-5807(02)00190-9
ESR1 (nuclear) estrogen receptor 1	It is crucial for liver lipid and carbohydrate metabolism. Its impaired function can lead to obesity and metabolic dysfunction.	10.1016/j.mce.2019.04.005
STAT3 signal transducer and activator of transcription 3	Fundamental in cell growth and apoptosis. it can be activated in response to various cytokines and growth factors. including *EGF. IFNs. IL5. IL6. LIF. HGF. and BMP2.*	STELZER. G. et al. 2016

KLF6 Kruppel like factor 6	Co-regulates lipid homeostasis. A study performed with *KLF6* knockdown revealed pathways associated to lipid homeostasis (cholesterol and triacylglycerol biosynthesis) which are down-regulated genes. in addition to *SREBF1* and *SREBF2*.	https://www.nature.com/articles/s41467-019-09116-x
SMAD3 SMAD family member 3	Activated in liver fibrosis. Involved in intracellular *TGF-β* signaling. body development. homeostasis and metabolism.	10.1369/0022155415627681
SOX9 SRY-box transcription factor 9	*FOXO* transcription factors *(FOXO1 and FOXO3)* promote *SOX9* expression when lipid levels are low and thus induce chondrogenic compromise. suppressing fatty acid oxidation. Furthermore. *SOX9* may be related to inhibition of Wnt signaling.	(1) STELZER. G. et al. 2016 (2)10.1002 / dvdy.22046
RXRA retinoid X receptor alpha	Related to adipogenic / lipogenic regulation. The SNPs ENHO. RXRA and *LXRA* were linked to epistatic interactions in dyslipidemia and myocardial infarction.	10.1186 / s12881-018-0708-4
TCF8 zinc finger E-box binding homeobox 1	It regulates endothelial invasion and may negatively regulate pathological angiogenesis.	10.1016/j.bbrc.2008.12.101
TSHZ1 teashirt zinc finger homeobox 1	It may be related to transcriptional regulation of the developmental processes.	STELZER. G. et al. 2016
TCF(LEF) lymphoid enhancer binding factor 1	In the nucleus. it binds to β-catenin and can activate transcription of *Wnt* target genes.	10.15252 / embj.201798873

Androgen receptor	Steroid-hormone activated transcription factor.	STELZER. G. et al.. (2016).
***SREBP2* precursor** sterol regulatory element binding transcription factor 2	Related to cholesterol homeostasis by regulating the transcription of sterol-regulated genes.	STELZER. G. et al.. (2016).

Table S5: Mechanisms and effects between transcription factors and DEG associated identified from the analysis networks (transcription factor) by MetaCore (Clarivate Analytics) [https://portal.genego.com/] from the list of differentially expressed genes of liver tissue of immunocastrated male pigs fed with two different soybean oil proportions in the diet (SOY1.5: 1.5 % and SOY3.0: 3.0 % of soybean oil).

From	To	Effect	Mechanism
ESR1 (nuclear)	*CRY2*	Transcription regulation	Inhibition
Beta-catenin	*Tcf(Lef)*	Complex formation	Activation
STAT3	*TERT*	Transcription regulation	Activation
GSK3 beta	*GSK3 beta*	Phosphorylation	Activation
STAT3	*Rb protein*	Transcription regulation	Activation
TCF8	*KLF6*	Transcription regulation	Activation
Androgen receptor	*E2F1*	Binding	Activation
ESR1 (nuclear)	*RXRA*	Transcription regulation	Inhibition
STAT3	*TPX2*	Transcription regulation	Activation
SMAD3	*AKT1*	Binding	Activation
Androgen receptor	*ESR1 (nuclear)*	Binding	Inhibition
HNF1-beta	*TCF8*	Transcription regulation	Activation
AKT1	*SMAD3*	Phosphorylation	Inhibition
Coumestrol intracellular	*Coumestrol + H(.2)O + ATP = PO(.4)('3-) + Coumestrol + ADP*	Technical	Technical
SOX9	*CDK1 (p34)*	Transcription regulation	Inhibition
Coumestrol intracellular	*CDK6*	Binding	Inhibition
HNF1-beta	*Rb protein*	Transcription regulation	Activation
KLF6	*SREBP2 precursor*	Transcription regulation	Activation
ATP cytoplasm	*Coumestrol + H(.2)O + ATP = PO(.4)('3-) + Coumestrol + ADP*	Technical	Technical
Androgen receptor	*SMAD3*	Binding	Inhibition
Beta-catenin	*EGFR*	co-regulation of transcription	Activation
H(.2)O + Rociletinib + ATP = PO(.4)('3-) + Rociletinib + ADP	*Rociletinib extracellular region*	Technical	Technical
ESR1 (nuclear)	*CDK6*	Transcription regulation	Inhibition
Androgen receptor	*SOX9*	Transcription regulation	Activation
AKT2	*ESR1 (nuclear)*	Phosphorylation	Activation
Androgen receptor	*AMD1*	Transcription regulation	Activation
Coumestrol intracellular	*ESR1 (nuclear)*	Binding	Activation

Androgen receptor	*CDC20*	Transcription regulation	Activation
Cyclin D1	*p21*	Binding	Activation
E2F1	*E2F1*	Transcription regulation	Activation
ESR1 (nuclear)	*PKHD1*	Transcription regulation	Activation
Coumestrol + H(.2)O + ATP = PO(.4)('3-) + Coumestrol + ADP	*PO(.4)('3-) cytoplasm*	Technical	Technical
ESR1 (nuclear)	*Tuftelin*	Transcription regulation	Inhibition
ABCG2	*H(.2)O + Rociletinib + ATP = PO(.4)('3-) + Rociletinib + ADP*	Transport catalysis	Activation
Cyclin D1	*CDK6*	Binding	Activation
TCF8	*ESR1 (nuclear)*	Transcription regulation	Inhibition
ESR1 (nuclear)	*PPIF*	Transcription regulation	Activation
EGFR	*AKT1*	Phosphorylation	Activation
AKT(PKB)	*GSK3 beta*	Phosphorylation	Inhibition
H(.2)O intracellular	*H(.2)O + Rociletinib + ATP = PO(.4)('3-) + Rociletinib + ADP*	Technical	Technical
E2F1	*ORC1L*	Transcription regulation	Activation
RXRA	*CYP26A1*	Transcription regulation	Activation
Coumestrol intracellular	*GSK3 beta*	Binding	Inhibition
STAT3	*CCRK*	Transcription regulation	Activation
ESR1 (nuclear)	*RPS21*	Transcription regulation	Activation
CDK4	*Rb protein*	Phosphorylation	Inhibition
ESR1 (nuclear)	*GABT*	Transcription regulation	Activation
E2F1	*CDK1 (p34)*	Transcription regulation	Activation
RXRA	*HNF1-beta*	Transcription regulation	Activation
STAT3	*AGP1 (ORM1)*	Transcription regulation	Activation
TCF8	*CDK4*	Transcription regulation	Activation
CDK6	*Rb protein*	Phosphorylation	Inhibition
GSK3 beta	*Cyclin D1*	Phosphorylation	Inhibition
Tenascin-C	*EGFR*	receptor binding	Activation
Androgen receptor	*STAT3*	Binding	Activation
ESR1 (nuclear)	*Tau (MAPT)*	Transcription regulation	Activation
HNF1-beta	*SREBP2 precursor*	Transcription regulation	Activation
TCF8	*Myosin VI*	Transcription regulation	Inhibition
H(.2)O intracellular	*Coumestrol + H(.2)O + ATP = PO(.4)('3-) + Coumestrol + ADP*	Technical	Technical

AKT1	*Androgen receptor*	Phosphorylation	Inhibition
E2F1	*Cyclin D1*	Transcription regulation	Activation
E2F1	*TSHZ1*	Transcription regulation	Activation
SMAD3	*ABCG2*	Transcription regulation	Inhibition
p21	*STAT3*	Binding	Inhibition
ACK1	*AKT1*	Binding	Activation
BI-2536 + ATP + H(.2)O = BI-2536 + ADP + PO(.4)('3-)	*BI-2536 extracellular region*	Technical	Technical
SOX9	*GSK3 beta*	Binding	Activation
AKT(PKB)	*SMAD3*	Binding	Inhibition
CDK1 (p34)	*AKT1*	Phosphorylation	Activation
Androgen receptor	*AGP1 (ORM1)*	Transcription regulation	Activation
ESR1 (nuclear)	*CYP2B6*	Transcription regulation	Activation
ACK1	*EGFR*	Binding	Activation
RXRA	*AGP1 (ORM1)*	Transcription regulation	Activation
Androgen receptor	*CDK4*	Transcription regulation	Activation
AKT(PKB)	*EGFR*	Phosphorylation	Activation
ESR1 (nuclear)	*TERT*	Transcription regulation	Activation
p21	*CDK4*	Binding	Inhibition
Rociletinib intracellular	H(.2)O + Rociletinib + ATP = PO(.4)('3-) + Rociletinib + ADP	Technical	Technical
STAT3	*TCF8*	Transcription regulation	Activation
p21	*Cyclin D1*	Binding	Inhibition
STAT3	*Beta-catenin*	Transcription regulation	Activation
GSK3 beta	*E2F1*	Phosphorylation	Inhibition
H(.2)O + Rociletinib + ATP = PO(.4)('3-) + Rociletinib + ADP	*ADP cytoplasm*	Technical	Technical
ACK1	*Androgen receptor*	Phosphorylation	Activation
H(.2)O intracellular	*BI-2536 + ATP + H(.2)O = BI-2536 + ADP + PO(.4)('3-)*	Technical	Technical
Nek2A	*CDC20*	Phosphorylation	Inhibition
Coumestrol + H(.2)O + ATP = PO(.4)('3-) + Coumestrol + ADP	*Coumestrol extracellular region*	Technical	Technical
Rociletinib intracellular	*ACK1*	Binding	Inhibition
SOX9	*Semaphorin 3A*	Transcription regulation	Inhibition
Androgen receptor	*GSK3 beta*	Transcription regulation	Inhibition
GSK3 beta	*Androgen receptor*	Phosphorylation	Inhibition
p21	*CDK6*	Binding	Inhibition
AKT2	*Beta-catenin*	Binding	Activation
Androgen receptor	*TCF8*	Transcription regulation	Activation
Beta-catenin	*SOX9*	co-regulation of transcription	Activation

STAT3	*CDK4*	Transcription regulation	Activation
Androgen receptor	*CDK1 (p34)*	Transcription regulation	Activation
Androgen receptor	*TERT*	Transcription regulation	Inhibition
STAT3	*CDK6*	Transcription regulation	Activation
Rb protein	*E2F1/DP1 complex*	Binding	Inhibition
STAT3	*5'-NTD*	Transcription regulation	Activation
p21	*ESR1 (nuclear)*	Binding	Activation
H(.2)O + Rociletinib + ATP = PO(.4)('3-) + Rociletinib + ADP	*PO(.4)('3-) cytoplasm*	Technical	Technical
Beta-catenin	*Androgen receptor*	Binding	Activation
BI-2536 intracellular	*Nek2A*	Binding	Inhibition
KLF6	*p21*	Transcription regulation	Activation
ESR1 (nuclear)	*C3orf26*	Transcription regulation	Activation
EGFR	*Beta-catenin*	Phosphorylation	Inhibition
SOX9	*Beta-catenin*	Binding	Inhibition
STAT3	*AKT1*	Transcription regulation	Activation
E2F1	*CDK4*	Transcription regulation	Activation
ABCG2	*Coumestrol + H(.2)O + ATP = PO(.4)('3-) + Coumestrol + ADP*	Transport catalysis	Activation
HNF1-beta	*LDHA*	Transcription regulation	Activation
ATP cytoplasm	*H(.2)O + Rociletinib + ATP = PO(.4)('3-) + Rociletinib + ADP*	Technical	Technical
KLF6	*E2F1*	Transcription regulation	Inhibition
ESR1 (nuclear)	*SOX9*	Transcription regulation	Inhibition
GSK3 beta	*ESR1 (nuclear)*	Phosphorylation	Activation
E2F1	*CDK6*	Transcription regulation	Activation
BI-2536 intracellular	*BI-2536 + ATP + H(.2)O = BI-2536 + ADP + PO(.4)('3-)*	Technical	Technical
HNF1-beta	*PKHD1*	Transcription regulation	Activation
SMAD3	*Tenascin-C*	Transcription regulation	Activation
Cyclin D1	*STAT3*	Binding	Inhibition
E2F1/DP1 complex	*CDK1 (p34)*	Transcription regulation	Activation
Tcf(Lef)	*Tenascin-C*	Transcription regulation	Activation
Cyclin D1	*Androgen receptor*	Binding	Inhibition
SMAD3	*TERT*	Transcription regulation	Inhibition
Tcf(Lef)	*Androgen receptor*	Transcription regulation	Activation
STAT3	*LDHA*	Transcription regulation	Activation
ESR1 (nuclear)	*D53*	Transcription regulation	Activation

Beta-catenin	*TCF8*	co-regulation of transcription	Activation
SMAD3	*SLC25A5*	Transcription regulation	Inhibition
RXRA	*EGFR*	Transcription regulation	Inhibition
STAT3	*SMAD3*	Transcription regulation	Inhibition
Beta-catenin	*AKT2*	co-regulation of transcription	Activation
STAT3	*p21*	Transcription regulation	Activation
ESR1 (nuclear)	*FLJ20366*	Transcription regulation	Activation
Coumestrol intracellular	*AKT1*	Binding	Inhibition
SOX9	*HNF1-beta*	Transcription regulation	Inhibition
CDK6	*Beta-catenin*	Phosphorylation	Inhibition
RXRA	*CD36*	Transcription regulation	Activation
Rb protein	*Androgen receptor*	Binding	Activation
AKT(PKB)	*ESR1 (nuclear)*	Phosphorylation	Activation
ESR1 (nuclear)	*GSK3 beta*	Transcription regulation	Activation
AKT1	*Beta-catenin*	Binding	Inhibition
STAT3	*STAT3*	Binding	Activation
ESR1 (nuclear)	*SLC38A2*	Transcription regulation	Activation
CDK1 (p34)	*Androgen receptor*	Phosphorylation	Activation
CDC20	*p21*	Binding	Inhibition
SMAD3	*5'-NTD*	Transcription regulation	Activation
Nek2A	*Beta-catenin*	Phosphorylation	Activation
AKT2	*p21*	Binding	Activation
EGFR	*STAT3*	Phosphorylation	Activation
ESR1 (nuclear)	*ABCG2*	Transcription regulation	Activation
Cyclin D1	*ESR1 (nuclear)*	Binding	Activation
SOX9	*ABCG2*	Transcription regulation	Activation
EGFR	*ESR1 (nuclear)*	Phosphorylation	Activation
TCF8	*Androgen receptor*	Transcription regulation	Activation
HNF1-beta	*SERPINA6*	Transcription regulation	Activation
Beta-catenin	*STAT3*	co-regulation of transcription	Activation
E2F1	*ACKR3*	Transcription regulation	Inhibition
ESR1 (nuclear)	*AKT2*	Transcription regulation	Activation
ESR1 (nuclear)	*AACS*	Transcription regulation	Inhibition
Androgen receptor	*CCRK*	Transcription regulation	Activation
BI-2536 extracellular region	*EGFR*	Binding	Inhibition
Rb protein	*STAT3*	Binding	Inhibition
Coumestrol intracellular	*ACK1*	Binding	Inhibition

AKT(PKB)	Androgen receptor	Phosphorylation	Inhibition
ABCG2	BI-2536 + ATP + H(.2)O = BI-2536 + ADP + PO(.4)('3-)	Transport catalysis	Activation
SOX9	*VNN1*	Transcription regulation	Activation
GSK3 beta	*STAT3*	Binding	Activation
ESR1 (nuclear)	*E2F1*	Transcription regulation	Activation
Androgen receptor	*Cyclin D1*	Transcription regulation	Inhibition
EGFR	*Cyclin D1*	Transcription regulation	Activation
GSK3 beta	*KLF6*	Phosphorylation	Activation
AKT1	*GSK3 beta*	Phosphorylation	Inhibition
EGFR	*E2F1*	Binding	Activation
p21	*CDK1 (p34)*	Binding	Inhibition
Tcf(Lef)	*Cyclin D1*	Transcription regulation	Activation
STAT3	*SOX9*	Transcription regulation	Activation
ESR1 (nuclear)	*ACOX2*	Transcription regulation	Activation
T3Rbeta/RXR-alpha	*SREBP2 precursor*	Transcription regulation	Activation
STAT3	*ESR1 (nuclear)*	Binding	Activation
ESR1 (nuclear)	*ACKR3*	Transcription regulation	Inhibition
STAT3	*GSK3 beta*	Transcription regulation	Inhibition
AKT1	*p21*	Phosphorylation	Activation
ACK1	*AKT(PKB)*	Phosphorylation	Activation
E2F1	*ABCG2*	Transcription regulation	Activation
EGFR	*EGFR*	Phosphorylation	Activation
GSK3 beta	*p21*	Phosphorylation	Inhibition
Androgen receptor	*ACKR3*	Transcription regulation	Inhibition
ESR1 (nuclear)	*STAT3*	Transcription regulation	Activation
E2F1	*TERT*	Transcription regulation	Activation
E2F1	*Androgen receptor*	Transcription regulation	Inhibition
E2F1	*Nek2A*	Transcription regulation	Activation
Androgen receptor	*p21*	Transcription regulation	Activation
SMAD3	*CDK4*	Transcription regulation	Activation
AKT(PKB)	*Beta-catenin*	Phosphorylation	Activation
SOX9	*SOX9*	Transcription regulation	Activation
Coumestrol intracellular	*CDK1 (p34)*	Binding	Inhibition
Rb protein	*E2F1*	Binding	Inhibition
Cyclin D1	*CDK4*	Binding	Activation
GSK3 beta	*SMAD3*	Phosphorylation	Inhibition
SMAD3	*Beta-catenin*	Binding	Activation

Rb protein	*TCF8*	co-regulation of transcription	Inhibition
SMAD3	*p21*	Transcription regulation	Activation
ATP cytoplasm	BI-2536 + ATP + H(.2)O = BI-2536 + ADP + PO(.4)('3-)	Technical	Technical
SMAD3	*SOX9*	Binding	Activation
E2F1	*EGFR*	Transcription regulation	Activation
ESR1 (nuclear)	*Cyclin D1*	co-regulation of transcription	Activation
SREBP2 precursor	*AACS*	Transcription regulation	Activation
TCF8	*SREBP2 precursor*	Transcription regulation	Inhibition
Androgen receptor	*EGFR*	Binding	Inhibition
E2F1	*Rb protein*	Transcription regulation	Activation
Rociletinib extracellular region	*EGFR*	Covalent modification	Inhibition
EGFR	*ABCG2*	co-regulation of transcription	Activation
BI-2536 + ATP + H(.2)O = BI-2536 + ADP + PO(.4)('3-)	ADP cytoplasm	Technical	Technical
Coumestrol intracellular	AKT3	Binding	Inhibition
SOX9	*RXRA*	Transcription regulation	Activation
RXRA	*Nek2A*	Transcription regulation	Activation
SOX9	*KLF6*	Transcription regulation	Activation
Beta-catenin	*Cyclin D1*	co-regulation of transcription	Activation
STAT3	*Androgen receptor*	Binding	Activation
E2F1	*TCF8*	Transcription regulation	Activation
SMAD3	*TMEFF1*	Transcription regulation	Activation
p21	*TCF8*	Binding	Inhibition
CDK6	*Androgen receptor*	Binding	Activation
Androgen receptor	*Beta-catenin*	Binding	Activation
ESR1 (nuclear)	*NEDD4L*	Transcription regulation	Inhibition
CDK4	*p21*	Binding	Inhibition
CDK1 (p34)	*Rb protein*	Phosphorylation	Inhibition
BI-2536 + ATP + H(.2)O = BI-2536 + ADP + PO(.4)('3-)	PO(.4)('3-) cytoplasm	Technical	Technical
Tcf(Lef)	*AKT1*	Transcription regulation	Activation
Coumestrol intracellular	*AKT2*	Binding	Inhibition
CDK1 (p34)	*CDC20*	Phosphorylation	Activation
Androgen receptor	*LDHA*	Transcription regulation	Activation
ESR1 (nuclear)	*ESR1 (nuclear)*	Transcription regulation	Activation
GSK3 beta	*Beta-catenin*	Phosphorylation	Inhibition
STAT3	*EGFR*	Transcription regulation	Inhibition
Androgen receptor	*AKT1*	Transcription regulation	Activation
Coumestrol + H(.2)O + ATP = PO(.4)('3-) + Coumestrol +	ADP cytoplasm	Technical	Technical

ADP			
CDK1 (p34)	*STAT3*	Phosphorylation	Inhibition
KLF6	*Cyclin D1*	Binding	Inhibition
RXRA	*GSK3 beta*	Binding	Inhibition
ESR1 (nuclear)	*LDHA*	Transcription regulation	Activation
RXRA	*CYP2B6*	Transcription regulation	Activation
Beta-catenin	*AKT1*	co-regulation of transcription	Activation
E2F1	*Beta-catenin*	Transcription regulation	Inhibition
p21	*E2F1*	Binding	Inhibition

APPENDIX C: SUPPLEMENTARY FILE
CHAPTER 4.

Table S1: Number of reads (*paired-end*) mapped in skeletal muscle and liver of pigs fed diets containing different oils (CO: canola oil 3%. SOY: soybean oil 3% and FO: fish oil 3%)

Samples (liver - CO)	Reads strandR1	Reads strandR2	Total reads	Trimmed readsR1	Trimmed readsR2	Total trimmed	unmapped (%)	multimapping (%)	noFeature (%)	ambiguous (%)
L2	22625726	22625726	45251452	22354833	22354833	44709666	1.47	11.99	8.22	6
L8	18550315	18550315	37100630	18347029	18347029	36694058	1.58	12.44	7.6	5.43
L9	13078142	13078142	26156284	12868810	12868810	25737620	6.85	15.75	5.88	7.07
L22	18727373	18727373	37454746	18476423	18476423	36952846	2.76	26.87	12.3	5
L24	21018509	21018509	42037018	20686969	20686969	41373938	2.62	16.94	8.54	5.52
L25	19481986	19481986	38963972	19207823	19207823	38415646	1.89	16.08	8.24	6.23
L39	15907071	15907071	31814142	15667843	15667843	31335686	2.51	13.74	7.41	5.77
L42	15106809	15106809	30213618	14853422	14853422	29706844	2.46	14.02	7.99	5.63
L44	14964925	14964925	29929850	14782639	14782639	29565278	1.95	13.15	7.69	6.05
L45	17147814	17147814	34295628	16936403	16936403	33872806	2.22	14.49	7.63	6.31
L50	15713304	15713304	31426608	15539525	15539525	31079050	1.74	14.28	8.53	5.93
L52	19119724	19119724	38239448	18847537	18847537	37695074	2.82	20.57	10.06	5.3
L58	15347709	15347709	30695418	15116354	15116354	30232708	2.48	15.37	9.5	5.66
L60	17303553	17303553	34607106	17087712	17087712	34175424	3.54	17.93	7.54	5.85
L64	17348463	17348463	34696926	17139807	17139807	34279614	2.26	13.22	8.16	5.41
L65	17104075	17104075	34208150	16912694	16912694	33825388	2.41	14.57	8.83	5.51
L67	18340432	18340432	36680864	18145135	18145135	36290270	2.17	14.45	8.83	6.03
L71	19927232	19927232	39854464	19659629	19659629	39319258	2.73	15.5	8.43	5.73
Total	316813162	316813162	633626324	312630587	312630587	625261174	-	-	-	-
Average	17600731	17600731	**35201462**	17368366	17368366	**34736732**	-	-	-	-

ummapped	7845556		
uniquely mapped	255720793		
% mapped	97.49	**% uniquely mapped**	81.8

Samples (liver - SOY)	Reads strandR1	Reads strandR2	Total reads	Trimmed readsR1	Trimmed readsR2	Total trimmed	unmapped (%)	multimapping (%)	noFeature (%)	ambiguous (%)
L3	17396801	17396801	34793602	17189863	17189863	34379726	1.46	9.4	6.87	6.15
L10	20704172	20704172	41408344	20449667	20449667	40899334	2.68	10.03	8.13	5.71
L11	15858812	15858812	31717624	15683401	15683401	31366802	1.87	13.15	6.65	5.94
L12	17957727	17957727	35915454	17714575	17714575	35429150	1.84	11.79	8.07	5.94
L18	16192070	16192070	32384140	15975133	15975133	31950266	2.72	16.35	8.33	6.51
L19	15751527	15751527	31503054	15526082	15526082	31052164	2.56	14.23	8.24	5.38
L26	16829185	16829185	33658370	16590646	16590646	33181292	2.24	14.84	7.7	6.2
L46	15265575	15265575	30531150	15009755	15009755	30019510	2.72	47.27	20.6	2.34
L53	14581821	14581821	29163642	14334854	14334854	28669708	2.64	21.17	9.94	6.03
L54	15593189	15593189	31186378	15384127	15384127	30768254	2.39	21.97	11.33	5.52
L55	18872901	18872901	37745802	18594669	18594669	37189338	2.51	17.98	9.45	5.48
L59	16293809	16293809	32587618	16054665	16054665	32109330	3.51	14.36	7.84	6.12
L61	16259565	16259565	32519130	15989887	15989887	31979774	2.91	50.46	20.61	2.2
L63	17530152	17530152	35060304	17310788	17310788	34621576	2.24	13.66	8.79	5.69
L68	18432836	18432836	36865672	18212361	18212361	36424722	2.33	22.78	10.58	5.3
L69	16561309	16561309	33122618	16355205	16355205	32710410	2.22	9.32	7.58	6.03
L70	17487210	17487210	34974420	17248945	17248945	34497890	2.96	17.34	8.84	5.13
L72	19141470	19141470	38282940	18873100	18873100	37746200	2.76	19.24	7.55	6.2
Total	306710131	306710131	613420262	302497723	302497723	604995446	-	-	-	-
Average	17039452	17039452	**34078903**	16805429	16805429	**33610858**	-	-	-	-
uniquely mapped	238028576									
% mapped	97.53									
% uniquely mapped	78.69									

Samples (muscle - CO)	Reads strandR1	Reads strandR2	Total reads	Trimmed readsR1	Trimmed readsR2	Total trimmed	unmapped (%)	multimapping (%)	noFeature (%)	ambiguous (%)
M2	17364843	17364843	34729686	16946235	16946235	33892470	2.12	2.82	10.28	7.56
M8	15199392	15199392	30398784	14962682	14962682	29925364	2.51	2.91	9.98	6.75
M9	15926565	15926565	31853130	15667645	15667645	31335290	2.67	2.95	8.36	7.91
M22	14082826	14082826	28165652	13904217	13904217	27808434	02.04	2.70	8.96	10.14
M24	17749077	17749077	35498154	17503812	17503812	35007624	1.44	3.15	9.37	10.42
M25	20402809	20402809	40805618	20128969	20128969	40257938	1.54	3.52	8.80	9.88
M39	16126360	16126360	32252720	15900769	15900769	31801538	2.83	3.15	9.32	8.48
M42	14685159	14685159	29370318	14474862	14474862	28949724	3.28	3.20	9.45	9.33
M44	15013989	15013989	30027978	14804781	14804781	29609562	3.18	2.88	10.98	8.58
M45	15638921	15638921	31277842	15394496	15394496	30788992	3.39	2.76	07.06	10.09
M50	17241661	17241661	34483322	16985985	16985985	33971970	2.88	2.71	10.46	7.82
M52	19645444	19645444	39290888	19371560	19371560	38743120	3.30	24.05	15.41	5.39
M58	15856234	15856234	31712468	15668613	15668613	31337226	3.83	2.76	8.92	7.47
M60	16839671	16839671	33679342	16626647	16626647	33253294	3.46	3.58	8.85	6.20
M64	19147912	19147912	38295824	18856580	18856580	37713160	4.17	2.71	11.00	08.01
M65	17786051	17786051	35572102	17549907	17549907	35099814	3.87	2.55	9.89	8.12
M67	17219806	17219806	34439612	17037421	17037421	34074842	03.03	3.10	10.28	7.24
M71	16185373	16185373	32370746	15985165	15985165	31970330	2.48	2.97	11.62	6.56
Total	302112093	302112093	604224186	297770346	297770346	595540692	-	-	-	-
Average	16784005	16784005	**33568010**	16542797	16542797	**33085594**	-	-	-	-
ummapped	8598753									
uniquely mapped	276239866									
% mapped	97.11									
% uniquely mapped	92.77									

Samples (muscle - SOY)	Reads strandR1	Reads strandR2	Total reads	Trimmed readsR1	Trimmed readsR2	Total trimmed	unmapped (%)	multimapping (%)	noFeature (%)	ambiguous (%)
M3	15646435	15646435	31292870	15396193	15396193	30792386	4.22	2.9	9.46	6.77
M10	13575043	13575043	27150086	13337731	13337731	26675462	2.29	2.8	13.14	6.46
M11	14777149	14777149	29554298	14513593	14513593	29027186	2.49	2.25	13.31	4.62
M12	16505168	16505168	33010336	16114942	16114942	32229884	2.6	2.75	8.2	8.91
M18	15403431	15403431	30806862	15179363	15179363	30358726	2.15	2.79	10.35	7.31
M19	14791761	14791761	29583522	14615040	14615040	29230080	3.16	2.7	11.68	7.85
M26	18888244	18888244	37776488	18587847	18587847	37175694	2.37	3.01	9.34	7.54
M46	14178120	14178120	28356240	14002783	14002783	28005566	1.67	2.17	13.98	5.14
M53	17380539	17380539	34761078	17151536	17151536	34303072	4.17	2.71	8.78	8.43
M54	17007569	17007569	34015138	16748500	16748500	33497000	3.78	3.09	10.33	7.87
M55	16423107	16423107	32846214	16211289	16211289	32422578	3.97	2.97	11.18	6.31
M59	15764683	15764683	31529366	15577575	15577575	31155150	2.89	3	8.85	6.94
M61	15556503	15556503	31113006	15332622	15332622	30665244	2.58	3.02	8.73	7.34
M63	16554614	16554614	33109228	16359501	16359501	32719002	3.09	2.71	6.96	8.57
M68	16181956	16181956	32363912	15955270	15955270	31910540	3.93	2.82	9.93	7.56
M69	16575604	16575604	33151208	16368158	16368158	32736316	3.01	2.61	9.86	7.59
M70	15648586	15648586	31297172	15462025	15462025	30924050	3.08	2.72	9.56	7.54
M72	16742006	16742006	33484012	16507152	16507152	33014304	3.44	2.82	9.73	7.81
Total	287600518	287600518	575201036	283421120	283421120	566842240	-	-	-	-
Average	15977807	15977807	**31955613**	15745618	15745618	**31491236**	-	-	-	-
mapped pairs	274717524									
uniquely mapped	266846154									
% mapped	96.93									
% uniquely mapped	94.15									

Samples (muscle - FO)	Reads strandR1	Reads strandR2	Total reads	Trimmed readsR1	Trimmed readsR2	Total trimmed	unmapped (%)	multimapping (%)	noFeature (%)	ambiguous (%)
M1	15998768	15998768	31997536	15638889	15638889	31277778	3.45	13.58	12.64	7.11
M5	17281531	17281531	34563062	17007517	17007517	34015034	03.05	2.37	13.49	5.30
M6	15538234	15538234	31076468	15239875	15239875	30479750	3.10	2.60	10.82	7.61
M15	14844386	14844386	29688772	14636260	14636260	29272520	2.53	2.69	11.20	7.21
M17	16392665	16392665	32785330	16202718	16202718	32405436	2.25	2.91	8.19	09.01
M20	16169941	16169941	32339882	15967385	15967385	31934770	2.37	2.58	14.36	5.26
M21	15005312	15005312	30010624	14811046	14811046	29622092	2.14	2.86	8.42	8.26
M23	16091446	16091446	32182892	15821624	15821624	31643248	3.25	2.82	08.07	10.61
M27	17787378	17787378	35574756	17535176	17535176	35070352	04.07	2.92	9.46	9.85
M29	21298897	21298897	42597794	21000833	21000833	42001666	4.20	03.02	9.86	6.28
M30	17825008	17825008	35650016	17532672	17532672	35065344	3.41	2.69	8.50	7.55
M31	18414810	18414810	36829620	18170684	18170684	36341368	3.30	2.63	14.98	5.71
M36	20797946	20797946	41595892	20529438	20529438	41058876	02.08	28.58	12.32	7.62
M38	16274958	16274958	32549916	16033199	16033199	32066398	2.94	3.30	8.22	7.85
M40	16747805	16747805	33495610	16506746	16506746	33013492	3.14	3.57	10.18	8.70
M48	13943169	13943169	27886338	13743287	13743287	27486574	03.09	2.70	14.37	5.51
M51	17057384	17057384	34114768	16827294	16827294	33654588	3.59	3.18	11.80	6.37
M57	17594247	17594247	35188494	17333194	17333194	34666388	3.33	2.90	9.78	6.71
Total	305063885	305063885	610127770	300537837	300537837	601075674	-	-	-	-
Average	16947994	16947994	**33895987**	16696547	16696547	**33393094**	-	-	-	-
ummapped	9293031									
uniquely mapped	275681351									
% mapped	96.91									
% uniquely mapped	91.73									

Samples (liver - FO)	Reads strandR1	Reads strandR2	Total reads	Trimmed readsR1	Trimmed reads2	Total trimmed	unmapped (%)	multimapping (%)	noFeature (%)	ambiguous (%)
L1	19949276	19949276	39898552	19701399	19701399	39402798	1.57	13.59	7.45	5.44
L5	17339439	17339439	34678878	17148130	17148130	34296260	1.48	11.23	7.76	6.35
L6	19414010	19414010	38828020	19187001	19187001	38374002	1.68	12.88	7.2	6.25
L15	16412046	16412046	32824092	16124060	16124060	32248120	3.03	11.94	6.72	5.95
L17	18290950	18290950	36581900	18070704	18070704	36141408	1.94	12.25	7.12	5.56
L20	18046573	18046573	36093146	17796077	17796077	35592154	2.77	11.76	7.98	5.77
L21	16976030	16976030	33952060	16724615	16724615	33449230	3.1	17.01	8.2	5.53
L23	16786868	16786868	33573736	16554651	16554651	33109302	2.72	18.58	8.49	5.66
L27	15501149	15501149	31002298	14976081	14976081	29952162	29.32	28.27	9.79	2.99
L29	18160475	18160475	36320950	17939448	17939448	35878896	2.28	12.62	7.4	5.8
L30	15871818	15871818	31743636	15637103	15637103	31274206	2.74	17.93	8.43	5.18
L31	16291833	16291833	32583666	16095109	16095109	32190218	2.3	10.9	8.27	5.96
L36	16700327	16700327	33400654	16489692	16489692	32979384	1.75	14.01	7.48	6.04
L38	15994395	15994395	31988790	15804552	15804552	31609104	1.68	13.73	7.91	6.47
L40	17437577	17437577	34875154	17123355	17123355	34246710	5.86	42.32	13.99	3.81
L48	15919420	15919420	31838840	15758525	15758525	31517050	1.47	13.51	6.24	6.91
L51	14367847	14367847	28735694	14149134	14149134	28298268	3.16	20.28	9.71	5.63
L57	19209410	19209410	38418820	18937596	18937596	37875192	2.78	16.36	8.52	5.88
Total	308669443	308669443	617338886	304217232	304217232	608434464	-	-	-	-
Average	17148302	17148302	**34296605**	16900957	16900957	**33801914**	-	-	-	-
mapped pairs	292669964									
uniquely mapped	242559550									
% mapped	96.2									
% uniquely mapped	79.73									

Table S2. Differently expressed genes of liver from immunocastrated male pigs fed diets containing different oils (Soybean Oil: SOY: 3.0%; Canola Oil: CO 3.0% Fisha Oil: FO: 3.0%).

Diet_comparison Muscle	Gene stable ID	Gene name	Gene description	log2 fold change	p-value	FDR
COvsSOY	ENSSSCG00000051166	*0*	0	-5.557956957	4.56E-10	7.20E-06
COvsSOY	ENSSSCG00000051302	*0*	0	-3.586988916	0.0001990215249	0.07134017024
COvsSOY	ENSSSCG00000017884	*TEKT1*	tektin 1 [Source:VGNC Symbol;Acc:VGNC:93867]	-2.660856482	8.55E-08	0.000272182461
COvsSOY	ENSSSCG00000051026	*0*	0	-2.433004063	1.55E-05	0.01284810193
COvsSOY	ENSSSCG00000010300	*MSS51*	MSS51 mitochondrial translational activator [Source:VGNC Symbol;Acc:VGNC:90428]	-2.195898443	5.96E-05	0.03473999991
COvsSOY	ENSSSCG00000012724	*SLITRK2*	SLIT and NTRK like family member 2 [Source:VGNC Symbol;Acc:VGNC:93207]	-2.127065866	0.0002036444356	0.07137511195
COvsSOY	ENSSSCG00000018044	*ALDH3A1*	aldehyde dehydrogenase 3 family member A1 [Source:VGNC Symbol;Acc:VGNC:85238]	-2.014610448	8.66E-08	0.000272182461
COvsSOY	ENSSSCG00000015726	*CNTNAP5*	contactin associated protein family member 5 [Source:VGNC Symbol;Acc:VGNC:95459]	-1.967061061	0.0002241562129	0.07363525723
COvsSOY	ENSSSCG00000005740	*SARDH*	sarcosine dehydrogenase [Source:VGNC Symbol;Acc:VGNC:92581]	-1.830622276	0.0002678187682	0.0767648501
COvsSOY	ENSSSCG00000045021	*0*	0	-1.779226119	0.0001844323712	0.0676480781
COvsSOY	ENSSSCG00000050531	*0*	0	-1.758996774	0.0002765519395	0.0767648501
COvsSOY	ENSSSCG00000022842	*0*	0	-1.732413387	5.31E-05	0.03348552298
COvsSOY	ENSSSCG00000022091	*SLITRK4*	SLIT and NTRK like family member 4 [Source:VGNC Symbol;Acc:VGNC:93209]	-1.628393671	0.0003512358815	0.08934987618
COvsSOY	ENSSSCG00000034866	*Novel gene*	transforming acidic coiled-coil-containing protein 1 [Source:NCBI gene (formerly Entrezgene);Acc:106506226]	-1.572733453	0.0002287679181	0.07363525723
COvsSOY	ENSSSCG00000000687	*CD4*	CD4 molecule [Source:VGNC Symbol;Acc:VGNC:86417]	-1.551331865	2.10E-06	0.003308761837
COvsSOY	ENSSSCG00000051428	*0*	0	-1.440741182	0.00033226303	0.08734087516
COvsSOY	ENSSSCG00000018042	*SLC47A2*	solute carrier family 47 member 2 [Source:VGNC Symbol;Acc:VGNC:99044]	-1.412610567	0.0002633668848	0.0767648501
COvsSOY	ENSSSCG00000003148	*DBP*	D-box binding PAR bZIP transcription factor [Source:VGNC Symbol;Acc:VGNC:87167]	-1.38984798	1.35E-05	0.01233598004
COvsSOY	ENSSSCG00000037534	*OPCML*	opioid binding protein/cell adhesion molecule like [Source:VGNC Symbol;Acc:VGNC:91047]	-1.3530521	0.0001630259132	0.06358185126

COvsSOY	ENSSSCG00000000795	*ADAMTS20*	ADAM metallopeptidase with thrombospondin type 1 motif 20 [Source:VGNC Symbol;Acc:VGNC:85082]	-1.295134688	0.000132682389	0.05812962886
COvsSOY	ENSSSCG00000006035	*ANGPT1*	angiopoietin 1 [Source:VGNC Symbol;Acc:VGNC:98732]	-1.22349093	0.0001249408999	0.05630193923
COvsSOY	ENSSSCG00000007235	*TPX2*	TPX2 microtubule nucleation factor [Source:VGNC Symbol;Acc:VGNC:95559]	-1.139824717	1.41E-05	0.01233598004
COvsSOY	ENSSSCG00000017109	*ADAMTS16*	ADAM metallopeptidase with thrombospondin type 1 motif 16 [Source:VGNC Symbol;Acc:VGNC:85078]	-1.119854853	0.00022629014	0.07363525723
COvsSOY	ENSSSCG00000001612	*Novel gene*	adenylate cyclase type 10 [Source:NCBI gene (formerly Entrezgene);Acc:100737927]	-1.112358295	0.0003075344986	0.08304187449
COvsSOY	ENSSSCG00000041411	*0*	0	-1.109813724	0.0002219546493	0.07363525723
COvsSOY	ENSSSCG00000007033	*AP3M2*	adaptor related protein complex 3 subunit mu 2 [Source:VGNC Symbol;Acc:VGNC:96369]	-1.088406134	2.67E-06	0.003834859366
COvsSOY	ENSSSCG00000040956	*0*	0	-1.081949507	2.98E-05	0.02114681315
COvsSOY	ENSSSCG00000014908	*CCDC89*	coiled-coil domain containing 89 [Source:VGNC Symbol;Acc:VGNC:86326]	-0.9500174139	0.0003457290503	0.08934987618
COvsSOY	ENSSSCG00000036454	*TMEM220*	transmembrane protein 220 [Source:VGNC Symbol;Acc:VGNC:94142]	-0.9388887915	0.0001720402066	0.06460519379
COvsSOY	ENSSSCG00000027093	*FOLH1B*	folate hydrolase 1B [Source:NCBI gene (formerly Entrezgene);Acc:397677]	-0.8696040607	7.81E-06	0.008795853327
COvsSOY	ENSSSCG00000009523	*Novel gene*	gamma-glutamylamine cyclotransferase [Source:VGNC Symbol;Acc:VGNC:88434]	-0.8017532098	0.000120842837	0.05605685955
COvsSOY	ENSSSCG00000018041	*ALDH3A2*	aldehyde dehydrogenase 3 family member A2 [Source:VGNC Symbol;Acc:VGNC:85239]	-0.7919963645	1.04E-07	0.000272182461
COvsSOY	ENSSSCG00000016164	*IKZF2*	IKAROS family zinc finger 2 [Source:VGNC Symbol;Acc:VGNC:95576]	-0.7681310818	1.09E-06	0.001917286295
COvsSOY	ENSSSCG00000017128	*Novel gene*	hexosaminidase D [Source:VGNC Symbol;Acc:VGNC:99001]	-0.6586778796	0.0001406330955	0.05994770761
COvsSOY	ENSSSCG00000003815	*ALG6*	ALG6 alpha-1.3-glucosyltransferase [Source:VGNC Symbol;Acc:VGNC:85253]	-0.6216957707	5.94E-05	0.03473999991
COvsSOY	ENSSSCG00000025130	*KLF12*	Kruppel like factor 12 [Source:VGNC Symbol;Acc:VGNC:89492]	-0.5920566198	0.0001178645083	0.05605685955
COvsSOY	ENSSSCG00000004859	*ZNF516*	zinc finger protein 516 [Source:VGNC Symbol;Acc:VGNC:95256]	-0.5527617769	4.07E-05	0.02672583573
COvsSOY	ENSSSCG00000015798	*ANKRD37*	ankyrin repeat domain 37 [Source:VGNC Symbol;Acc:VGNC:96223]	-0.4855811898	0.0003690578141	0.09239333085
COvsSOY	ENSSSCG00000011157	*PITRM1*	pitrilysin metallopeptidase 1 [Source:VGNC Symbol;Acc:VGNC:95855]	-	0.0001590699886	0.06358185126

				0.4545092336		
COvsSOY	ENSSSCG00000004996	*KLHL28*	kelch like family member 28 [Source:VGNC Symbol;Acc:VGNC:89523]	-0.4436486819	1.13E-05	0.01184420241
COvsSOY	ENSSSCG00000009021	*LRBA*	LPS responsive beige-like anchor protein [Source:VGNC Symbol;Acc:VGNC:98074]	-0.4226228222	0.000154826099	0.06358185126
COvsSOY	ENSSSCG00000014903	*CCDC90B*	coiled-coil domain containing 90B [Source:VGNC Symbol;Acc:VGNC:86328]	-0.3938304294	3.11E-06	0.004093171178
COvsSOY	ENSSSCG00000001074	*KDM1B*	lysine demethylase 1B [Source:VGNC Symbol;Acc:VGNC:89409]	-0.3910347611	6.55E-05	0.03473999991
COvsSOY	ENSSSCG00000034450	*ABHD10*	abhydrolase domain containing 10. depalmitoylase [Source:VGNC Symbol;Acc:VGNC:84969]	-0.3774574955	0.0002711961697	0.0767648501
COvsSOY	ENSSSCG00000004963	*Novel gene*	acidic nuclear phosphoprotein 32 family member A [Source:NCBI gene (formerly Entrezgene);Acc:100155298]	-0.3324796963	6.18E-05	0.03473999991
COvsSOY	ENSSSCG00000027293	*TNPO1*	transportin 1 [Source:VGNC Symbol;Acc:VGNC:94287]	-0.3216982197	0.0004120032986	0.09997101577
COvsSOY	ENSSSCG00000038329	*PIGK*	phosphatidylinositol glycan anchor biosynthesis class K [Source:VGNC Symbol;Acc:VGNC:98194]	-0.2909184568	0.0003106435832	0.08304187449
COvsSOY	ENSSSCG00000027389	*HERPUD2*	HERPUD family member 2 [Source:VGNC Symbol;Acc:VGNC:88853]	0.2212253704	0.0002444616087	0.0767648501
COvsSOY	ENSSSCG00000008678	*SLBP*	transmembrane protein 129. E3 ubiquitin ligase [Source:VGNC Symbol;Acc:VGNC:94076]	0.3080526023	0.0001189661213	0.05605685955
COvsSOY	ENSSSCG00000031532	*GBGT1*	globoside alpha-1.3-N-acetylgalactosaminyltransferase 1 (FORS blood group) [Source:NCBI gene (formerly Entrezgene);Acc:110256486]	0.3731168115	0.000264089364	0.0767648501
COvsSOY	ENSSSCG00000040740	*Novel gene*	chromosome 14 C22orf39 homolog [Source:NCBI gene (formerly Entrezgene);Acc:100154344]	0.5272156562	0.0002711852065	0.0767648501
COvsSOY	ENSSSCG00000038829	*Novel gene*	putative MORF4 family-associated protein 1-like protein UPP [Source:NCBI gene (formerly Entrezgene);Acc:100621428]	0.6672219249	2.63E-05	0.01978916165
COvsSOY	ENSSSCG00000016334	*SCLY*	selenocysteine lyase [Source:VGNC Symbol;Acc:VGNC:98302]	0.9087373147	6.83E-05	0.03473999991
COvsSOY	ENSSSCG00000006761	*DCLRE1B*	DNA cross-link repair 1B [Source:VGNC Symbol;Acc:VGNC:87186]	1.005942004	6.63E-05	0.03473999991
COvsSOY	ENSSSCG00000010210	*SLC16A9*	solute carrier family 16 member 9 [Source:VGNC Symbol;Acc:VGNC:92949]	1.105107927	1.30E-05	0.01233598004
COvsSOY	ENSSSCG00000009578	*Novel gene*	cyclin dependent kinase 20 [Source:NCBI gene (formerly Entrezgene);Acc:100157041]	1.171261119	5.58E-08	0.000272182461
COvsSOY	ENSSSCG00000024892	*NSG1*	neuronal vesicle trafficking associated 1 [Source:VGNC Symbol;Acc:VGNC:90907]	1.285452398	2.32E-05	0.01831335243
COvsSOY	ENSSSCG00000032849	*MLPH*	melanophilin [Source:VGNC Symbol;Acc:VGNC:96225]	1.298926223	0.0001652837878	0.06358185126

COvsSOY	ENSSSCG00000011195	*GALNT15*	polypeptide N-acetylgalactosaminyltransferase 15 [Source:VGNC Symbol;Acc:VGNC:88331]	1.605055336	4.52E-07	0.001018682538
COvsSOY	ENSSSCG00000051557	*0*	0	1.732401329	5.97E-08	0.000272182461
COvsSOY	ENSSSCG00000033993	*PLCXD3*	phosphatidylinositol specific phospholipase C X domain containing 3 [Source:VGNC Symbol;Acc:VGNC:91524]	1.79533196	3.72E-06	0.004513179556
COvsSOY	ENSSSCG00000003565	*NR0B2*	nuclear receptor subfamily 0 group B member 2 [Source:VGNC Symbol;Acc:VGNC:90868]	2.14787518	0.0002774281293	0.0767648501
COvsSOY	ENSSSCG00000009182	*ADH1C*	alcohol dehydrogenase 1C (class I). gamma polypeptide [Source:NCBI gene (formerly Entrezgene);Acc:100512615]	2.339575371	3.08E-05	0.02114681315
COvsSOY	ENSSSCG00000044549	*0*	0	2.911745277	0.0004086149822	0.09997101577
COvsSOY	ENSSSCG00000049049	*0*	0	3.069822416	6.38E-07	0.00125777602

Diet_comparison Muscle	**Gene stable ID**	***Gene name***	**Gene description**	**log2 fold change**	**p-value**	**FDR**
SOYvsFO	ENSSSCG00000051166	*0*	0	-4.993630706	4.30E-09	5.61E-05
SOYvsFO	ENSSSCG00000003374	*ESPN*	espin [Source:VGNC Symbol;Acc:VGNC:97054]	-4.810388295	2.28E-06	0.002065883007
SOYvsFO	ENSSSCG00000012138	*ACE2*	angiotensin I converting enzyme 2 [Source:VGNC Symbol;Acc:VGNC:85008]	-4.33272784	7.66E-07	0.0008238380319
SOYvsFO	ENSSSCG00000006719	*Novel gene*	hydroxy-delta-5-steroid dehydrogenase. 3 beta- and steroid delta-isomerase 1 [Source:NCBI gene (formerly Entrezgene);Acc:445539]	-4.163738381	0.0001382955306	0.02032826099
SOYvsFO	ENSSSCG00000003894	*CYP4B1*	cytochrome P450 4B1 [Source:NCBI gene (formerly Entrezgene);Acc:100523909]	-4.140311833	1.10E-07	0.0002249582568
SOYvsFO	ENSSSCG00000032374	*SULT1B1*	sulfotransferase family cytosolic 1B member 1 [Source:NCBI gene (formerly Entrezgene);Acc:100624541]	-4.128554903	0.000358284527	0.0320795851
SOYvsFO	ENSSSCG00000046097	*0*	0	-4.071387042	6.46E-05	0.01310977365
SOYvsFO	ENSSSCG00000029744	*PLCH2*	phospholipase C eta 2 [Source:VGNC Symbol;Acc:VGNC:91522]	-4.06388246	0.0002854429563	0.02922052359
SOYvsFO	ENSSSCG00000005474	*SAL1*	salivary lipocalin [Source:NCBI gene (formerly Entrezgene);Acc:396739]	-4.032483887	3.10E-08	0.0001173311129
SOYvsFO	ENSSSCG00000015799	*KLKB1*	kallikrein B1 [Source:VGNC Symbol;Acc:VGNC:96397]	-3.826298711	0.00297991998	0.09873388783
SOYvsFO	ENSSSCG00000007642	*Novel gene*	alpha-2-glycoprotein 1. zinc-binding [Source:VGNC Symbol;Acc:VGNC:85710]	-3.784140337	5.54E-07	0.0006810923942
SOYvsFO	ENSSSCG00000028411	*MC5R*	melanocortin 5 receptor [Source:HGNC Symbol;Acc:HGNC:6933]	-3.746510304	0.001155396203	0.06028356025
SOYvsFO	ENSSSCG00000000577	*GYS2*	glycogen synthase 2 [Source:VGNC Symbol;Acc:VGNC:88761]	-3.672578092	8.31E-06	0.004025924256
SOYvsFO	ENSSSCG00000006245	*SDR16C5*	short chain dehydrogenase/reductase family 16C member 5 [Source:VGNC Symbol;Acc:VGNC:98853]	-3.622877301	1.44E-06	0.00138259839

SOYvsFO	ENSSSCG00000022258	*Novel gene*	antileukoproteinase [Source:NCBI gene (formerly Entrezgene);Acc:100512873]	-3.563162604	4.09E-08	0.0001173311129
SOYvsFO	ENSSSCG00000039985	*CES1*	liver carboxylesterase [Source:NCBI gene (formerly Entrezgene);Acc:100736962]	-3.55925038	4.56E-06	0.003014969705
SOYvsFO	ENSSSCG00000026718	*PLCH1*	phospholipase C eta 1 [Source:VGNC Symbol;Acc:VGNC:91521]	-3.550580742	0.0001562299523	0.02076808349
SOYvsFO	ENSSSCG00000038107	*Novel gene*	serine peptidase inhibitor Kazal type 2 [Source:NCBI gene (formerly Entrezgene);Acc:100520393]	-3.511692508	0.001498662613	0.0678263148
SOYvsFO	ENSSSCG00000014570	*NRIP3*	TMEM9 domain family member B [Source:NCBI gene (formerly Entrezgene);Acc:100519788]	-3.388386989	2.56E-06	0.002130424726
SOYvsFO	ENSSSCG00000014977	*PGR*	progesterone receptor [Source:VGNC Symbol;Acc:VGNC:91362]	-3.382677082	0.000193371002	0.02445290068
SOYvsFO	ENSSSCG00000021222	*Novel gene*	tryptase [Source:NCBI gene (formerly Entrezgene);Acc:397389]	-3.379574819	0.001706557118	0.07235403464
SOYvsFO	ENSSSCG00000022153	*SULT1C2*	sulfotransferase 1C2 [Source:NCBI gene (formerly Entrezgene);Acc:100623541]	-3.373859753	0.0002278741507	0.02620717765
SOYvsFO	ENSSSCG00000046536	*0*	0	-3.37274398	3.85E-05	0.00966181679
SOYvsFO	ENSSSCG00000051302	*0*	0	-3.361800487	0.0006579831345	0.04386044165
SOYvsFO	ENSSSCG00000040934	*ISX*	intestine specific homeobox [Source:VGNC Symbol;Acc:VGNC:96164]	-3.331173234	0.001831136151	0.07533942472
SOYvsFO	ENSSSCG00000038322	*Novel gene*	diacylglycerol O-acyltransferase 2-like [Source:NCBI gene (formerly Entrezgene);Acc:110259135]	-3.329791974	5.56E-05	0.01194883741
SOYvsFO	ENSSSCG00000048885	*0*	0	-3.297543569	6.71E-05	0.01310977365
SOYvsFO	ENSSSCG00000047413	*OTOS*	otospiralin [Source:NCBI gene (formerly Entrezgene);Acc:100525436]	-3.277561775	2.04E-08	0.0001171956594
SOYvsFO	ENSSSCG00000014426	*Novel gene*	serine protease inhibitor Kazal-type 9 [Source:NCBI gene (formerly Entrezgene);Acc:100513074]	-3.257066514	0.001745739869	0.07269548249
SOYvsFO	ENSSSCG00000008034	*NOXO1*	NADPH oxidase organizer 1 [Source:VGNC Symbol;Acc:VGNC:90834]	-3.250340179	2.86E-05	0.008490693145
SOYvsFO	ENSSSCG00000021241	*ADAMTS13*	ADAM metallopeptidase with thrombospondin type 1 motif 13 [Source:VGNC Symbol;Acc:VGNC:85075]	-3.219627142	3.88E-06	0.00267009565
SOYvsFO	ENSSSCG00000002803	*CCDC113*	coiled-coil domain containing 113 [Source:VGNC Symbol;Acc:VGNC:86247]	-3.208521927	0.0002610177077	0.02823259457
SOYvsFO	ENSSSCG00000033822	*THRSP*	thyroid hormone responsive [Source:NCBI gene (formerly Entrezgene);Acc:100512730]	-3.202338723	1.43E-05	0.005845002307
SOYvsFO	ENSSSCG00000027404	*UNC93A*	unc-93 homolog A [Source:VGNC Symbol;Acc:VGNC:94711]	-3.17937063	1.23E-05	0.005459864706
SOYvsFO	ENSSSCG00000007507	*PCK1*	phosphoenolpyruvate carboxykinase 1 [Source:VGNC Symbol;Acc:VGNC:96469]	-3.159226429	9.30E-05	0.0162119407
SOYvsFO	ENSSSCG00000007063	*ANKEF1*	ankyrin repeat and EF-hand domain containing 1 [Source:VGNC	-3.148121973	0.000668659126	0.04408662364

			Symbol;Acc:VGNC:95662]			
SOYvsFO	ENSSSCG00000039815	*Novel gene*	uncharacterized LOC100517809 [Source:NCBI gene (formerly Entrezgene);Acc:100517809]	-3.130808108	0.0001800891877	0.02326995716
SOYvsFO	ENSSSCG00000039103	*ADIPOQ*	adiponectin. C1Q and collagen domain containing [Source:VGNC Symbol;Acc:VGNC:85140]	-3.128104939	2.60E-06	0.002130424726
SOYvsFO	ENSSSCG00000002825	*Novel gene*	carboxylesterase 1 [Source:NCBI gene (formerly Entrezgene);Acc:397478]	-3.100789799	8.26E-06	0.004025924256
SOYvsFO	ENSSSCG00000009789	*HCAR1*	hydroxycarboxylic acid receptor 1 [Source:VGNC Symbol;Acc:VGNC:88797]	-3.090018238	1.96E-05	0.00662185122
SOYvsFO	ENSSSCG00000049501	*0*	0	-3.082152596	0.0005998568099	0.04150893779
SOYvsFO	ENSSSCG00000000151	*Novel gene*	apolipoprotein L6 [Source:NCBI gene (formerly Entrezgene);Acc:100518305]	-3.072528775	5.53E-05	0.01194883741
SOYvsFO	ENSSSCG00000024325	*SGK2*	serum/glucocorticoid regulated kinase 2 [Source:VGNC Symbol;Acc:VGNC:95597]	-3.041416366	5.67E-05	0.01204440753
SOYvsFO	ENSSSCG00000022568	*TMPRSS3*	transmembrane serine protease 3 [Source:VGNC Symbol;Acc:VGNC:94235]	-3.037935981	0.0001813102837	0.02326995716
SOYvsFO	ENSSSCG00000000892	*HAL*	histidine ammonia-lyase [Source:VGNC Symbol;Acc:VGNC:88775]	-3.037886677	0.002228444919	0.08404560463
SOYvsFO	ENSSSCG00000039644	*Novel gene*	transient receptor potential cation channel subfamily M member 5 [Source:NCBI gene (formerly Entrezgene);Acc:100533558]	-3.022784656	5.53E-07	0.0006810923942
SOYvsFO	ENSSSCG00000017522	*SP6*	Sp6 transcription factor [Source:VGNC Symbol;Acc:VGNC:93363]	-3.015005655	0.0003906621747	0.03309659153
SOYvsFO	ENSSSCG00000017086	*SLC36A2*	solute carrier family 36 member 2 [Source:VGNC Symbol;Acc:VGNC:93089]	-3.010212119	8.39E-06	0.004025924256
SOYvsFO	ENSSSCG00000001844	*PLIN1*	perilipin 1 [Source:VGNC Symbol;Acc:VGNC:91557]	-2.985904618	5.27E-06	0.00309956594
SOYvsFO	ENSSSCG00000038839	*TTC36*	tetratricopeptide repeat domain 36 [Source:VGNC Symbol;Acc:VGNC:94549]	-2.984454643	0.002554279961	0.08965001381
SOYvsFO	ENSSSCG00000032036	*0*	0	-2.982140318	0.0009061667514	0.05372335221
SOYvsFO	ENSSSCG00000049307	*0*	0	-2.974007672	0.0003393319428	0.03194691242
SOYvsFO	ENSSSCG00000047207	*0*	0	-2.969759667	0.001545067705	0.06927686309
SOYvsFO	ENSSSCG00000044047	*0*	0	-2.968886125	0.002016864721	0.08047804984
SOYvsFO	ENSSSCG00000006003	*MAL2*	mal. T cell differentiation protein 2 [Source:VGNC Symbol;Acc:VGNC:98818]	-2.94760268	6.19E-06	0.003434888406
SOYvsFO	ENSSSCG00000002990	*0*	0	-2.926485956	0.0004091327	0.03399161437
SOYvsFO	ENSSSCG00000040277	*0*	0	-2.908477765	0.000403950754	0.03388851252

SOYvsFO	ENSSSCG00000046768	*0*	0	-2.901603377	0.0009152626643	0.05390646336
SOYvsFO	ENSSSCG00000017470	*TNS4*	tensin 4 [Source:VGNC Symbol;Acc:VGNC:94297]	-2.899557932	0.0004085525058	0.03399161437
SOYvsFO	ENSSSCG00000015873	*ACVR1C*	activin A receptor type 1C [Source:VGNC Symbol;Acc:VGNC:95873]	-2.885168274	4.12E-05	0.009939015695
SOYvsFO	ENSSSCG00000013031	*KCNK4*	potassium two pore domain channel subfamily K member 4 [Source:VGNC Symbol;Acc:VGNC:89371]	-2.882637946	9.52E-05	0.0162119407
SOYvsFO	ENSSSCG00000031976	*ANKRD53*	ankyrin repeat domain 53 [Source:VGNC Symbol;Acc:VGNC:85343]	-2.882233323	0.0001207376853	0.01853970278
SOYvsFO	ENSSSCG00000049866	*0*	0	-2.878654326	2.15E-05	0.007113168151
SOYvsFO	ENSSSCG00000000781	*ABCD2*	ATP binding cassette subfamily D member 2 [Source:VGNC Symbol;Acc:VGNC:84962]	-2.874720248	2.80E-05	0.008448837776
SOYvsFO	ENSSSCG00000044466	*0*	0	-2.868249491	0.001725727074	0.07241648016
SOYvsFO	ENSSSCG00000040164	*Novel gene*	lipocalin 12 [Source:VGNC Symbol;Acc:VGNC:89660]	-2.859641207	0.00129587061	0.06316634762
SOYvsFO	ENSSSCG00000007346	*Novel gene*	adipogenin [Source:VGNC Symbol;Acc:VGNC:96182]	-2.824222108	3.93E-05	0.00966181679
SOYvsFO	ENSSSCG00000044197	*0*	0	-2.789448203	0.002990146551	0.09873388783
SOYvsFO	ENSSSCG00000017801	*0*	0	-2.782395804	1.82E-05	0.006467956366
SOYvsFO	ENSSSCG00000000893	*AMDHD1*	amidohydrolase domain containing 1 [Source:VGNC Symbol;Acc:VGNC:85275]	-2.770312704	1.74E-05	0.006467956366
SOYvsFO	ENSSSCG00000005852	*ENTPD8*	ectonucleoside triphosphate diphosphohydrolase 8 [Source:VGNC Symbol;Acc:VGNC:87717]	-2.742259134	0.0002560223698	0.02799032089
SOYvsFO	ENSSSCG00000002490	*GSC*	goosecoid homeobox [Source:VGNC Symbol;Acc:VGNC:88714]	-2.737004213	0.000442115463	0.03531648183
SOYvsFO	ENSSSCG00000013056	*LGALS12*	galectin 12 [Source:VGNC Symbol;Acc:VGNC:89692]	-2.672964863	6.78E-05	0.01310977365
SOYvsFO	ENSSSCG00000017498	*PPP1R1B*	protein phosphatase 1 regulatory inhibitor subunit 1B [Source:VGNC Symbol;Acc:VGNC:91728]	-2.657733243	7.69E-05	0.01407674647
SOYvsFO	ENSSSCG00000038215	*Novel gene*	collagen alpha-4(VI) chain-like [Source:NCBI gene (formerly Entrezgene);Acc:100517188]	-2.643051116	0.002426038987	0.08638306109
SOYvsFO	ENSSSCG00000021386	*PTGR1*	prostaglandin reductase 1 [Source:VGNC Symbol;Acc:VGNC:91957]	-2.632997029	2.75E-06	0.002148380002
SOYvsFO	ENSSSCG00000036261	*CROCC2*	ciliary rootlet coiled-coil. rootletin family member 2 [Source:VGNC Symbol;Acc:VGNC:96358]	-2.615590995	7.03E-05	0.0133282276
SOYvsFO	ENSSSCG00000012926	*PC*	pyruvate carboxylase [Source:NCBI gene (formerly Entrezgene);Acc:397630]	-2.611660558	5.31E-06	0.00309956594
SOYvsFO	ENSSSCG00000023859	*LRRTM1*	leucine rich repeat transmembrane neuronal 1 [Source:VGNC Symbol;Acc:VGNC:89863]	-2.608034068	0.002155157297	0.08329077572

SOYvsFO	ENSSSCG00000010647	*ADRB1*	adrenoceptor beta 1 [Source:NCBI gene (formerly Entrezgene);Acc:397355]	-2.604171106	0.0001454310059	0.02076808349
SOYvsFO	ENSSSCG00000036013	*Novel gene*	trypsinogen [Source:NCBI gene (formerly Entrezgene);Acc:100302368]	-2.59528827	5.82E-05	0.01205974666
SOYvsFO	ENSSSCG00000003846	*Novel gene*	GLIS family zinc finger 1 [Source:NCBI gene (formerly Entrezgene);Acc:100515552]	-2.591796793	0.001326416478	0.063719862
SOYvsFO	ENSSSCG00000045432	*0*	0	-2.584566701	0.001221271717	0.06232472104
SOYvsFO	ENSSSCG00000008090	*IL1A*	interleukin 1 alpha [Source:VGNC Symbol;Acc:VGNC:89091]	-2.569646708	0.0006557218728	0.04386044165
SOYvsFO	ENSSSCG00000042003	*0*	0	-2.541626632	0.002048878027	0.08094294436
SOYvsFO	ENSSSCG00000011630	*ACKR4*	atypical chemokine receptor 4 [Source:VGNC Symbol;Acc:VGNC:85013]	-2.531080534	2.96E-05	0.008634008145
SOYvsFO	ENSSSCG00000010478	*FFAR4*	free fatty acid receptor 4 [Source:NCBI gene (formerly Entrezgene);Acc:116183081]	-2.506313463	0.0001498572006	0.02076808349
SOYvsFO	ENSSSCG00000009798	*B3GNT4*	UDP-GlcNAc:betaGal beta-1.3-N-acetylglucosaminyltransferase 4 [Source:VGNC Symbol;Acc:VGNC:85725]	-2.48884895	0.001915223705	0.07755890604
SOYvsFO	ENSSSCG00000011557	*CIDEC*	cell death inducing DFFA like effector c [Source:VGNC Symbol;Acc:VGNC:86700]	-2.488694303	1.70E-05	0.006467956366
SOYvsFO	ENSSSCG00000017383	*Novel gene*	membrane primary amine oxidase-like [Source:NCBI gene (formerly Entrezgene);Acc:110256000]	-2.485883081	1.05E-07	0.0002249582568
SOYvsFO	ENSSSCG00000042679	*0*	0	-2.476987761	0.0004214983919	0.03451871116
SOYvsFO	ENSSSCG00000046652	*0*	0	-2.470527802	0.0009370231469	0.05462686129
SOYvsFO	ENSSSCG00000016617	*WNT16*	Wnt family member 16 [Source:VGNC Symbol;Acc:VGNC:94967]	-2.470412147	0.001980809212	0.07959335707
SOYvsFO	ENSSSCG00000032580	*MGST1*	microsomal glutathione S-transferase 1 [Source:NCBI gene (formerly Entrezgene);Acc:397567]	-2.427713774	1.76E-05	0.006467956366
SOYvsFO	ENSSSCG00000046684	*0*	0	-2.426931456	4.16E-05	0.009939015695
SOYvsFO	ENSSSCG00000024249	*GABRR2*	gamma-aminobutyric acid type A receptor subunit rho2 [Source:NCBI gene (formerly Entrezgene);Acc:100522289]	-2.423405596	0.0001517982126	0.02076808349
SOYvsFO	ENSSSCG00000039569	*0*	0	-2.421264021	0.0005195446176	0.03819615319
SOYvsFO	ENSSSCG00000036236	*ELOVL6*	ELOVL fatty acid elongase 6 [Source:VGNC Symbol;Acc:VGNC:87662]	-2.401298246	6.90E-06	0.003709940729
SOYvsFO	ENSSSCG00000013292	*PRR5L*	proline rich 5 like [Source:VGNC Symbol;Acc:VGNC:91862]	-2.398237187	3.91E-05	0.00966181679
SOYvsFO	ENSSSCG00000002866	*CEBPA*	CCAAT enhancer binding protein alpha [Source:VGNC Symbol;Acc:VGNC:86531]	-2.397620365	2.53E-05	0.007920901766
SOYvsFO	ENSSSCG00000041248	*Novel gene*	zinc finger BED-type containing 3 [Source:NCBI gene (formerly Entrezgene);Acc:100521776]	-2.381487002	4.89E-06	0.00309956594

SOYvsFO	ENSSSCG00000041483	*0*	0	-2.381094324	0.0003560836602	0.0320795851
SOYvsFO	ENSSSCG00000010479	*RBP4*	retinol binding protein 4 [Source:VGNC Symbol;Acc:VGNC:92164]	-2.369276201	0.0001789202832	0.02326995716
SOYvsFO	ENSSSCG00000006359	*ADAMTS4*	ADAM metallopeptidase with thrombospondin type 1 motif 4 [Source:VGNC Symbol;Acc:VGNC:85084]	-2.351514612	0.001366255015	0.06440109696
SOYvsFO	ENSSSCG00000024685	*GRIA2*	glutamate ionotropic receptor AMPA type subunit 2 [Source:VGNC Symbol;Acc:VGNC:88671]	-2.349775953	0.0003786233674	0.03272143052
SOYvsFO	ENSSSCG00000037735	*Novel gene*	hydroxycarboxylic acid receptor 2 [Source:NCBI gene (formerly Entrezgene);Acc:102164386]	-2.332935201	0.0007720887743	0.04826173176
SOYvsFO	ENSSSCG00000034623	*Novel gene*	ADAM3b [Source:NCBI gene (formerly Entrezgene);Acc:100049687]	-2.32830315	0.0001481268329	0.02076808349
SOYvsFO	ENSSSCG00000022842	*0*	0	-2.32421739	4.49E-07	0.0006439956156
SOYvsFO	ENSSSCG00000005952	*LRRC6*	leucine rich repeat containing 6 [Source:VGNC Symbol;Acc:VGNC:98083]	-2.314634022	0.002844119008	0.09590815431
SOYvsFO	ENSSSCG00000003399	*RBP7*	retinol binding protein 7 [Source:VGNC Symbol;Acc:VGNC:92165]	-2.3143336	6.78E-05	0.01310977365
SOYvsFO	ENSSSCG00000016516	*ATP6V0A4*	ATPase H+ transporting V0 subunit a4 [Source:VGNC Symbol;Acc:VGNC:85665]	-2.305578302	5.05E-05	0.01143863171
SOYvsFO	ENSSSCG00000033425	*ST6GALNAC5*	ST6 N-acetylgalactosaminide alpha-2.6-sialyltransferase 5 [Source:VGNC Symbol;Acc:VGNC:93513]	-2.298258592	0.0001533108996	0.02076808349
SOYvsFO	ENSSSCG00000010529	*SFRP5*	secreted frizzled related protein 5 [Source:VGNC Symbol;Acc:VGNC:92777]	-2.296878394	1.96E-05	0.00662185122
SOYvsFO	ENSSSCG00000034882	*0*	0	-2.290516803	0.0003388661725	0.03194691242
SOYvsFO	ENSSSCG00000040464	*LEP*	leptin [Source:VGNC Symbol;Acc:VGNC:89684]	-2.289185751	0.0004550987679	0.03548275244
SOYvsFO	ENSSSCG00000046916	*0*	0	-2.281180406	5.38E-05	0.01185930097
SOYvsFO	ENSSSCG00000047540	*Novel gene*	0	-2.25334194	0.00161238018	0.07157576844
SOYvsFO	ENSSSCG00000004676	*DUOXA2*	dual oxidase maturation factor 2 [Source:VGNC Symbol;Acc:VGNC:87472]	-2.239868426	0.002005777613	0.08022177532
SOYvsFO	ENSSSCG00000011186	*COL6A5*	collagen type VI alpha 5 chain [Source:VGNC Symbol;Acc:VGNC:86879]	-2.218251134	0.00266095266	0.09134344083
SOYvsFO	ENSSSCG00000000591	*PIK3C2G*	phosphatidylinositol-4-phosphate 3-kinase catalytic subunit type 2 gamma [Source:VGNC Symbol;Acc:VGNC:91438]	-2.208208199	0.0004932900054	0.03737269389
SOYvsFO	ENSSSCG00000005452	*C9orf152*	chromosome 1 C9orf152 homolog [Source:VGNC Symbol;Acc:VGNC:85972]	-2.206444834	0.002896616263	0.0967301097
SOYvsFO	ENSSSCG00000036572	*BCO1*	beta-carotene oxygenase 1 [Source:VGNC Symbol;Acc:VGNC:85789]	-2.187435175	0.0001492543707	0.02076808349
SOYvsFO	ENSSSCG00000041487	*0*	0	-2.178949282	0.0003539552358	0.0320795851

SOYvsFO	ENSSSCG00000046138	*0*	0	-2.172772425	0.00233173828	0.0854889379
SOYvsFO	ENSSSCG00000035402	*RGS9*	regulator of G protein signaling 9 [Source:VGNC Symbol;Acc:VGNC:92270]	-2.169626761	0.0001339823777	0.01986404251
SOYvsFO	ENSSSCG00000041147	*0*	0	-2.168997048	0.0004590926908	0.03556520764
SOYvsFO	ENSSSCG00000032687	*CYP4V2*	cytochrome P450. family 4. subfamily v. polypeptide 2 [Source:NCBI gene (formerly Entrezgene);Acc:100113469]	-2.165975329	1.83E-05	0.006467956366
SOYvsFO	ENSSSCG00000007718	*CLDN4*	claudin 4 [Source:NCBI gene (formerly Entrezgene);Acc:733578]	-2.158251057	0.001295698192	0.06316634762
SOYvsFO	ENSSSCG00000037706	*PRKAR2B*	protein kinase cAMP-dependent type II regulatory subunit beta [Source:VGNC Symbol;Acc:VGNC:91805]	-2.151100842	3.53E-05	0.009478470008
SOYvsFO	ENSSSCG00000014861	*MOGAT2*	2-acylglycerol O-acyltransferase 2-like [Source:NCBI gene (formerly Entrezgene);Acc:110255553]	-2.140173365	0.001294296982	0.06316634762
SOYvsFO	ENSSSCG00000051032	*0*	0	-2.129382083	0.0006393889257	0.04339349133
SOYvsFO	ENSSSCG00000009662	*STMN4*	stathmin 4 [Source:VGNC Symbol;Acc:VGNC:93562]	-2.128894494	0.0002808711911	0.02892468709
SOYvsFO	ENSSSCG00000039677	*CHRNA4*	cholinergic receptor nicotinic alpha 4 subunit [Source:VGNC Symbol;Acc:VGNC:95915]	-2.126365861	0.002770605265	0.09398199084
SOYvsFO	ENSSSCG00000011911	*DRD3*	dopamine receptor D3 [Source:VGNC Symbol;Acc:VGNC:87445]	-2.125253768	0.00242538204	0.08638306109
SOYvsFO	ENSSSCG00000031228	*OPRL1*	opioid related nociceptin receptor 1 [Source:VGNC Symbol;Acc:VGNC:96461]	-2.123102087	0.0007773287416	0.04826173176
SOYvsFO	ENSSSCG00000035460	*0*	0	-2.120831662	0.001497666635	0.0678263148
SOYvsFO	ENSSSCG00000011250	*ACAA1*	acetyl-CoA acyltransferase 1 [Source:VGNC Symbol;Acc:VGNC:84995]	-2.112966351	3.28E-05	0.009094657695
SOYvsFO	ENSSSCG00000042806	*C1orf146*	chromosome 1 open reading frame 146 [Source:HGNC Symbol;Acc:HGNC:24032]	-2.10786489	0.002594043952	0.09030038651
SOYvsFO	ENSSSCG00000005272	*NMRK1*	nicotinamide riboside kinase 1 [Source:VGNC Symbol;Acc:VGNC:90800]	-2.102397645	2.24E-05	0.007148986444
SOYvsFO	ENSSSCG00000003088	*APOE*	apolipoprotein E [Source:NCBI gene (formerly Entrezgene);Acc:397576]	-2.097220926	0.0001858846608	0.02368032886
SOYvsFO	ENSSSCG00000031851	*CBR2*	carbonyl reductase 2 [Source:NCBI gene (formerly Entrezgene);Acc:396780]	-2.086916673	0.001101735298	0.05921138642
SOYvsFO	ENSSSCG00000015550	*RGS16*	regulator of G protein signaling 16 [Source:VGNC Symbol;Acc:VGNC:92262]	-2.080755617	0.0002456342676	0.02743128659
SOYvsFO	ENSSSCG00000003788	*PTGER3*	prostaglandin E receptor 3 [Source:VGNC Symbol;Acc:VGNC:98225]	-2.076257911	0.0002699303377	0.02876163552
SOYvsFO	ENSSSCG00000017605	*MMD*	monocyte to macrophage differentiation associated [Source:VGNC Symbol;Acc:VGNC:90264]	-2.070065666	3.51E-06	0.002514953036
SOYvsFO	ENSSSCG00000015732	*TFCP2L1*	transcription factor CP2 like 1 [Source:VGNC	-2.061128109	0.0008479811145	0.05099153569

			Symbol;Acc:VGNC:95864]			
SOYvsFO	ENSSSCG00000050531	*0*	0	-2.03352215	0.0006690666805	0.04408662364
SOYvsFO	ENSSSCG00000012512	*ZMAT1*	zinc finger matrin-type 1 [Source:VGNC Symbol;Acc:VGNC:95175]	-2.032090588	0.0003019400047	0.02984347242
SOYvsFO	ENSSSCG00000000362	*RDH5*	retinol dehydrogenase 5 [Source:VGNC Symbol;Acc:VGNC:92191]	-2.019533012	0.001353571038	0.06440109696
SOYvsFO	ENSSSCG00000008141	*ST6GAL2*	ST6 beta-galactoside alpha-2.6-sialyltransferase 2 [Source:VGNC Symbol;Acc:VGNC:93508]	-2.009082236	0.0007746590006	0.04826173176
SOYvsFO	ENSSSCG00000011850	*Novel gene*	mucin 4. cell surface associated [Source:NCBI gene (formerly Entrezgene);Acc:100157344]	-2.002502386	0.00236410521	0.08585399169
SOYvsFO	ENSSSCG00000025005	*B4GALT6*	beta-1.4-galactosyltransferase 6 [Source:VGNC Symbol;Acc:VGNC:85734]	-1.963689	0.0002776155074	0.02876163552
SOYvsFO	ENSSSCG00000003882	*SLC5A9*	solute carrier family 5 member 9 [Source:VGNC Symbol;Acc:VGNC:93149]	-1.931851079	0.002186600672	0.08351911876
SOYvsFO	ENSSSCG00000006852	*NTNG1*	netrin G1 [Source:VGNC Symbol;Acc:VGNC:90935]	-1.929901843	0.002146914617	0.08329077572
SOYvsFO	ENSSSCG00000031813	*XKR4*	XK related 4 [Source:VGNC Symbol;Acc:VGNC:98900]	-1.926295223	0.0001472379295	0.02076808349
SOYvsFO	ENSSSCG00000008237	*RETSAT*	retinol saturase [Source:VGNC Symbol;Acc:VGNC:92225]	-1.923486768	1.01E-05	0.004685307343
SOYvsFO	ENSSSCG00000011579	*PPARG*	peroxisome proliferator activated receptor gamma [Source:VGNC Symbol;Acc:VGNC:91684]	-1.915401152	0.0002416745127	0.02734419914
SOYvsFO	ENSSSCG00000042365	*0*	0	-1.910836359	8.55E-05	0.0151618868
SOYvsFO	ENSSSCG00000018044	*ALDH3A1*	aldehyde dehydrogenase 3 family member A1 [Source:VGNC Symbol;Acc:VGNC:85238]	-1.893445962	1.18E-07	0.0002249582568
SOYvsFO	ENSSSCG00000000721	*Novel gene*	dual specificity tyrosine phosphorylation regulated kinase 4 [Source:VGNC Symbol;Acc:VGNC:97971]	-1.885594803	0.0009475173539	0.05476956043
SOYvsFO	ENSSSCG00000036520	*EFNA5*	ephrin A5 [Source:VGNC Symbol;Acc:VGNC:87575]	-1.867962928	8.43E-06	0.004025924256
SOYvsFO	ENSSSCG00000014097	*Novel gene*	phosphodiesterase 8B [Source:NCBI gene (formerly Entrezgene);Acc:100522306]	-1.863153459	0.002498972143	0.08788818594
SOYvsFO	ENSSSCG00000031216	*HS3ST6*	heparan sulfate-glucosamine 3-sulfotransferase 6 [Source:VGNC Symbol;Acc:VGNC:88980]	-1.860967541	0.0001050633074	0.01737383424
SOYvsFO	ENSSSCG00000024149	*ELOVL5*	ELOVL fatty acid elongase 5 [Source:VGNC Symbol;Acc:VGNC:87661]	-1.84876564	6.56E-05	0.01310977365
SOYvsFO	ENSSSCG00000033688	*ZDHHC22*	zinc finger DHHC-type palmitoyltransferase 22 [Source:VGNC Symbol;Acc:VGNC:95124]	-1.846810788	0.0002733417771	0.02876163552
SOYvsFO	ENSSSCG00000002257	*MCTP2*	multiple C2 and transmembrane domain containing 2 [Source:VGNC Symbol;Acc:VGNC:90084]	-1.845882496	0.0009056162619	0.05372335221
SOYvsFO	ENSSSCG00000003640	*GRIK3*	glutamate ionotropic receptor kainate type subunit 3 [Source:VGNC	-1.842937661	0.0003727733006	0.03254291992

			Symbol;Acc:VGNC:88679]			
SOYvsFO	ENSSSCG00000038824	*FRRS1L*	ferric chelate reductase 1 like [Source:VGNC Symbol;Acc:VGNC:88245]	-1.830024037	0.0001569863271	0.02076808349
SOYvsFO	ENSSSCG00000002552	*TDRD9*	tudor domain containing 9 [Source:VGNC Symbol;Acc:VGNC:93851]	-1.790013914	0.0001271939479	0.0190215784
SOYvsFO	ENSSSCG00000044065	*0*	0	-1.771969363	0.000202932872	0.02487210892
SOYvsFO	ENSSSCG00000015135	*SORL1*	sortilin related receptor 1 [Source:NCBI gene (formerly Entrezgene);Acc:100626812]	-1.759212388	0.0002032818222	0.02487210892
SOYvsFO	ENSSSCG00000039797	*APCDD1*	APC down-regulated 1 [Source:VGNC Symbol;Acc:VGNC:85406]	-1.757601876	0.0002731662948	0.02876163552
SOYvsFO	ENSSSCG00000042401	*0*	0	-1.756650933	0.0003857839783	0.03307561776
SOYvsFO	ENSSSCG00000000672	*CLSTN3*	calsyntenin 3 [Source:VGNC Symbol;Acc:VGNC:86786]	-1.753471406	0.001266417591	0.06316634762
SOYvsFO	ENSSSCG00000005830	*Novel gene*	coiled-coil domain containing 183 [Source:NCBI gene (formerly Entrezgene);Acc:100513066]	-1.737984438	0.002280141737	0.08543328451
SOYvsFO	ENSSSCG00000036011	*ISLR2*	immunoglobulin superfamily containing leucine rich repeat 2 [Source:VGNC Symbol;Acc:VGNC:89227]	-1.733465817	0.001370554802	0.06440109696
SOYvsFO	ENSSSCG00000005287	*PSAT1*	phosphoserine aminotransferase 1 [Source:VGNC Symbol;Acc:VGNC:91893]	-1.728173983	0.0002307415332	0.02628008535
SOYvsFO	ENSSSCG00000029468	*P2RX3*	purinergic receptor P2X 3 [Source:VGNC Symbol;Acc:VGNC:91120]	-1.726775304	0.001128674911	0.0600958239
SOYvsFO	ENSSSCG00000049474	*0*	0	-1.708671696	0.0009933153506	0.05637966138
SOYvsFO	ENSSSCG00000017884	*TEKT1*	tektin 1 [Source:VGNC Symbol;Acc:VGNC:93867]	-1.706715304	0.001623742696	0.07160288945
SOYvsFO	ENSSSCG00000037318	*TRABD2B*	TraB domain containing 2B [Source:VGNC Symbol;Acc:VGNC:94356]	-1.705989688	0.0002030889906	0.02487210892
SOYvsFO	ENSSSCG00000015355	*DGKB*	diacylglycerol kinase beta [Source:VGNC Symbol;Acc:VGNC:87270]	-1.703859714	0.0007513777528	0.04806780918
SOYvsFO	ENSSSCG00000021557	*SULT1A3*	sulfotransferase family 1A member 3 [Source:NCBI gene (formerly Entrezgene);Acc:396640]	-1.700074306	5.81E-05	0.01205974666
SOYvsFO	ENSSSCG00000037918	*ADIRF*	adipogenesis regulatory factor [Source:VGNC Symbol;Acc:VGNC:85142]	-1.692663633	0.0003590793941	0.0320795851
SOYvsFO	ENSSSCG00000009613	*DMTN*	dematin actin binding protein [Source:VGNC Symbol;Acc:VGNC:87358]	-1.692581709	0.0002073267646	0.02493430558
SOYvsFO	ENSSSCG00000002993	*CYP2A19*	cytochrome P450 2A19 [Source:NCBI gene (formerly Entrezgene);Acc:403149]	-1.682358131	0.0005154361971	0.03819615319
SOYvsFO	ENSSSCG00000024860	*Novel gene*	sodium/glucose cotransporter 1-like [Source:NCBI gene (formerly Entrezgene);Acc:102159834]	-1.677753596	5.41E-06	0.00309956594
SOYvsFO	ENSSSCG00000017747	*RAB11FIP4*	RAB11 family interacting protein 4 [Source:VGNC Symbol;Acc:VGNC:92041]	-1.668839419	0.000772618015	0.04826173176

SOYvsFO	ENSSSCG00000029606	*AOX1*	aldehyde oxidase 1 [Source:NCBI gene (formerly Entrezgene);Acc:100523701]	-1.66512304	0.0005197057708	0.03819615319
SOYvsFO	ENSSSCG00000010184	*AGT*	angiotensinogen [Source:VGNC Symbol;Acc:VGNC:85190]	-1.660187594	0.00176685376	0.07322012281
SOYvsFO	ENSSSCG00000040681	*FABP4*	fatty acid binding protein 4. adipocyte [Source:NCBI gene (formerly Entrezgene);Acc:399533]	-1.660151728	0.0007681091025	0.04826173176
SOYvsFO	ENSSSCG00000049283	*0*	0	-1.657760689	9.47E-05	0.0162119407
SOYvsFO	ENSSSCG00000016487	*MGAM2*	maltase-glucoamylase 2 (putative) [Source:NCBI gene (formerly Entrezgene);Acc:100623494]	-1.656793214	0.0002189585028	0.02602928751
SOYvsFO	ENSSSCG00000030626	*ALDH1L1*	aldehyde dehydrogenase 1 family member L1 [Source:VGNC Symbol;Acc:VGNC:97881]	-1.655312417	0.0005765441029	0.04030652635
SOYvsFO	ENSSSCG00000045083	*0*	0	-1.64234389	0.002215559046	0.08374709408
SOYvsFO	ENSSSCG00000016830	*PRLR*	prolactin receptor [Source:VGNC Symbol;Acc:VGNC:91819]	-1.641324063	0.001693616369	0.0722749735
SOYvsFO	ENSSSCG00000006491	*Novel gene*	progestin and adipoQ receptor family member 6 [Source:VGNC Symbol;Acc:VGNC:91176]	-1.614916299	0.0002053796745	0.02487408199
SOYvsFO	ENSSSCG00000034087	*TNFSF15*	TNF superfamily member 15 [Source:VGNC Symbol;Acc:VGNC:94271]	-1.609663605	0.001533702067	0.06920132207
SOYvsFO	ENSSSCG00000010554	*SCD*	stearoyl-CoA desaturase [Source:NCBI gene (formerly Entrezgene);Acc:396670]	-1.604179071	4.43E-05	0.01016099889
SOYvsFO	ENSSSCG00000045639	*0*	0	-1.596448132	0.0007683003502	0.04826173176
SOYvsFO	ENSSSCG00000016199	*CYP27A1*	cytochrome P450. family 27. subfamily A. polypeptide 1 [Source:NCBI gene (formerly Entrezgene);Acc:100126282]	-1.587898825	0.0001136418039	0.01793038297
SOYvsFO	ENSSSCG00000036469	*0*	0	-1.569262344	0.002644090591	0.09112839677
SOYvsFO	ENSSSCG00000040779	*Novel gene*	cystathionine beta-synthase [Source:NCBI gene (formerly Entrezgene);Acc:110256498]	-1.561549692	1.64E-05	0.006467956366
SOYvsFO	ENSSSCG00000016672	*ADCYAP1R1*	ADCYAP receptor type I [Source:VGNC Symbol;Acc:VGNC:85115]	-1.550025005	0.001658637808	0.07200289865
SOYvsFO	ENSSSCG00000003825	*CYP2J34*	cytochrome P450 2J2 [Source:NCBI gene (formerly Entrezgene);Acc:100524940]	-1.54317936	0.00247516469	0.08764042677
SOYvsFO	ENSSSCG00000036438	*GPX3*	glutathione peroxidase 3 [Source:VGNC Symbol;Acc:VGNC:98026]	-1.53995039	0.0004975162562	0.03752756392
SOYvsFO	ENSSSCG00000028627	*Novel gene*	cytochrome P450 2G1 [Source:NCBI gene (formerly Entrezgene);Acc:100737508]	-1.538344652	0.002336395246	0.0854889379
SOYvsFO	ENSSSCG00000000551	*ARNTL2*	aryl hydrocarbon receptor nuclear translocator like 2 [Source:NCBI gene (formerly Entrezgene);Acc:100625791]	-1.53665663	0.0006618671361	0.04394900002
SOYvsFO	ENSSSCG00000040337	*AK4*	adenylate kinase 4 [Source:VGNC Symbol;Acc:VGNC:85209]	-1.523011182	0.001145108641	0.06019228851
SOYvsFO	ENSSSCG00000026297	*KLB*	klotho beta [Source:VGNC Symbol;Acc:VGNC:89485]	-1.522895997	0.001312703027	0.06341535579

SOYvsFO	ENSSSCG00000016437	*Novel gene*	WD repeat domain 86 [Source:NCBI gene (formerly Entrezgene);Acc:100739295]	-1.518324906	0.002481735541	0.08764042677
SOYvsFO	ENSSSCG00000024162	*Novel gene*	cell death inducing DFFA like effector a [Source:NCBI gene (formerly Entrezgene);Acc:100127171]	-1.513688823	3.77E-05	0.00966181679
SOYvsFO	ENSSSCG00000013388	*PDE3B*	phosphodiesterase 3B [Source:VGNC Symbol;Acc:VGNC:91253]	-1.501189679	0.000527171759	0.03857298083
SOYvsFO	ENSSSCG00000016519	*AKR1D1*	aldo-keto reductase family 1 member D1 [Source:VGNC Symbol;Acc:VGNC:85230]	-1.499293833	0.0005490947107	0.03952320758
SOYvsFO	ENSSSCG00000009477	*EDNRB*	endothelin receptor type B [Source:VGNC Symbol;Acc:VGNC:87550]	-1.484972104	3.28E-06	0.002453930897
SOYvsFO	ENSSSCG00000032684	*BOK*	BCL2 family apoptosis regulator BOK [Source:VGNC Symbol;Acc:VGNC:95496]	-1.483266783	0.0008439377341	0.05098748974
SOYvsFO	ENSSSCG00000045880	*0*	0	-1.479788057	0.0005737104311	0.04027213059
SOYvsFO	ENSSSCG00000027854	*HSD17B6*	17-beta-hydroxysteroid dehydrogenase type 6 [Source:NCBI gene (formerly Entrezgene);Acc:100620470]	-1.478123491	0.00259687969	0.09030038651
SOYvsFO	ENSSSCG00000034786	*HACD2*	3-hydroxyacyl-CoA dehydratase 2 [Source:VGNC Symbol;Acc:VGNC:88766]	-1.470521925	0.0005576120235	0.03962732058
SOYvsFO	ENSSSCG00000032417	*NGF*	nerve growth factor [Source:VGNC Symbol;Acc:VGNC:98826]	-1.438387043	0.0004916803928	0.03737269389
SOYvsFO	ENSSSCG00000045021	*0*	0	-1.427157865	0.0006266845215	0.04276873175
SOYvsFO	ENSSSCG00000015022	*LAYN*	layilin [Source:VGNC Symbol;Acc:VGNC:89651]	-1.425323035	0.000804191228	0.04957161555
SOYvsFO	ENSSSCG00000001203	*ZSCAN9*	zinc finger and SCAN domain containing 9 [Source:VGNC Symbol;Acc:VGNC:95332]	-1.413946648	0.0004132184414	0.03416601324
SOYvsFO	ENSSSCG00000038575	*0*	0	-1.386129564	0.002290228208	0.0854889379
SOYvsFO	ENSSSCG00000051428	*0*	0	-1.382330157	6.53E-09	5.61E-05
SOYvsFO	ENSSSCG00000042995	*0*	0	-1.369202646	0.001044753268	0.05838710885
SOYvsFO	ENSSSCG00000000687	*CD4*	CD4 molecule [Source:VGNC Symbol;Acc:VGNC:86417]	-1.361925219	7.31E-05	0.0136150245
SOYvsFO	ENSSSCG00000015802	*Novel gene*	family with sequence similarity 149 member A [Source:VGNC Symbol;Acc:VGNC:96044]	-1.358195634	0.002057469439	0.08094294436
SOYvsFO	ENSSSCG00000025870	*HEPACAM2*	HEPACAM family member 2 [Source:VGNC Symbol;Acc:VGNC:88846]	-1.357764782	0.0004559651291	0.03548275244
SOYvsFO	ENSSSCG00000001435	*AGPAT1*	1-acylglycerol-3-phosphate O-acyltransferase 1 [Source:VGNC Symbol;Acc:VGNC:85183]	-1.353507061	0.0001549969617	0.02076808349
SOYvsFO	ENSSSCG00000003793	*LRRC7*	leucine rich repeat containing 7 [Source:NCBI gene (formerly Entrezgene);Acc:100516204]	-1.353427671	0.002382301685	0.08589271358
SOYvsFO	ENSSSCG00000004885	*CDH19*	cadherin 19 [Source:VGNC Symbol;Acc:VGNC:86482]	-1.352166435	0.001664222897	0.07200289865

SOYvsFO	ENSSSCG00000006309	*CD247*	CD247 molecule [Source:VGNC Symbol;Acc:VGNC:86401]	-1.329466273	0.0008421063621	0.05098748974
SOYvsFO	ENSSSCG00000032941	*SIK2*	salt inducible kinase 2 [Source:VGNC Symbol;Acc:VGNC:92872]	-1.320321196	0.0004283682144	0.03475036109
SOYvsFO	ENSSSCG00000009486	*SLITRK6*	SLIT and NTRK like family member 6 [Source:VGNC Symbol;Acc:VGNC:93211]	-1.313430449	0.001234266615	0.06247052669
SOYvsFO	ENSSSCG00000010340	*PRXL2A*	peroxiredoxin like 2A [Source:VGNC Symbol;Acc:VGNC:91892]	-1.304206191	0.0004431592766	0.03531648183
SOYvsFO	ENSSSCG00000003018	*LIPE*	lipase E. hormone sensitive type [Source:VGNC Symbol;Acc:VGNC:98493]	-1.300015738	0.001368562576	0.06440109696
SOYvsFO	ENSSSCG00000009759	*SCARB1*	scavenger receptor class B member 1 [Source:VGNC Symbol;Acc:VGNC:92613]	-1.289779122	0.0003675904207	0.03241959003
SOYvsFO	ENSSSCG00000018042	*SLC47A2*	solute carrier family 47 member 2 [Source:VGNC Symbol;Acc:VGNC:99044]	-1.289548258	0.0001752578477	0.02300827836
SOYvsFO	ENSSSCG00000036751	*PPM1H*	protein phosphatase. Mg2+/Mn2+ dependent 1H [Source:VGNC Symbol;Acc:VGNC:91708]	-1.288157752	0.001217743318	0.06232472104
SOYvsFO	ENSSSCG00000027443	*MRAS*	muscle RAS oncogene homolog [Source:VGNC Symbol;Acc:VGNC:90340]	-1.281774326	0.000511406897	0.03819615319
SOYvsFO	ENSSSCG00000035554	*LHFPL3*	LHFPL tetraspan subfamily member 3 [Source:VGNC Symbol;Acc:VGNC:89706]	-1.278517552	0.001418154537	0.06573968119
SOYvsFO	ENSSSCG00000015914	*SCN7A*	sodium voltage-gated channel alpha subunit 7 [Source:VGNC Symbol;Acc:VGNC:95480]	-1.26569248	0.0004792795829	0.03679754583
SOYvsFO	ENSSSCG00000047361	*0*	0	-1.264210389	0.0004474518368	0.03546210456
SOYvsFO	ENSSSCG00000000419	*RDH16*	retinol dehydrogenase 16 [Source:NCBI gene (formerly Entrezgene);Acc:100626199]	-1.261866278	0.0001132333845	0.01793038297
SOYvsFO	ENSSSCG00000051482	*0*	0	-1.260311045	0.0002571502907	0.02799032089
SOYvsFO	ENSSSCG00000022196	*CCT6B*	chaperonin containing TCP1 subunit 6B [Source:VGNC Symbol;Acc:VGNC:86384]	-1.258414212	0.0001132864377	0.01793038297
SOYvsFO	ENSSSCG00000014894	*Novel gene*	teneurin transmembrane protein 4 [Source:NCBI gene (formerly Entrezgene);Acc:100514784]	-1.255194506	0.001092973014	0.05910990531
SOYvsFO	ENSSSCG00000012731	*Novel gene*	iduronate 2-sulfatase [Source:NCBI gene (formerly Entrezgene);Acc:100512880]	-1.251838234	0.0004673599022	0.03604329865
SOYvsFO	ENSSSCG00000047596	*0*	0	-1.244501293	0.001712589013	0.07236635344
SOYvsFO	ENSSSCG00000009336	*RXFP2*	relaxin family peptide receptor 2 [Source:VGNC Symbol;Acc:VGNC:92526]	-1.243467348	0.001331071162	0.06376535335
SOYvsFO	ENSSSCG00000009169	*SLC39A8*	solute carrier family 39 member 8 [Source:VGNC Symbol;Acc:VGNC:93109]	-1.216620412	0.0009293843661	0.05436582424
SOYvsFO	ENSSSCG00000029944	*FASN*	fatty acid synthase [Source:VGNC Symbol;Acc:VGNC:88016]	-1.216105687	0.002737033744	0.09321090361

SOYvsFO	ENSSSCG00000009128	*AP1AR*	family with sequence similarity 241 member A [Source:NCBI gene (formerly Entrezgene);Acc:102158861]	-1.210025892	0.001429673029	0.06609547516
SOYvsFO	ENSSSCG00000039961	*Novel gene*	serine protease 33-like [Source:NCBI gene (formerly Entrezgene);Acc:110256121]	-1.206554521	0.003038321104	0.09896410294
SOYvsFO	ENSSSCG00000028612	*PTPRS*	protein tyrosine phosphatase receptor type S [Source:VGNC Symbol;Acc:VGNC:91994]	-1.204810346	0.00237124352	0.08585399169
SOYvsFO	ENSSSCG00000032723	*ACER3*	alkaline ceramidase 3 [Source:NCBI gene (formerly Entrezgene);Acc:100524160]	-1.197154807	0.001309137297	0.06341535579
SOYvsFO	ENSSSCG00000008013	*IGFALS*	insulin like growth factor binding protein acid labile subunit [Source:NCBI gene (formerly Entrezgene);Acc:397322]	-1.19345802	0.001399705043	0.0652361174
SOYvsFO	ENSSSCG00000041675	*0*	0	-1.189358327	0.001257160093	0.06303393374
SOYvsFO	ENSSSCG00000039573	*SLPI*	secretory leukocyte peptidase inhibitor [Source:NCBI gene (formerly Entrezgene);Acc:396886]	-1.188094043	0.002141517391	0.08329077572
SOYvsFO	ENSSSCG00000032320	*TCIM*	transcriptional and immune response regulator [Source:VGNC Symbol;Acc:VGNC:95587]	-1.186964003	0.001091475722	0.05910990531
SOYvsFO	ENSSSCG00000023264	*IDH1*	isocitrate dehydrogenase (NADP(+)) 1 [Source:NCBI gene (formerly Entrezgene);Acc:102166364]	-1.173863765	0.0001543808237	0.02076808349
SOYvsFO	ENSSSCG00000017492	*ORMDL3*	ORMDL sphingolipid biosynthesis regulator 3 [Source:VGNC Symbol;Acc:VGNC:91064]	-1.169146179	0.0002965740951	0.02982737595
SOYvsFO	ENSSSCG00000005910	*TMEM249*	transmembrane protein 249 [Source:VGNC Symbol;Acc:VGNC:94156]	-1.163172899	0.0005613875036	0.03973144974
SOYvsFO	ENSSSCG00000041180	*0*	0	-1.157118004	0.001442137139	0.06633604773
SOYvsFO	ENSSSCG00000006890	*ABCA4*	ATP binding cassette subfamily A member 4 [Source:VGNC Symbol;Acc:VGNC:84948]	-1.147606181	0.001237914288	0.06247052669
SOYvsFO	ENSSSCG00000037637	*GGH*	gamma-glutamyl hydrolase [Source:NCBI gene (formerly Entrezgene);Acc:100154232]	-1.140635741	0.001288610035	0.06316634762
SOYvsFO	ENSSSCG00000020657	*BCAM*	basal cell adhesion molecule [Source:VGNC Symbol;Acc:VGNC:96620]	-1.13332832	0.001142486505	0.06019228851
SOYvsFO	ENSSSCG00000028341	*Novel gene*	synaptotagmin-15 [Source:NCBI gene (formerly Entrezgene);Acc:100625711]	-1.124622918	0.0003016227404	0.02984347242
SOYvsFO	ENSSSCG00000039188	*AK8*	adenylate kinase 8 [Source:VGNC Symbol;Acc:VGNC:85213]	-1.112188827	0.0004520664073	0.03548275244
SOYvsFO	ENSSSCG00000006082	*MATN2*	matrilin 2 [Source:VGNC Symbol;Acc:VGNC:90043]	-1.096386303	9.36E-05	0.0162119407
SOYvsFO	ENSSSCG00000022014	*DCDC2B*	doublecortin domain containing 2B [Source:VGNC Symbol;Acc:VGNC:87182]	-1.096080366	0.001089857315	0.05910990531
SOYvsFO	ENSSSCG00000030016	*PDE9A*	phosphodiesterase 9A [Source:VGNC Symbol;Acc:VGNC:91264]	-1.094612647	0.00274618244	0.09333763953
SOYvsFO	ENSSSCG00000009092	*TRPC3*	transient receptor potential cation channel subfamily C member 3 [Source:VGNC Symbol;Acc:VGNC:94461]	-1.093033404	0.0002039171623	0.02487210892

SOYvsFO	ENSSSCG00000037487	*Novel gene*	membrane primary amine oxidase [Source:NCBI gene (formerly Entrezgene);Acc:100520329]	-1.091438276	0.002056169366	0.08094294436
SOYvsFO	ENSSSCG00000009873	*DTX1*	deltex E3 ubiquitin ligase 1 [Source:VGNC Symbol;Acc:VGNC:87466]	-1.082144472	0.002135640937	0.08329077572
SOYvsFO	ENSSSCG00000022395	*SLC25A35*	solute carrier family 25 member 35 [Source:VGNC Symbol;Acc:VGNC:93011]	-1.078408674	1.27E-05	0.005459864706
SOYvsFO	ENSSSCG00000007710	*MLXIPL*	MLX interacting protein like [Source:VGNC Symbol;Acc:VGNC:90263]	-1.065896011	0.001838818854	0.07547495619
SOYvsFO	ENSSSCG00000017734	*Novel gene*	rhomboid like 3 [Source:VGNC Symbol;Acc:VGNC:92279]	-1.059146447	0.0005136166288	0.03819615319
SOYvsFO	ENSSSCG00000033745	*0*	0	-1.055354144	0.0009049583189	0.05372335221
SOYvsFO	ENSSSCG00000017392	*CCR10*	C-C motif chemokine receptor 10 [Source:VGNC Symbol;Acc:VGNC:86369]	-1.045390354	0.002058945506	0.08094294436
SOYvsFO	ENSSSCG00000017743	*CRLF3*	cytokine receptor like factor 3 [Source:VGNC Symbol;Acc:VGNC:86999]	-1.035101249	0.000840949002	0.05098748974
SOYvsFO	ENSSSCG00000037744	*ZNF483*	zinc finger protein 483 [Source:VGNC Symbol;Acc:VGNC:95248]	-1.03354292	0.001238658542	0.06247052669
SOYvsFO	ENSSSCG00000003744	*MOCOS*	molybdenum cofactor sulfurase [Source:VGNC Symbol;Acc:VGNC:90294]	-1.021932152	0.0009520493207	0.05476956043
SOYvsFO	ENSSSCG00000014434	*IL17B*	interleukin 17B [Source:VGNC Symbol;Acc:VGNC:99764]	-1.02031235	0.00236704695	0.08585399169
SOYvsFO	ENSSSCG00000026818	*Novel gene*	CST telomere replication complex component 1 [Source:VGNC Symbol;Acc:VGNC:87056]	-1.017445856	1.30E-05	0.005459864706
SOYvsFO	ENSSSCG00000042541	*0*	0	-1.017219442	7.05E-05	0.0133282276
SOYvsFO	ENSSSCG00000015023	*Novel gene*	ALG9 alpha-1.2-mannosyltransferase [Source:NCBI gene (formerly Entrezgene);Acc:100519965]	-1.015731141	0.0008449490974	0.05098748974
SOYvsFO	ENSSSCG00000001612	*Novel gene*	adenylate cyclase type 10 [Source:NCBI gene (formerly Entrezgene);Acc:100737927]	-1.014574232	0.002194999512	0.08351911876
SOYvsFO	ENSSSCG00000014219	*CDO1*	cysteine dioxygenase type 1 [Source:VGNC Symbol;Acc:VGNC:86518]	-1.011665922	0.0002762402566	0.02876163552
SOYvsFO	ENSSSCG00000050213	*0*	0	-1.011616693	7.36E-05	0.0136150245
SOYvsFO	ENSSSCG00000003148	*DBP*	D-box binding PAR bZIP transcription factor [Source:VGNC Symbol;Acc:VGNC:87167]	-0.9858513984	0.001207443272	0.06217248323
SOYvsFO	ENSSSCG00000032213	*DBI*	diazepam binding inhibitor. acyl-CoA binding protein [Source:HGNC Symbol;Acc:HGNC:2690]	-0.9755846737	0.0008151387947	0.04988881492
SOYvsFO	ENSSSCG00000048434	*0*	0	-0.9748661726	0.0004435608836	0.03531648183
SOYvsFO	ENSSSCG00000014314	*Novel gene*	F-box and leucine rich repeat protein 21. pseudogene [Source:NCBI gene (formerly Entrezgene);Acc:100517085]	-0.9731632326	0.001484950215	0.06756130634

SOYvsFO	ENSSSCG00000010258	*AIFM2*	apoptosis inducing factor mitochondria associated 2 [Source:VGNC Symbol;Acc:VGNC:85199]	-0.9651020611	0.0003573815704	0.0320795851
SOYvsFO	ENSSSCG00000007100	*SLC24A3*	solute carrier family 24 member 3 [Source:VGNC Symbol;Acc:VGNC:95501]	-0.9646591445	0.0005675931182	0.04000601002
SOYvsFO	ENSSSCG00000008852	*MAP9*	microtubule associated protein 9 [Source:NCBI gene (formerly Entrezgene);Acc:100512295]	-0.9631345279	0.002268727277	0.08535312189
SOYvsFO	ENSSSCG00000034811	*QDPR*	quinoid dihydropteridine reductase [Source:VGNC Symbol;Acc:VGNC:98232]	-0.9617516105	3.18E-05	0.008964072604
SOYvsFO	ENSSSCG00000010638	*TCF7L2*	transcription factor 7 like 2 [Source:VGNC Symbol;Acc:VGNC:93825]	-0.9560103053	0.002273039297	0.08535312189
SOYvsFO	ENSSSCG00000027525	*DHCR24*	tetratricopeptide repeat domain 22 [Source:NCBI gene (formerly Entrezgene);Acc:100620707]	-0.9503063473	3.47E-05	0.009467952064
SOYvsFO	ENSSSCG00000023478	*SLC46A1*	solute carrier family 46 member 1 [Source:VGNC Symbol;Acc:VGNC:93126]	-0.9434147255	0.001735302435	0.07243624098
SOYvsFO	ENSSSCG00000000720	*AKAP3*	A-kinase anchoring protein 3 [Source:VGNC Symbol;Acc:VGNC:85218]	-0.9412855225	3.13E-05	0.008964072604
SOYvsFO	ENSSSCG00000011129	*ITIH5*	inter-alpha-trypsin inhibitor heavy chain 5 [Source:VGNC Symbol;Acc:VGNC:95966]	-0.9398589312	0.002730049588	0.09315752542
SOYvsFO	ENSSSCG00000041951	*0*	0	-0.9365572724	0.0009090298577	0.05372335221
SOYvsFO	ENSSSCG00000037745	*Novel gene*	zinc finger and BTB domain containing 3 [Source:VGNC Symbol;Acc:VGNC:95067]	-0.9327362518	0.0005298560811	0.03857298083
SOYvsFO	ENSSSCG00000034689	*GPIHBP1*	glycosylphosphatidylinositol anchored high density lipoprotein binding protein 1 [Source:VGNC Symbol;Acc:VGNC:88588]	-0.9257555428	0.002135915337	0.08329077572
SOYvsFO	ENSSSCG00000009666	*EPHX2*	epoxide hydrolase 2 [Source:NCBI gene (formerly Entrezgene);Acc:414425]	-0.9235108953	0.001442591107	0.06633604773
SOYvsFO	ENSSSCG00000001780	*FAH*	fumarylacetoacetate hydrolase [Source:VGNC Symbol;Acc:VGNC:87881]	-0.9196801096	0.001362141243	0.06440109696
SOYvsFO	ENSSSCG00000013512	*PLIN4*	perilipin 4 [Source:VGNC Symbol;Acc:VGNC:91560]	-0.9127146312	0.002050898128	0.08094294436
SOYvsFO	ENSSSCG00000032977	*PPP1R3E*	protein phosphatase 1 regulatory subunit 3E [Source:VGNC Symbol;Acc:VGNC:91738]	-0.9075539647	0.003014030184	0.09873388783
SOYvsFO	ENSSSCG00000031407	*STKLD1*	serine/threonine kinase like domain containing 1 [Source:VGNC Symbol;Acc:VGNC:93559]	-0.9070522225	0.0001250349981	0.01886273594
SOYvsFO	ENSSSCG00000015819	*PLPP5*	phospholipid phosphatase 5 [Source:VGNC Symbol;Acc:VGNC:96061]	-0.9048277341	0.0002748210285	0.02876163552
SOYvsFO	ENSSSCG00000030386	*NUP205*	nucleoporin 205 [Source:VGNC Symbol;Acc:VGNC:90976]	-0.9021639292	0.00173061829	0.07241648016

SOYvsFO	ENSSSCG00000018056	*SRCIN1*	SRC kinase signaling inhibitor 1 [Source:VGNC Symbol;Acc:VGNC:93448]	-0.8876013095	0.001015024451	0.05723406723
SOYvsFO	ENSSSCG00000025777	*ESR1*	estrogen receptor 1 [Source:NCBI gene (formerly Entrezgene);Acc:397435]	-0.8805557853	0.002431224954	0.08638885694
SOYvsFO	ENSSSCG00000008901	*PAICS*	phosphoribosylaminoimidazole carboxylase and phosphoribosylaminoimidazolesuccinocarboxamide synthase [Source:VGNC Symbol;Acc:VGNC:91156]	-0.8764021987	0.0005315616035	0.03857298083
SOYvsFO	ENSSSCG00000034360	*CELSR2*	cadherin EGF LAG seven-pass G-type receptor 2 [Source:VGNC Symbol;Acc:VGNC:98748]	-0.874790368	0.001092560152	0.05910990531
SOYvsFO	ENSSSCG00000029538	*PPP2R1B*	protein phosphatase 2 scaffold subunit Abeta [Source:VGNC Symbol;Acc:VGNC:91747]	-0.8637971271	0.001043775807	0.05838710885
SOYvsFO	ENSSSCG00000023186	*CA4*	carbonic anhydrase 4 [Source:VGNC Symbol;Acc:VGNC:86100]	-0.8616758729	0.0002936909228	0.0298048322
SOYvsFO	ENSSSCG00000027903	*Novel gene*	phylloquinone omega-hydroxylase CYP4F2-like [Source:NCBI gene (formerly Entrezgene);Acc:110259328]	-0.8586685368	0.002571427997	0.0900680625
SOYvsFO	ENSSSCG00000051601	*0*	0	-0.8542989593	0.001459815173	0.0667710142
SOYvsFO	ENSSSCG00000007033	*AP3M2*	adaptor related protein complex 3 subunit mu 2 [Source:VGNC Symbol;Acc:VGNC:96369]	-0.8542926941	0.0002239341961	0.02620717765
SOYvsFO	ENSSSCG00000006324	*Novel gene*	aldehyde dehydrogenase 9 family member A1 [Source:NCBI gene (formerly Entrezgene);Acc:100153809]	-0.8530042856	0.002409916628	0.08629926059
SOYvsFO	ENSSSCG00000017198	*ACOX1*	acyl-CoA oxidase 1 [Source:VGNC Symbol;Acc:VGNC:85020]	-0.8521935564	0.0003407781975	0.03194691242
SOYvsFO	ENSSSCG00000004666	*Novel gene*	sulfide quinone oxidoreductase [Source:NCBI gene (formerly Entrezgene);Acc:100154990]	-0.852121892	0.002618977362	0.09080881588
SOYvsFO	ENSSSCG00000002314	*SMOC1*	SPARC related modular calcium binding 1 [Source:VGNC Symbol;Acc:VGNC:93259]	-0.8519488655	0.0006478022093	0.04351914998
SOYvsFO	ENSSSCG00000009492	*GPR180*	G protein-coupled receptor 180 [Source:VGNC Symbol;Acc:VGNC:88621]	-0.8419530767	0.0002633287279	0.02830454664
SOYvsFO	ENSSSCG00000027093	*FOLH1B*	folate hydrolase 1B [Source:NCBI gene (formerly Entrezgene);Acc:397677]	-0.8379555142	1.45E-06	0.00138259839
SOYvsFO	ENSSSCG00000050958	*0*	0	-0.8317336325	0.002591570485	0.09030038651
SOYvsFO	ENSSSCG00000016705	*HOXA3*	homeobox A3 [Source:VGNC Symbol;Acc:VGNC:88938]	-0.8296955526	0.0002285775467	0.02620717765
SOYvsFO	ENSSSCG00000009523	*Novel gene*	gamma-glutamylamine cyclotransferase [Source:VGNC Symbol;Acc:VGNC:88434]	-0.8293639195	0.001994987149	0.07997619812

SOYvsFO	ENSSSCG00000016703	*HOXA5*	homeobox A5 [Source:VGNC Symbol;Acc:VGNC:88939]	-0.7955454261	0.002868618105	0.09652457889
SOYvsFO	ENSSSCG00000009524	*TMTC4*	transmembrane O-mannosyltransferase targeting cadherins 4 [Source:VGNC Symbol;Acc:VGNC:94244]	-0.7732323916	0.0002442234959	0.02743128659
SOYvsFO	ENSSSCG00000010053	*Novel gene*	sperm antigen with calponin homology and coiled-coil domains 1 like [Source:NCBI gene (formerly Entrezgene);Acc:100519740]	-0.76594899	0.0002508747398	0.02783576629
SOYvsFO	ENSSSCG00000003815	*ALG6*	ALG6 alpha-1.3-glucosyltransferase [Source:VGNC Symbol;Acc:VGNC:85253]	-0.7636474339	1.93E-07	0.0003310800826
SOYvsFO	ENSSSCG00000027801	*VTN*	vitronectin [Source:VGNC Symbol;Acc:VGNC:98411]	-0.7550315032	0.002311388466	0.0854889379
SOYvsFO	ENSSSCG00000005668	*SH3GLB2*	SH3 domain containing GRB2 like. endophilin B2 [Source:VGNC Symbol;Acc:VGNC:92827]	-0.7531788965	0.0006040887168	0.04155647101
SOYvsFO	ENSSSCG00000028431	*HSD17B4*	hydroxysteroid 17-beta dehydrogenase 4 [Source:VGNC Symbol;Acc:VGNC:99760]	-0.748606307	0.0005539018638	0.0395269886
SOYvsFO	ENSSSCG00000022705	*SALL2*	spalt like transcription factor 2 [Source:VGNC Symbol;Acc:VGNC:92562]	-0.7476840018	0.001408525823	0.06546980297
SOYvsFO	ENSSSCG00000017635	*MKS1*	MKS transition zone complex subunit 1 [Source:VGNC Symbol;Acc:VGNC:96589]	-0.7466333379	0.0019714041	0.07940095483
SOYvsFO	ENSSSCG00000004205	*ARHGAP18*	Rho GTPase activating protein 18 [Source:VGNC Symbol;Acc:VGNC:85460]	-0.7401087286	0.0009505084303	0.05476956043
SOYvsFO	ENSSSCG00000023814	*FAIM*	Fas apoptotic inhibitory molecule [Source:VGNC Symbol;Acc:VGNC:87882]	-0.7194184989	0.002820053377	0.09541406709
SOYvsFO	ENSSSCG00000031683	*Novel gene*	putative surface protein SACOL0050 [Source:NCBI gene (formerly Entrezgene);Acc:102166270]	-0.7148230318	0.002299136938	0.0854889379
SOYvsFO	ENSSSCG00000015250	*ADAMTS15*	ADAM metallopeptidase with thrombospondin type 1 motif 15 [Source:VGNC Symbol;Acc:VGNC:85077]	-0.7142146973	0.002167668779	0.08334463949
SOYvsFO	ENSSSCG00000041416	*0*	0	-0.7070902347	0.002477976472	0.08764042677
SOYvsFO	ENSSSCG00000034614	*Novel gene*	RFT1 homolog [Source:NCBI gene (formerly Entrezgene);Acc:100622175]	-0.6939173852	0.00216505975	0.08334463949
SOYvsFO	ENSSSCG00000011470	*ABHD6*	abhydrolase domain containing 6. acylglycerol lipase [Source:VGNC Symbol;Acc:VGNC:84982]	-0.6933982654	0.002335796912	0.0854889379
SOYvsFO	ENSSSCG00000018041	*ALDH3A2*	aldehyde dehydrogenase 3 family member A2 [Source:VGNC Symbol;Acc:VGNC:85239]	-0.6865164741	2.46E-07	0.0003839651565
SOYvsFO	ENSSSCG00000025357	*LDAH*	lipid droplet associated hydrolase [Source:VGNC Symbol;Acc:VGNC:89666]	-0.6682150631	0.001682707111	0.07200289865
SOYvsFO	ENSSSCG00000003478	*CROCC*	ciliary rootlet coiled-coil. rootletin [Source:VGNC Symbol;Acc:VGNC:97946]	-0.6658411629	0.001080219341	0.05910990531

SOYvsFO	ENSSSCG00000007247	*KIF3B*	kinesin family member 3B [Source:VGNC Symbol;Acc:VGNC:96392]	-0.6520266887	0.002181594659	0.08351911876
SOYvsFO	ENSSSCG00000037598	*SNX10*	sorting nexin 10 [Source:VGNC Symbol;Acc:VGNC:93303]	-0.6356411305	0.002882006119	0.09661742931
SOYvsFO	ENSSSCG00000002265	*FAM174B*	family with sequence similarity 174 member B [Source:VGNC Symbol;Acc:VGNC:87932]	-0.6306567784	0.003059179481	0.09926748815
SOYvsFO	ENSSSCG00000016866	*GHR*	growth hormone receptor [Source:NCBI gene (formerly Entrezgene);Acc:397488]	-0.6296906312	0.0002250786536	0.02620717765
SOYvsFO	ENSSSCG00000017420	*CNP*	2'.3'-cyclic nucleotide 3' phosphodiesterase [Source:VGNC Symbol;Acc:VGNC:86840]	-0.6231192362	0.002629541642	0.0909916643
SOYvsFO	ENSSSCG00000027381	*GGCX*	gamma-glutamyl carboxylase [Source:VGNC Symbol;Acc:VGNC:88435]	-0.6170030989	0.002983120853	0.09873388783
SOYvsFO	ENSSSCG00000048082	*0*	0	-0.5971003897	0.001672003955	0.07200289865
SOYvsFO	ENSSSCG00000002298	*ZFYVE26*	zinc finger FYVE-type containing 26 [Source:VGNC Symbol;Acc:VGNC:95160]	-0.5892741252	0.001274828003	0.06316634762
SOYvsFO	ENSSSCG00000023728	*TECTA*	tubulin-specific chaperone cofactor E-like protein [Source:NCBI gene (formerly Entrezgene);Acc:100523684]	-0.5837585274	0.0002267843425	0.02620717765
SOYvsFO	ENSSSCG00000031139	*IKZF4*	IKAROS family zinc finger 4 [Source:VGNC Symbol;Acc:VGNC:89075]	-0.5525916205	0.000996937953	0.05639914117
SOYvsFO	ENSSSCG00000012102	*Novel gene*	transducin beta like 1 X-linked [Source:NCBI gene (formerly Entrezgene);Acc:102166569]	-0.5512753061	0.002946727327	0.09802285604
SOYvsFO	ENSSSCG00000006678	*FCGR1A*	Fc fragment of IgG. high affinity Ia. receptor (CD64) [Source:NCBI gene (formerly Entrezgene);Acc:613130]	-0.5166103113	0.001830945656	0.07533942472
SOYvsFO	ENSSSCG00000008604	*WDR35*	WD repeat domain 35 [Source:VGNC Symbol;Acc:VGNC:94916]	-0.5160250363	0.000147024488	0.02076808349
SOYvsFO	ENSSSCG00000014580	*RIC3*	RIC3 acetylcholine receptor chaperone [Source:VGNC Symbol;Acc:VGNC:92300]	-0.5120355578	0.002823919069	0.09541406709
SOYvsFO	ENSSSCG00000040334	*CBX6*	chromobox 6 [Source:VGNC Symbol;Acc:VGNC:97915]	-0.5096738469	0.00147885243	0.06746234507
SOYvsFO	ENSSSCG00000022282	*BDH2*	3-hydroxybutyrate dehydrogenase 2 [Source:VGNC Symbol;Acc:VGNC:85793]	-0.4964017527	6.56E-05	0.01310977365
SOYvsFO	ENSSSCG00000016971	*MCCC2*	methylcrotonoyl-CoA carboxylase 2 [Source:VGNC Symbol;Acc:VGNC:90064]	-0.4955924191	0.001646217189	0.07200289865
SOYvsFO	ENSSSCG00000033626	*SREBF1*	sterol regulatory element binding transcription factor 1 [Source:VGNC Symbol;Acc:VGNC:99083]	-0.4899446085	0.001708090363	0.07235403464
SOYvsFO	ENSSSCG00000007998	*RHBDL1*	rhomboid like 1 [Source:VGNC Symbol;Acc:VGNC:92277]	-0.4880396018	0.00167687896	0.07200289865

SOYvsFO	ENSSSCG00000021138	*CEP250*	centrosomal protein 250 [Source:VGNC Symbol;Acc:VGNC:95888]	-0.4811796034	0.0003404684546	0.03194691242
SOYvsFO	ENSSSCG00000038081	*AGPAT3*	1-acylglycerol-3-phosphate O-acyltransferase 3 [Source:VGNC Symbol;Acc:VGNC:85185]	-0.4777034506	0.002939667761	0.0979775313
SOYvsFO	ENSSSCG00000005620	*SH2D3C*	SH2 domain containing 3C [Source:VGNC Symbol;Acc:VGNC:92810]	-0.4715098419	0.001156737695	0.06028356025
SOYvsFO	ENSSSCG00000023080	*TPP1*	tripeptidyl peptidase 1 [Source:VGNC Symbol;Acc:VGNC:94342]	-0.4656455535	0.0003172793965	0.03118040607
SOYvsFO	ENSSSCG00000010826	*MTARC2*	mitochondrial amidoxime reducing component 2 [Source:HGNC Symbol;Acc:HGNC:26064]	-0.4632254012	0.001250351948	0.06287588537
SOYvsFO	ENSSSCG00000009021	*LRBA*	LPS responsive beige-like anchor protein [Source:VGNC Symbol;Acc:VGNC:98074]	-0.4565753995	0.0003436550062	0.03194691242
SOYvsFO	ENSSSCG00000002660	*MTHFSD*	methenyltetrahydrofolate synthetase domain containing [Source:VGNC Symbol;Acc:VGNC:90452]	-0.4413873825	3.76E-05	0.00966181679
SOYvsFO	ENSSSCG00000011896	*ADPRH*	ADP-ribosylarginine hydrolase [Source:VGNC Symbol;Acc:VGNC:85151]	-0.437878836	0.002993160281	0.09873388783
SOYvsFO	ENSSSCG00000004897	*ZCCHC2*	zinc finger CCHC-type containing 2 [Source:VGNC Symbol;Acc:VGNC:95109]	-0.4227643308	0.003010573573	0.09873388783
SOYvsFO	ENSSSCG00000009713	*CLCN3*	chloride voltage-gated channel 3 [Source:VGNC Symbol;Acc:VGNC:86727]	-0.4225102869	9.92E-05	0.01656344371
SOYvsFO	ENSSSCG00000035393	*SAAL1*	tryptophan hydroxylase 1 [Source:NCBI gene (formerly Entrezgene);Acc:100511002]	-0.4149916994	0.0003376559349	0.03194691242
SOYvsFO	ENSSSCG00000011157	*PITRM1*	pitrilysin metallopeptidase 1 [Source:VGNC Symbol;Acc:VGNC:95855]	-0.3990634654	0.000616703925	0.04225527531
SOYvsFO	ENSSSCG00000017895	*RABEP1*	rabaptin. RAB GTPase binding effector protein 1 [Source:VGNC Symbol;Acc:VGNC:99032]	-0.3962516955	6.80E-07	0.000779345682
SOYvsFO	ENSSSCG00000037077	*SHMT2*	serine hydroxymethyltransferase 2 [Source:VGNC Symbol;Acc:VGNC:92856]	-0.3902528461	0.002362843672	0.08585399169
SOYvsFO	ENSSSCG00000004349	*FAXC*	coenzyme Q3. methyltransferase [Source:NCBI gene (formerly Entrezgene);Acc:100152047]	-0.383229533	0.0009706964915	0.05563767323
SOYvsFO	ENSSSCG00000005613	*LRSAM1*	leucine rich repeat and sterile alpha motif containing 1 [Source:VGNC Symbol;Acc:VGNC:89864]	-0.3814371667	0.002027883463	0.08073041621
SOYvsFO	ENSSSCG00000014903	*CCDC90B*	coiled-coil domain containing 90B [Source:VGNC Symbol;Acc:VGNC:86328]	-0.3567966288	0.0001123855064	0.01793038297
SOYvsFO	ENSSSCG00000023604	*LAP3*	leucine aminopeptidase 3 [Source:VGNC Symbol;Acc:VGNC:89635]	-0.3482198987	0.001091968197	0.05910990531
SOYvsFO	ENSSSCG00000038231	*ABCD4*	ATP binding cassette subfamily D member 4 [Source:VGNC Symbol;Acc:VGNC:84964]	-0.3427026137	0.0001418868867	0.02067941252

SOYvsFO	ENSSSCG00000009338	*Novel gene*	FRY microtubule binding protein [Source:NCBI gene (formerly Entrezgene);Acc:100155799]	-0.3349112053	0.001045658188	0.05838710885
SOYvsFO	ENSSSCG00000000612	*ATF7IP*	activating transcription factor 7 interacting protein [Source:VGNC Symbol;Acc:VGNC:85611]	-0.3320385497	0.001889481132	0.07682103192
SOYvsFO	ENSSSCG00000010799	*COG7*	component of oligomeric golgi complex 7 [Source:VGNC Symbol;Acc:VGNC:86859]	-0.331149645	0.0009522094761	0.05476956043
SOYvsFO	ENSSSCG00000007466	*SLC9A8*	solute carrier family 9 member A8 [Source:VGNC Symbol;Acc:VGNC:95943]	-0.3291555299	0.002334693292	0.0854889379
SOYvsFO	ENSSSCG00000006192	*LACTB2*	lactamase beta 2 [Source:VGNC Symbol;Acc:VGNC:89615]	-0.3212189385	0.001111096306	0.05940210345
SOYvsFO	ENSSSCG00000028973	*PHACTR4*	phosphatase and actin regulator 4 [Source:VGNC Symbol;Acc:VGNC:98531]	-0.304943316	4.28E-05	0.0100371659
SOYvsFO	ENSSSCG00000014280	*Novel gene*	RAD50 double strand break repair protein [Source:NCBI gene (formerly Entrezgene);Acc:100522666]	-0.3041308365	0.0007579154488	0.04826173176
SOYvsFO	ENSSSCG00000003110	*ZC3H4*	zinc finger CCCH-type containing 4 [Source:VGNC Symbol;Acc:VGNC:95097]	-0.3035889272	0.0001190563783	0.01844623057
SOYvsFO	ENSSSCG00000017744	*SUZ12*	SUZ12 polycomb repressive complex 2 subunit [Source:VGNC Symbol;Acc:VGNC:93638]	-0.3001196246	0.001213880826	0.06231738043
SOYvsFO	ENSSSCG00000010025	*LIMK2*	LIM domain kinase 2 [Source:VGNC Symbol;Acc:VGNC:89728]	-0.2784994477	0.0003253077616	0.03160815189
SOYvsFO	ENSSSCG00000016070	*GTF3C3*	general transcription factor IIIC subunit 3 [Source:VGNC Symbol;Acc:VGNC:96339]	-0.2759700849	0.001642735644	0.07200289865
SOYvsFO	ENSSSCG00000003339	*INTS11*	integrator complex subunit 11 [Source:VGNC Symbol;Acc:VGNC:89159]	-0.2726576145	0.001916649324	0.07755890604
SOYvsFO	ENSSSCG00000029094	*PIK3R4*	phosphoinositide-3-kinase regulatory subunit 4 [Source:VGNC Symbol;Acc:VGNC:91446]	-0.2630790846	0.001299243139	0.06316634762
SOYvsFO	ENSSSCG00000005984	*ZHX1*	zinc fingers and homeoboxes 1 [Source:VGNC Symbol;Acc:VGNC:95164]	-0.2550499202	0.0007431704689	0.04786908511
SOYvsFO	ENSSSCG00000038682	*TAF1D*	TATA-box binding protein associated factor. RNA polymerase I subunit D [Source:VGNC Symbol;Acc:VGNC:93714]	-0.2375881412	0.0007665880904	0.04826173176
SOYvsFO	ENSSSCG00000005011	*NEMF*	nuclear export mediator factor [Source:VGNC Symbol;Acc:VGNC:90685]	-0.2366610335	0.0007429686241	0.04786908511
SOYvsFO	ENSSSCG00000001362	*MDC1*	mediator of DNA damage checkpoint 1 [Source:NCBI gene (formerly Entrezgene);Acc:100144453]	-0.2356554958	0.0003642531211	0.03229085142
SOYvsFO	ENSSSCG00000026959	*NPAT*	nuclear protein. coactivator of histone transcription [Source:VGNC Symbol;Acc:VGNC:90840]	-0.2288752412	0.001703571564	0.07235403464
SOYvsFO	ENSSSCG00000038943	*TOM1*	target of myb1 membrane trafficking protein [Source:VGNC Symbol;Acc:VGNC:95552]	0.2063651943	0.003075878625	0.09962139471

SOYvsFO	ENSSSCG00000013395	*BTBD10*	BTB domain containing 10 [Source:VGNC Symbol;Acc:VGNC:99595]	0.2255212967	0.0008122769718	0.04988881492
SOYvsFO	ENSSSCG00000009563	*TMCO3*	transmembrane and coiled-coil domains 3 [Source:VGNC Symbol;Acc:VGNC:94050]	0.2367702976	0.002197481816	0.08351911876
SOYvsFO	ENSSSCG00000025164	*TSC22D4*	TSC22 domain family protein 4 [Source:NCBI gene (formerly Entrezgene);Acc:100514038]	0.2531209313	0.002377980505	0.08589271358
SOYvsFO	ENSSSCG00000014855	*RPS3*	ribosomal protein S3 [Source:NCBI gene (formerly Entrezgene);Acc:733671]	0.2605943664	0.0002539802407	0.02799032089
SOYvsFO	ENSSSCG00000031627	*WBP4*	WW domain binding protein 4 [Source:VGNC Symbol;Acc:VGNC:94900]	0.2615215223	0.001087001067	0.05910990531
SOYvsFO	ENSSSCG00000020725	*ERBB3*	erb-b2 receptor tyrosine kinase 3 [Source:VGNC Symbol;Acc:VGNC:87760]	0.2625162544	0.002658892046	0.09134344083
SOYvsFO	ENSSSCG00000003580	*EYA3*	EYA transcriptional coactivator and phosphatase 3 [Source:VGNC Symbol;Acc:VGNC:87852]	0.2665908913	0.001193376824	0.06181835729
SOYvsFO	ENSSSCG00000038466	*EIF4E2*	eukaryotic translation initiation factor 4E family member 2 [Source:VGNC Symbol;Acc:VGNC:96269]	0.2990750363	0.0009254821115	0.05432232544
SOYvsFO	ENSSSCG00000017772	*SDF2*	stromal cell derived factor 2 [Source:VGNC Symbol;Acc:VGNC:98306]	0.3189350031	0.001636829835	0.07199539513
SOYvsFO	ENSSSCG00000036014	*RPLP0*	ribosomal protein lateral stalk subunit P0 [Source:NCBI gene (formerly Entrezgene);Acc:100049695]	0.3220940336	0.001267985682	0.06316634762
SOYvsFO	ENSSSCG00000041401	*0*	0	0.3276967683	0.001084062713	0.05910990531
SOYvsFO	ENSSSCG00000004207	*0*	0	0.3511383706	0.001138411954	0.06019228851
SOYvsFO	ENSSSCG00000004926	*PDCD7*	programmed cell death 7 [Source:NCBI gene (formerly Entrezgene);Acc:100152985]	0.3731484944	0.001865988372	0.07622628985
SOYvsFO	ENSSSCG00000006530	*EFNA1*	ephrin A1 [Source:VGNC Symbol;Acc:VGNC:98789]	0.42822058	0.0006846825157	0.04492024267
SOYvsFO	ENSSSCG00000025245	*ARMC5*	armadillo repeat containing 5 [Source:VGNC Symbol;Acc:VGNC:85529]	0.4405465676	0.0005515507512	0.03952320758
SOYvsFO	ENSSSCG00000006581	*Novel gene*	S100 calcium binding protein A16 [Source:NCBI gene (formerly Entrezgene);Acc:100155146]	0.4449736593	0.002300998765	0.0854889379
SOYvsFO	ENSSSCG00000038234	*TMEM175*	transmembrane protein 175 [Source:VGNC Symbol;Acc:VGNC:94111]	0.4536587794	0.002323509542	0.0854889379
SOYvsFO	ENSSSCG00000036529	*Novel gene*	RIO kinase 2 [Source:NCBI gene (formerly Entrezgene);Acc:100511553]	0.4577284063	0.0003598793877	0.0320795851
SOYvsFO	ENSSSCG00000037755	*NSMCE2*	NSE2 (MMS21) homolog. SMC5-SMC6 complex SUMO ligase [Source:VGNC Symbol;Acc:VGNC:98828]	0.4691965201	0.001397486397	0.0652361174
SOYvsFO	ENSSSCG00000026414	*0*	0	0.4888496962	9.81E-05	0.01654717889
SOYvsFO	ENSSSCG00000035293	*Novel gene*	insulin like growth factor 2 [Source:NCBI gene (formerly Entrezgene);Acc:396916]	0.4933799444	0.001147526647	0.06019228851

SOYvsFO	ENSSSCG00000034980	*IRF8*	interferon regulatory factor 8 [Source:VGNC Symbol;Acc:VGNC:89211]	0.5126148966	0.002719162729	0.09297049825
SOYvsFO	ENSSSCG00000001787	*IL16*	interleukin 16 [Source:VGNC Symbol;Acc:VGNC:89084]	0.5549611149	0.0001132143979	0.01793038297
SOYvsFO	ENSSSCG00000023315	*THOC6*	THO complex 6 [Source:VGNC Symbol;Acc:VGNC:93959]	0.5601745794	0.001945352605	0.07853561996
SOYvsFO	ENSSSCG00000038829	*Novel gene*	putative MORF4 family-associated protein 1-like protein UPP [Source:NCBI gene (formerly Entrezgene);Acc:100621428]	0.604657803	7.78E-05	0.01408785653
SOYvsFO	ENSSSCG00000036521	*TNFSF13*	TNF superfamily member 13 [Source:VGNC Symbol;Acc:VGNC:98380]	0.6354385599	0.0004152301672	0.03416807855
SOYvsFO	ENSSSCG00000003616	*FAM167B*	family with sequence similarity 167 member B [Source:VGNC Symbol;Acc:VGNC:87925]	0.6472855184	0.001546826109	0.06927686309
SOYvsFO	ENSSSCG00000040461	*CDKN1C*	cyclin dependent kinase inhibitor 1C [Source:VGNC Symbol;Acc:VGNC:86516]	0.6621212023	0.0004273034606	0.03475036109
SOYvsFO	ENSSSCG00000033833	*DUSP18*	dual specificity phosphatase 18 [Source:NCBI gene (formerly Entrezgene);Acc:100156909]	0.6624241225	0.0006426094742	0.04339349133
SOYvsFO	ENSSSCG00000010981	*NUDT2*	nudix hydrolase 2 [Source:VGNC Symbol;Acc:VGNC:96457]	0.6739100102	0.002199916316	0.08351911876
SOYvsFO	ENSSSCG00000009896	*BICDL1*	BICD family like cargo adaptor 1 [Source:VGNC Symbol;Acc:VGNC:85820]	0.6883737096	0.002322290711	0.0854889379
SOYvsFO	ENSSSCG00000003219	*FAM71E1*	family with sequence similarity 71 member E1 [Source:VGNC Symbol;Acc:VGNC:87979]	0.6937838093	2.24E-05	0.007148986444
SOYvsFO	ENSSSCG00000016571	*0*	0	0.7051618386	0.003003231977	0.09873388783
SOYvsFO	ENSSSCG00000011723	*MME*	membrane metalloendopeptidase [Source:VGNC Symbol;Acc:VGNC:90265]	0.7180394811	0.001618965805	0.07157576844
SOYvsFO	ENSSSCG00000031374	*0*	0	0.7232833858	0.0003779508737	0.03272143052
SOYvsFO	ENSSSCG00000021184	*OSGIN2*	oxidative stress induced growth inhibitor family member 2 [Source:VGNC Symbol;Acc:VGNC:91080]	0.7561649403	0.0006009841556	0.04150893779
SOYvsFO	ENSSSCG00000025589	*SMIM26*	small integral membrane protein 26 [Source:HGNC Symbol;Acc:HGNC:43430]	0.7586815639	0.001858805046	0.07611364089
SOYvsFO	ENSSSCG00000010655	*GFRA1*	GDNF family receptor alpha 1 [Source:VGNC Symbol;Acc:VGNC:88428]	0.7833114578	0.0007193503213	0.04668447859
SOYvsFO	ENSSSCG00000036941	*AKR1E2*	aldo-keto reductase family 1 member E2 [Source:VGNC Symbol;Acc:VGNC:96003]	0.8167867967	0.0003600046473	0.0320795851
SOYvsFO	ENSSSCG00000033526	*BAG2*	BAG cochaperone 2 [Source:VGNC Symbol;Acc:VGNC:85744]	0.8524050327	0.001537091815	0.06920132207
SOYvsFO	ENSSSCG00000024671	*WNT9A*	Wnt family member 9A [Source:VGNC Symbol;Acc:VGNC:94978]	0.8690737677	0.0004019241961	0.03388378591
SOYvsFO	ENSSSCG00000015570	*IVNS1ABP*	influenza virus NS1A binding protein [Source:NCBI gene (formerly Entrezgene);Acc:100302027]	0.8727405853	0.003022345515	0.09877797734

SOYvsFO	ENSSSCG00000024752	*ALDH4A1*	aldehyde dehydrogenase 4 family member A1 [Source:VGNC Symbol;Acc:VGNC:85240]	0.9143896295	0.002889890397	0.09669325884
SOYvsFO	ENSSSCG00000046155	*0*	0	0.9170379085	1.28E-05	0.005459864706
SOYvsFO	ENSSSCG00000015037	*IL18*	interleukin 18 [Source:NCBI gene (formerly Entrezgene);Acc:397057]	0.9323366495	0.001299463322	0.06316634762
SOYvsFO	ENSSSCG00000021041	*Novel gene*	peptidase M20 domain containing 1 [Source:NCBI gene (formerly Entrezgene);Acc:100627595]	0.9346364175	0.00175745992	0.07300675292
SOYvsFO	ENSSSCG00000044010	*0*	0	0.9584477754	0.003049366662	0.0991361207
SOYvsFO	ENSSSCG00000022635	*BEX4*	brain expressed X-linked 4 [Source:NCBI gene (formerly Entrezgene);Acc:100627578]	0.9653356324	0.0003865681573	0.03307561776
SOYvsFO	ENSSSCG00000038579	*DKKL1*	dickkopf like acrosomal protein 1 [Source:VGNC Symbol;Acc:VGNC:87324]	0.9736537408	0.0009814588203	0.05589115494
SOYvsFO	ENSSSCG00000010507	*TLL2*	tolloid like 2 [Source:VGNC Symbol;Acc:VGNC:94019]	1.030323622	0.001669870021	0.07200289865
SOYvsFO	ENSSSCG00000046723	*0*	0	1.047843323	0.00259906334	0.09030038651
SOYvsFO	ENSSSCG00000014448	*ARSI*	arylsulfatase family member I [Source:HGNC Symbol;Acc:HGNC:32521]	1.066907519	0.0005175666017	0.03819615319
SOYvsFO	ENSSSCG00000007816	*IL21R*	interleukin 21 receptor [Source:VGNC Symbol;Acc:VGNC:89096]	1.106847749	0.001228967865	0.06247052669
SOYvsFO	ENSSSCG00000016334	*SCLY*	selenocysteine lyase [Source:VGNC Symbol;Acc:VGNC:98302]	1.11538992	4.32E-05	0.0100371659
SOYvsFO	ENSSSCG00000017251	*SOX9*	SRY-box transcription factor 9 [Source:VGNC Symbol;Acc:VGNC:99053]	1.128716007	0.0007518456024	0.04806780918
SOYvsFO	ENSSSCG00000034185	*SNORA73*	Small nucleolar RNA SNORA73 family [Source:RFAM;Acc:RF00045]	1.135158775	0.001615817877	0.07157576844
SOYvsFO	ENSSSCG00000011195	*GALNT15*	polypeptide N-acetylgalactosaminyltransferase 15 [Source:VGNC Symbol;Acc:VGNC:88331]	1.140262694	0.002075599933	0.08131245479
SOYvsFO	ENSSSCG00000001247	*ZFP57*	ZFP57 zinc finger protein [Source:NCBI gene (formerly Entrezgene);Acc:100141415]	1.148217645	0.002873623933	0.09652457889
SOYvsFO	ENSSSCG00000016557	*CPA1*	carboxypeptidase A1 [Source:VGNC Symbol;Acc:VGNC:86930]	1.14884741	0.001292573826	0.06316634762
SOYvsFO	ENSSSCG00000046945	*0*	0	1.158698843	0.00114798643	0.06019228851
SOYvsFO	ENSSSCG00000017770	*PROCA1*	protein interacting with cyclin A1 [Source:VGNC Symbol;Acc:VGNC:91828]	1.162591798	0.001322510723	0.06371019446
SOYvsFO	ENSSSCG00000013892	*KCNN1*	potassium calcium-activated channel subfamily N member 1 [Source:VGNC Symbol;Acc:VGNC:89379]	1.163911469	0.002488939915	0.08771473086
SOYvsFO	ENSSSCG00000041461	*0*	0	1.167575421	0.002171089574	0.08334463949
SOYvsFO	ENSSSCG00000006140	*CA2*	carbonic anhydrase 2 [Source:VGNC Symbol;Acc:VGNC:98746]	1.170838357	0.0002194584654	0.02602928751

SOYvsFO	ENSSSCG00000010607	*COL17A1*	collagen type XVII alpha 1 chain [Source:VGNC Symbol;Acc:VGNC:86868]	1.19315618	0.002400779068	0.08629926059
SOYvsFO	ENSSSCG00000012066	*KCNJ15*	potassium inwardly rectifying channel subfamily J member 15 [Source:VGNC Symbol;Acc:VGNC:89355]	1.194318125	0.001173653515	0.06098034183
SOYvsFO	ENSSSCG00000010530	*CRTAC1*	cartilage acidic protein 1 [Source:VGNC Symbol;Acc:VGNC:87004]	1.196827336	0.0003235143108	0.03160815189
SOYvsFO	ENSSSCG00000022846	*SLC4A3*	solute carrier family 4 member 3 [Source:VGNC Symbol;Acc:VGNC:95505]	1.198545724	0.0004877173639	0.03727894767
SOYvsFO	ENSSSCG00000051557	*0*	0	1.202311461	0.0003713553326	0.03254291992
SOYvsFO	ENSSSCG00000044892	*0*	0	1.20764796	0.001807807829	0.07473720922
SOYvsFO	ENSSSCG00000043645	*0*	0	1.253319755	8.06E-05	0.01443176942
SOYvsFO	ENSSSCG00000003508	*KIF17*	kinesin family member 17 [Source:VGNC Symbol;Acc:VGNC:98486]	1.261669433	0.00172913837	0.07241648016
SOYvsFO	ENSSSCG00000014823	*P2RY6*	pyrimidinergic receptor P2Y6 [Source:VGNC Symbol;Acc:VGNC:91128]	1.269576484	0.001359308143	0.06440109696
SOYvsFO	ENSSSCG00000010039	*SLC5A4*	solute carrier family 5 member 4 [Source:NCBI gene (formerly Entrezgene);Acc:397376]	1.278955614	1.84E-05	0.006467956366
SOYvsFO	ENSSSCG00000008449	*SLC3A1*	solute carrier family 3 member 1 [Source:VGNC Symbol;Acc:VGNC:93111]	1.291258836	0.0004314768345	0.03483820939
SOYvsFO	ENSSSCG00000010077	*Novel gene*	immunoglobulin lambda-like polypeptide 5 [Source:NCBI gene (formerly Entrezgene);Acc:100523213]	1.300943184	0.00234127746	0.0854889379
SOYvsFO	ENSSSCG00000023539	*MBOAT2*	membrane bound O-acyltransferase domain containing 2 [Source:VGNC Symbol;Acc:VGNC:90058]	1.303490913	0.000117509203	0.01837202976
SOYvsFO	ENSSSCG00000050092	*0*	0	1.306456548	0.001099268097	0.05921138642
SOYvsFO	ENSSSCG00000033637	*Novel gene*	chromosome 13 C3orf52 homolog [Source:VGNC Symbol;Acc:VGNC:85935]	1.324839687	0.002405865767	0.08629926059
SOYvsFO	ENSSSCG00000043494	*0*	0	1.354354715	0.0004499792029	0.03548275244
SOYvsFO	ENSSSCG00000023004	*FZD9*	frizzled class receptor 9 [Source:VGNC Symbol;Acc:VGNC:88284]	1.363186426	0.001066931217	0.05910990531
SOYvsFO	ENSSSCG00000000937	*MYF5*	myogenic factor 5 [Source:VGNC Symbol;Acc:VGNC:90508]	1.392420274	0.001725710054	0.07241648016
SOYvsFO	ENSSSCG00000018063	*0*	0	1.395575914	0.0002946169016	0.0298048322
SOYvsFO	ENSSSCG00000045913	*0*	0	1.421895702	0.002643888881	0.09112839677
SOYvsFO	ENSSSCG00000032795	*IL1RL1*	interleukin 1 receptor like 1 [Source:NCBI gene (formerly Entrezgene);Acc:100127134]	1.450424106	0.0005505267715	0.03952320758
SOYvsFO	ENSSSCG00000000749	*SLC6A12*	solute carrier family 6 member 12 [Source:VGNC Symbol;Acc:VGNC:93155]	1.45111788	0.001453012994	0.06663711325

SOYvsFO	ENSSSCG00000037347	*Novel gene*	R3H and coiled-coil domain-containing protein 1-like [Source:NCBI gene (formerly Entrezgene);Acc:110258721]	1.466124195	0.00157140442	0.07019483954
SOYvsFO	ENSSSCG00000017909	*CHRNE*	cholinergic receptor nicotinic epsilon subunit [Source:HGNC Symbol;Acc:HGNC:1966]	1.484008236	0.001300202759	0.06316634762
SOYvsFO	ENSSSCG00000006745	*CASQ2*	calsequestrin 2 [Source:VGNC Symbol;Acc:VGNC:86206]	1.551022577	0.0001225419002	0.01865022654
SOYvsFO	ENSSSCG00000038600	*PRSS8*	serine protease 8 [Source:VGNC Symbol;Acc:VGNC:91888]	1.602243854	0.001683054149	0.07200289865
SOYvsFO	ENSSSCG00000010201	*RASGEF1A*	RasGEF domain family member 1A [Source:VGNC Symbol;Acc:VGNC:92108]	1.611503237	0.0006434085527	0.04339349133
SOYvsFO	ENSSSCG00000017915	*VMO1*	vitelline membrane outer layer 1 homolog [Source:VGNC Symbol;Acc:VGNC:94833]	1.61393017	0.0003427684297	0.03194691242
SOYvsFO	ENSSSCG00000010162	*SLC35F3*	solute carrier family 35 member F3 [Source:VGNC Symbol;Acc:VGNC:93083]	1.660544126	0.002714118721	0.09297049825
SOYvsFO	ENSSSCG00000011259	*SCN5A*	sodium voltage-gated channel alpha subunit 5 [Source:VGNC Symbol;Acc:VGNC:92637]	1.692452596	0.001207408102	0.06217248323
SOYvsFO	ENSSSCG00000009498	*Novel gene*	multidrug resistance-associated protein 4 [Source:NCBI gene (formerly Entrezgene);Acc:100738425]	1.711802414	0.000686941727	0.04492024267
SOYvsFO	ENSSSCG00000021569	*MMP25*	matrix metallopeptidase 25 [Source:VGNC Symbol;Acc:VGNC:90276]	1.737928301	0.001112191959	0.05940210345
SOYvsFO	ENSSSCG00000031106	*PLA2G2D*	phospholipase A2 group IID [Source:VGNC Symbol;Acc:VGNC:91491]	1.765580927	0.003026863243	0.09877797734
SOYvsFO	ENSSSCG00000018699	*0*	0	1.778425969	0.003006149248	0.09873388783
SOYvsFO	ENSSSCG00000023031	*TNNT2*	Sus scrofa troponin T2. cardiac type (TNNT2). transcript variant 4. mRNA. [Source:RefSeq mRNA;Acc:NM_001353845]	1.792034031	0.0003589031552	0.0320795851
SOYvsFO	ENSSSCG00000044382	*0*	0	1.849708608	0.001054642114	0.05869817176
SOYvsFO	ENSSSCG00000004225	*TPD52L1*	TPD52 like 1 [Source:VGNC Symbol;Acc:VGNC:94334]	1.921342506	0.001381167415	0.06472293515
SOYvsFO	ENSSSCG00000008118	*PROM2*	prominin 2 [Source:VGNC Symbol;Acc:VGNC:91833]	1.952329371	0.0005813251142	0.04047623204
SOYvsFO	ENSSSCG00000004357	*SIM1*	SIM bHLH transcription factor 1 [Source:VGNC Symbol;Acc:VGNC:92876]	2.05018456	0.002319377943	0.0854889379
SOYvsFO	ENSSSCG00000010601	*CALHM1*	calcium homeostasis modulator protein 2 [Source:NCBI gene (formerly Entrezgene);Acc:100157433]	2.092432136	0.002155079336	0.08329077572
SOYvsFO	ENSSSCG00000037292	*PLA2G4E*	phospholipase A2 group IVE [Source:VGNC Symbol;Acc:VGNC:91497]	2.168358099	0.0009737725109	0.05563767323
SOYvsFO	ENSSSCG00000004803	*ACTC1*	actin alpha cardiac muscle 1 [Source:VGNC Symbol;Acc:VGNC:85040]	2.177356405	0.0002989772658	0.02984347242
SOYvsFO	ENSSSCG00000005486	*KIF12*	kinesin family member 12 [Source:VGNC Symbol;Acc:VGNC:89453]	2.179414256	0.001577288068	0.07027513004
SOYvsFO	ENSSSCG00000010632	*TECTB*	tectorin beta [Source:VGNC Symbol;Acc:VGNC:93860]	2.197342221	0.002413649514	0.08629926059

SOYvsFO	ENSSSCG00000011277	*CCK*	cholecystokinin [Source:VGNC Symbol;Acc:VGNC:86334]	2.289480942	0.0008038247327	0.04957161555
SOYvsFO	ENSSSCG00000017307	*MYL4*	myosin light chain 4 [Source:VGNC Symbol;Acc:VGNC:90516]	2.328312564	0.001670852503	0.07200289865
SOYvsFO	ENSSSCG00000037563	*5_8S_rRNA*	5.8S ribosomal RNA [Source:RFAM;Acc:RF00002]	2.34533725	2.59E-05	0.007957577524
SOYvsFO	ENSSSCG00000033532	*SBK2*	serine/threonine-protein kinase SBK2 [Source:NCBI gene (formerly Entrezgene);Acc:100621492]	2.450149641	0.0008868008831	0.05314007522
SOYvsFO	ENSSSCG00000038816	*Novel gene*	crystallin alpha A [Source:NCBI gene (formerly Entrezgene);Acc:110256286]	2.53380691	0.001879439839	0.07659385391
SOYvsFO	ENSSSCG00000032708	*Metazoa_SRP*	Metazoan signal recognition particle RNA [Source:RFAM;Acc:RF00017]	2.675036028	0.002215660414	0.08374709408
SOYvsFO	ENSSSCG00000038965	*ARC*	activity regulated cytoskeleton associated protein [Source:VGNC Symbol;Acc:VGNC:85442]	2.731971872	0.0002003004392	0.02487210892
SOYvsFO	ENSSSCG00000049049	*0*	0	2.827826477	3.89E-08	0.0001173311129
SOYvsFO	ENSSSCG00000038188	*Novel gene*	left-right determination factor 2 [Source:NCBI gene (formerly Entrezgene);Acc:100524517]	2.847450779	0.001349670065	0.06440109696
SOYvsFO	ENSSSCG00000042075	*0*	0	2.851245126	0.0007075230516	0.04609083879
SOYvsFO	ENSSSCG00000034943	*GDF6*	growth differentiation factor 6 [Source:VGNC Symbol;Acc:VGNC:88402]	2.852921915	0.001652760444	0.07200289865
SOYvsFO	ENSSSCG00000007760	*PRSS36*	serine protease 36 [Source:NCBI gene (formerly Entrezgene);Acc:100511374]	2.895938259	3.75E-05	0.00966181679
SOYvsFO	ENSSSCG00000040520	*0*	0	3.013728621	0.002061461195	0.08094294436
SOYvsFO	ENSSSCG00000043795	*0*	0	3.128603657	5.29E-05	0.01182006514
SOYvsFO	ENSSSCG00000032177	*MYO3B*	myosin IIIB [Source:NCBI gene (formerly Entrezgene);Acc:100621555]	3.449198172	0.0003885236303	0.03307836333
SOYvsFO	ENSSSCG00000023048	*Metazoa_SRP*	Metazoan signal recognition particle RNA [Source:RFAM;Acc:RF00017]	3.528337675	0.0003412774317	0.03194691242

Diet_comparison Muscle	**Gene stable ID**	***Gene name***	**Gene description**	**log2 fold change**	**p-value**	**FDR**
COxFO	ENSSSCG00000051166	*0*	0	-4.844835369	1.32E-07	0.0005892058173
COxFO	ENSSSCG00000049731	*0*	0	-4.209527935	4.44E-05	0.0441086194
COxFO	ENSSSCG00000022568	*TMPRSS3*	transmembrane serine protease 3 [Source:VGNC Symbol;Acc:VGNC:94235]	-3.475449751	5.32E-05	0.05002488318
COxFO	ENSSSCG00000036013	*Novel gene*	trypsinogen [Source:NCBI gene (formerly Entrezgene);Acc:100302368]	-2.417277954	2.05E-05	0.0333156122
COxFO	ENSSSCG00000032691	*ANKRD66*	ankyrin repeat domain 66 [Source:NCBI gene (formerly Entrezgene);Acc:100155360]	-2.327352614	0.000142857338	0.09595204146

COxFO	ENSSSCG00000046916	*0*	0	-2.146114042	0.0001009240549	0.07846187064
COxFO	ENSSSCG00000018044	*ALDH3A1*	aldehyde dehydrogenase 3 family member A1 [Source:VGNC Symbol;Acc:VGNC:85238]	-2.072835213	5.01E-09	8.96E-05
COxFO	ENSSSCG00000010554	*SCD*	stearoyl-CoA desaturase [Source:NCBI gene (formerly Entrezgene);Acc:396670]	-1.622802592	2.31E-05	0.0344399524
COxFO	ENSSSCG00000016487	*MGAM2*	maltase-glucoamylase 2 (putative) [Source:NCBI gene (formerly Entrezgene);Acc:100623494]	-1.547529388	2.89E-05	0.03694680982
COxFO	ENSSSCG00000000687	*CD4*	CD4 molecule [Source:VGNC Symbol;Acc:VGNC:86417]	-1.524053018	1.84E-05	0.03289038034
COxFO	ENSSSCG00000041416	*0*	0	-1.018312212	1.18E-06	0.004206143557
COxFO	ENSSSCG00000040956	*0*	0	-0.9231303829	3.67E-05	0.03859256411
COxFO	ENSSSCG00000027093	*FOLH1B*	folate hydrolase 1B [Source:NCBI gene (formerly Entrezgene);Acc:397677]	-0.9134023154	1.14E-05	0.02923389134
COxFO	ENSSSCG00000000720	*AKAP3*	A-kinase anchoring protein 3 [Source:VGNC Symbol;Acc:VGNC:85218]	-0.8842699301	3.37E-06	0.01004930785
COxFO	ENSSSCG00000038963	*Novel gene*	protein kinase X-linked [Source:NCBI gene (formerly Entrezgene);Acc:106504268]	-0.8492753879	0.0001661572463	0.09900466846
COxFO	ENSSSCG00000015786	*PRIMPOL*	primase and DNA directed polymerase [Source:VGNC Symbol;Acc:VGNC:96133]	-0.7005861528	0.0001381103196	0.09595204146
COxFO	ENSSSCG00000018041	*ALDH3A2*	aldehyde dehydrogenase 3 family member A2 [Source:VGNC Symbol;Acc:VGNC:85239]	-0.6022289152	2.75E-05	0.03694680982
COxFO	ENSSSCG00000009093	*BBS7*	Bardet-Biedl syndrome 7 [Source:HGNC Symbol;Acc:HGNC:18758]	-0.5535627345	0.0001771796539	0.09900466846
COxFO	ENSSSCG00000038960	*Novel gene*	heparan-alpha-glucosaminide N-acetyltransferase [Source:NCBI gene (formerly Entrezgene);Acc:100517562]	-0.5449831267	0.0001144656979	0.08528171437
COxFO	ENSSSCG00000003815	*ALG6*	ALG6 alpha-1.3-glucosyltransferase [Source:VGNC Symbol;Acc:VGNC:85253]	-0.5008557874	3.49E-05	0.03859256411
COxFO	ENSSSCG00000009021	*LRBA*	LPS responsive beige-like anchor protein [Source:VGNC Symbol;Acc:VGNC:98074]	-0.4708032916	3.42E-05	0.03859256411
COxFO	ENSSSCG00000010523	*HOGA1*	4-hydroxy-2-oxoglutarate aldolase 1 [Source:VGNC Symbol;Acc:VGNC:88927]	0.5003355871	0.0001749343858	0.09900466846
COxFO	ENSSSCG00000036941	*AKR1E2*	aldo-keto reductase family 1 member E2 [Source:VGNC Symbol;Acc:VGNC:96003]	1.214382566	4.56E-08	0.0004077674524
COxFO	ENSSSCG00000043494	*0*	0	1.335536516	0.0001506294319	0.09619303115
COxFO	ENSSSCG00000044892	*0*	0	1.366640616	0.0001650882429	0.09900466846

COxFO	ENSSSCG00000000917	*KERA*	keratocan [Source:VGNC Symbol;Acc:VGNC:89420]	1.544921063	8.52E-05	0.0692154631
COxFO	ENSSSCG00000023031	*TNNT2*	Sus scrofa troponin T2. cardiac type (TNNT2). transcript variant 4. mRNA. [Source:RefSeq mRNA;Acc:NM_001353845]	1.999612855	1.68E-05	0.03289038034
COxFO	ENSSSCG00000044272	*0*	0	2.068659236	1.79E-05	0.03289038034
COxFO	ENSSSCG00000018005	*MYH8*	myosin-8 [Source:NCBI gene (formerly Entrezgene);Acc:110255887]	2.492362984	6.43E-05	0.05747591422
COxFO	ENSSSCG00000005486	*KIF12*	kinesin family member 12 [Source:VGNC Symbol;Acc:VGNC:89453]	2.597817667	0.0001448859191	0.09595204146
COxFO	ENSSSCG00000031581	*Novel gene*	otoraplin [Source:NCBI gene (formerly Entrezgene);Acc:110258854]	2.695572634	8.16E-05	0.0692154631
COxFO	ENSSSCG00000049049	*0*	0	2.922677979	9.90E-08	0.0005892058173

Diet_comparison Liver	**Gene stable ID**	***Gene name***	**Gene description**	**log2 fold change**	**p-value**	**FDR**
COvsSOY	ENSSSCG00000014861	*MOGAT2*	2-acylglycerol O-acyltransferase 2-like [Source:NCBI gene (formerly Entrezgene);Acc:110255553]	-4.717780986	5.42E-07	0.002977668262
COvsSOY	ENSSSCG00000051166	*0*	0	-3.850692626	2.69E-05	0.01583287404
COvsSOY	ENSSSCG00000026176	*CHRM3*	cholinergic receptor muscarinic 3 [Source:VGNC Symbol;Acc:VGNC:86664]	-3.171524715	0.0001103036005	0.03663125592
COvsSOY	ENSSSCG00000043197	*0*	0	-2.589521718	3.61E-05	0.01917459384
COvsSOY	ENSSSCG00000051024	*0*	0	-2.574375048	4.15E-05	0.02092120428
COvsSOY	ENSSSCG00000015747	*Novel gene*	myomesin 2 [Source:NCBI gene (formerly Entrezgene);Acc:100523824]	-2.461046333	1.72E-05	0.01583287404
COvsSOY	ENSSSCG00000003006	*CYP2B22*	cytochrome P450 2B4-like [Source:NCBI gene (formerly Entrezgene);Acc:102165015]	-2.449178341	5.72E-06	0.009426908959
COvsSOY	ENSSSCG00000047471	*0*	0	-2.331963203	0.0007409049285	0.09436330265
COvsSOY	ENSSSCG00000006238	*CYP7A1*	cytochrome P450 family 7 subfamily A member 1 [Source:VGNC Symbol;Acc:VGNC:98774]	-2.31140525	0.0007497326933	0.09436330265
COvsSOY	ENSSSCG00000038322	*Novel gene*	diacylglycerol O-acyltransferase 2-like [Source:NCBI gene (formerly Entrezgene);Acc:110259135]	-2.230329329	9.00E-06	0.01293576522
COvsSOY	ENSSSCG00000010632	*TECTB*	tectorin beta [Source:VGNC Symbol;Acc:VGNC:93860]	-2.221151576	7.46E-05	0.02735053857
COvsSOY	ENSSSCG00000014314	*Novel gene*	F-box and leucine rich repeat protein 21. pseudogene [Source:NCBI gene (formerly Entrezgene);Acc:100517085]	-2.178512609	4.06E-06	0.009258811916
COvsSOY	ENSSSCG00000051703	*0*	0	-2.1126961	0.0006397871167	0.08680212563
COvsSOY	ENSSSCG00000050735	*0*	0	-2.059416769	1.73E-05	0.01583287404
COvsSOY	ENSSSCG00000022842	*0*	0	-1.993629255	1.53E-05	0.01583287404

COvsSOY	ENSSSCG00000009798	*B3GNT4*	UDP-GlcNAc:betaGal beta-1.3-N-acetylglucosaminyltransferase 4 [Source:VGNC Symbol;Acc:VGNC:85725]	-1.91733984	3.91E-07	0.002977668262
COvsSOY	ENSSSCG00000010428	*DKK1*	dickkopf WNT signaling pathway inhibitor 1 [Source:VGNC Symbol;Acc:VGNC:87321]	-1.882122573	1.05E-05	0.01329622636
COvsSOY	ENSSSCG00000038171	*Novel gene*	acyl-coenzyme A amino acid N-acyltransferase 2 [Source:NCBI gene (formerly Entrezgene);Acc:100515185]	-1.800675981	0.0004505587887	0.07819803482
COvsSOY	ENSSSCG00000002475	*SERPINA6*	serpin family A member 6 [Source:NCBI gene (formerly Entrezgene);Acc:396736]	-1.74269664	2.87E-06	0.009258811916
COvsSOY	ENSSSCG00000003148	*DBP*	D-box binding PAR bZIP transcription factor [Source:VGNC Symbol;Acc:VGNC:87167]	-1.574868024	2.02E-07	0.002977668262
COvsSOY	ENSSSCG00000034656	*RTN4R*	reticulon 4 receptor [Source:NCBI gene (formerly Entrezgene);Acc:100152289]	-1.521982675	0.0006065389675	0.08643669018
COvsSOY	ENSSSCG00000001612	*Novel gene*	adenylate cyclase type 10 [Source:NCBI gene (formerly Entrezgene);Acc:100737927]	-1.463994535	0.0004648604093	0.07979309744
COvsSOY	ENSSSCG00000041847	*0*	0	-1.439824303	4.47E-05	0.02106788877
COvsSOY	ENSSSCG00000034894	*NKAIN3*	sodium/potassium transporting ATPase interacting 3 [Source:VGNC Symbol;Acc:VGNC:90755]	-1.434260115	0.0007799180231	0.09596483854
COvsSOY	ENSSSCG00000046097	*0*	0	-1.431880163	0.0002839248955	0.05779448985
COvsSOY	ENSSSCG00000045889	*0*	0	-1.420145153	2.57E-05	0.01583287404
COvsSOY	ENSSSCG00000045401	*0*	0	-1.415811071	0.0005244695439	0.08314859461
COvsSOY	ENSSSCG00000050399	*0*	0	-1.378612886	0.0008759773192	0.09869048179
COvsSOY	ENSSSCG00000017963	*Novel gene*	dynein axonemal heavy chain 2 [Source:VGNC Symbol;Acc:VGNC:87370]	-1.354492474	1.82E-05	0.01583287404
COvsSOY	ENSSSCG00000000415	*SDR9C7*	short chain dehydrogenase/reductase family 9C member 7 [Source:VGNC Symbol;Acc:VGNC:92664]	-1.337743262	0.0001459136244	0.04374225161
COvsSOY	ENSSSCG00000034993	*NREP*	neuronal regeneration related protein [Source:NCBI gene (formerly Entrezgene);Acc:100037285]	-1.301584143	0.0001110845946	0.03663125592
COvsSOY	ENSSSCG00000037616	*SULT1C4*	sulfotransferase 1C4-like [Source:NCBI gene (formerly Entrezgene);Acc:100624389]	-1.287929781	0.0004808801659	0.08005826242
COvsSOY	ENSSSCG00000011673	*Novel gene*	tetraspanin-6 [Source:NCBI gene (formerly Entrezgene);Acc:100739719]	-1.262563409	0.0007473457321	0.09436330265
COvsSOY	ENSSSCG00000003891	*CYP4A24*	cytochrome P450 4A24 [Source:NCBI gene (formerly Entrezgene);Acc:403326]	-1.249195405	0.0004867126601	0.08005826242
COvsSOY	ENSSSCG00000014311	*SLC25A48*	solute carrier family 25 member 48 [Source:VGNC Symbol;Acc:VGNC:93021]	-1.244778251	0.0002212852933	0.05341704999
COvsSOY	ENSSSCG00000006808	*SLC16A4*	solute carrier family 16 member 4 [Source:VGNC	-1.233908313	0.0006895432816	0.09095351702

			Symbol;Acc:VGNC:92944]			
COvsSOY	ENSSSCG00000033099	*ASPRV1*	aspartic peptidase retroviral like 1 [Source:VGNC Symbol;Acc:VGNC:85587]	-1.209817365	2.14E-05	0.01583287404
COvsSOY	ENSSSCG00000016129	*GPR1*	G protein-coupled receptor 1 [Source:VGNC Symbol;Acc:VGNC:96331]	-1.206880742	0.0001524824675	0.04470982782
COvsSOY	ENSSSCG00000048436	*0*	0	-1.198808059	0.0005840497061	0.08643669018
COvsSOY	ENSSSCG00000010664	*ENO4*	enolase 4 [Source:VGNC Symbol;Acc:VGNC:87704]	-1.180093048	5.07E-05	0.02142786959
COvsSOY	ENSSSCG00000010432	*Novel gene*	N-acylsphingosine amidohydrolase 2 [Source:VGNC Symbol;Acc:VGNC:97888]	-1.175909313	0.0005702239883	0.08643669018
COvsSOY	ENSSSCG00000017781	*PIPOX*	peroxisomal sarcosine oxidase [Source:NCBI gene (formerly Entrezgene);Acc:100515508]	-1.12364014	3.09E-05	0.01696364634
COvsSOY	ENSSSCG00000033997	*Novel gene*	zinc finger and SCAN domain-containing protein 2-like [Source:NCBI gene (formerly Entrezgene);Acc:110257542]	-1.113904427	0.0001741193201	0.04706359589
COvsSOY	ENSSSCG00000003044	*LYPD4*	LY6/PLAUR domain containing 4 [Source:VGNC Symbol;Acc:VGNC:89912]	-1.095964437	0.0008798823886	0.09869048179
COvsSOY	ENSSSCG00000051384	*0*	0	-1.090353674	0.0002671955931	0.05648103767
COvsSOY	ENSSSCG00000008888	*NPY1R*	neuropeptide Y receptor Y1 [Source:VGNC Symbol;Acc:VGNC:90865]	-1.089532829	0.0008037445538	0.0981640015
COvsSOY	ENSSSCG00000044746	*0*	0	-1.057520519	0.0002291331693	0.05341704999
COvsSOY	ENSSSCG00000033189	*Novel gene*	FAM3 metabolism regulating signaling molecule D [Source:NCBI gene (formerly Entrezgene);Acc:100621654]	-1.022093414	2.23E-05	0.01583287404
COvsSOY	ENSSSCG00000018091	*ND5*	mitochondrially encoded NADH:ubiquinone oxidoreductase core subunit 5 [Source:VGNC Symbol;Acc:VGNC:99796]	-0.9961061529	3.66E-06	0.009258811916
COvsSOY	ENSSSCG00000015243	*PRDM10*	PR/SET domain 10 [Source:VGNC Symbol;Acc:VGNC:91773]	-0.9946818832	0.0002764527051	0.05697690253
COvsSOY	ENSSSCG00000036933	*NR1D1*	nuclear receptor subfamily 1 group D member 1 [Source:VGNC Symbol;Acc:VGNC:90869]	-0.9870627232	0.0005762371039	0.08643669018
COvsSOY	ENSSSCG00000039188	*AK8*	adenylate kinase 8 [Source:VGNC Symbol;Acc:VGNC:85213]	-0.9579059719	0.0002548063061	0.05502523086
COvsSOY	ENSSSCG00000032687	*CYP4V2*	cytochrome P450. family 4. subfamily v. polypeptide 2 [Source:NCBI gene (formerly Entrezgene);Acc:100113469]	-0.9560581905	1.94E-05	0.01583287404
COvsSOY	ENSSSCG00000046729	*0*	0	-0.9398096038	9.41E-06	0.01293576522
COvsSOY	ENSSSCG00000018092	*ND6*	mitochondrially encoded NADH:ubiquinone oxidoreductase core subunit 6 [Source:VGNC Symbol;Acc:VGNC:99797]	-0.9286856954	2.06E-05	0.01583287404
COvsSOY	ENSSSCG00000051779	*0*	0	-0.8948897459	0.0006550289587	0.08780583309

COvsSOY	ENSSSCG00000027991	*Novel gene*	sodium channel epithelial 1 subunit delta [Source:VGNC Symbol;Acc:VGNC:92642]	-0.8943805618	0.000593240228	0.08643669018
COvsSOY	ENSSSCG00000051054	*0*	0	-0.8876479806	0.0006024122156	0.08643669018
COvsSOY	ENSSSCG00000001048	*ADTRP*	androgen dependent TFPI regulating protein [Source:VGNC Symbol;Acc:VGNC:85161]	-0.8631585564	0.0008537406433	0.09869048179
COvsSOY	ENSSSCG00000013270	*CRY2*	cryptochrome circadian regulator 2 [Source:VGNC Symbol;Acc:VGNC:87012]	-0.8608730522	1.17E-05	0.01373286453
COvsSOY	ENSSSCG00000034069	*0*	0	-0.8376712739	0.000396744872	0.07433556192
COvsSOY	ENSSSCG00000013043	*MACROD1*	mono-ADP ribosylhydrolase 1 [Source:VGNC Symbol;Acc:VGNC:98096]	-0.8190970904	0.0007211698104	0.0936271483
COvsSOY	ENSSSCG00000041180	*0*	0	-0.7941344077	0.000365789362	0.06932339081
COvsSOY	ENSSSCG00000026473	*ABCA8*	ATP-binding cassette sub-family A member 8 [Source:NCBI gene (formerly Entrezgene);Acc:100520512]	-0.7910886918	0.0004374509645	0.07775408713
COvsSOY	ENSSSCG00000043977	*Novel gene*	cytochrome c oxidase subunit 6B1-like [Source:NCBI gene (formerly Entrezgene);Acc:100519366]	-0.789408221	8.79E-05	0.0315152198
COvsSOY	ENSSSCG00000010879	*KIF26B*	kinesin family member 26B [Source:VGNC Symbol;Acc:VGNC:96087]	-0.766712149	2.41E-05	0.01583287404
COvsSOY	ENSSSCG00000006213	*Novel gene*	alcohol dehydrogenase iron containing 1 [Source:VGNC Symbol;Acc:VGNC:98730]	-0.7488334346	0.0001041612331	0.03654064705
COvsSOY	ENSSSCG00000037808	*0*	0	-0.7457271124	3.31E-06	0.009258811916
COvsSOY	ENSSSCG00000040838	*AGBL2*	ATP/GTP binding protein like 2 [Source:VGNC Symbol;Acc:VGNC:85176]	-0.7404512644	0.0004731665578	0.07979309744
COvsSOY	ENSSSCG00000022953	*PTER*	phosphotriesterase related [Source:VGNC Symbol;Acc:VGNC:96514]	-0.7398139504	0.000879181234	0.09869048179
COvsSOY	ENSSSCG00000018087	*ND4*	mitochondrially encoded NADH:ubiquinone oxidoreductase core subunit 4 [Source:VGNC Symbol;Acc:VGNC:99795]	-0.7280364527	0.0001378815205	0.04209982427
COvsSOY	ENSSSCG00000027903	*Novel gene*	phylloquinone omega-hydroxylase CYP4F2-like [Source:NCBI gene (formerly Entrezgene);Acc:110259328]	-0.7072196383	0.0001968936933	0.05152989232
COvsSOY	ENSSSCG00000007636	*GJC3*	gap junction protein gamma 3 [Source:VGNC Symbol;Acc:VGNC:88470]	-0.6872467916	0.0004400489459	0.07775408713
COvsSOY	ENSSSCG00000025876	*PBLD*	phenazine biosynthesis like protein domain containing [Source:VGNC Symbol;Acc:VGNC:91201]	-0.6845349813	0.0002547136565	0.05502523086
COvsSOY	ENSSSCG00000014110	*DMGDH*	dimethylglycine dehydrogenase [Source:VGNC Symbol;Acc:VGNC:87347]	-0.6717715723	4.35E-05	0.02106788877

COvsSOY	ENSSSCG00000011949	*CEP97*	centrosomal protein 97 [Source:NCBI gene (formerly Entrezgene);Acc:100521822]	-0.648134564	0.0004742675612	0.07979309744
COvsSOY	ENSSSCG00000011802	*KNG1*	kininogen 1 [Source:VGNC Symbol;Acc:VGNC:89557]	-0.6468489909	0.0003105750301	0.06169591683
COvsSOY	ENSSSCG00000000659	*Novel gene*	ovostatin homolog 2 [Source:NCBI gene (formerly Entrezgene);Acc:100524679]	-0.6462323544	0.000415773314	0.07639773741
COvsSOY	ENSSSCG00000046214	*IFT22*	intraflagellar transport 22 [Source:NCBI gene (formerly Entrezgene);Acc:100519188]	-0.6327936155	0.0007595440598	0.09487395801
COvsSOY	ENSSSCG00000018075	*COX1*	mitochondrially encoded cytochrome c oxidase I [Source:VGNC Symbol;Acc:VGNC:99790]	-0.629175199	0.0001084239419	0.03663125592
COvsSOY	ENSSSCG00000037312	*Novel gene*	transmembrane protein 234 [Source:VGNC Symbol;Acc:VGNC:94148]	-0.6286385295	3.02E-05	0.01696364634
COvsSOY	ENSSSCG00000000926	*CEP290*	centrosomal protein 290 [Source:VGNC Symbol;Acc:VGNC:86567]	-0.6283979696	0.0006819842141	0.09068190099
COvsSOY	ENSSSCG00000017604	*HLF*	HLF transcription factor. PAR bZIP family member [Source:VGNC Symbol;Acc:VGNC:88896]	-0.6274973184	0.0008662589421	0.09869048179
COvsSOY	ENSSSCG00000044227	*NRG4*	neuregulin 4 [Source:NCBI gene (formerly Entrezgene);Acc:100516621]	-0.6236486946	2.23E-05	0.01583287404
COvsSOY	ENSSSCG00000014368	*Novel gene*	uncharacterized LOC100513976 [Source:NCBI gene (formerly Entrezgene);Acc:100513976]	-0.6203166225	5.99E-05	0.02408594067
COvsSOY	ENSSSCG00000003815	*ALG6*	ALG6 alpha-1.3-glucosyltransferase [Source:VGNC Symbol;Acc:VGNC:85253]	-0.6073164649	2.45E-05	0.01583287404
COvsSOY	ENSSSCG00000016295	*NGEF*	neuronal guanine nucleotide exchange factor [Source:VGNC Symbol;Acc:VGNC:96443]	-0.6023512937	0.0002279490497	0.05341704999
COvsSOY	ENSSSCG00000015281	*PLEKHA6*	pleckstrin homology domain containing A6 [Source:VGNC Symbol;Acc:VGNC:91536]	-0.5659438105	0.0006075116708	0.08643669018
COvsSOY	ENSSSCG00000046546	*0*	0	-0.5632895485	0.0008937940126	0.09957348433
COvsSOY	ENSSSCG00000007094	*DZANK1*	double zinc ribbon and ankyrin repeat domains 1 [Source:VGNC Symbol;Acc:VGNC:95675]	-0.5556057266	0.0008591884513	0.09869048179
COvsSOY	ENSSSCG00000005272	*NMRK1*	nicotinamide riboside kinase 1 [Source:VGNC Symbol;Acc:VGNC:90800]	-0.539410743	0.000157833349	0.04486821136
COvsSOY	ENSSSCG00000009818	*IFT81*	intraflagellar transport 81 [Source:VGNC Symbol;Acc:VGNC:89051]	-0.5315682215	0.0005002589355	0.08086538557
COvsSOY	ENSSSCG00000028446	*PCBP4*	poly(rC) binding protein 4 [Source:NCBI gene (formerly Entrezgene);Acc:100620941]	-0.5269764595	7.36E-05	0.02735053857
COvsSOY	ENSSSCG00000036411	*ACOT13*	acyl-CoA thioesterase 13 [Source:VGNC Symbol;Acc:VGNC:85018]	-0.5222191549	0.0007721438971	0.09572262087

COvsSOY	ENSSSCG00000035675	*Novel gene*	methyltransferase like 7A [Source:NCBI gene (formerly Entrezgene);Acc:110258456]	-0.5218343802	0.0006308621506	0.08668045949
COvsSOY	ENSSSCG00000005082	*PCNX4*	pecanex 4 [Source:HGNC Symbol;Acc:HGNC:20349]	-0.4969388241	0.0003576470972	0.06856843418
COvsSOY	ENSSSCG00000029494	*RBBP9*	RB binding protein 9. serine hydrolase [Source:VGNC Symbol;Acc:VGNC:96532]	-0.4918763955	5.29E-05	0.02180126607
COvsSOY	ENSSSCG00000034811	*QDPR*	quinoid dihydropteridine reductase [Source:VGNC Symbol;Acc:VGNC:98232]	-0.4917238342	0.0008446393387	0.09869048179
COvsSOY	ENSSSCG00000001074	*KDM1B*	lysine demethylase 1B [Source:VGNC Symbol;Acc:VGNC:89409]	-0.4855998252	0.0002162602688	0.05321939273
COvsSOY	ENSSSCG00000014170	*CAST*	calpastatin [Source:VGNC Symbol;Acc:VGNC:99603]	-0.4855452469	0.0002569712989	0.05502523086
COvsSOY	ENSSSCG00000015405	*CD36*	CD36 molecule [Source:NCBI gene (formerly Entrezgene);Acc:733702]	-0.4783217922	0.000583431248	0.08643669018
COvsSOY	ENSSSCG00000025910	*ZNF277*	zinc finger protein 277 [Source:VGNC Symbol;Acc:VGNC:95215]	-0.4309302596	4.98E-05	0.02142786959
COvsSOY	ENSSSCG00000014903	*CCDC90B*	coiled-coil domain containing 90B [Source:VGNC Symbol;Acc:VGNC:86328]	-0.4203926589	0.0002875394713	0.05781647321
COvsSOY	ENSSSCG00000032028	*0*	0	-0.389499994	0.0002012731242	0.05185298861
COvsSOY	ENSSSCG00000034407	*AMN1*	antagonist of mitotic exit network 1 homolog [Source:VGNC Symbol;Acc:VGNC:97883]	-0.3683622974	0.0002109065662	0.05321939273
COvsSOY	ENSSSCG00000009944	*CORO1C*	coronin 1C [Source:VGNC Symbol;Acc:VGNC:86914]	-0.3610697918	0.0004904102684	0.08005826242
COvsSOY	ENSSSCG00000004952	*SMAD3*	SMAD family member 3 [Source:VGNC Symbol;Acc:VGNC:93217]	-0.3173857025	0.0008597437264	0.09869048179
COvsSOY	ENSSSCG00000008529	*YPEL5*	yippee like 5 [Source:VGNC Symbol;Acc:VGNC:95039]	-0.2918382389	0.00057103154	0.08643669018
COvsSOY	ENSSSCG00000027779	*TMEM259*	transmembrane protein 259 [Source:VGNC Symbol;Acc:VGNC:94162]	0.2476064203	0.0006422767665	0.08680212563
COvsSOY	ENSSSCG00000007896	*TXNDC11*	thioredoxin domain containing 11 [Source:VGNC Symbol;Acc:VGNC:94603]	0.3552634198	0.0006081183928	0.08643669018
COvsSOY	ENSSSCG00000010585	*ACTR1A*	actin related protein 1A [Source:VGNC Symbol;Acc:VGNC:85049]	0.3570786896	0.0002143501758	0.05321939273
COvsSOY	ENSSSCG00000009758	*DHX37*	DEAH-box helicase 37 [Source:VGNC Symbol;Acc:VGNC:87293]	0.3611122345	0.0002711148913	0.0565840801
COvsSOY	ENSSSCG00000012653	*ZDHHC9*	zinc finger DHHC-type palmitoyltransferase 9 [Source:VGNC Symbol;Acc:VGNC:95131]	0.3939007094	0.0001545645431	0.04470982782
COvsSOY	ENSSSCG00000000120	*ANKRD54*	ankyrin repeat domain 54 [Source:VGNC Symbol;Acc:VGNC:85344]	0.441288276	0.0002414074655	0.05502523086

COvsSOY	ENSSSCG00000014558	*SIRT3*	sirtuin 3 [Source:VGNC Symbol;Acc:VGNC:92886]	0.4498969734	6.48E-05	0.02543902437
COvsSOY	ENSSSCG00000025564	*GAS2L1*	growth arrest specific 2 like 1 [Source:VGNC Symbol;Acc:VGNC:88355]	0.4614206778	0.0005527415189	0.08597737891
COvsSOY	ENSSSCG00000007749	*Novel gene*	mitochondrial ribosomal protein S17 [Source:NCBI gene (formerly Entrezgene);Acc:100624266]	0.5060610874	0.0006166034791	0.08663904854
COvsSOY	ENSSSCG00000034265	*DESI1*	desumoylating isopeptidase 1 [Source:VGNC Symbol;Acc:VGNC:87263]	0.5067387438	0.0006300425079	0.08668045949
COvsSOY	ENSSSCG00000008019	*JPT2*	Jupiter microtubule associated homolog 2 [Source:NCBI gene (formerly Entrezgene);Acc:474165]	0.5257768199	0.0004170182173	0.07639773741
COvsSOY	ENSSSCG00000007840	*POLR3E*	RNA polymerase III subunit E [Source:VGNC Symbol;Acc:VGNC:91657]	0.5690657641	0.0008145039411	0.09864886242
COvsSOY	ENSSSCG00000035867	*GFOD1*	glucose-fructose oxidoreductase domain containing 1 [Source:VGNC Symbol;Acc:VGNC:88424]	0.5717269808	0.0008256636956	0.09864886242
COvsSOY	ENSSSCG00000027827	*GALE*	UDP-galactose-4-epimerase [Source:VGNC Symbol;Acc:VGNC:88325]	0.5776757013	0.000531609826	0.08347793153
COvsSOY	ENSSSCG00000005930	*SLC45A4*	solute carrier family 45 member 4 [Source:VGNC Symbol;Acc:VGNC:93125]	0.5819862754	5.05E-06	0.009258811916
COvsSOY	ENSSSCG00000009215	*ABCG2*	ATP-binding cassette. sub-family G (WHITE). member 2 [Source:NCBI gene (formerly Entrezgene);Acc:397073]	0.5953792091	2.69E-05	0.01583287404
COvsSOY	ENSSSCG00000035344	*UBE2S*	ubiquitin conjugating enzyme E2 S [Source:VGNC Symbol;Acc:VGNC:94651]	0.6109117162	0.0005229199159	0.08314859461
COvsSOY	ENSSSCG00000028124	*SNRPN*	small nuclear ribonucleoprotein polypeptide N [Source:NCBI gene (formerly Entrezgene);Acc:100626432]	0.6271581418	0.00035344691	0.06856038414
COvsSOY	ENSSSCG00000011798	*Novel gene*	DnaJ heat shock protein family (Hsp40) member B11 [Source:NCBI gene (formerly Entrezgene);Acc:100152894]	0.6520956575	0.0008203843209	0.09864886242
COvsSOY	ENSSSCG00000024045	*CASTOR2*	cytosolic arginine sensor for mTORC1 subunit 2 [Source:NCBI gene (formerly Entrezgene);Acc:100620792]	0.6672481284	0.0006200514148	0.08663904854
COvsSOY	ENSSSCG00000029097	*RCC1*	regulator of chromosome condensation 1 [Source:VGNC Symbol;Acc:VGNC:92175]	0.6708235938	0.0001344056188	0.04209982427
COvsSOY	ENSSSCG00000017203	*GALK1*	galactokinase 1 [Source:VGNC Symbol;Acc:VGNC:88326]	0.6886798402	0.0002300224739	0.05341704999
COvsSOY	ENSSSCG00000016957	*CD180*	CD180 molecule [Source:VGNC Symbol;Acc:VGNC:86392]	0.7455772974	0.0001860595462	0.04947983543
COvsSOY	ENSSSCG00000032914	*MANF*	mesencephalic astrocyte derived neurotrophic factor [Source:VGNC Symbol;Acc:VGNC:89973]	0.7837257492	0.0007150836888	0.09357380842
COvsSOY	ENSSSCG00000035565	*CCDC134*	coiled-coil domain containing 134 [Source:VGNC Symbol;Acc:VGNC:86256]	0.7908220854	7.05E-05	0.02704686912
COvsSOY	ENSSSCG00000013397	*ARNTL*	aryl hydrocarbon receptor nuclear translocator like [Source:VGNC Symbol;Acc:VGNC:96796]	0.8229834706	0.000437647896	0.07775408713
COvsSOY	ENSSSCG00000015106	*HYOU1*	hypoxia up-regulated 1 [Source:VGNC Symbol;Acc:VGNC:89014]	0.8629960569	0.0001296940426	0.04192932107

COvsSOY	ENSSSCG00000039626	*DERL3*	derlin 3 [Source:VGNC Symbol;Acc:VGNC:87262]	0.9745665153	0.0001680808808	0.04618862605
COvsSOY	ENSSSCG00000000981	*CRELD2*	cysteine rich with EGF like domains 2 [Source:VGNC Symbol;Acc:VGNC:97942]	1.05718406	4.19E-05	0.02092120428
COvsSOY	ENSSSCG00000029790	*PCYOX1*	prenylcysteine oxidase 1 [Source:VGNC Symbol;Acc:VGNC:91235]	1.090026006	0.0001648977517	0.0460819344
COvsSOY	ENSSSCG00000051557	*0*	0	1.108718568	4.81E-05	0.02142786959
COvsSOY	ENSSSCG00000043973	*0*	0	1.10893414	0.0004432850673	0.07775408713
COvsSOY	ENSSSCG00000008386	*KIAA1841*	KIAA1841 [Source:VGNC Symbol;Acc:VGNC:89447]	1.289747179	4.72E-06	0.009258811916
COvsSOY	ENSSSCG00000045759	*0*	0	1.393756901	0.0007294050915	0.09395649335
COvsSOY	ENSSSCG00000031106	*PLA2G2D*	phospholipase A2 group IID [Source:VGNC Symbol;Acc:VGNC:91491]	1.430682083	0.000247697742	0.05502523086
COvsSOY	ENSSSCG00000017885	*SMTNL2*	smoothelin like 2 [Source:VGNC Symbol;Acc:VGNC:93268]	1.498691673	0.0001362820854	0.04209982427
COvsSOY	ENSSSCG00000022945	*UCHL1*	ubiquitin C-terminal hydrolase L1 [Source:VGNC Symbol;Acc:VGNC:94680]	1.663720451	0.0008794863501	0.09869048179
COvsSOY	ENSSSCG00000039880	*Novel gene*	C-type lectin domain family 12 member B [Source:NCBI gene (formerly Entrezgene);Acc:100520308]	1.685946683	4.89E-05	0.02142786959
COvsSOY	ENSSSCG00000045703	*Novel gene*	ring finger protein 212 [Source:NCBI gene (formerly Entrezgene);Acc:110262032]	2.097760733	0.0002569068834	0.05502523086
COvsSOY	ENSSSCG00000003797	*DIRAS3*	DIRAS family GTPase 3 [Source:VGNC Symbol;Acc:VGNC:87314]	2.362930421	0.0003247394066	0.06374170638

Diet_comparison Liver	**Gene stable ID**	***Gene name***	**Gene description**	**log2 fold change**	**p-value**	**FDR**
SOYvsFO	ENSSSCG00000015610	*SYT14*	synaptotagmin 14 [Source:NCBI gene (formerly Entrezgene);Acc:100512917]	-3.943536968	2.75E-05	0.02054624254
SOYvsFO	ENSSSCG00000026333	*GTSF1*	gametocyte specific factor 1 [Source:VGNC Symbol;Acc:VGNC:88746]	-3.504394144	4.08E-05	0.02317733235
SOYvsFO	ENSSSCG00000006238	*CYP7A1*	cytochrome P450 family 7 subfamily A member 1 [Source:VGNC Symbol;Acc:VGNC:98774]	-2.770032202	0.0001635170193	0.04646499621
SOYvsFO	ENSSSCG00000050735	*0*	0	-2.304389014	2.40E-05	0.01896429359
SOYvsFO	ENSSSCG00000022842	*0*	0	-2.2814004	5.02E-05	0.02446163621
SOYvsFO	ENSSSCG00000038322	*Novel gene*	diacylglycerol O-acyltransferase 2-like [Source:NCBI gene (formerly Entrezgene);Acc:110259135]	-2.278392365	2.58E-06	0.004574378918
SOYvsFO	ENSSSCG00000003006	*CYP2B22*	cytochrome P450 2B4-like [Source:NCBI gene (formerly Entrezgene);Acc:102165015]	-2.185967764	8.11E-05	0.03032901868
SOYvsFO	ENSSSCG00000044512	*Novel gene*	CD200 receptor 1 like [Source:NCBI gene (formerly Entrezgene);Acc:100516043]	-2.072634966	0.0002369628612	0.04809669045

SOYvsFO	ENSSSCG00000043197	*0*	0	-2.002378584	0.0006842389018	0.08750066737
SOYvsFO	ENSSSCG00000044322	*0*	0	-1.960987451	0.0002299430478	0.04809669045
SOYvsFO	ENSSSCG00000029796	*KBTBD11*	kelch repeat and BTB domain containing 11 [Source:VGNC Symbol;Acc:VGNC:96196]	-1.955893674	0.0002739843751	0.05332561645
SOYvsFO	ENSSSCG00000010632	*TECTB*	tectorin beta [Source:VGNC Symbol;Acc:VGNC:93860]	-1.779120582	0.000516166485	0.07560508679
SOYvsFO	ENSSSCG00000001863	*TMEM266*	transmembrane protein 266 [Source:VGNC Symbol;Acc:VGNC:94166]	-1.737415191	8.37E-05	0.03048964443
SOYvsFO	ENSSSCG00000037430	*COL6A6*	collagen type VI alpha 6 chain [Source:NCBI gene (formerly Entrezgene);Acc:100516642]	-1.709299034	0.0008667938538	0.09473390058
SOYvsFO	ENSSSCG00000005180	*BNC2*	basonuclin 2 [Source:VGNC Symbol;Acc:VGNC:85852]	-1.625164315	0.0007661177009	0.09147059071
SOYvsFO	ENSSSCG00000045889	*0*	0	-1.554843888	1.41E-06	0.004012858058
SOYvsFO	ENSSSCG00000041847	*0*	0	-1.397939074	0.0001977637024	0.04763555944
SOYvsFO	ENSSSCG00000009798	*B3GNT4*	UDP-GlcNAc:betaGal beta-1.3-N-acetylglucosaminyltransferase 4 [Source:VGNC Symbol;Acc:VGNC:85725]	-1.392796044	0.0003534297215	0.06123816442
SOYvsFO	ENSSSCG00000034360	*CELSR2*	cadherin EGF LAG seven-pass G-type receptor 2 [Source:VGNC Symbol;Acc:VGNC:98748]	-1.372133477	1.45E-05	0.01376640887
SOYvsFO	ENSSSCG00000003882	*SLC5A9*	solute carrier family 5 member 9 [Source:VGNC Symbol;Acc:VGNC:93149]	-1.369135849	0.0001062919711	0.03610414569
SOYvsFO	ENSSSCG00000011294	*GASK1A*	golgi associated kinase 1A [Source:VGNC Symbol;Acc:VGNC:88361]	-1.356281413	0.0001250583532	0.04038247915
SOYvsFO	ENSSSCG00000003148	*DBP*	D-box binding PAR bZIP transcription factor [Source:VGNC Symbol;Acc:VGNC:87167]	-1.272308341	5.78E-05	0.02650219601
SOYvsFO	ENSSSCG00000050178	*0*	0	-1.227247002	0.0005890056263	0.07821113961
SOYvsFO	ENSSSCG00000012380	*P2RY4*	pyrimidinergic receptor P2Y4 [Source:VGNC Symbol;Acc:VGNC:91127]	-1.017062886	0.0001623559142	0.04646499621
SOYvsFO	ENSSSCG00000033997	*Novel gene*	zinc finger and SCAN domain-containing protein 2-like [Source:NCBI gene (formerly Entrezgene);Acc:110257542]	-1.012946489	7.62E-05	0.02927026331
SOYvsFO	ENSSSCG00000033189	*Novel gene*	FAM3 metabolism regulating signaling molecule D [Source:NCBI gene (formerly Entrezgene);Acc:100621654]	-0.9956226794	0.0006130526232	0.07991056578
SOYvsFO	ENSSSCG00000017781	*PIPOX*	peroxisomal sarcosine oxidase [Source:NCBI gene (formerly Entrezgene);Acc:100515508]	-0.9819005182	0.000784852581	0.09246292718
SOYvsFO	ENSSSCG00000005221	*SPATA6L*	spermatogenesis associated 6 like [Source:VGNC Symbol;Acc:VGNC:93388]	-0.9595732245	0.0009285806349	0.09652866114
SOYvsFO	ENSSSCG00000016129	*GPR1*	G protein-coupled receptor 1 [Source:VGNC Symbol;Acc:VGNC:96331]	-0.9521089852	0.000798292928	0.09249956969
SOYvsFO	ENSSSCG00000018092	*ND6*	mitochondrially encoded NADH:ubiquinone oxidoreductase core subunit	-	0.0002044029562	0.04763555944

			6 [Source:VGNC Symbol;Acc:VGNC:99797]	0.9243504441		
SOYvsFO	ENSSSCG00000015243	*PRDM10*	PR/SET domain 10 [Source:VGNC Symbol;Acc:VGNC:91773]	-0.8690498065	0.0008925550102	0.09604749279
SOYvsFO	ENSSSCG00000044483	*0*	0	-0.8646843804	5.17E-05	0.02446163621
SOYvsFO	ENSSSCG00000046729	*0*	0	-0.8620968979	0.0001092678959	0.03610414569
SOYvsFO	ENSSSCG00000004181	*VNN1*	vanin 1 [Source:NCBI gene (formerly Entrezgene);Acc:397246]	-0.8419576068	1.40E-06	0.004012858058
SOYvsFO	ENSSSCG00000026473	*ABCA8*	ATP-binding cassette sub-family A member 8 [Source:NCBI gene (formerly Entrezgene);Acc:100520512]	-0.8069555537	1.86E-05	0.01601334164
SOYvsFO	ENSSSCG00000017635	*MKS1*	MKS transition zone complex subunit 1 [Source:VGNC Symbol;Acc:VGNC:96589]	-0.8034196331	0.0006988498518	0.08750066737
SOYvsFO	ENSSSCG00000028572	*Novel gene*	period circadian regulator 3 [Source:NCBI gene (formerly Entrezgene);Acc:100627898]	-0.7681589668	0.000289956453	0.05464790052
SOYvsFO	ENSSSCG00000041180	*0*	0	-0.7525130618	0.000456626801	0.0737244726
SOYvsFO	ENSSSCG00000015120	*USP2*	ubiquitin specific peptidase 2 [Source:VGNC Symbol;Acc:VGNC:94751]	-0.7449764398	0.0005769286681	0.07806669063
SOYvsFO	ENSSSCG00000023320	*CYP3A29*	cytochrome P450. subfamily IIIA. polypeptide 22 [Source:NCBI gene (formerly Entrezgene);Acc:100144468]	-0.7158580236	0.0008007775248	0.09249956969
SOYvsFO	ENSSSCG00000013270	*CRY2*	cryptochrome circadian regulator 2 [Source:VGNC Symbol;Acc:VGNC:87012]	-0.670701433	0.0009091271123	0.09608132434
SOYvsFO	ENSSSCG00000014368	*Novel gene*	uncharacterized LOC100513976 [Source:NCBI gene (formerly Entrezgene);Acc:100513976]	-0.6490259412	0.0007874446923	0.09246292718
SOYvsFO	ENSSSCG00000016295	*NGEF*	neuronal guanine nucleotide exchange factor [Source:VGNC Symbol;Acc:VGNC:96443]	-0.6488462559	0.0002257820092	0.04809669045
SOYvsFO	ENSSSCG00000035774	*ERRFI1*	ERBB receptor feedback inhibitor 1 [Source:VGNC Symbol;Acc:VGNC:87784]	-0.6466640551	3.69E-05	0.02185770277
SOYvsFO	ENSSSCG00000011970	*CMSS1*	cms1 ribosomal small subunit homolog [Source:VGNC Symbol;Acc:VGNC:96723]	-0.6280729268	6.53E-05	0.02797946364
SOYvsFO	ENSSSCG00000047750	*0*	0	-0.6221514915	0.0005146924382	0.07560508679
SOYvsFO	ENSSSCG00000037808	*0*	0	-0.6178073621	0.0008282965474	0.09306329645
SOYvsFO	ENSSSCG00000039681	*B9D1*	B9 domain containing 1 [Source:VGNC Symbol;Acc:VGNC:85737]	-0.6006800836	0.0003421861681	0.06015594808

SOYvsFO	ENSSSCG00000027903	*Novel gene*	phylloquinone omega-hydroxylase CYP4F2-like [Source:NCBI gene (formerly Entrezgene);Acc:110259328]	-0.5979406289	0.0004695800151	0.07496396465
SOYvsFO	ENSSSCG00000028724	*N6AMT1*	N-6 adenine-specific DNA methyltransferase 1 [Source:NCBI gene (formerly Entrezgene);Acc:100623424]	-0.5794791651	3.37E-05	0.02155608755
SOYvsFO	ENSSSCG00000024158	*ANO1*	anoctamin 1 [Source:VGNC Symbol;Acc:VGNC:85354]	-0.5788259053	0.0002351209951	0.04809669045
SOYvsFO	ENSSSCG00000011023	*ZNF438*	zinc finger protein 438 [Source:NCBI gene (formerly Entrezgene);Acc:100519167]	-0.5679686225	0.0005754519382	0.07806669063
SOYvsFO	ENSSSCG00000007094	*DZANK1*	double zinc ribbon and ankyrin repeat domains 1 [Source:VGNC Symbol;Acc:VGNC:95675]	-0.5548601334	0.0002110162536	0.04763555944
SOYvsFO	ENSSSCG00000009852	*VSIG10*	V-set and immunoglobulin domain containing 10 [Source:NCBI gene (formerly Entrezgene);Acc:100153531]	-0.5507573895	0.0001806620164	0.04753418387
SOYvsFO	ENSSSCG00000021941	*Novel gene*	zinc finger with KRAB and SCAN domains 1 [Source:NCBI gene (formerly Entrezgene);Acc:102162731]	-0.5489048534	0.0007402336637	0.09060412889
SOYvsFO	ENSSSCG00000035038	*CGNL1*	cingulin like 1 [Source:VGNC Symbol;Acc:VGNC:86616]	-0.5351346612	0.0001982016966	0.04763555944
SOYvsFO	ENSSSCG00000007247	*KIF3B*	kinesin family member 3B [Source:VGNC Symbol;Acc:VGNC:96392]	-0.5300905344	6.73E-05	0.02797946364
SOYvsFO	ENSSSCG00000014170	*CAST*	calpastatin [Source:VGNC Symbol;Acc:VGNC:99603]	-0.5212565036	0.0002995353694	0.05527011076
SOYvsFO	ENSSSCG00000011397	*SLC38A3*	solute carrier family 38 member 3 [Source:VGNC Symbol;Acc:VGNC:93095]	-0.5191798228	0.0004917948737	0.07513356522
SOYvsFO	ENSSSCG00000003428	*MTHFR*	methylenetetrahydrofolate reductase [Source:VGNC Symbol;Acc:VGNC:90451]	-0.5180908197	0.0001287255708	0.04064295355
SOYvsFO	ENSSSCG00000017492	*ORMDL3*	ORMDL sphingolipid biosynthesis regulator 3 [Source:VGNC Symbol;Acc:VGNC:91064]	-0.5119874869	0.000899093225	0.09604749279
SOYvsFO	ENSSSCG00000000038	*CYB5R3*	NADH-cytochrome b5 reductase 3-like [Source:NCBI gene (formerly Entrezgene);Acc:100524254]	-0.511454435	0.0005599578102	0.07724155891
SOYvsFO	ENSSSCG00000014903	*CCDC90B*	coiled-coil domain containing 90B [Source:VGNC Symbol;Acc:VGNC:86328]	-0.5027944664	2.39E-07	0.00169442425
SOYvsFO	ENSSSCG00000027865	*GALC*	galactosylceramidase [Source:VGNC Symbol;Acc:VGNC:88324]	-0.4963153077	0.0005278687661	0.07575716594
SOYvsFO	ENSSSCG00000001074	*KDM1B*	lysine demethylase 1B [Source:VGNC Symbol;Acc:VGNC:89409]	-0.4759609741	0.0003045441549	0.05547388913
SOYvsFO	ENSSSCG00000016826	*RAD1*	RAD1 checkpoint DNA exonuclease [Source:VGNC Symbol;Acc:VGNC:92051]	-0.4758463783	0.0009731301354	0.09805838981
SOYvsFO	ENSSSCG00000011888	*GPR156*	G protein-coupled receptor 156 [Source:VGNC Symbol;Acc:VGNC:88610]	-0.4638427507	0.0009375672323	0.09652866114

SOYvsFO	ENSSSCG00000035757	*SSBP2*	single stranded DNA binding protein 2 [Source:VGNC Symbol;Acc:VGNC:93480]	-0.4622693097	0.0001966992253	0.04763555944
SOYvsFO	ENSSSCG00000029494	*RBBP9*	RB binding protein 9. serine hydrolase [Source:VGNC Symbol;Acc:VGNC:96532]	-0.4569985531	0.0001060714812	0.03610414569
SOYvsFO	ENSSSCG00000040003	*UAP1L1*	UDP-N-acetylglucosamine pyrophosphorylase 1 like 1 [Source:VGNC Symbol;Acc:VGNC:94627]	-0.4565263938	0.0002356064647	0.04809669045
SOYvsFO	ENSSSCG00000039972	*Novel gene*	protein CutA homolog [Source:NCBI gene (formerly Entrezgene);Acc:102164650]	-0.4265448069	0.0001933824071	0.04763555944
SOYvsFO	ENSSSCG00000021784	*TBCK*	TBC1 domain containing kinase [Source:VGNC Symbol;Acc:VGNC:93786]	-0.4264937967	0.0007001730304	0.08750066737
SOYvsFO	ENSSSCG00000016611	*CADPS2*	calcium dependent secretion activator 2 [Source:VGNC Symbol;Acc:VGNC:86137]	-0.4200466608	0.0003429498729	0.06015594808
SOYvsFO	ENSSSCG00000028446	*PCBP4*	poly(rC) binding protein 4 [Source:NCBI gene (formerly Entrezgene);Acc:100620941]	-0.4134305915	0.0009347890976	0.09652866114
SOYvsFO	ENSSSCG00000017676	*BCAS3*	BCAS3 microtubule associated cell migration factor [Source:VGNC Symbol;Acc:VGNC:85772]	-0.4055445318	0.0003965441573	0.06628352219
SOYvsFO	ENSSSCG00000039013	*NOTUM*	notum. palmitoleoyl-protein carboxylesterase [Source:VGNC Symbol;Acc:VGNC:90826]	-0.4001440076	0.0004886611292	0.07513356522
SOYvsFO	ENSSSCG00000011193	*BTD*	biotinidase [Source:VGNC Symbol;Acc:VGNC:85911]	-0.3845175772	0.0002494904717	0.04992620595
SOYvsFO	ENSSSCG00000025910	*ZNF277*	zinc finger protein 277 [Source:VGNC Symbol;Acc:VGNC:95215]	-0.3809661106	0.0009940343919	0.09876392056
SOYvsFO	ENSSSCG00000004952	*SMAD3*	SMAD family member 3 [Source:VGNC Symbol;Acc:VGNC:93217]	-0.3779015205	0.0002113049773	0.04763555944
SOYvsFO	ENSSSCG00000025682	*ACTR6*	actin related protein 6 [Source:VGNC Symbol;Acc:VGNC:85052]	-0.3755240887	6.06E-05	0.02690833346
SOYvsFO	ENSSSCG00000038682	*TAF1D*	TATA-box binding protein associated factor. RNA polymerase I subunit D [Source:VGNC Symbol;Acc:VGNC:93714]	-0.3739946953	0.0002693279308	0.05314737835
SOYvsFO	ENSSSCG00000011477	*ACOX2*	acyl-CoA oxidase 2 [Source:VGNC Symbol;Acc:VGNC:85021]	-0.3725213723	0.0004123853364	0.06782446436
SOYvsFO	ENSSSCG00000032028	*0*	0	-0.3711251101	0.0002059758617	0.04763555944
SOYvsFO	ENSSSCG00000006303	*DCAF6*	DDB1 and CUL4 associated factor 6 [Source:VGNC Symbol;Acc:VGNC:87177]	-0.3638247986	0.0001588748086	0.04646499621
SOYvsFO	ENSSSCG00000037245	*HNRNPDL*	heterogeneous nuclear ribonucleoprotein D like [Source:NCBI gene (formerly Entrezgene);Acc:100511704]	-0.3373615547	0.0005158357	0.07560508679
SOYvsFO	ENSSSCG00000025675	*EEF2*	eukaryotic translation elongation factor 2 [Source:VGNC Symbol;Acc:VGNC:87556]	-0.2605863397	0.000546690082	0.07690468005

SOYvsFO	ENSSSCG00000028287	*C2orf68*	chromosome 3 C2orf68 homolog [Source:VGNC Symbol;Acc:VGNC:86023]	-0.2028125812	0.0008425596683	0.09306329645
SOYvsFO	ENSSSCG00000015560	*ARPC5*	actin related protein 2/3 complex subunit 5 [Source:VGNC Symbol;Acc:VGNC:85539]	0.2864219872	0.0007082331607	0.08750066737
SOYvsFO	ENSSSCG00000046439	*GNG10*	G protein subunit gamma 10 [Source:NCBI gene (formerly Entrezgene);Acc:100515992]	0.3102831441	0.0007600924918	0.09147059071
SOYvsFO	ENSSSCG00000037595	*Novel gene*	adaptor related protein complex 3 subunit sigma 1 [Source:NCBI gene (formerly Entrezgene);Acc:100736866]	0.3285272329	0.0008179536216	0.09306329645
SOYvsFO	ENSSSCG00000022353	*RAP1GDS1*	Rap1 GTPase-GDP dissociation stimulator 1 [Source:VGNC Symbol;Acc:VGNC:92087]	0.3455830807	0.0002166767954	0.04763555944
SOYvsFO	ENSSSCG00000036106	*TUBG1*	tubulin gamma 1 [Source:HGNC Symbol;Acc:HGNC:12417]	0.3477962747	0.0005448516903	0.07690468005
SOYvsFO	ENSSSCG00000014924	*CTSC*	cathepsin C [Source:VGNC Symbol;Acc:VGNC:87075]	0.3524594742	7.38E-05	0.02914211072
SOYvsFO	ENSSSCG00000035618	*PGAM5*	PGAM family member 5. mitochondrial serine/threonine protein phosphatase [Source:NCBI gene (formerly Entrezgene);Acc:106508765]	0.3660697793	0.0005533214551	0.07707442387
SOYvsFO	ENSSSCG00000008348	*PLEK*	pleckstrin [Source:VGNC Symbol;Acc:VGNC:91531]	0.3686742841	0.0007461066357	0.09060412889
SOYvsFO	ENSSSCG00000006538	*FLAD1*	flavin adenine dinucleotide synthetase 1 [Source:NCBI gene (formerly Entrezgene);Acc:100153896]	0.3710504688	0.000704429642	0.08750066737
SOYvsFO	ENSSSCG00000004470	*HMGN3*	high mobility group nucleosomal binding domain 3 [Source:VGNC Symbol;Acc:VGNC:88908]	0.3838903459	2.06E-06	0.004574378918
SOYvsFO	ENSSSCG00000008298	*DUSP11*	dual specificity phosphatase 11 [Source:VGNC Symbol;Acc:VGNC:87477]	0.4220517563	0.0004847764966	0.07513356522
SOYvsFO	ENSSSCG00000011755	*NCEH1*	neutral cholesterol ester hydrolase 1 [Source:VGNC Symbol;Acc:VGNC:98147]	0.434876322	0.0009129348808	0.09608132434
SOYvsFO	ENSSSCG00000023866	*ACSF3*	acyl-CoA synthetase family member 3 [Source:VGNC Symbol;Acc:VGNC:85032]	0.436047099	0.0005854092536	0.07821113961
SOYvsFO	ENSSSCG00000033180	*PSMD10*	proteasome 26S subunit. non-ATPase 10 [Source:VGNC Symbol;Acc:VGNC:91918]	0.4445947142	0.0004782013869	0.07513356522
SOYvsFO	ENSSSCG00000025564	*GAS2L1*	growth arrest specific 2 like 1 [Source:VGNC Symbol;Acc:VGNC:88355]	0.4782541032	0.0003611330383	0.06181901455
SOYvsFO	ENSSSCG00000017673	*INTS2*	integrator complex subunit 2 [Source:VGNC Symbol;Acc:VGNC:89162]	0.4789756366	0.000500151739	0.07559740328
SOYvsFO	ENSSSCG00000015037	*IL18*	interleukin 18 [Source:NCBI gene (formerly Entrezgene);Acc:397057]	0.493713191	0.000173855456	0.04753418387
SOYvsFO	ENSSSCG00000038234	*TMEM175*	transmembrane protein 175 [Source:VGNC Symbol;Acc:VGNC:94111]	0.5134499588	0.000315286826	0.05670373701
SOYvsFO	ENSSSCG00000011398	*SEMA3F*	semaphorin 3F [Source:VGNC Symbol;Acc:VGNC:92698]	0.5330856851	0.0006037392614	0.07942525394
SOYvsFO	ENSSSCG00000024495	*0*	0	0.5480387265	0.0009652220781	0.09805838981

SOYvsFO	ENSSSCG00000027665	*Novel gene*	tyrosine-protein phosphatase non-receptor type substrate 1 [Source:NCBI gene (formerly Entrezgene);Acc:102161654]	0.5511979339	0.0009923115516	0.09876392056
SOYvsFO	ENSSSCG00000036265	*0*	0	0.6194686191	0.0005244410603	0.07575716594
SOYvsFO	ENSSSCG00000023078	*WDR4*	WD repeat domain 4 [Source:VGNC Symbol;Acc:VGNC:94919]	0.6482625356	0.0002907149062	0.05464790052
SOYvsFO	ENSSSCG00000017203	*GALK1*	galactokinase 1 [Source:VGNC Symbol;Acc:VGNC:88326]	0.6483006901	6.89E-05	0.02797946364
SOYvsFO	ENSSSCG00000008727	*MSX1*	msh homeobox 1 [Source:VGNC Symbol;Acc:VGNC:90431]	0.6642167199	0.0008355689123	0.09306329645
SOYvsFO	ENSSSCG00000008677	*Novel gene*	transforming acidic coiled-coil containing protein 3 [Source:VGNC Symbol;Acc:VGNC:93699]	0.6759170646	0.0003764273733	0.06367000142
SOYvsFO	ENSSSCG00000008383	*Novel gene*	activator of HSP90 ATPase homolog 2. pseudogene [Source:NCBI gene (formerly Entrezgene);Acc:110260004]	0.6983465051	0.0002923170355	0.05464790052
SOYvsFO	ENSSSCG00000004750	*OIP5*	Opa interacting protein 5 [Source:VGNC Symbol;Acc:VGNC:91029]	0.7144803195	4.30E-05	0.02350708916
SOYvsFO	ENSSSCG00000004291	*NT5E*	5'-nucleotidase ecto [Source:VGNC Symbol;Acc:VGNC:90925]	0.7328507787	1.92E-05	0.01601334164
SOYvsFO	ENSSSCG00000024973	*Novel gene*	guanylate binding protein 1. interferon-inducible [Source:NCBI gene (formerly Entrezgene);Acc:100151938]	0.7443994395	0.0008352940917	0.09306329645
SOYvsFO	ENSSSCG00000010495	*ALDH18A1*	aldehyde dehydrogenase 18 family member A1 [Source:VGNC Symbol;Acc:VGNC:85237]	0.7451703276	1.22E-06	0.004012858058
SOYvsFO	ENSSSCG00000016322	*ACKR3*	atypical chemokine receptor 3 [Source:VGNC Symbol;Acc:VGNC:96017]	0.7497894604	4.96E-05	0.02446163621
SOYvsFO	ENSSSCG00000009904	*DYNLL1*	dynein light chain LC8-type 1 [Source:VGNC Symbol;Acc:VGNC:87500]	0.7784879967	3.28E-06	0.005177025879
SOYvsFO	ENSSSCG00000040207	*P2RY2*	purinergic receptor P2Y2 [Source:VGNC Symbol;Acc:VGNC:98173]	0.7980382591	0.0001462486324	0.04517175151
SOYvsFO	ENSSSCG00000039626	*DERL3*	derlin 3 [Source:VGNC Symbol;Acc:VGNC:87262]	0.8448444425	0.0002179273201	0.04763555944
SOYvsFO	ENSSSCG00000000981	*CRELD2*	cysteine rich with EGF like domains 2 [Source:VGNC Symbol;Acc:VGNC:97942]	0.8597075895	0.0002158525404	0.04763555944
SOYvsFO	ENSSSCG00000029449	*Novel gene*	proteoglycan 4 [Source:NCBI gene (formerly Entrezgene);Acc:100518683]	0.8681266609	3.24E-05	0.02155608755
SOYvsFO	ENSSSCG00000004125	*STX11*	syntaxin 11 [Source:VGNC Symbol;Acc:VGNC:93585]	0.8741302021	3.49E-05	0.02155608755
SOYvsFO	ENSSSCG00000025308	*IL17D*	interleukin 17D [Source:NCBI gene (formerly Entrezgene);Acc:100738902]	0.8900402138	0.0001524903994	0.04609752329
SOYvsFO	ENSSSCG00000016957	*CD180*	CD180 molecule [Source:VGNC Symbol;Acc:VGNC:86392]	0.8958052986	1.43E-05	0.01376640887
SOYvsFO	ENSSSCG00000047793	*0*	0	0.8984888817	8.98E-06	0.01159623939
SOYvsFO	ENSSSCG00000014766	*OR51E1*	olfactory receptor 51E1 [Source:NCBI gene (formerly Entrezgene);Acc:100737531]	0.9563302553	0.0006301772459	0.08139598463

SOYvsFO	ENSSSCG00000006287	*SELL*	selectin L [Source:NCBI gene (formerly Entrezgene);Acc:100127147]	1.035853145	3.00E-05	0.02128094501
SOYvsFO	ENSSSCG00000021161	*CKS2*	CDC28 protein kinase regulatory subunit 2 [Source:NCBI gene (formerly Entrezgene);Acc:100520933]	1.071701546	1.10E-05	0.01197387463
SOYvsFO	ENSSSCG00000051557	*0*	0	1.104600574	7.56E-06	0.01073875662
SOYvsFO	ENSSSCG00000004225	*TPD52L1*	TPD52 like 1 [Source:VGNC Symbol;Acc:VGNC:94334]	1.173842651	0.0008449581392	0.09306329645
SOYvsFO	ENSSSCG00000038929	*CEMIP*	cell migration inducing hyaluronidase 1 [Source:VGNC Symbol;Acc:VGNC:86542]	1.335091538	0.0004153102758	0.06782446436
SOYvsFO	ENSSSCG00000039880	*Novel gene*	C-type lectin domain family 12 member B [Source:NCBI gene (formerly Entrezgene);Acc:100520308]	1.412840377	0.0009690654476	0.09805838981
SOYvsFO	ENSSSCG00000021041	*Novel gene*	peptidase M20 domain containing 1 [Source:NCBI gene (formerly Entrezgene);Acc:100627595]	1.5050296	2.50E-06	0.004574378918
SOYvsFO	ENSSSCG00000010532	*LOXL4*	lysyl oxidase like 4 [Source:VGNC Symbol;Acc:VGNC:89783]	1.537783259	2.10E-07	0.00169442425
SOYvsFO	ENSSSCG00000008875	*RXFP1*	relaxin family peptide receptor 1 [Source:VGNC Symbol;Acc:VGNC:92525]	1.603285224	0.000177542953	0.04753418387
SOYvsFO	ENSSSCG00000005948	*TG*	thyroglobulin [Source:VGNC Symbol;Acc:VGNC:93926]	1.647223305	0.0008960665608	0.09604749279
SOYvsFO	ENSSSCG00000031106	*PLA2G2D*	phospholipase A2 group IID [Source:VGNC Symbol;Acc:VGNC:91491]	1.652094949	0.0001092336442	0.03610414569
SOYvsFO	ENSSSCG00000034829	*0*	0	1.807588728	0.0001756955624	0.04753418387
SOYvsFO	ENSSSCG00000026043	*Novel gene*	transglutaminase 3 [Source:NCBI gene (formerly Entrezgene);Acc:100153042]	1.897670016	1.09E-05	0.01197387463
SOYvsFO	ENSSSCG00000040707	*Novel gene*	RAS and EF-hand domain containing [Source:VGNC Symbol;Acc:VGNC:96130]	1.942030954	4.81E-05	0.02446163621

Table S3: Pathway maps by MetaCore software (p-value <0.1) from the list of differentially expressed genes (FDR 10%) in the liver of immunocastrated male pigs fed with different oil sources (SOY: 3.0% soybean oil *vs* FO: 3.0% fish oil)

Pathway Maps	p-value	Network Objects from Active Data
TNF-alpha. IL-1 beta induce dyslipidemia and inflammation in obesity and type 2 diabetes in adipocytes	1.165E-04	*AZGP1. PDE3B. APOE. Perilipin. LIPS*
Putative pathways for stimulation of fat cell differentiation by Bisphenol A	4.803E-04	*PPAR-gamma. TCF7L2 (TCF4). SCD. C/EBPalpha*
Signal transduction_WNT/Beta-catenin signaling in tissue homeostasis	1.367E-03	*TCF7L2 (TCF4). Tcf(Lef). WNT. PPCKC*
Fenofibrate in treatment of type 2 diabetes and metabolic syndrome X	2.894E-03	*RBP4. ACOX1. SR-BI*
Pioglitazone and Rosiglitazone in treatment of type 2 diabetes and metabolic syndrome X	3.244E-03	*PPAR-gamma. PPCKC. SR-BI*
Adiponectin in pathogenesis of type 2 diabetes	4.446E-03	*SCD. PPCKC. ACOX1*
Influence of low doses of Arsenite on glucose uptake in adipocytes	5.377E-03	*PPAR-gamma. KIF3B. C/EBPalpha*
Role of IL-6 in obesity and type 2 diabetes in adipocytes	5.884E-03	*PPAR-gamma. Perilipin. LIPS*
Dysregulation of Adiponectin secretion from adipocytes in obesity. type 2 diabetes and metabolic syndrome X	9.516E-03	*PPAR-gamma. IL-18. C/EBPalpha*
Regulation of metabolism_Bile acids regulation of glucose and lipid metabolism via FXR	1.173E-02	*APOE. SCD. PPCKC*
Transport_HDL-mediated reverse cholesterol transport	1.252E-02	*APOE. CES1. SR-BI*
Role of inflammasome in macrophages. adipocytes and pancreatic beta cells in type 2 diabetes	1.801E-02	*IL-18. ChREBP*
Regulation of lipid metabolism_Insulin regulation of fatty acid metabolism	1.967E-02	*PDE3B. SCD. Perilipin. LIPS*
Regulation of lipid metabolism_Regulation of fatty acid synthesis: NLTP and EHHADH	2.204E-02	*PPAR-gamma. ACAA1*
Glucagon-induced glucose upregulation in type 2 diabetes in liver	2.218E-02	*GYS2. PYC. PPCKC*
Androstenedione and testosterone biosynthesis and metabolism p.1	2.448E-02	*HSD3B1. HSD3B2. CYP2A13*
Role of ER stress in obesity and type 2 diabetes	2.448E-02	*PPAR-gamma. SCD. C/EBPalpha*
Signal transduction_Production and main functions of biologically active prostaglandins and Thromboxane A2	3.079E-02	*PPAR-gamma. ABCC4. PGE2R3*
Triacylglycerol biosynthesis in obesity and diabetes mellitus. type II	3.106E-02	*MOGAT2. PLCA*
Triacylglycerol metabolism p.1	3.214E-02	*ALD9A1. AL3A2. PLCA*
Inhibition of oligodendrocyte precursor cells differentiation by Wnt signaling in multiple sclerosis	3.351E-02	*TCF7L2 (TCF4). WNT*
Role of Diethylhexyl Phthalate and Tributyltin in fat cell differentiation	4.129E-02	*PPAR-gamma. C/EBPalpha*
Regulation of lipid metabolism_RXR-dependent regulation of lipid metabolism via PPAR. RAR and VDR	4.682E-02	*PPAR-gamma. SCD*
Role of adipose tissue hypoxia in obesity and type 2 diabetes	4.682E-02	*PPAR-gamma. C/EBPalpha*
Selective Insulin resistance in type 2 diabetes in liver	5.259E-02	*GYS2. PPCKC*
Cortisol biosynthesis from Cholesterol	7.130E-02	*HSD3B1. HSD3B2*
VLDL. LDL dyslipidemia in type 2 diabetes and metabolic syndrome X	7.460E-02	*APOE. SR-BI*

CHDI_Correlations from Replication data_Causal network (negative correlations)	7.795E-02	*TCF7L2 (TCF4). WNT*
Regulation of metabolism_Role of Adiponectin in regulation of metabolism	8.828E-02	*PPCKC. ACOX1*